POLITECNICO DI TORINO

Corso di Laurea Magistrale in Ingegneria Civile

Master Thesis

Application of B.I.M. methodology for long steel deck bridge

Lectures:

Prof. Rosario CERAVOLO

Eng. Andrea ALBERTO, phD.

Candidate:

Pier Paolo CAIRO

Marzo 2020

CONTENTS

FIGURE INDEX

TABLE INDEX

ABSTRACT

La scelta di sviluppare la tesi adottando la metodologia B.I.M. (Building Information Modeling) è dovuta al fatto che il B.I.M. rappresenta il metodo di progettazione innovativo che nei prossimi anni troverà larga scala di applicazione nella progettazione, sia in campo edilizio che non. Questa metodica, che già da qualche anno sta sostituendo i metodi tradizionali di progettazione, ha il vantaggio di inglobare in un singolo modello tutte le fasi progettuali, operative e di manutenzione dal progetto costruttivo. Esse saranno visualizzate a 360 gradi dai tecnici grazie al concetto essenziale di "interoperabilità" tra discipline.

La prima parte della tesi è dedicata allo studio progettuale di un viadotto a struttura composta. Il viadotto presenta una larghezza complessiva di 13,5m, in senso longitudinale è costituito da tre campate di luce +49,5, + 70,0, +49,5m misurate in asse agli appoggi. L'impalcato è realizzato con una sezione mista acciaio-calcestruzzo ed è costituito da due travi principali metalliche di altezza costante pari 2,5m e una trave pilota centrale di altezza pari a 0,45m. La struttura è segmentata da 8 diverse tipologie di conci, presenta 4 tipologie di diaframmi trasversali, irrigidite nel piano orizzontali da controventi superiori e inferiori con distribuzione variabile longitudinalmente. All'estradosso delle travi è solidarizzata la soletta in calcestruzzo, mediante uso di predalles, per mezzo di connettori a taglio opportunamente saldati sulla piattabanda superiore delle travi principali, al fine di garantire il comportamento torsionale.

La seconda parte della tesi riguarda l'applicazione del B.I.M. della struttura in esame, utilizzata per incrementare il livello di dettaglio e verificare l'interoperabilità tra i modelli strutturali nelle specifiche verifiche progettuali. La progettazione B.I.M. è indipendente dai software che si utilizzano. In caso sono state utilizzate 3 tipologie di programmi per ottenere indipendentemente senza vincoli: la modellazione dell'impalcato mediante elementi superficiali bidimensionali (elementi al continuo) ed elementi di tipo trave (teoria di De Saint Venant), con successivo calcolo strutturale sotto carico. Successivamente sono stati analizzati i giunti trave-trave, identificandoli tutti come giunti a completo ripristino. Infine, la terza tipologia è stata impiegata per incrementare il livello di dettaglio (LOD) degli elementi in struttura metallica e renderli gestibili in officina.

ABSTRACT

The choice to develop the thesis by adopting the B.I.M. (Building Information Modeling) methodology is due to the fact that the B.I.M. represents the innovative design method that in the coming years will find wide application in the design, both in the building and non-building field. This method, which has been replacing traditional design methods for some years now, has the advantage of incorporating in a single model all the design, operational and maintenance phases of the construction project. They will be displayed at 360 degrees by technicians thanks to the essential concept of "interoperability" between disciplines.

The first part of the thesis is dedicated to the design study of a viaduct with a compound structure. The viaduct has a total width of 13.5m, in the longitudinal direction it consists of three spans of +49.5, +70.0, +49.5m measured in axis to the supports. The deck is made of a mixed steel-concrete section and consists of two main metal beams with a constant height of 2.5m and a central pilot beam with a height of 0.45m. The structure is segmented by 8 different types of segments and has 4 types of transverse diaphragms, stiffened in the horizontal plane by upper and lower bracing with longitudinally variable distribution. The concrete slab is solidified to the extrados of the beams, by means of predalles, by means of shear connectors suitably welded to the upper flange of the main beams, in order to guarantee the torsional behaviour.

The second part of the thesis concerns the application of the B.I.M. methodology of the structure, used to increase the level of detail and verify the interoperability between the structural models in the specific design checks. The B.I.M. design is independent of the software used. In this case, 3 types of programs have been used to obtain independently without constraints: the deck modelling using two-dimensional surface elements (continuous elements) and beam type elements (De Saint Venant's theory), with subsequent structural calculation under load. Subsequently the beam-beam joints were analysed, identifying them all as fully restored bolted joints. Finally, the third type was used to increase the level of detail (LOD) of the metal structure elements and make them manageable in the workshop.

1. INTRODUCTION

The case study that we are going to analyse is a bridge with a metal carpentry deck, developed in three spans with a different linear curvature of each segment. This is due of geometrical and topography consideration, environment and landscape impositions. The site where the work is presented is an area of high seismicity.

The main thesis purpose is to verify the static and dynamic behaviour of each deck elements, with particular attention to the deformation and internal stress in order to apply the B.I.M methodology to check the local effects in some nodes and increase the level of details.

The research was carried out using the finite element model, approaching both continuous and linear elements. In fact, it was decided to produce the main beams of the deck as continuous elements and the relative transversal and horizontal reinforcements as linear one, following the De Saint Venant's theory. The choice to carry out a continuous analysis was dictated by the need to explore in detail the stress effects that are generated for each combination of applied load. These results give us the mastery and control to fully understand how the deck behaves. This does not preclude the creation of a synthetic model, which is a useful, intuitive and fast tool for carrying out specific checks of bending moment and shear forces, specially for traffic check .

1.1. DECK

The deck consists of 3 types of elements: longitudinal main beams, transverse diaphragms and upper and lower horizontal bracing. The truss segments are connected to each other by means of bolted fully restored joints.

In the longitudinal direction, the viaduct consists of 3 spans, the first and third of 49500mm and the second span of 70000mm. At the extrados of the beams is positioned a system of predalles connected bend over by a concrete slab. All set by means of shear connectors, suitably positioned and welded in the upper flanges of the main beams. The predalles and slab system, including the casting of concrete, has a total thickness of 280mm.

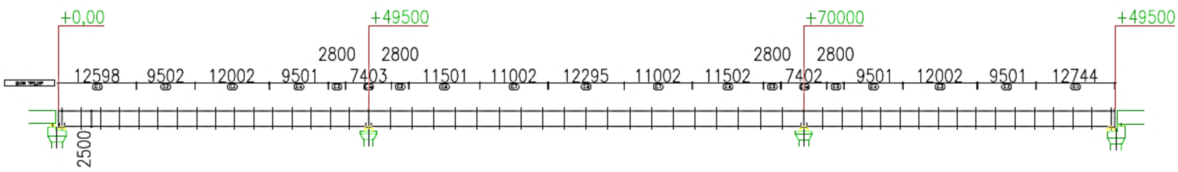

Figure 1:longitudinal profile of the deck. All measures are in mm.

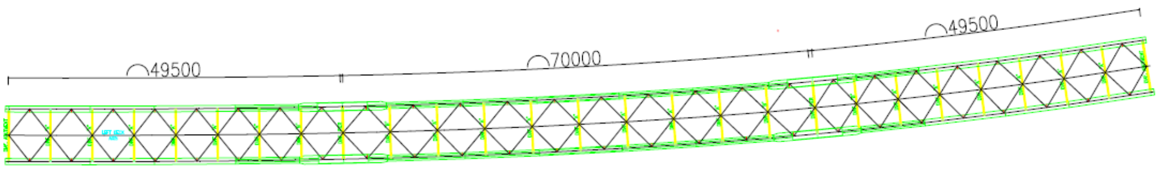

Figure 2: Longitudinal profile of lower braces. All measures are in mm.

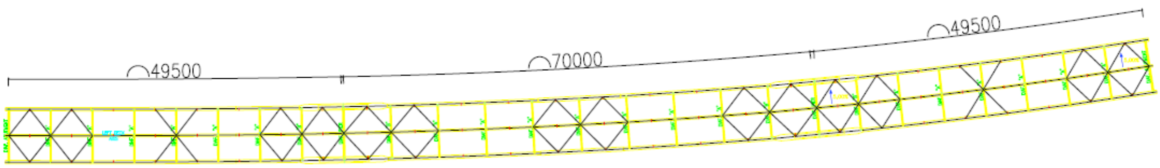

Figure 3: Longitudinal profile of upper braces. All measures are in mm.

1.2. CRITERIA FOR CALCULATION

The general safety criteria for the calculation actions and the characteristics of the materials have been taken in accordance with by Ministerial law (D.M. 17.01.2018) and 'Technical construction standards' (NTC2018) and its explanatory circular. According to the chapter §2.4 of NTC2018, the nominal project life of construction, $\mathbf{V_N}$ is generally defined as a number in which it is expected the durability, surely subjected to the necessary maintenance and keep it a specific performance level. In this case we deal with a construction with high performance levels; for this means that $\mathbf{V_N}$ is equal to 100 years. Of course, need to define as well the class of use and its coefficient, $\mathbf{C_U}$**.** As defined before, the construction of a strategic functions as the bridge, the class of use is the fourth, IV, with use's coefficient equivalent to 2.0. Summing it all up in briefly:

- V_N = 100 years.

- Class of use = IV.

- C_U = 2.0.

1.3 EXECUTION CLASS

The EN 1090 Introduce the meaning of execution classes, EXC, each with its own requirements set. So, basically the EXC is determined by the designer and owner of the construction works in order to apply to the whole structure, parts or specific details the circumstances activities and verification. The choose of EXC is made by taking into account the type of material, reliability of construction and potential failure.

Table 1: Execution class determination

EXC Determination							
Consequence class		CC1		CC2		CC3	
Service category		SC1	SC2	SC1	SC2	SC1	SC2
Production category	PC1	EXC1	EXC2	EXC2	EXC3	$\boxed{\text{EXC3}}$	EXC3
	PC2	EXC2	EXC2	EXC2	EXC3	EXC3	EXC4

The consequence class, CC, aims to define the differentiation of structural reliability for buildings, from the point of view of malfunction, according to the impact on the population, environment, human and social life. As far as the classes of service and production category, SC and PC, are concerned, they are necessary to take into account the structural behaviour of the work that will be designed and subsequently built. therefore, dissipative and non-dissipative behaviour will be distinguished from the load situation, i.e. whether we are in the dynamic or static case.

For this case, we assume: CC3, SC2 and PC1. Therefore, the work will be realized in the execution class of **EXC3.**

1.4. MATERIAL USED

1.4.1. REINFORCEMENT STEEL (C.A)

For carpentry steel, the density value is assumed to be $\gamma_s = 7850\,\frac{daN}{m^3}$

- The characteristic yielding strength $f_{syk} = 4500\,\frac{daN}{cm^2}$
- The characteristic failure strength $f_{suk} = 5400\,\frac{daN}{cm^2}$

SLU condition $f_{syd} = \frac{4500}{1{,}15} = 3913\,\frac{daN}{cm^2}$

SLE condition $f_{syd} = \frac{4500}{1{,}25} = 3600\,\frac{daN}{cm^2}$

1.4.2. STEELWORK

The steel used for the construction of the main deck is type S355, having the following technical characteristics:

- The characteristic yielding strength $f_{ayk} = 3550\,\frac{daN}{cm^2}$
- The characteristic failure strength $f_{auk} = 5100\,\frac{daN}{cm^2}$

SLU condition $f_{ayd} = \frac{3550}{1{,}05} = 3381\,\frac{daN}{cm^2}$

1.4.3. CONCRETE

Below are the main mechanical characteristics and properties defined in accordance with the reference standard (NTC2018). For concrete the following weight per unit volume is assumed: $\gamma_{CLS} = 2500\,\frac{daN}{m^3}$.

Table 2: Concrete parameters

Concrete class C30/37

Cubic characteristic compressive strength	$R_{ck} = 37$	$\frac{N}{mm^2}$
Cylindrical characteristic compressive strength	$f_{ck} = 30$	$\frac{N}{mm^2}$
Average compressive strength	$f_{cm} = 38$	$\frac{N}{mm^2}$
Cylindrical compressive strength design	$f_{cd} = 18.81$	$\frac{N}{mm^2}$
Average tensile strength	$f_{ctm} = 3.3$	$\frac{N}{mm^2}$
Characteristic tensile strength (fractile 5%)	$f_{ctk,5\%} = 2.33$	$\frac{N}{mm^2}$
Characteristic tensile strength (95% fractile)	$f_{ctk,95\%} = 4.33$	$\frac{N}{mm^2}$
Average tensile strength for bending	$f_{cfm} = 3.72$	$\frac{N}{mm^2}$
Design tensile strength	$f_{ctd} = 1.55$	$\frac{N}{mm^2}$

Tangential resistance characteristic	$f_{bk} = 4.88$	$\frac{N}{mm^2}$
Tangential adhesion strength steel-cls calculation	$f_{bd} = 3.25$	$\frac{N}{mm^2}$
Average instantaneous elastic modulus (secant)	$E_{cm} = 34330{,}8$	$\frac{N}{mm^2}$
Maximum compression stress in operation (rare combination)	$\sigma = 19.92$	$\frac{N}{mm^2}$
Maximum compressive stress in operation (almost perm. comb.)	$\sigma = 14{,}94$	$\frac{N}{mm^2}$
Exposure class	XF4	-
Maximum water/cement ratio	0,45	-
Minimum cement content	360	$\frac{kg}{mc}$
Consistency class (Slump)	S4	-
Maximum aggregate size	30	mm

1.5. EFFECTIVE WIDTH OF CONCRETE SLAB

As we know, the effective width of concrete slab positioned over the main beam should be evaluated as:

$$b_{eff} = b_0 + b_{e1} + b_{e2}$$

Where each term means:

b_0, distance between shear connectors.

$b_{ei} = \left(\frac{L_e}{8}; b_i - \frac{b_0}{2}\right)$, is the effective width of each side, left and right of composed cross-section.

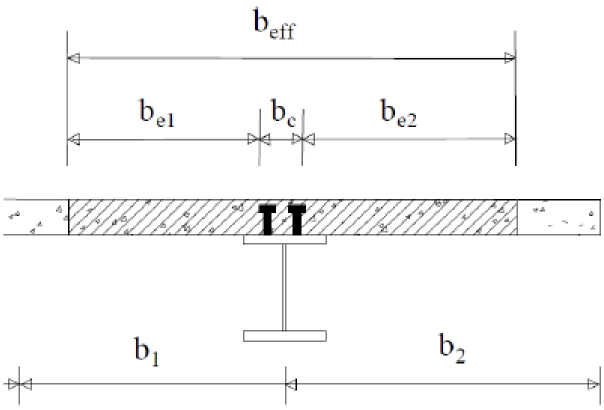

Figure 4:Effective width of the concrete slab

we remind you that the rules give us information on how to evaluate this effective width, according to the following scheme:

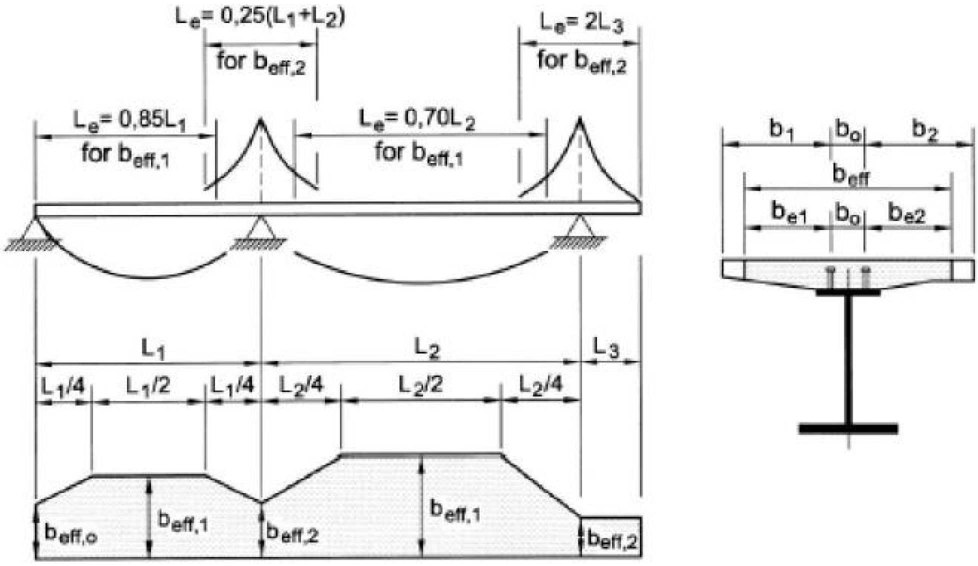

Figure 5:Determination of effective length.

For the end supports the formula becomes:

$$b_{eff} = b_0 + \beta_1 \cdot b_{e1} + \beta_2 \cdot b_{e2}$$

Where, $\beta_i = \left(0{,}55 + 0{,}025 \cdot \frac{L_e}{b_{ei}}\right) \leq 1{,}00$, is an end support coefficient.

Using the formulations expressed above, we can define the real widths for each span. It is obtained:

Table 3:Effective width for the external main longitudinal beams.

BEAM 1-3												
		QUOIN	**X [mm]**	**Le [mm]**	**b_0 [mm]**	**b_1 [mm]**	**b_2 [mm]**	**b_{e1} [mm]**	**b_{e2} [mm]**	**β_1**	**β_2**	**b_{eff} [mm]**
P1		0	0	42075	400	1950	1425	1750	1225	1	1	3375
	C1	12598	12598	42075	400	1950	1425	1750	1225	1	1	3375
	C2	9502	22100	42075	200	1950	1425	1850	1325	1	1	3375
	C3	12002	34102	42075	200	1950	1425	1850	1325	1	1	3375
	C4	9501	43603	42075	200	1950	1425	1850	1325	1	1	3375
	C5	2800	46403	29875	400	1950	1425	1750	1225	1	1	3375
P2	**C5a**	7403	53806	29875	400	1950	1425	1750	1225	1	1	3375
	C5	2800	56606	29875	400	1950	1425	1750	1225	1	1	3375
	C6	11501	68107	49000	200	1950	1425	1850	1325	1	1	3375
	C7	11002	79109	49000	200	1950	1425	1850	1325	1	1	3375
	C8	12295	91404	49000	200	1950	1425	1850	1325	1	1	3375
	C7	11002	102406	49000	200	1950	1425	1850	1325	1	1	3375
	C6	11502	113908	49000	200	1950	1425	1850	1325	1	1	3375
	C5	2800	116708	29875	400	1950	1425	1750	1225	1	1	3375
P3	**C5a**	7402	124110	29875	400	1950	1425	1750	1225	1	1	3375
	C5	2800	126910	29875	400	1950	1425	1750	1225	1	1	3375
	C4	9501	136411	42075	200	1950	1425	1850	1325	1	1	3375
	C3	12002	148413	42075	200	1950	1425	1850	1325	1	1	3375
	C2	9501	157914	42075	400	1950	1425	1750	1225	1	1	3375
P4	**C1**	12744	170658	42075	400	1950	1425	1750	1225	1	1	3375

Table 4: Effective width of pilot beam

PILOT BEAM												
		QUOIN	**X [mm]**	**Le [mm]**	**b_0 [mm]**	**b_1 [mm]**	**b_2 [mm]**	**b_{e1} [mm]**	**b_{e2} [mm]**	**β_1**	**β_2**	**b_{eff} [mm]**
P1		0	0	42075	0	1950	1950	1950	1950	1	1	3900
	C1	12598	12598	42075	0	1950	1950	1950	1950	1	1	3900
	C2	9502	22100	42075	0	1950	1950	1950	1950	1	1	3900
	C3	12002	34102	42075	0	1950	1950	1950	1950	1	1	3900
	C4	9501	43603	42075	0	1950	1950	1950	1950	1	1	3900
	C5	2800	46403	29875	0	1950	1950	1950	1950	1	1	3900
P2	**C5a**	7403	53806	29875	0	1950	1950	1950	1950	1	1	3900
	C5	2800	56606	29875	0	1950	1950	1950	1950	1	1	3900
	C6	11501	68107	49000	0	1950	1950	1950	1950	1	1	3900
	C7	11002	79109	49000	0	1950	1950	1950	1950	1	1	3900
	C8	12295	91404	49000	0	1950	1950	1950	1950	1	1	3900
	C7	11002	102406	49000	0	1950	1950	1950	1950	1	1	3900
	C6	11502	113908	49000	0	1950	1950	1950	1950	1	1	3900
	C5	2800	116708	29875	0	1950	1950	1950	1950	1	1	3900
P3	**C5a**	7402	124110	29875	0	1950	1950	1950	1950	1	1	3900
	C5	2800	126910	29875	0	1950	1950	1950	1950	1	1	3900
	C4	9501	136411	42075	0	1950	1950	1950	1950	1	1	3900
	C3	12002	148413	42075	0	1950	1950	1950	1950	1	1	3900
	C2	9501	157914	42075	0	1950	1950	1950	1950	1	1	3900
P4	**C1**	12744	170658	42075	0	1950	1950	1950	1950	1	1	3900

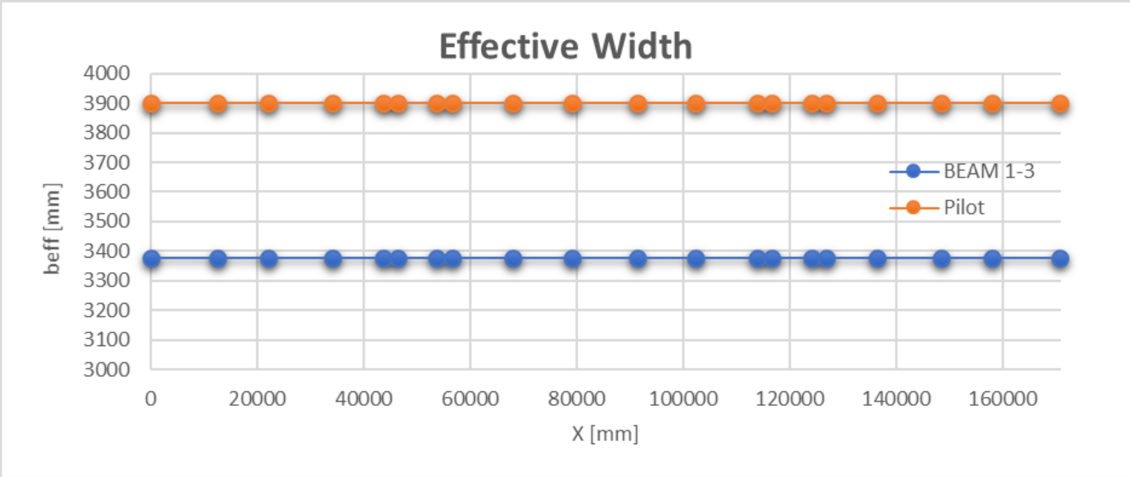

Figure 6:Final result of Effective width for each segment.

The beams 1 and 3 are the external and the Pilot one is the internal one, which is the smallest in term of cross-section.

1.6. GEOMETRICAL PROPERTIES

1.6.1. MAIN BEAMS

As said in the introduction, the deck is composed of 3 main beams. In the table below, all geometric characteristics for each beam segment that the viaduct is composed are described. We remember that the asymmetric beam option has been chosen for dependent load reasons.

Another important feature of the deck is the connection between the welded beams. They are joined by means of fully restored bolted joints, that is, bolted both on the web and in the flanges.

In order to overcome the negative moment present in the internal supports and the excessive deformation that characterizes the central span, as expressed in the table, a double flange upper and lower have been designed. They also have the function of increasing the moment of inertia and the general robustness of the beam.

Table 5: Main Beams properties.

MAIN BEAMS											
		C1	**C2**	**C3**	**C4**	**C5**	**C5a**	**C6**	**C7**	**C8**	**Pilot**
h	mm	2500	2500	2500	2500	2500	2500	2500	2500	2500	450
$\mathbf{b_{up}}$	mm	500	500	500	500	900	900	500	500	600	350
$\mathbf{b_{up,2}}$	mm	-	-	-	-	-	600	-	-	-	-
$\mathbf{b_{low}}$	mm	900	900	900	900	1250	1250	1250	900	900	350
$\mathbf{b_{low,2}}$	mm	-	-	-	400	400	900	600	400	600	-
$\mathbf{t_{f,Up}}$	mm	25	25	30	30	30	40	40	30	30	16
$\mathbf{t_{f,Up,2}}$	mm	-	-	-	-	-	40	-	-	-	-
$\mathbf{t_{f,Low}}$	mm	35	35	35	35	35	35	35	35	35	16
$\mathbf{t_{f,Low,2}}$	mm	-	-	-	20	25	35	25	35	35	-
$\mathbf{t_w}$	mm	18	16	16	22	28	28	22	16	16	10
$\mathbf{h_w}$	mm	2440	2440	2440	2415	2410	2360	2400	2400	2400	418
A	mm^2	87920,0	83040,0	83040,0	107630,0	148230,0	192330,0	114300,0	98900,0	108509,4	15700,0
$\mathbf{I_x}$	mm^4	1,68E+11	1,58E+11	1,58E+11	2,03E+11	3,07E+11	4,45E+11	2,32E+11	1,73E+11	1,90E+11	1,37E+09
$\mathbf{I_y}$	mm^4	2,39E+09	2,39E+09	2,39E+09	2,55E+09	7,66E+09	1,04E+10	2,68E+09	2,63E+09	3,27E+09	1,14E+08
Yg	mm	969,4	954,6	954,6	947,5	1006,4	1071,6	993,1	848,4	838,9	225

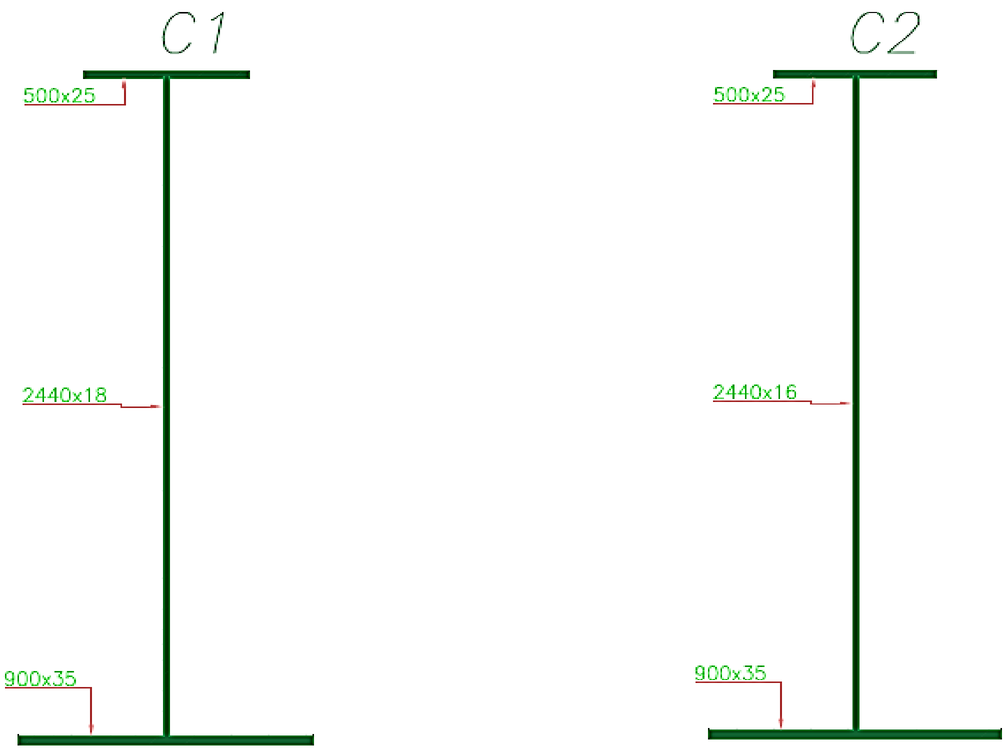

Figure 7: C1 and C2 cross-sections. Values in mm.

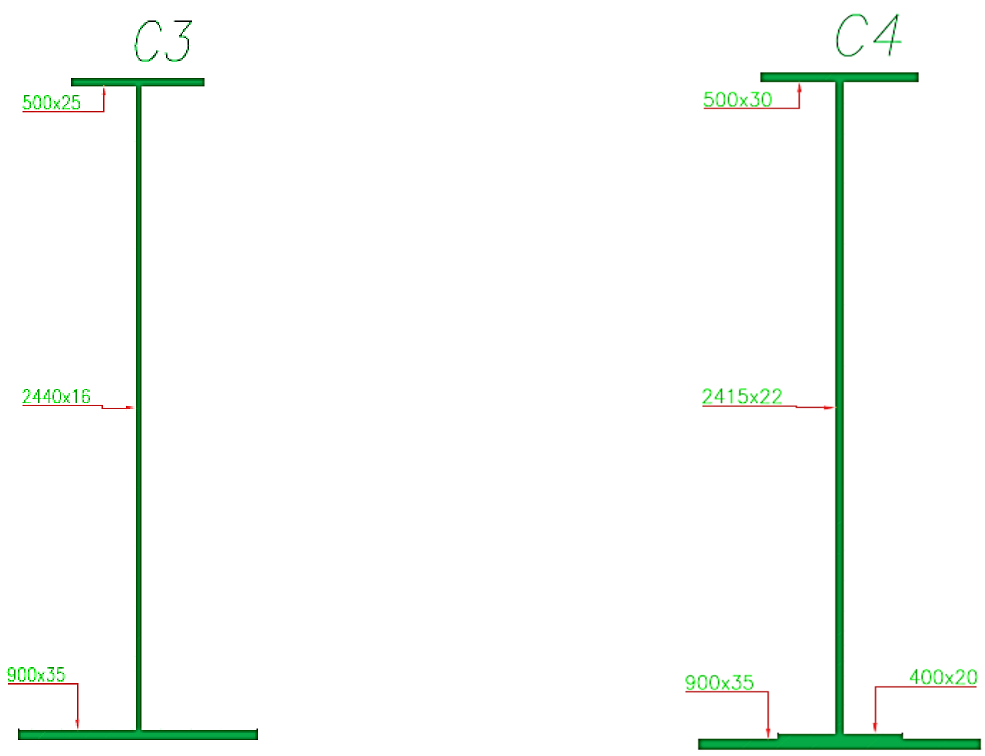

Figure 8: C3 and C4 cross-sections. Values in mm.

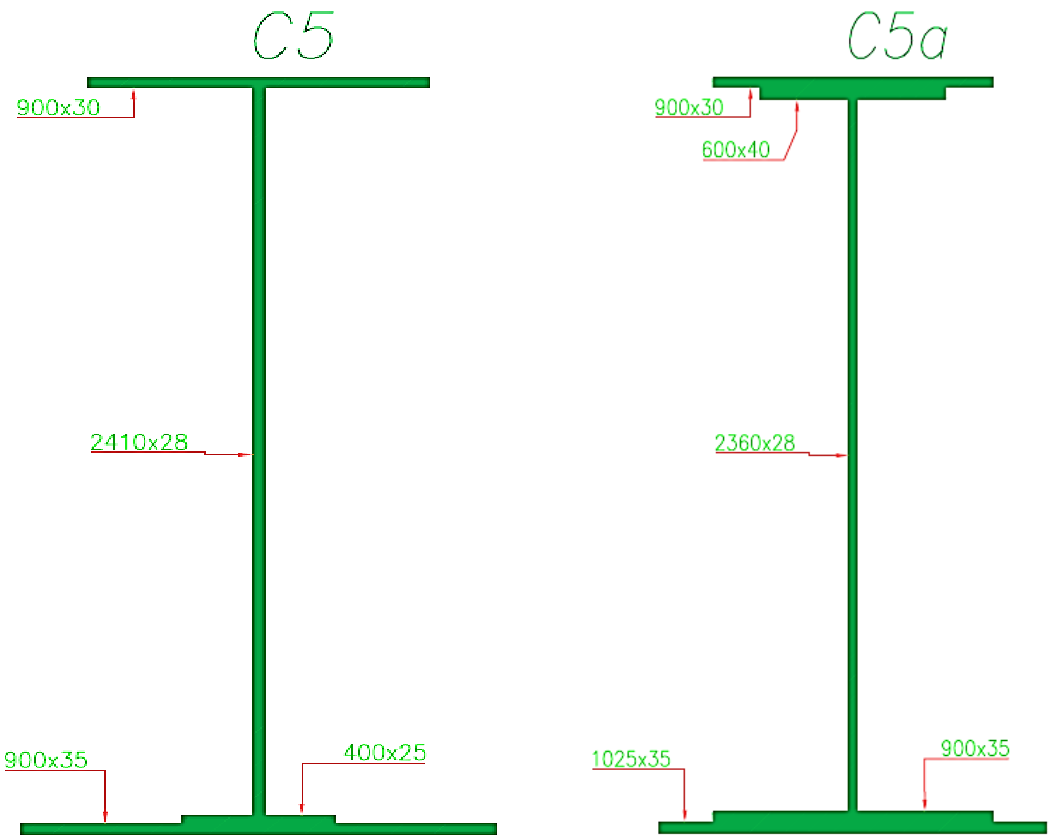

Figure 9: C5 and C5a cross-sections. Values in mm.

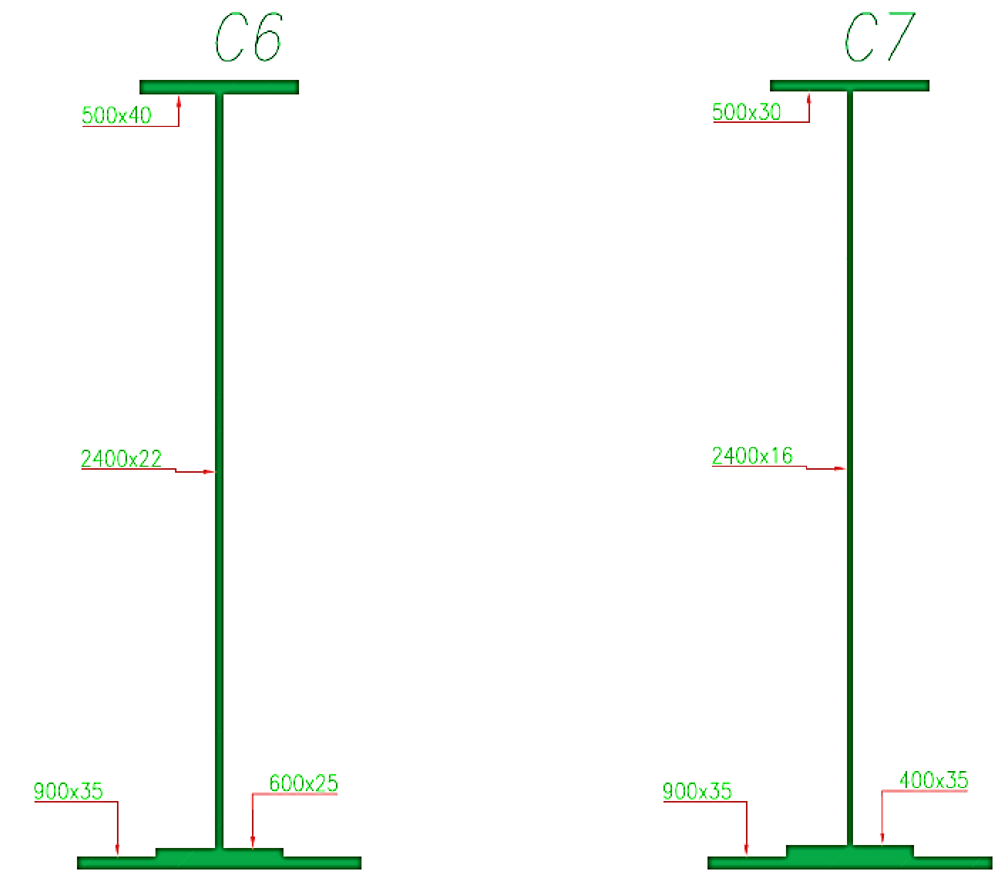

Figure 10: C6 and C7 cross-sections. Values in mm.

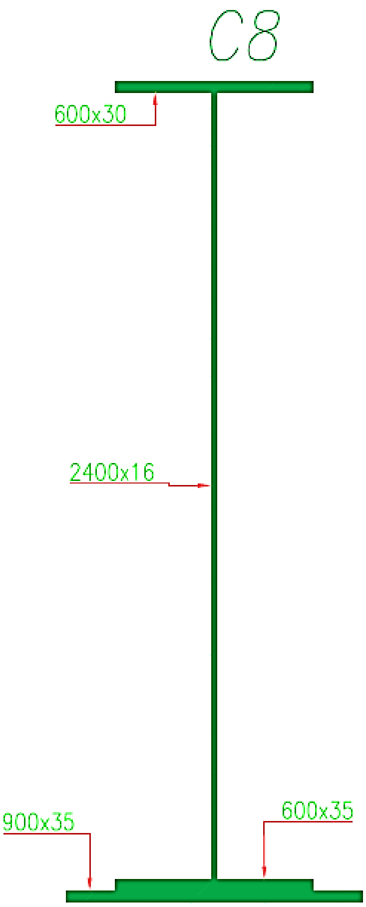

Figure 11:C8 cross-section. Values in mm.

1.6.2. DIAFRAGM

For the type of bridge being treated, i.e. a type of box deck with a mixed steel-concrete structure, transverse stiffeners called diaphragms are required. They have the function of stiffening the structure itself and reduce the buckling effect of the longitudinal main beams.

Describing in more detail, the longitudinal beams are joined by 27 diaphragms, having different spacing and following the same curvature of the deck in order to be orthogonal to them. They are made up of composite angular profiles, 2L composition, of equal sides. There are 4 configurations, as described in detail in the table below.

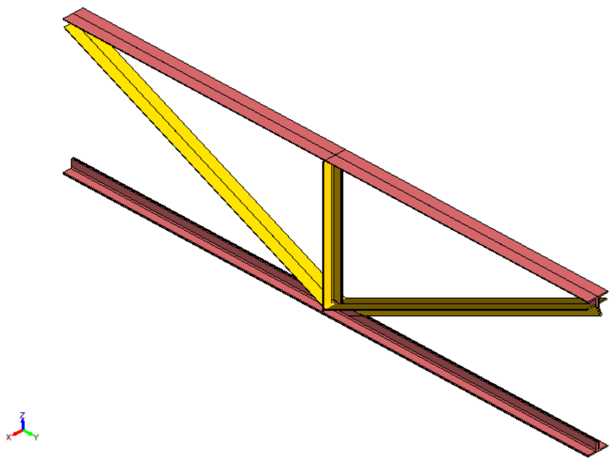

Figure 12: Diaphragm scheme in axonometric view. Source Advance design model.

Table 6: Diaphragm cross section type.

DIAPHRAGM TRUSS - A							
NAME	Weight	Dimension		Area	Moment of inertia	Modulus of flexural strenght	Radius of inertia
	p	b	s	A	$I_x=I_y$	$W_x=W_y$	$i_x=i_y$
-	kg/m	mm	mm	cm^2	cm^4	cm^3	cm
100x10	15,1	100	10	19,2	177	24,6	3,04
80x8	9,66	80	8	12,3	72,2	12,6	2,42
DIAPHRAGM TRUSS - B							
NAME	Weight	Dimension		Area	Moment of inertia	Modulus of flexural strenght	Radius of inertia
	p	b	s	A	$I_x=I_y$	$W_x=W_y$	$i_x=i_y$
-	kg/m	mm	mm	cm^2	cm^4	cm^3	cm
120x10	18,2	120	10	23,2	313	36	3,67
100x10	15,1	100	10	19,2	177	24,6	3,04
DIAPHRAGM TRUSS - ABUTMENT							
NAME	Weight	Dimension		Area	Moment of inertia	Modulus of flexural strenght	Radius of inertia
	p	b	s	A	$I_x=I_y$	$W_x=W_y$	$i_x=i_y$
-	kg/m	mm	mm	cm^2	cm^4	cm^3	cm
150x18	40,1	150	18	51	1050	98,7	4,54
150x15	33,8	150	15	43	898	83,5	4,57
DIAPHRAGM TRUSS - PIER							
NAME	Weight	Dimension		Area	Moment of inertia	Modulus of flexural strenght	Radius of inertia
	p	b	s	A	$I_x=I_y$	$W_x=W_y$	$i_x=i_y$
-	kg/m	mm	mm	cm^2	cm^4	cm^3	cm
180x18	48,6	180	18	61,9	1866	145	5,49
150x15	33,8	150	15	43	898	83,5	4,57

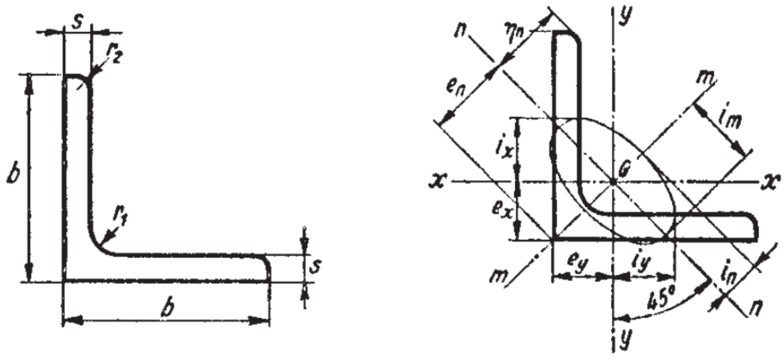

Figure 13: Cross section of one diaphragm element.

It should be noted that for each arrangement the first table reference refers to the horizontally positioned profiles; in opposite, the second profile refers to the diagonal and vertical elements. They are named on position function.

1.6.3. HORIZONTAL BRACE

The viaduct has an additional degree of stiffening from a torsional point of view and reduce the warping effect, i.e. the presence of bracing. They are arranged on two levels, upper and lower. The braces are connected to the main beams and the diaphragm system by means of bolted joints.

The beams themselves have the same composite of diaphragm elements.

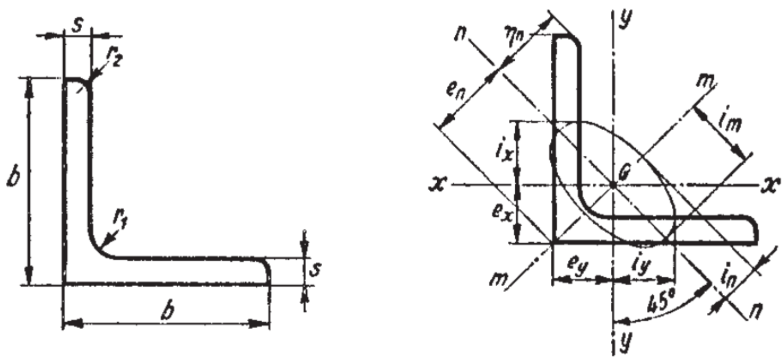

Figure 14: Cross section of single brace element.

Table 7: Brace girder cross-sectional properties.

BRACE GIRDER TRUSS															
NAME		**Weight**	**Dimension**				**Area**	**Moment of inertia**			**Modulus of flexural strenght**		**Radius of inertia**		
		p	**b**	**s**	**r_1**	**r_2**	**A**	**I_x=I_y**	**I_m**	**I_n**	**W_x=W_y**	**$W_{n,min}$**	**i_x=i_y**	**i_m**	**i_n**
	-	kg/m	mm	mm	mm	mm	cm^2	cm^4	cm^4	cm^4	cm^3	cm^3	cm	cm	cm
LOWER PLAN	**100x10**	15,1	100	10	12	6	19,2	177	280	73	24,6	18,3	3,04	3,82	1,95
UPPER PLAN	**80x8**	9,66	80	8	10	5	12,3	72,2	115	29,9	12,6	9,37	2,42	3,06	1,56

α	51,5	°
α	0,898845	rad

2. LOAD ANALYSIS

In this chapter we want to describe in detail the loads used and all the loading conditions to be carried out according to Eurocode and Italian technical standard.

2.1. DEAD LOAD - Deck

As previously defined in the characteristics of the materials used, the deck is made steel elements with a weight per unit volume of 7850 kg/m3. In the continuous analysis, each single element has been characterized by this mechanical characteristic.

The figure below conceptually represents the typical cross-section of the deck.

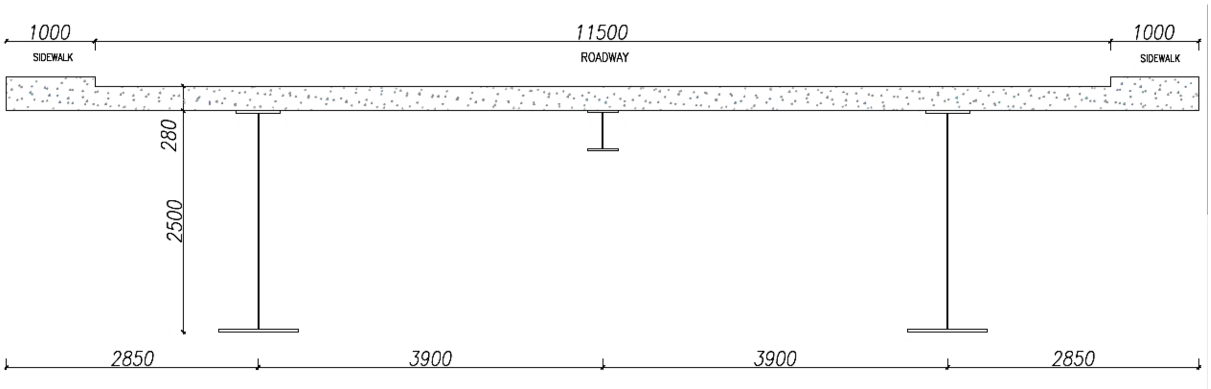

Figure 15: General Scheme of cross section. Values in mm.

2.2. PERMANENT LOADS

From the schematic section of the deck, we can see what permanent loading agents there might be. In a more explicit way, afterwards, we will analyse them.

$q_{predalles} = 0{,}06 \cdot 2500 = 150\ kg/m^2$. Predalles own weight.

$q_{c\_casting} = 0{,}22\ \cdot 2500 = 550\ kg/m^2$. Casting concrete over the predalles.

$q_{sidewalk} = 0{,}20 \cdot 2500 = 500\ kg/m^2$. Sidewalk for pedestrian.

$q_{binder} = 0{,}10 \cdot 1750 = 175\ kg/m^2$. Surface finishing layer.

The actions described above are to be considered as agents on the deck.

2.3. ACCIDENTAL LOADS

2.3.1. TRAFFIC LOADS

The EN 1991-2 standard defines traffic load models for the design of road bridges, footbridges and railway bridges. For the design of new bridges, EN 1991-2 is intended to be used, for direct application, together with the EN 1990-1999 Eurocodes. It is intended to be used as a design guide. They will have to be compared with the national reference guides.

As defined, EN 1991-2 specifies the imposed loads (models and representative values) associated with road traffic, pedestrian actions and rail traffic which include, when relevant, dynamic effects and centrifugal, braking and acceleration actions and accidental design actions.

For normal conditions of use (i.e. excluding any accidental situation), traffic and pedestrian loads should be considered as variable actions. The various representative values are:

- characteristic values.
- frequent values.
- quasi-permanent values.

The following table explains the bases for the calibration of the main load models for road bridges and footbridges.

Traffic Load Models	Characteristic values	Frequent values	Quasi-permanent values
Road bridges			
LM1 (4.3.2)	1000 year return period (or probability of exceedance of 5% in 50 years) for traffic on the main roads in Europe (α factors equal to 1, see 4.3.2).	1 week return period for traffic on the main roads in Europe (α factors equal to 1, see 4.3.2).	Calibration in accordance with definition given in EN 1990.
LM2 (4.3.3)	1000 year return period (or probability of exceedance of 5% in 50 years) for traffic on the main roads in Europe (β factor equal to 1, see 4.3.3).	1 week return period for traffic on the main roads in Europe (β factor equal to 1, see 4.3.3).	Not relevant
LM3 (4.3.4)	Set of nominal values. Basic values defined in annex A are derived from a synthesis based on various national regulations.	Not relevant	Not relevant
LM4 (4.3.5)	Nominal value deemed to represent the effects of a crowd. Defined with reference to existing national standards.	Not relevant	Not relevant
Footbridges			
Uniformly distributed load (5.3.2.1)	Nominal value deemed to represent the effects of a crowd. Defined with reference to existing national standards.	Equivalent static force calibrated on the basis of 2 pedestrians/m^2 (in the absence of particular dynamic behaviour). It can be considered, for footbridges in urban areas, as a load of 1 week return period.	Calibration in accordance with definition given in EN 1990.
Concentrated load (5.3.2.2)	Nominal value. Defined with reference to existing national standards.	Not relevant	Not relevant
Service vehicle (5.3.2.3)	Nominal value. As specified or given in 5.6.3.	Not relevant	Not relevant

Figure 16: Load model characteristics. Source: EN 1991-2.

The calculation model used for the design of this bridge is Load model 1, LM1, concentrated and uniformly distributed loads, which cover most of the effects of the traffic of lorries and cars. This model should be used for general and local verifications.

In order to describe the actions that are part of this variable action, there is a need to specify what the moving loads are. They are loads due to road traffic, such as vehicles, trucks, lorries and other special transport vehicles for industrial transport. Taking into account all the pedestrian and transient components that may arise during their lifetime.

2.3.2. DIVISIONS OF THE CARRIAGEWAY INTO NOTIONAL LANES

The carriageway area, its width "*w*", shall be considered as an entity between kerbs and/or any internal road limitations. National regulations shall describe what widths, if any, are required depending on the road class and type. The number of notional lanes should be defined in accordance with the principles used in the following table:

Carriageway width w	**Number of notional lanes**	**Width of a notional lane** w_l	**Width of the remaining area**
$w < 5{,}4$ m	$n_l = 1$	3 m	w - 3 m
$5{,}4 \text{ m} \leq w < 6$ m	$n_l = 2$	$\frac{w}{2}$	0
$6 \text{ m} \leq w$	$n_l = Int\left(\frac{w}{3}\right)$	3 m	$w - 3 \times n_l$
NOTE For example, for a carriageway width equal to 11m, $n_l = Int\left(\frac{w}{3}\right) = 3$, and the width of the remaining area is 11 - 3×3 = 2m.			

Figure 17: Classification of notional lanes. Source EN1991

In this case, the number of notional lanes are **3** with a remaining area such as 2,5m.

2.3.3. LOAD MODEL 1, LM1

Traffic loads are performed with the LM1 because give us general and local information and effect verifications. Basically, the model consists of 2 partial system:

- TS, tandem system. It is a double axle concentrated loads, each having a certain load declared form the rules.
- UDL, uniformed distributed loads, that has weight per square metre along the notional lane. The UDL should be applied only in the unfavourable position along the deck.

The following scheme represents the variable loads applied for traffic loads.

Table 8: Traffic loads

Position	TS [kN]	UDL [kN/m^2]
Notional lane 1	300	9,00
Notional lane 2	200	2,50
Notional lane 3	100	2,50
Remaining area	-	2,50

As previously defined in the description of the variable load, the calculation scheme is that of longitudinal main beams with lateral cantilevers, loaded from time-to-time by distributed loads of width 3.00 or variable according to the destination of use, arranged in such a way as to obtain and determine the heaviest loading conditions on the external beams or on the middle beam.

2.3.4. DISPERSAL OF CONCENTRATED LOADS

As already mentioned, concentrated loads are difficult to evaluate on continuous elements because they do not become part of De Sain Venant's theory, so they must be considered as special loads in order to be evaluated with special check.

The dispersal underneath the footprint of concentrated load should be taken at a spread to depth of 1/1, goes down on 45°. The picture shows briefly the local effect.

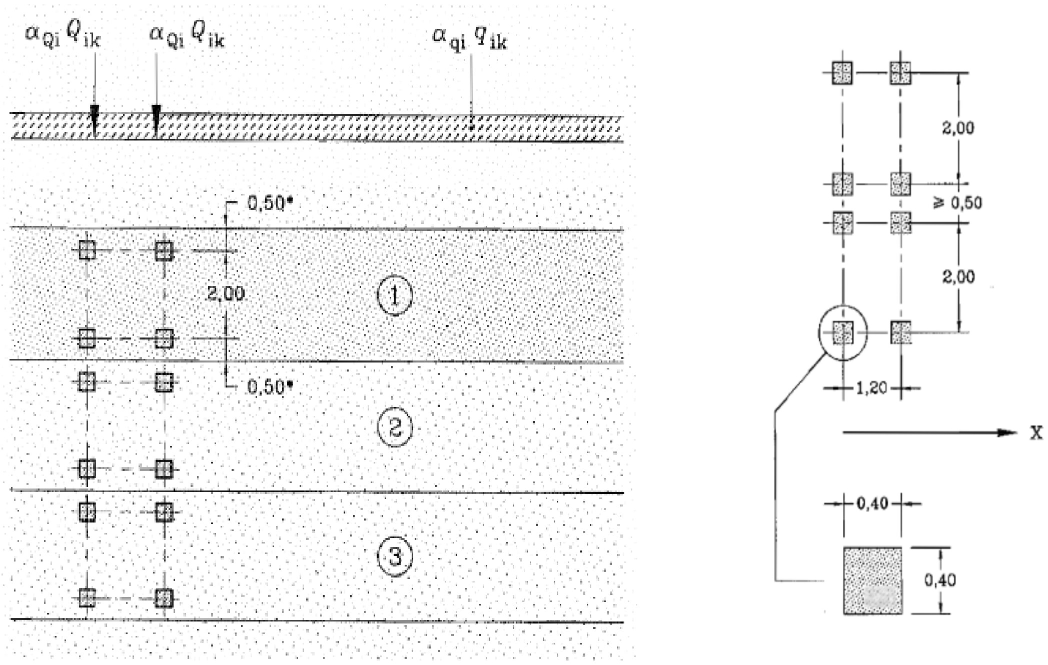

Figure 18: Geometrical condition of LM1. Source EN1991

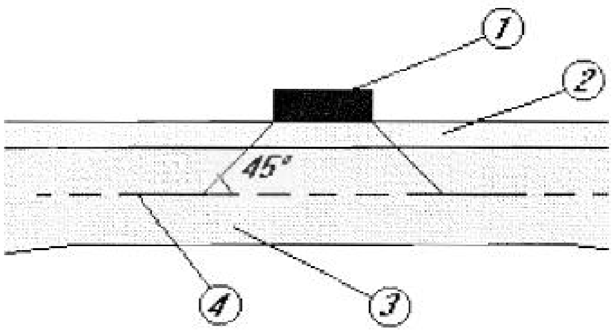

Figure 19: Representation of load distribution through the pavement. Source EN 1991

Where,

- 1, wheel contact pressure.
- 2, Pavement layer.
- 3, concrete slab.
- 4, middle surface of concrete slab.

2.3.5. HORIZONTAL FORCES – BRAKING, ACCELERATION & CENTRIFUGAL.

When carrying out verifications due to horizontal actions caused by moving elements, the characteristic component of this must be taken into account.

A braking force, Q_{lk}, should be taken as a longitudinal force acting at the surfacing level of carriageway. Its characteristic value is limited to 900kN for the total width of the bridge, and of course, shall be calculated as a fraction of the maximum of the vertical loads coming from the LM1 on notional lane 1. The formula is the following:

$$Q_{lk} = 0{,}6(2Q_{1k}) + 0{,}1 \cdot q_{1k} \cdot w \cdot L$$

Where,

- w, notional lane width.
- L, bridge length.
- q_{1k}, UDL corresponded.

The loads are taken from the table 9 below.

It must be remembered, assessing this force, it must be positioned along the notional lane axis.

Acceleration forces should be taken with the same magnitude of the braking one but in the opposite direction.

Centrifugal force. It is an action acting at the carriageway level, both transversely and in radial direction due to its vector components. In this specific case, it will not be included in the calculation of dynamic actions, since it is dependent on the radius of curvature of the road path.

2.4. VARIABLE LOADS

2.4.1. WIND EFFECTS

The wind action is calculated according to chapter §3.3 of NTC2018 in accordance with Eurocode EN 1991-1-4. This action is comparable to a static horizontal action, having orthogonal direction to the axis of the bridge and in projection in the vertical plane of the involved surfaces. In the case of a loaded bridge, the exposed surface increases due to the presence of moving vehicles. This surface is such as a continuous rectangular wall 3 metres above the road surface.

2.4.1.1. REFERENCE BASE VELOCITY

The basic reference speed v_b is the average value over 10 minutes, at 10 m above ground level on flat and homogeneous ground of exposure category II (see Table 3.3.II NTC2018), referring to a return period TR = 50 years. The table below expresses the reference values in order to evaluate the base velocity.

Zona	Descrizione	$v_{b,0}$ [m/s]	a_0 [m]	k_s
1	Valle d'Aosta, Piemonte, Lombardia, Trentino Alto Adige, Veneto, Friuli Venezia Giulia (con l'eccezione della provincia di Trieste)	25	1000	0,40
2	Emilia Romagna	25	750	0,45
3	Toscana, Marche, Umbria, Lazio, Abruzzo, Molise, Puglia, Campania, Basilicata, Calabria (esclusa la provincia di Reggio Calabria)	27	500	0,37
4	Sicilia e provincia di Reggio Calabria	28	500	0,36
5	Sardegna (zona a oriente della retta congiungente Capo Teulada con l'Isola di Maddalena)	28	750	0,40
6	Sardegna (zona a occidente della retta congiungente Capo Teulada con l'Isola di Maddalena)	28	500	0,36
7	Liguria	28	1000	0,54
8	Provincia di Trieste	30	1500	0,50
9	Isole (con l'eccezione di Sicilia e Sardegna) e mare aperto	31	500	0,32

Figure 20: Description of italian zone. Source NTC 2018.

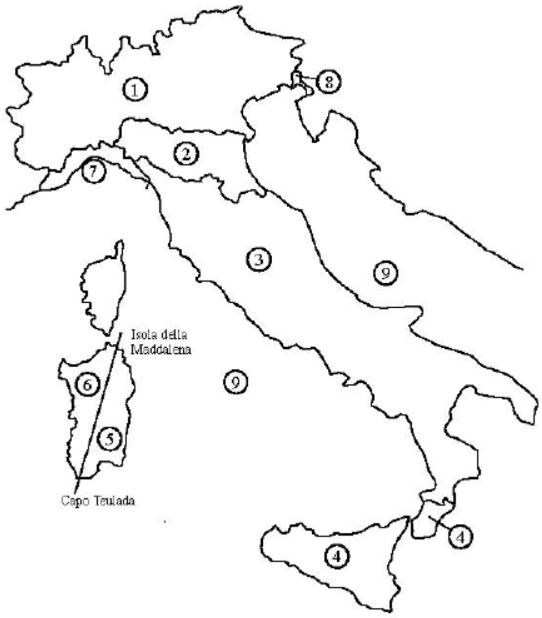

Figure 21:Geographical subdivision of base reference velocity. Source NTC2018

As defined in the technical standards:

$$v_b = v_{b0} \cdot c_a$$

$$\begin{cases} c_a = 1, & a_s \leq a_0 \\ c_a = 1 + k_s \left(\frac{a_s}{a_0} - 1 \right) & a_0 < a_s < 1500m \end{cases}$$

In this case, we obtain:

$v_b = 27 \cdot 1 = 27\ m/s$

2.4.1.2. WIND KINETIC PRESSURE

For the calculation of the reference kinetic pressure q_b (in N/m2), expression in the chapter §3.3.4 of the NTC18 has been used.

$$q_b = \frac{1}{2} \cdot \rho \cdot v_r^2 = 492{,}08\ N/m^2$$

Where *r* is the air standard density, equal to 1,25 kg/m^3; v_r is the reference velocity.

2.4.1.3. EXPOSURE COEFFICIENT

As described in the Italian technical standard, the exposure coefficient depends directly on the height on the ground of the point in question, the topography of the surrounding terrain. The parameters that become part of the calculation are stretches linked to tabular values present in the NTC18, such as according to the exposure class, ground roughness and distance from the sea, this coefficient can be easily calculated.

In accordance to the rule, the coefficient is evaluated as:

$$c_e(z) = k_r^2 \cdot c_t \cdot \ln\left(\frac{z}{z_0}\right) \cdot \left[7 + c_t \cdot \ln\left(\frac{z}{z_0}\right)\right], \quad z \geq z_0$$
$$c_e(z) = c_e(z_{min}), \quad z < z_{min}$$

.

Categoria di esposizione del sito	K_r	z_0 [m]	z_{min} [m]
I	0,17	0,01	2
II	0,19	0,05	4
III	0,20	0,10	5
IV	0,22	0,30	8
V	0,23	0,70	12

Figure 22: Exposure coefficients related to each case. Source NTC 2018.

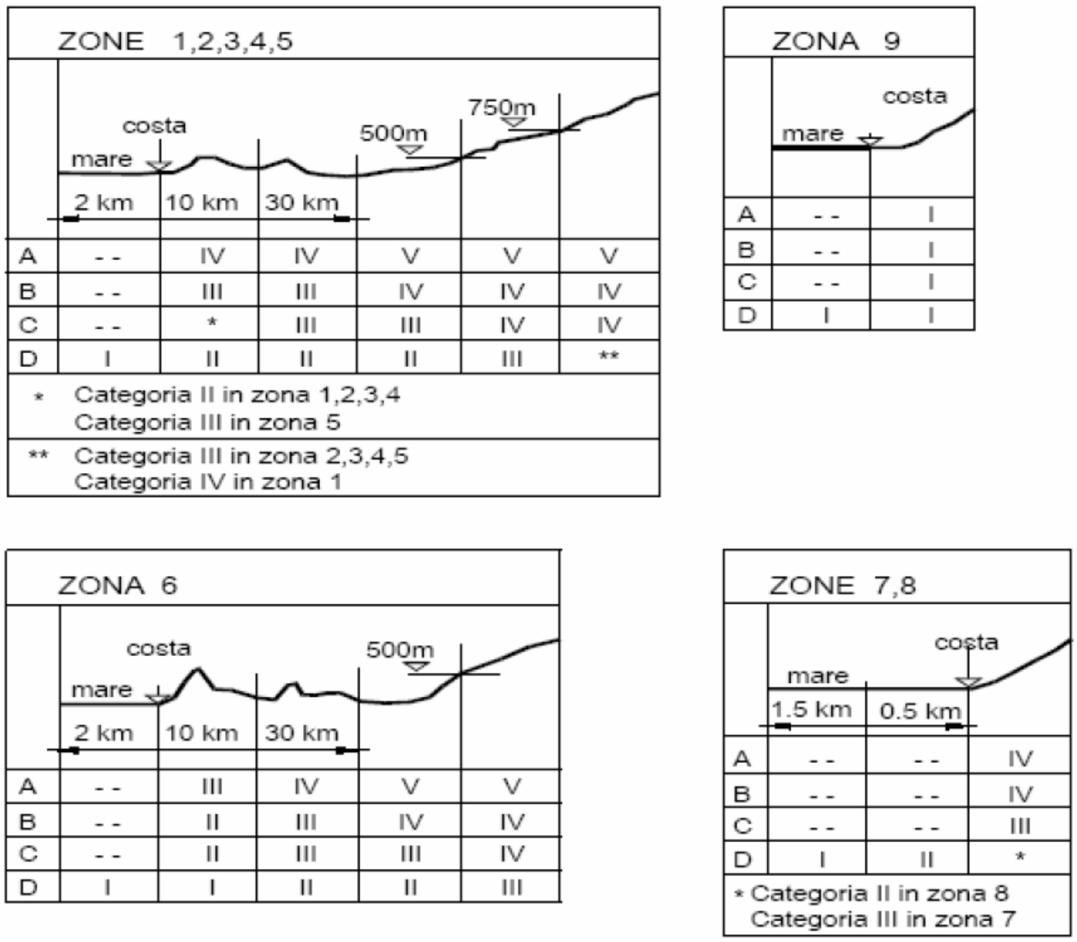

Figure 23: Definition of the class of exposure related to the case. Source NTC2018.

Subsequently, all the values used for the calculation will be described in a summary form.

Table 9: Reference Parameters of wind.

BASE REFERENCE VELOCITY		
a_s	238	m
a_0	500	m
k_s	0,37	-
$v_{b,0}$	27	m/s
c_a	1	
v_b	27	m/s
REFERENCE VELOCITY		
c_r	1,0392386	
T_R	100	anni
v_r	28,059441	m/s
KINETIC BASE PRESSURE		
q_r	492,08265	N/m2
EXPOSURE CLASS PARAMETERS		
Exposure class		IV
Roughness ground		B
k_r	0,22	m
z_0	0,3	m
z_{min}	8	-
c_t	1	-
c_d	1	-
φ	1	-
c_p	1,4	-
d	3900	mm
h	2500	mm
d/h	1,56	-
μ	0,2	-

Table 10:Geometrical values and pressures.

ELEVETION			EXPOSURE COEFFICCIENT					
Z_1	9,7	m	c_e	1,7625321	-			
Z_2	10,1	m	c_e	1,7898992	-			
Z_3	13,1	m	c_e	1,9698166	-			
LATERAL PRESSURE			**DOWNWIND**			**DOWNWIND**		
p_1	1214,2361	N/m2	p_1	242,84721	N/m2	p_1	48,569443	N/m2
p_2	1233,0897	N/m2	p_2	246,61793	N/m2	p_2	49,323586	N/m2
p_3	1357,0376	N/m2	p_3	271,40752	N/m2	p_3	54,281504	N/m2

2.4.1.4. LOCAL DYNAMIC EFFECT

In this chapter we are going to analyze the effects of local instability that could occur caused by the wind. They are directly related to the frequencies of the structure under examination and the average speed that the site is characteristic of it. First of all, the calculations for the determination of the frequency proper to the structure will be made and then the steps for the calculation of the frequency due to the effect of the wind action and control of the lock-in phenomenon will follow.

2.4.1.4.1. STRUCTURAL NATURAL FREQUENCY

In order to understand the own frequency of the structure, the natural one, the EN 1991-1-4 defines a guideline procedure for dynamic response of itself. The equation F.6 describes the fundamental vertical bending frequency of girder bridge from:

$$n_{1,B} = \frac{k^2}{2\pi L^2}\sqrt{\frac{EI_b}{m}}$$

Where,

- L is the main span length.
- E is the Young Modulus.
- I_b is the second moment inertia of cross-section at mid-span.
- m is the mass per unit length of full cross section.
- K is a dimensionless factor.

Other important fundamental frequency for what concern bridge case is the torsional frequency. The Eurocode defines approximately as:

$$n_{1,T} = n_{1,B}\sqrt{P_1(P_2 + P_3)}$$

Where,

P1, P2 and P3 are coefficients defined on Eurocode.

The following table are summarized the own frequency of structure.

Table 11: Bending and Torsional frequency of the bridge

BENDING FREQUENCY		
m_{perm}	1600	Kg/m^2
	1600	Kg/m
m_{dead}	1832,975	Kg/m
tot	3432,975	Kg/m
L	70	m
I_{tot}	0,78861	m^4
k	3,65	-
E	2,1E+11	N/m^2
ν_{1B}	**4,113128683**	**[Hz]**
T	0,243123928	s
ω	25,84354971	rad/s

TORSIONAL FREQUENCY		
b	13,5	m
r	2,083	m
ds/t	606,2461	-
A_{tot}	0,232399	m_2
J	0,000356	m^4
I_p	27838,31	m^6
P_1	22,47477	
P_2	0,023807	
P_3	3,93E-08	
ν_{1B}	**3,008679**	**[Hz]**
T	0,332372	s
ω	18,90409	rad/s

As we can see in tab.11, they represent the characteristic frequencies of the structure. Naturally, as previously mentioned, they will have to be compared with the dynamic action of the wind and then with modal analysis due to the earthquake, to avoid possible resonance scenarios.

2.4.1.4.2. WIND NATURAL FREQUENCY

In order to rigorously calculate the frequency of the wind in question, we have used Eurocode 1 part 4 and a study conducted by the National Research Council (CNR), a study carried out on 19 February 2009. Having no suitable software available to be able to discretize the action of the wind in order to visualize the effects that could occur in the structure, we made use of European legislation and national studies, as mentioned above.

The procedure that follows will be at the end the natural frequency of the wind on our structure and to evaluate the dynamic longitudinal coefficient, a dimensional quantity that has the effect of modifying the static actions calculated above.

The calculation procedure will indeed be as follows:

1) Assignment of the reference structural model. This means that we can choose if the structure has a vertical structure, horizontal structure or point structure. Of course, the structure has an horizontal behaviour and the reference height will be calculate as: $z_e = h_1 + \frac{h}{2} \geq z_{min}$.

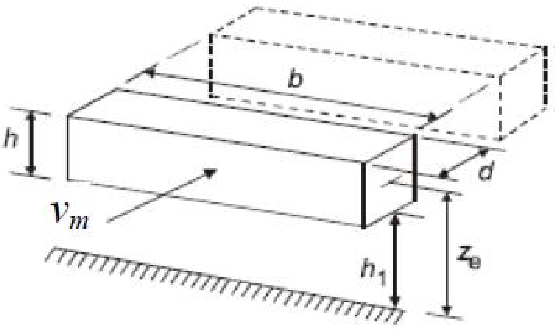

Figure 24:Structure description with respect to the structural model.

2) Assignment of geometric parameters b, h, z_e.
3) Assessment of average wind speed $v_m(z_e)$.
4) Assessment of integral turbulence scale $L_v(z_e)$. it should be evaluated by using a chart on function of exposure class.

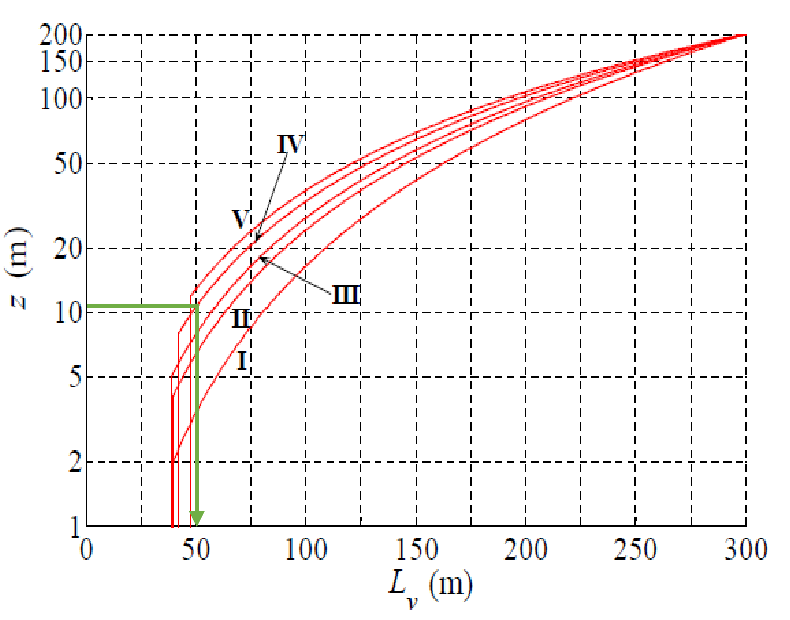

Figure 25:Integral turbulence scale chart.

5) Assessment of turbulence intensity $I_v(z_e)$. is easily using a chat to establish which is the correct value, as did with the turbulence scale.

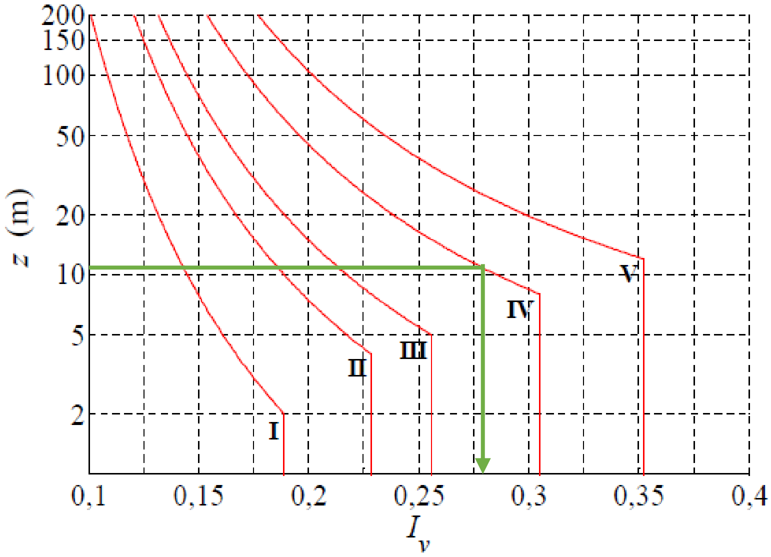

Figure 26:Turbulence intensity chart.

6) Assignment of dynamic parameters n_D and ξ_D. the first term represents the bending moment frequency of the structure. The second value is linked to the dumping factor of the bridge.
7) Assessment of quasi-static response factor B. Quasi-static response factor, which takes into account the not perfect correlation of agent pressure on the structure.
8) Evaluation of the S_D parameter. Critical relative damping ratio for the first mode of the structure in the direction of the wind.
9) Evaluation of expected frequency υ_D.
10) Evaluation of dynamic coefficient c_{dD}.

The following table, table 12, is used to summarize all values and easily check.

Table 12: Wind frequency

Isolated Deck		
g_D	3,898	-
$I_v\ (z_e)$	0,6	-
z_e	10,15	m
B^2	0,669	-
$R_D{}^2$	0,168	-
$L_v\ (z_e)$	50	m
S_D	0,037	-
v_m	28,059	m/s
n_D	4,113	Hz
n_h	3,459	Hz
n_b	7,916	Hz
R_h	0,247	-
R_b	0,118	-
ξ_D	0,005	-
υ_d	**1,843**	**Hz**
T	600	s
G_D	5,278	-
c_{dD}	**1,015**	**-**

2.4.1.4.3. VORTEX SEPARATION FROM STEEL BEAM

A body immersed in a fluid current produces, in general, a trail formed by trains of vortexes (von Karman's path) that detach alternately from the body itself with a frequency of $\mathbf{n_s}$ provided by Strouhal's number:

$$n_s = \frac{S_t \cdot v_m}{b}$$

Where,

- St, is a dimensionless parameter called Strouhal Number that is a function of body shape.

- v_m, is the reference velocity evaluated before.

- b, is the main transversal dimension.

This phenomenon is also called lock-in. it is an event of aeroelastic instability that occurs when the transverse vibration frequency of the body equals the detachment frequency of vortexes, which is linked directly the flutter phenomenon. In other words this phenomena happens when the vortex shedding frequency becomes close to a natural frequency of vibration of the structure. When this happens large and damaging vibrations can result because the excitement of the first mode is maximum when the detachment of the vortices is resonant in the middle of the span.

It is also helpful assess the effects of the detachment of the vortices for all critical speeds, in order to satisfy this relationship:

$$v_{cr} = \frac{n_T \cdot b}{S_t} < v_m$$

Table 13: Strouhal parameters

St	0,140	-
$\mathbf{v_m}$	28,059	m/s
b	1250	mm
$\mathbf{n_s}$	**3,143**	**Hz**
$\mathbf{n_T}$	3,009	Hz
$\mathbf{v_{crit}}$	26,863	m/s

2.5. SEISMIC LOAD

2.5.1. DETERMINATION OF SEISMIC ACTION

Design seismic actions are defined from the basic seismic hazard of the construction site. It constitutes the primary knowledge element for the determination of seismic actions. The seismic hazard is defined in terms of maximum expected horizontal acceleration a_g in free field conditions on a rigid reference site with horizontal topographic surface, as well as in terms of ordinates of the acceleration elastic response spectrum corresponding to *Se (T),* with reference to probability of P_{VR} exceeding, in the period V_R .

2.5.1.1. NOMINAL LIFE

The nominal life of a structural work is understood as the number of years in which the structure, provided that it is subject to routine maintenance, it must be able to be used for its intended purpose. The nominal life is therefore assumed to be V_N = 100 years.

2.5.1.2. CLASS OF USE

In the presence of seismic actions, with reference to the consequences of an interruption of operations or a possible collapse, the constructions are divided into classes of use. In this case, reference is made to Class IV.

The coefficient of use is therefore assumed to be c_U = 2,0. The following table sum up the general characteristics.

VITA NOMINALE V_N	VALORI DI V_R			
	CLASSE D'USO			
	I	II	III	IV
≤ 10	35	35	35	35
≥ 50	≥ 35	≥ 50	≥ 75	≥ 100
≥ 100	≥ 70	≥ 100	≥ 150	≥ 200

Figure 27: Reference life determination. Source NTC 2018

The seismic actions related to each construction are evaluated in relation to a reference period V_R which is obtained, for each type of construction, by multiplying the nominal life V_N by the use coefficient c_U. This coefficient is a function of the class of use.

$$V_R = V_N \cdot c_U = 100 \cdot 2 = 200\ years$$

2.5.1.3. LIMIT STATES AND THEIR PROBABILITY

With regard to seismic actions, the limit states, both service and ultimate, are identified by referring to the performance of the construction as a whole, including structural and non-structural.

The serviceability limit states, SLS, are:

- Operating Limit State (SLO): after the earthquake, the construction, including structural elements, non-structural elements and equipment relevant to its function, must not suffer significant damage and interruptions in use;
- Damage Limit State (SLD): following the earthquake, the construction as a whole, including structural and non-structural elements, suffers damage such as to avoid risk to users and not to significantly compromise the capacity of resistance and stiffness against vertical and horizontal actions, remaining immediately usable even if part of the equipment is interrupted.

The ultimate limit states, ULS, are:

- Life Safety Limit State (SLV): as a consequence of the earthquake, the construction is subject to breakage and collapse of non-structural and engineering components and significant damage to the structural components to which is associated a significant loss of rigidity with respect to horizontal actions; the construction instead retains a part resistance and stiffness for vertical actions and a safety margin against collapse for horizontal seismic actions;
- Collapse Prevention Limit State (SLC): after the earthquake, the construction suffers serious breakage and collapse of non-structural and plant components and very serious damage to structural components; the construction still retains a safety margin for vertical actions and a small safety margin against collapse for horizontal seismic actions. of the horizontal action collapse.

The probability of exceeding, P_{VR}, in the reference period, to which reference should be made in order to identify the seismic action acting in each of the limit states considered, are reported in the next table.

Table 14: Limit state probability

Limit State		Probability of exceeding
Serviceability Limit State	SLO	81%
	SLD	63%
Ultimate Limit State	SLV	10%
	SLC	5%

2.5.1.4. DESIGN PARAMETERS

The spectral shapes are defined, for each of the probabilities of being exceeded during the P_{VR} reference period, from the values of the following parameters:

- a_g, is the design ground acceleration.
- F_0, maximum value of the spectrum amplification factor under horizontal acceleration.
- T_C^*, reference value for the determination of the start period of the constant velocity section of the spectrum under horizontal acceleration.

The spectral shapes predicted by NTCs are characterised by selected exceedance probabilities and reference life. To this purpose, they must be fixed:

- V_R, reference life of the construction;
- P_{VR}, the probabilities of exceedance in the reference life associated with the limit states considered and identify the corresponding seismic actions from the available seismic hazard data.

For this reason, it is convenient to use the return period as a parameter characterizing the seismic hazard. of seismic action T_R, expressed in years. Fixed the V_R reference life, the two parameters T_R and P_{VR} are immediately expressible, one in relation to the other, by using the following expression:

$$T_R = -\frac{V_R}{\ln(1 - P_{VR})}$$

The values of the seismic hazard parameters are shown in the following table. The values have been elaborated by the "National Institute of Geophysics and Volcanology". As defined in the introductory description of the report, the site is located in a highly seismic zone, classified as zone 1 according to the "general criteria for the identification of seismic zones and the updating of their lists".

In order to define the design seismic action and in compliance with Italian technical regulations, the simplified approach of the analysis was adopted, using the elastic response spectrum of the horizontal component, which is based on the identification of reference subsoil categories, topographical conditions and probability of exceedance mentioned above.

The elastic components are summarized in the following expressions:

$$0 \le T \le T_B \qquad S_e(T) = a_g \cdot S \cdot \eta \cdot F_0 \cdot \left[\frac{T}{T_B} + \frac{1}{\eta \cdot F_0} \cdot \left(1 - \frac{T}{T_B}\right)\right].$$

$$T_B \le T \le T_C \qquad S_e(T) = a_g \cdot S \cdot \eta \cdot F_0.$$

$$T_C \le T \le T_D \qquad S_e(T) = a_g \cdot S \cdot \eta \cdot F_0 \cdot \left(\frac{T_C}{T}\right).$$

$$T_D \le T \qquad S_e(T) = a_g \cdot S \cdot \eta \cdot F_0 \cdot \left(\frac{T_C \cdot T_D}{T^2}\right).$$

Where,

- S, it is the coefficient that takes into account the subsoil category and topographical conditions by means of the following report: $S = S_S \cdot S_T$. S_S the stratigraphic amplification coefficient and S_T the topographic amplification coefficient shown in the following tables.
- η, is the factor that alters the elastic spectrum for conventional viscous damping coefficients ξ other than 5%, by the relationship: $\eta = \sqrt{10/(5+\xi)} \ge 0{,}55$, where ξ (expressed as a percentage) it is assessed on the basis of materials, structural type and foundation soil;
- F_0, is the factor that quantifies the maximum spectral amplification, on a rigid horizontal reference site, and has a minimum value of 2.2;
- T_0, is the period corresponding to the beginning of the period at constant speed of the spectrum, given by: $T_C = C_c \cdot T_C^*$;
- T_B, the period corresponding to the beginning of the constant accelerating section of the spectrum, given by the ratio $T_C = T_C/3$;
- T_D, is the period corresponding to the beginning of the constant-shift section of the spectrum, expressed in seconds through the relationship: $T_C = 4{,}0 \cdot \frac{a_g}{g} + 1{,}6$.

Figure 28:Definition of soil category

Categoria sottosuolo	S_S	C_C
A	1,00	1,00
B	$1{,}00 \le 1{,}40 - 0{,}40 \cdot F_o \cdot \frac{a_g}{g} \le 1{,}20$	$1{,}10 \cdot (T_C^*)^{-0{,}20}$
C	$1{,}00 \le 1{,}70 - 0{,}60 \cdot F_o \cdot \frac{a_g}{g} \le 1{,}50$	$1{,}05 \cdot (T_C^*)^{-0{,}33}$
D	$0{,}90 \le 2{,}40 - 1{,}50 \cdot F_o \cdot \frac{a_g}{g} \le 1{,}80$	$1{,}25 \cdot (T_C^*)^{-0{,}50}$
E	$1{,}00 \le 2{,}00 - 1{,}10 \cdot F_o \cdot \frac{a_g}{g} \le 1{,}60$	$1{,}15 \cdot (T_C^*)^{-0{,}40}$

Figure 29: Topographic definition

Categoria topografica	Ubicazione dell'opera o dell'intervento	S_T
T1	-	1,0
T2	In corrispondenza della sommità del pendio	1,2
T3	In corrispondenza della cresta di un rilievo con pendenza media minore o uguale a 30°	1,2
T4	In corrispondenza della cresta di un rilievo con pendenza media maggiore di 30°	1,4

Table 15: Limit state parameters and values

Limit State	Probability of exceeding	T_R	a_g	F_0	T_C^*
		[years]	[g]	[-]	[sec]
SLO	81%	120	0,145	2,343	0,331
SLD	63%	201	0,186	2,374	0,346
SLV	10%	1898	0,463	2,505	0,435
SLC	5%	2475	0,511	2,521	0,447

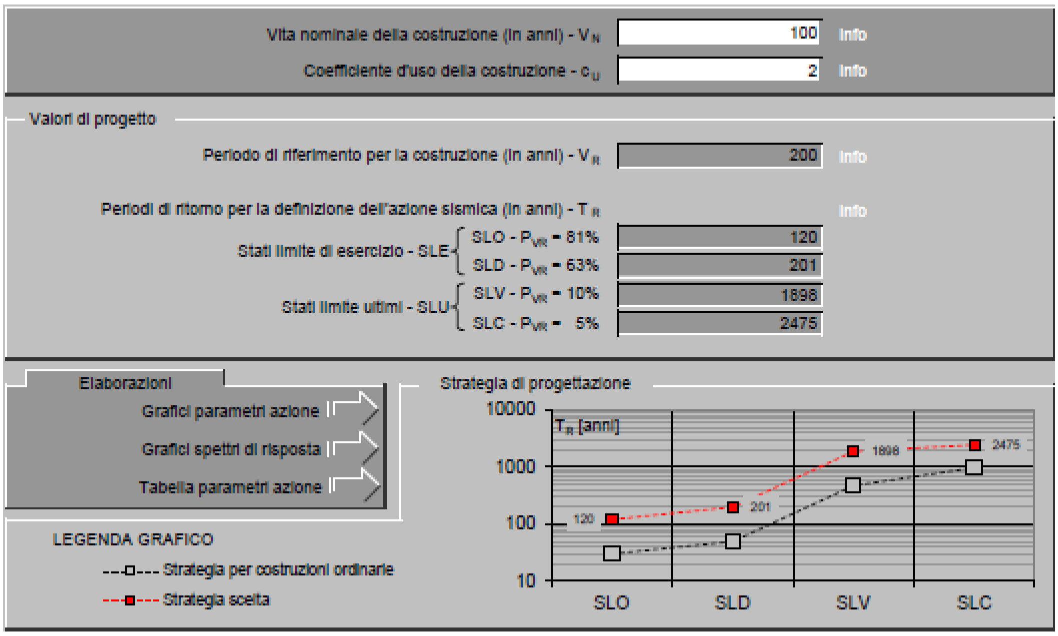

Figure 30:Reference life determination.

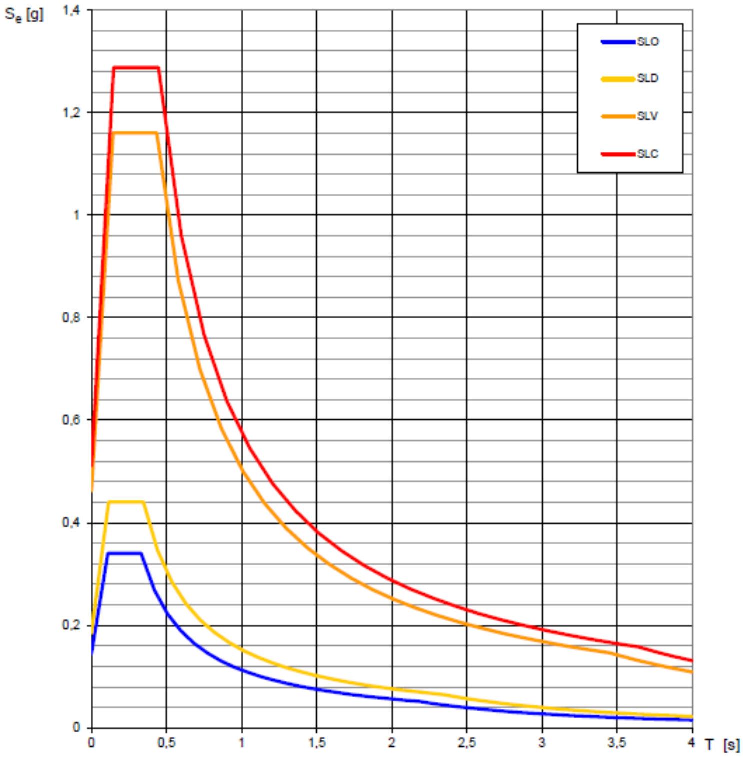

Figure 31:Limit state curves.

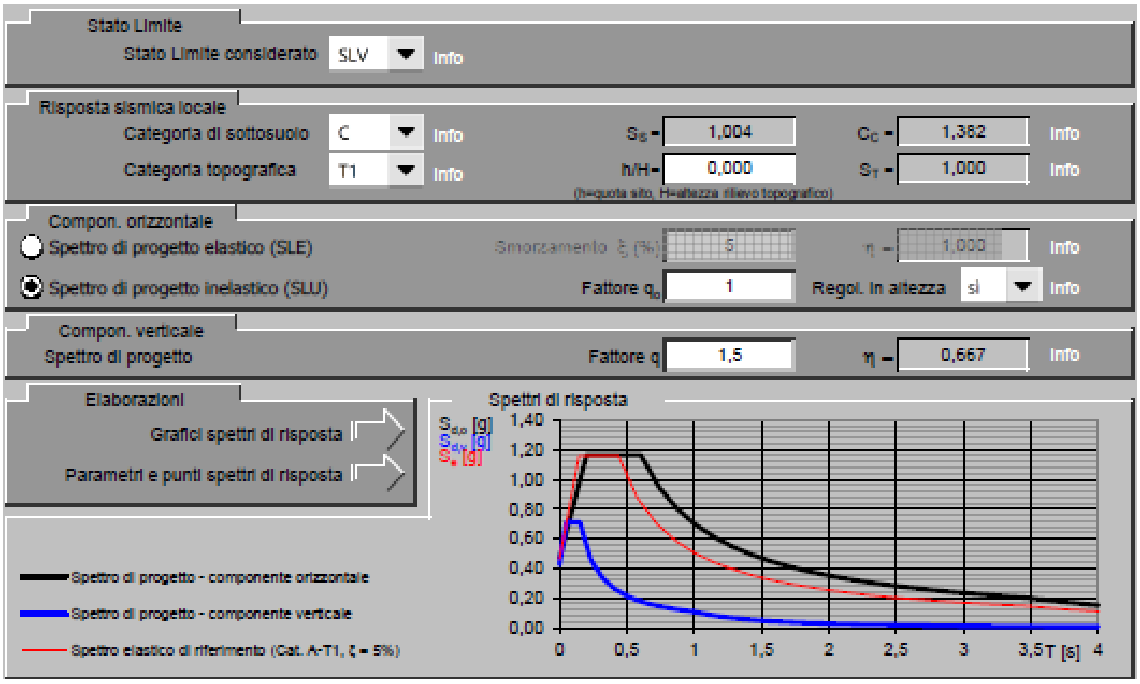

Figure 32: Limit state parameters

Table 16: Design seismic parameters

Design Parameters	a_g $[g]$	F_0 $[s]$	T_C^* $[s]$	T_B $[s]$	T_C $[s]$	T_D $[s]$
	0.463	2.505	0.435	0.201	0.602	3.453

2.6. TEMPERATURE EFFECT

Daily and seasonal variations in outdoor temperature, sun radiation and convection lead to variations in the temperature distribution in the individual structural elements.

The severity of thermal actions is generally influenced by several factors, such as the climatic conditions of the site, exposure, the overall mass of the structure and the possible presence of insulating non-structural elements.

2.6.1. UNIFORM THERMAL VARIATION

The uniform temperature component depends of course on the minimum and maximum temperature which the bridge achieves. Following the European standard EN 1991-1-5, which describes that the temperature variation of a composite deck, i.e. of type 2, the maximum and minimum values can be defined as:

$$T_{e,max} = T_{max} + 4 = 41{,}5 + 4 = 45{,}5°C.$$

$$T_{e,min} = T_{min} + 4 = -4{,}1 + 4 = 0{,}1°C.$$

2.7. SHRINKAGE EFFECTS

Shrinkage and creep, as we know, are time-dependent characteristics of concrete. The effects could generally be taken into account for the verification of SLS. Of course, when they are considered, should be evaluated under the quasi-permanent combination of the design situation considered.

The parameters for axial deformation due to shrinkage of the concrete slab are indicated and described in Eurocode 2, EN 1992-1.

Now, the parameters are evaluated.

$A_c = concrete\ cross - sectional\ area = 3999999{,}99\ mm^2.$

$u = exposed\ perimeter = 28000{,}00\ mm.$

$h_0 = notional\ size = 2 \cdot \frac{A_c}{u} = 285{,}71 mm.$

$E_{cm} = Young\ modulus\ of\ concrete = 22000\ \left(\frac{f_{cm}}{10}\right)^{0,3} = 34330{,}8\ N/mm^2.$

$E_s = Young\ modulus\ of\ steel = 210000\ N/mm^2.$

2.7.1. RHEOLOGIC EFFECTS

Rheologic effects depend on the ambient humidity, dimension of the element and concrete composition, such as defined above. Creep is also influence by the degree of maturation of concrete when the load will be applied and of course on its magnitude.

It is useful introduce a creep coefficient $\varphi(t, t_0)$ related to concrete young modulus tangent, $E_c = 1{,}05\ E_{cm}$.

2.7.2. TIME AND ENVIRONMENT

$t_0 = 2\ d$. Represents the beginning of drying creep

$t_0 = 28\ d$. It defines the day of permanent loads application

$t_0 = 2\ d$. It defines the day of shrinkage application

$t = V_N = 100\ y = 36525\ d.$

In this specific analysis will be considered a relative humidity equal to 75%, $RH = 75\%$.

2.7.3. ELASTIC MODULUS

The phenomenon of viscosity has the effect of increasing deformation over time caused by a load kept constant for a long period. However, the viscous deformations occur without changing the stress state. The phenomenon of viscosity is assimilated to a fictitious decrease in the modulus of elasticity of the concrete over time (in reality, the mechanical characteristics of the concrete improve over time so that the modulus of elasticity, understood as the ratio of stress to deformation under a short duration load, increases over time). The modulus of elasticity therefore goes from the initial value at the instant t_0 of application of the load to the conventional final value at time t.

So, the variation of the modulus of elasticity with time can be estimated by:

$$E_{cm}(t) = \left(\frac{f_{cm}(t)}{f_{cm}}\right)^{0,3} E_{cm}$$

2.7.4. SHRINKAGE EVALUATION

The total shrinkage strain is composed of two elements, the drying and autogenous strain. The drying shrinkage develops slowly, since it starts the migration of water through the concrete. Instead, the autogenous shrinkage strain develops during the hardening phase of concrete, after some days of concrete casting. The last one is a linear function of concrete strength and should be considered when the new added concrete is cast against hardened one.

$$\varepsilon_{cs} = \varepsilon_{cd} + \varepsilon_{ca}$$

Where,

ε_{cs}, is the total shrinkage strain.

ε_{cd}, is the drying shrinkage strain.

ε_{ca}, is the autogenous shrinkage strain.

The development of the drying shrinkage strain follows from:

$$\varepsilon_{cd}(t) = \beta_{ds}(t, t_s) \cdot k_h \cdot \varepsilon_{cd,0}$$

Where,

k_h is a coefficient depending on the notional size. This case it is 0,78.

t is the age of concrete at the moment considered.

t_s is the age of the concrete at the beginning of drying shrinkage.

The autogenous shrinkage strain is defined as:

$$\varepsilon_{ca} = \beta_{as}(t)\varepsilon_{ca}(\infty)$$

Table 17:Shrinkage parameters

Time t=2 days

COMPRESSIVE STRENGTH AT Time t		
fcm	38,00	N/mm2
b_cc	0,35	
t	2,00	days
fcm(t)	13,41	N/mm2
TENSILE STRENGTH		
fctm	3,33	N/mm2
a	1,00	
t	2,00	
b_cc	0,35	
fctm(t)	1,18	N/mm2
VARIATION OF YOUNG MODULUS		
Ecm	34330,80	N/mm2
b_cc	0,35	
t	2,00	days
fcm(t)	13,41	N/mm2
Ecm(t)	25115,72	N/mm2
DRYING SHRINKAGE		
e_cd0	0,35	‰
k_h	0,78	-
b_ds		-
t_s	2,00	days
t	2,00	days
h_0	285,71	mm
e_cd		‰
AUTOGENOUS SHRINKAGE		
e_ca (∞)	0,05	‰
b_as	0,25	-
t	2,00	days
e_ca (t)	0,01	‰

Time t=7 days

COMPRESSIVE STRENGTH AT Time t		
fcm	38,00	N/mm2
b_cc	0,68	
t	7,00	days
fcm(t)	25,99	N/mm2
TENSILE STRENGTH		
fctm	3,33	N/mm2
a	1,00	
t	7,00	
b_cc	0,68	
fctm(t)	2,28	N/mm2
VARIATION OF YOUNG MODULUS		
Ecm	34330,80	N/mm2
b_cc	0,68	
t	7,00	days
fcm(t)	25,99	N/mm2
Ecm(t)	30631,93	N/mm2
DRYING SHRINKAGE		
e_cd0	0,35	‰
k_h	0,78	-
b_ds	2,17	-
t_s	2,00	days
t	7,00	days
h_0	285,71	mm
e_cd	0,60	‰
AUTOGENOUS SHRINKAGE		
e_ca (∞)	0,05	‰
b_as	0,41	-
t	7,00	days
e_ca (t)	0,02	‰

Time t=28 days

COMPRESSIVE STRENGTH AT Time t		
fcm	38,00	N/mm2
b_cc	1,00	
t	28,00	days
fcm(t)	38,00	N/mm2
TENSILE STRENGTH		
fctm	3,33	N/mm2
a	0,67	
t	28,00	
b_cc	1,00	
fctm(t)	3,33	N/mm2
VARIATION OF YOUNG MODULUS		
Ecm	34330,80	N/mm2
b_cc	1,00	
t	28,00	days
fcm(t)	38,00	N/mm2
Ecm(t)	34330,80	N/mm2
DRYING SHRINKAGE		
e_cd0	0,35	‰
k_h	0,78	-
b_ds	2,17	-
t_s	2,00	days
t	28,00	days
h_0	285,71	mm
e_cd	0,60	‰
AUTOGENOUS SHRINKAGE		
e_ca (∞)	0,05	‰
b_as	0,65	-
t	28,00	days
e_ca (t)	0,03	‰

Time t=36525 days

COMPRESSIVE STRENGTH AT Time t		
fcm	38,00	N/mm2
b_cc	1,45	
t	36525,00	days
fcm(t)	54,99	N/mm2
TENSILE STRENGTH		
fctm	3,33	N/mm2
a	0,67	
t	36525,00	
b_cc	1,28	
fctm(t)	4,26	N/mm2
VARIATION OF YOUNG MODULUS		
Ecm	34330,80	N/mm2
b_cc	1,45	
t	36525,00	days
fcm(t)	54,99	N/mm2
Ecm(t)	38355,06	N/mm2
DRYING SHRINKAGE		
e_cd0	0,35	‰
k_h	0,78	-
b_ds	2,17	-
t_s	2,00	days
t	36525,00	days
h_0	285,71	mm
e_cd	0,60	‰
AUTOGENOUS SHRINKAGE		
e_ca (∞)	0,05	‰
b_as	1,00	-
t	36525,00	days
e_ca (t)	0,05	‰

2.7.5. VISCOUS EFFECTS ON YOUNG MODULUS

For loads with a duration that should causing the creep phenomena, the total deformation including creep may be calculated by using an effective modulus of elasticity in according the following expression:

$$E_c = \frac{E_{cm}}{1+\varphi(t,t_0)}$$

Where, $\varphi(t,t_0)$ is the creep coefficient relevant for the load and time interval.

$$\varphi(t,t_0) = \varphi_0 \cdot \beta_c(t,t_0)$$

$$\varphi(t,t_0) = \left[1 + \frac{1-\frac{RH}{100}}{0{,}1\cdot\sqrt[3]{h_0}} \cdot \left(\frac{35}{fcm}\right)^{0,7}\right] \cdot \left(\frac{35}{fcm}\right)^{0,2} \cdot \frac{16{,}8}{\sqrt{fcm}} \cdot \frac{1}{0{,}1+t_0^{0,2}} \cdot \left[\frac{t-t_0}{(1{,}5\cdot(1+(0{,}012\cdot RH)^{18})\cdot h_0+250)+t-t_0}\right]^{0,3}.$$

Summing up all calculation, the following table denotes all characteristics values.

Table 18: Effective Elastic modulus during the time.

	ϕ_(t,t$_0$)	$E_{cm}(t,t_0)$	n
ACCIDENTAL LOADS	-	34330,80	6,12
SHRINKAGE	2,99	12973,67	16,19
PERMANENT	1,83	11414,08	18,40
SEATTLEMENT	1,83	9184,63	22,86

3. LOAD COMBINATION CRITERIONS

This chapter will analyse the safety verification criteria for the actions described in the previous chapter and their application to structural models.

The Ultimate Limit States are listed below:

- loss of balance of the structure or part of it;
- excessive displacements or deformations;
- achievement of the maximum resistance capacity of parts of structures, connections, foundations;
- achievement of the maximum resistance capacity of the structure as a whole;
- achievement of collapse mechanisms in the soil;
- failure of membranes and fatigue connections;
- failure of membranes and connections due to other time-dependent effects;
- instability of parts of the structure or the entire structure.

The main Exercise Limit States are listed below:

- local damage (e.g. excessive cracking of the concrete) which can reduce the
- durability of the structure, its efficiency or its appearance;
- displacements and deformations that may limit the use of the construction, its efficiency or appearance; and
- appearance;
- displacements and deformations that may impair the efficiency and appearance of non
- structural, plant, machinery;
- vibrations that could compromise the use of the construction;
- fatigue damage that may compromise durability;
- corrosion and/or excessive degradation of materials depending on the exposure environment.

As far as the crack verification is concerned, the verification is conducted in accordance with CIRCULAR 21 January 2009, no. 7, "Instructions for the application of the Updating of the Technical standards for construction" referred to in the Ministerial Decree of 17 January 2018.
The characteristic crack verification width, w_k can be calculated with the expression:

$$w_k = 1{,}7\ \cdot \varepsilon_{sm} \cdot \Delta_{sm}$$

Where,
ε_{sm}, is the average unit deformation of reinforcement.

$$\varepsilon_{sm} = \frac{\left[\sigma_s - k_t\left(\frac{f_{ctm}}{\rho_{eff}}\right)\left(1 + \alpha_e \rho_{eff}\right)\right]}{E_s}$$

σ_s, is the tension stress in the reinforcement considering the cracked section.
α_e, is he ration E_s/E_{cm}.
ρ_{eff}, is the ratio $A_s/A_{c,eff}$. $A_{c,eff}$ is the effective concrete area without reinforcement.
k_t, is a partial coefficient linked to the load duration.
Δ_{sm}, is the average distance between the cracks.

If we want to check the distance of cracks or the max span between bars in easily and indirect way, NTC18 give us two important tables in order to check in quickly way the reinforcements. The tables are represented next.

Table 19:Maximum diameter of bar to crack control. NTC2018

Tensione nell'acciaio σ_s [MPa]	Diametro massimo ϕ delle barre (mm)		
	w_3 = 0,4 mm	w_2 = 0,3 mm	w_1 = 0,2 mm
160	40	32	25
200	32	25	16
240	20	16	12
280	16	12	8
320	12	10	6
360	10	8	-

Table 20: Maximum span between bars to crack control. NTC2018

Tensione nell'acciaio σ_s [MPa]	Spaziatura massima s delle barre (mm)		
	w_3 = 0,4 mm	w_2 = 0,3 mm	w_1 = 0,2 mm
160	300	300	200
200	300	250	150
240	250	200	100
280	200	150	50
320	150	100	-
360	100	50	-

3.1. SAFETY CONTROL

For the assessment of the safety of constructions, scientifically probabilistic criteria must be adopted proven. In the following, the criteria of the semi probabilistic method to limit states based on use are standardized partial safety coefficients, applicable in most cases; this method is called the first level method. For works of importance, higher-level methods may be adopted, taken from documentation proven technique.

In the semi-probabilistic method at the limit states, structural safety must be verified by comparing the resistance and the effect of the actions. For safety Structural, the resistance of the materials and the actions are represented by the characteristic values, $\mathbf{R_{ki}}$ and $\mathbf{E_{kj}}$ defined, respectively, as the lower fractile of the resistances and the (upper or lower) fractionality of actions that minimize security. In general, fractile is assumed to be equal at 5%. For sizes with small coefficients of variation, i.e. for sizes that do not concern univocally resistances or actions, can be considered fractile of 50% (median). The verification of the safety regarding the ultimate limit states of resistance is carried out with the "method of the partial coefficients" of safety expressed by the formal equation:

$$R_d \geq E_d$$

Where,

R_d, is the design resistance, evaluated on the basis of the design values of the resistance of the materials and values nominal of the quantities involved;

E_d, is the project value of the effect of the actions, evaluated based on the project values $E_{dj} = E_{kj} \cdot \gamma_j$.

3.2. LOAD COMBINATIONS

The chapter 5 of the NTC deals with general criteria and technical guidance for the design and execution of road bridges and railways. In particular, with regard to road bridges, in addition to the main geometric characteristics, are defined the different possible actions agents and assigned load schemes corresponding to the action's variable by traffic. The road and rail load schemes to be used for static and fatigue testing are generally coherent with the schemes UNI EN 1991-2.

The term "bridges" also includes all those works that, in relation to their different destinations, are normally indicated by special names, such as: viaducts, underpasses or overpasses, elevated roads, etc.

For the purposes of this regulation, the width of the roadway of the bridge means the distance measured orthogonally to the road axis.

In the case of hydraulic compatibility is necessary an accurate definition of return time of flood such as T_R=200 years. It will be very important to describe and specify in the hydraulic and hydrogeological report all the aspects that determine the feasibility of such.

The actions to be considered when designing road bridges are: permanent actions; distortions and deformations imposed; variable actions from traffic; variable actions (thermal variations, hydrodynamic thrusts, wind, snow and actions on railings); the passive resistances of the constraints; impacts on road safety barriers of vehicles; seismic actions; accidental actions.

Load Combinations. The load combinations to be considered for verification shall be determined in such a way as to ensure safety in accordance with as prescribed in Chapter §2. For the purpose of determining the characteristic values of traffic-based actions, combinations of the following shall generally be considered shown in table below:

Table 21: Characteristics action values due traffic loads.

	Carichi sulla superficie carrabile					Carichi su marciapiedi e piste ciclabili non sormontabili
	Carichi verticali			*Carichi orizzontali*		*Carichi verticali*
Gruppo di azioni	Modello principale (schemi di carico 1, 2, 3, 4 e 6)	Veicoli speciali	Folla (Schema di carico 5)	Frenatura	Forza centrifuga	Carico uniformemente distribuito
1	Valore caratteristico					Schema di carico 5 con valore di combinazione 2,5KN/m²
2a	Valore frequente			Valore caratteristico		
2b	Valore frequente				Valore caratteristico	
3 (*)						Schema di carico 5 con valore caratteristico 5,0KN/m²
4 (**)			Schema di carico 5 con valore caratteristico 5,0KN/m²			Schema di carico 5 con valore caratteristico 5,0KN/m²
5 (***)	Da definirsi per il singolo progetto	Valore caratteristico o nominale				

(*) Ponti pedonali
(**) Da considerare solo se richiesto dal particolare progetto (ad es. ponti in zona urbana)
(***) Da considerare solo se si considerano veicoli speciali

The table provides values of partial safety factor of the actions to be taken in the analysis for the determination of the effects in the ultimate limit states check. The meaning of the symbols are the following:

γ_{G1}, partial coefficient for dead load.

γ_{G2}, partial coefficient for not structural loads.

γ_{Q}, partial coefficient for traffic loads.

γ_{Qi}, partial factor for variable loads.

Table 22:Partial coefficient for ULS load combinations.

		Coefficiente	EQU(1)	A1	A2
Azioni permanenti g_1 e g_3	favorevoli sfavorevoli	γ_{G1} e γ_{G3}	0,90 1,10	1,00 1,35	1,00 1,00
Azioni permanenti non strutturali (2) g_2	favorevoli sfavorevoli	γ_{G2}	0,00 1,50	0,00 1,50	0,00 1,30
Azioni variabili da traffico	favorevoli sfavorevoli	γ_Q	0,00 1,35	0,00 1,35	0,00 1,15
Azioni variabili	favorevoli sfavorevoli	γ_{Qi}	0,00 1,50	0,00 1,50	0,00 1,30
Distorsioni e presollecita-zioni di progetto	favorevoli sfavorevoli	$\gamma_{\varepsilon1}$	0,90 1,00(3)	1,00 1,00(4)	1,00 1,00
Ritiro e viscosità, Cedimenti vincolari	favorevoli sfavorevoli	$\gamma_{\varepsilon2}$, $\gamma_{\varepsilon3}$, $\gamma_{\varepsilon4}$	0,00 1,20	0,00 1,20	0,00 1,00

Other values of partial coefficients are given in the table 25 below; the values of the combination coefficients ψ_{0j}, ψ_{1j} and ψ_{2j} for the different categories of actions are shown as:

Table 23:Partial combination coefficients for variable loads.

Azioni	Gruppo di azioni (Tab. 5.1.IV)	Coefficiente ψ_0 di combinazione	Coefficiente ψ_1 (valori frequenti)	Coefficiente ψ_2 (valori quasi permanenti)
Azioni da traffico	Schema 1 (carichi tandem)	0,75	0,75	0,0
	Schemi 1, 5 e 6 (carichi distribuiti	0,40	0,40	0,0
	Schemi 3 e 4 (carichi concentrati)	0,40	0,40	0,0
	Schema 2	0,0	0,75	0,0
	2	0,0	0,0	0,0
	3	0,0	0,0	0,0
	4 (folla)	--	0,75	0,0
	5	0,0	0,0	0,0
Vento	a ponte scarico SLU e SLE	0,6	0,2	0,0
	in esecuzione	0,8	0,0	0,0
	a ponte carico SLU e SLE	0,6	0,0	0,0
Neve	SLU e SLE	0,0	0,0	0,0
	in esecuzione	0,8	0,6	0,5
Temperatura	SLU e SLE	0,6	0,6	0,5

3.2.1. ULS AND SLS LOAD COMBINATIONS

In accordance with the §2.5.3 of Ministerial Decree 27/01/18, the following combinations of actions are defined for the purpose of checking the limit states:

1) Fundamental combination, generally used for ultimate limit states (U.L.S.)

$$\gamma_{G1} \cdot G_1 + \gamma_{G2} \cdot G_2 + \gamma_{Q1} \cdot Q_{k1} + \gamma_{Q2} \cdot \psi_{02} \cdot Q_{k2} + \gamma_{Q3} \cdot \psi_{03} \cdot Q_{k3} + \cdots$$

2) Characteristic combination (rare), generally used for irreversible limit states (S.L.S.)

$$G_1 + G_2 + Q_{k1} + \psi_{02} \cdot Q_{k2} + \psi_{03} \cdot Q_{k3} + \cdots$$

3) Frequent combination, generally used for reversible operating limit states (S.L.S.)

$$G_1 + G_2 + \psi_{11} \cdot Q_{k1} + \psi_{22} \cdot Q_{k2} + \psi_{23} \cdot Q_{k3} + \cdots$$

4) quasi-permanent combination, generally used for long-term effects (S.L.S.)

$$G_1 + G_2 + \psi_{21} \cdot Q_{k1} + \psi_{22} \cdot Q_{k2} + \psi_{23} \cdot Q_{k3} + \cdots$$

5) Exceptional combination, used for the final limit states related to exceptional actions A.

$$G_1 + G_2 + A_D + \psi_{21} \cdot Q_{k1} + \psi_{22} \cdot Q_{k2} + \psi_{23} \cdot Q_{k3} + \cdots$$

3.2.2. SEISMIC LOAD COMBINATIONS

The reference linear analysis method to determine the effects of seismic action on both dissipative systems both on non-dissipative systems, is modal analysis with response spectrum or dynamic linear analysis. The linear dynamic analysis consists on:

- determining the vibration modes of the construction (modal analysis);
- calculation of the effects of seismic action, represented by the design response spectrum, for each of the modes of vibration detected;
- combination of these effects.

All modes with significant participating mass must be considered. It is appropriate in this respect consider all modes with a participating mass greater than 5% and in any case a number of modes whose mass total participant is more than 85%.

The checks on the final or operating limit states must be carried out for the combination of the seismic actions with the other actions, as suggested by the technical regulations:

$$G_1 + G_2 + E + \sum \psi_{2j} \cdot Q_{kj}$$

The effects of seismic action will be evaluated taking into account the masses associated with the following gravitational loads:

$$G_1 + G_2 + \sum \psi_{2j} \cdot Q_{kj}$$

Using the Advance design calculation program, the following seismic load combinations have been defined according to Newmark's coefficients:

1) $1{,}00 \cdot E_x + 0{,}30 \cdot E_y + 0{,}30 \cdot E_z$. Longitudinal actions as dominant.
2) $0{,}30 \cdot E_x + 1{,}00 \cdot E_y + 0{,}30 \cdot E_z$. Transversal actions as dominant.
3) $0{,}30 \cdot E_x + 0{,}30 \cdot E_y + 1{,}00 \cdot E_z$. Vertical actions as dominant.

3.2.3. GENERAL STRUCTURAL MODEL

The stress calculation was carried out using the finite element code provide by Advance Design. The entire structure was discretized into a surface and plate elements. The stress analysis was carried out in several distinct phases.

Phase 1. Stress analysis by steel own weight and slab own weight; in the beam frame the inertia of the longitudinal and transoms only was considered.

Phase 2. Analysis of stresses due to permanent loads; in the frame girders the contribution of the inertia of the reinforced concrete slab to the longitudinal beams was considered, with homogenisation coefficient **n=18,40**.

Phase 2b. Analysis of stresses due to loads due to shrinkage; the contribution of the inertia of the reinforced concrete slab to the longitudinal beams was considered in the lattice girders, with homogenisation coefficient **n=16,19**.

Phase 2c. Analysis of stresses induced by differential failure; in the lattice girders the contribution of the inertia of the AC slab to the longitudinal beams was considered, with homogenisation coefficient **n=22,86**.

Phase 3. Analysis of stresses due to accidental loads (vehicles, crowd, wind); the contribution of the inertia of the reinforced concrete slab to the longitudinal beams was considered in the lattice girders, with homogenisation coefficient **n=6,12**.

Phase 3f. Analysis of stresses due to accidental fatigue loads; the contribution of the inertia of the reinforced concrete slab to the longitudinal beams was considered in the lattice girders, with homogenization coefficient **n=6,12**.

Seismic phase. Analysis of stresses due to seismic loads; the contribution of the inertia of the reinforced concrete slab to the longitudinal beams has been considered in the lattice girders, with homogenization coefficient **n=6,12**. The modal analysis was carried out with reference to the three main directions, with the X and Y axes coinciding respectively with the longitudinal and transversal direction of the decks, and the Z axis coinciding with the vertical direction. The modal combinations were performed with the CQC rule.

Deformation phase. Analysis of the upper bracing by own weight steel and slab; in the frame girders the inertia of the longitudinal and cross beams only was considered.

4. STRESS ANALYSIS

As mentioned in the introduction to the thesis, this project consists of surface elements and not linear beam-type elements. Defining this approach, it is of limited usefulness to view the results in terms of bending moment and shear force, but it is an excellent measure of control to visualize the results due to the different combinations as a function of displacement and internal stress.

4.1. GRAPHICAL RESULTS

This paragraph will display the results obtained using the Advance Design software with regard to the displacements and the stress state for the different load combinations and load phases. The pictures plotted have different unit of major: displacements are plotted in term of millimetres and the stress tension are function of Von Mises state of stress in N/mm^2.

As defined in the introduction, the essential reason for this thesis is to verify what are the substantial differences between a continuous model and the classic De Saint Venant model.

As will be shown in the following figures, the model is characterized by surface elements for the main beams and beam elements for transverse stiffeners, such as diaphragms and braces.

In addition, another linear model of equal character is created to compare results and to have an easier calculation and verification proposed by the Italian regulations in force.

In fact, the linear model was mainly useful for the calculation of crowd and vehicular load, which through the tool offered in the Advance Design package, was easy to use and display the results, both from the tensional and force aspects.

4.1.1. STEEL DECK – PHASE 1

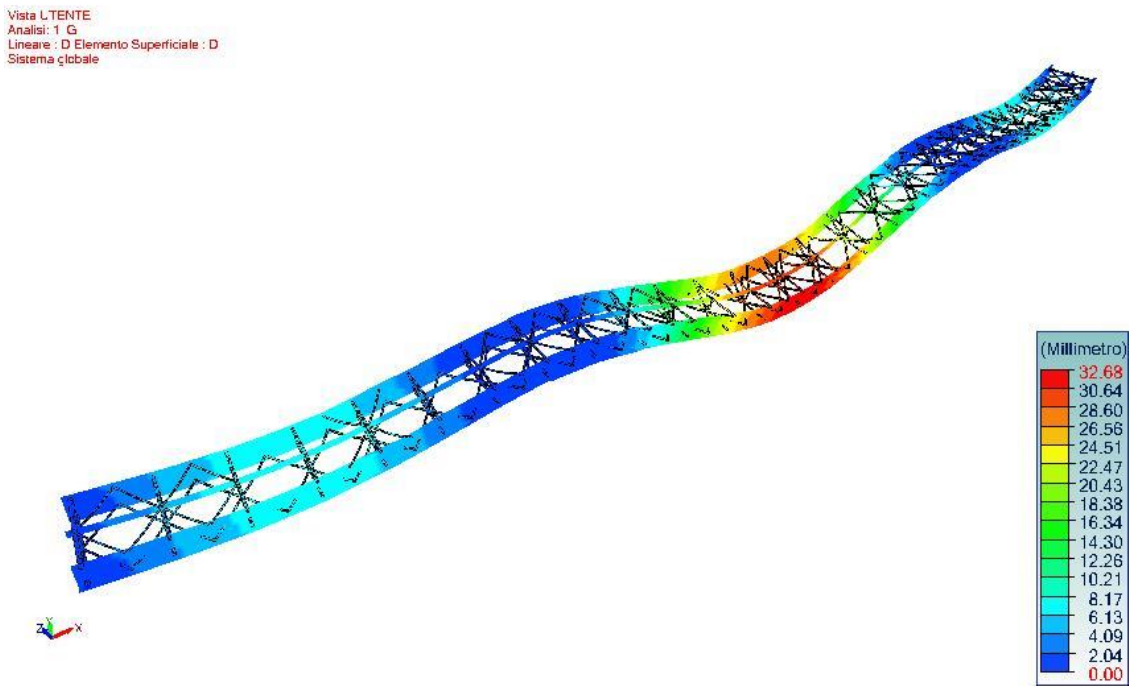

Figure 33: Displacement due to dead load

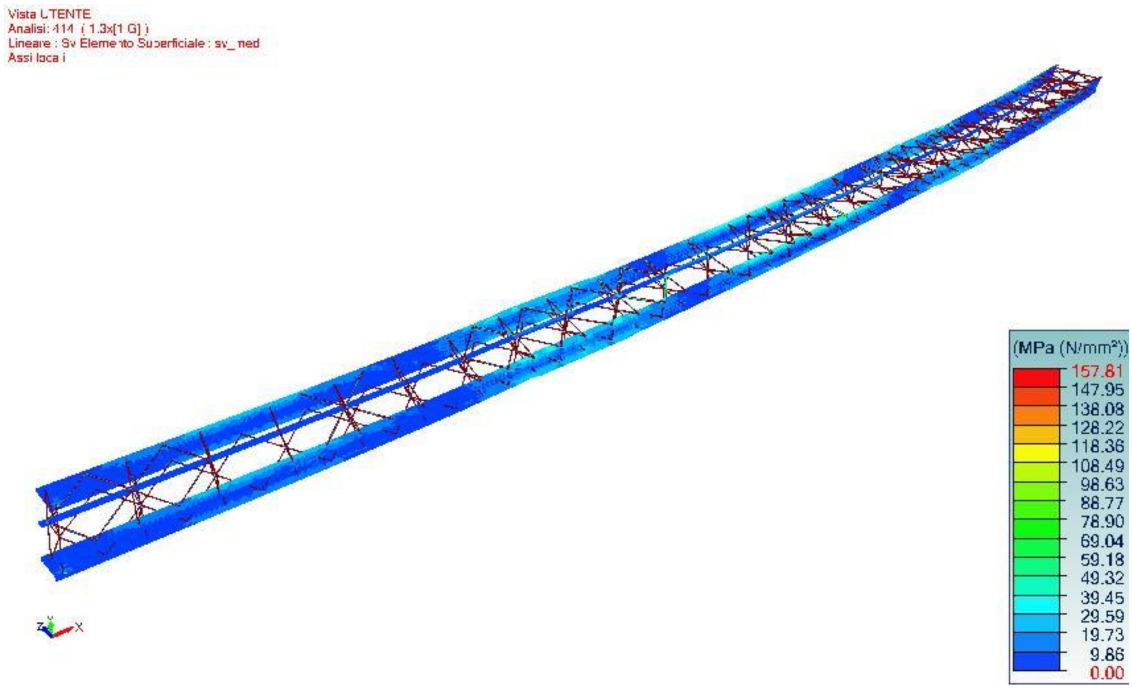

Figure 34: Von Mises Tension due to dead load

4.1.2. STEEL DECK WITH PREDALLES – PHASE 1

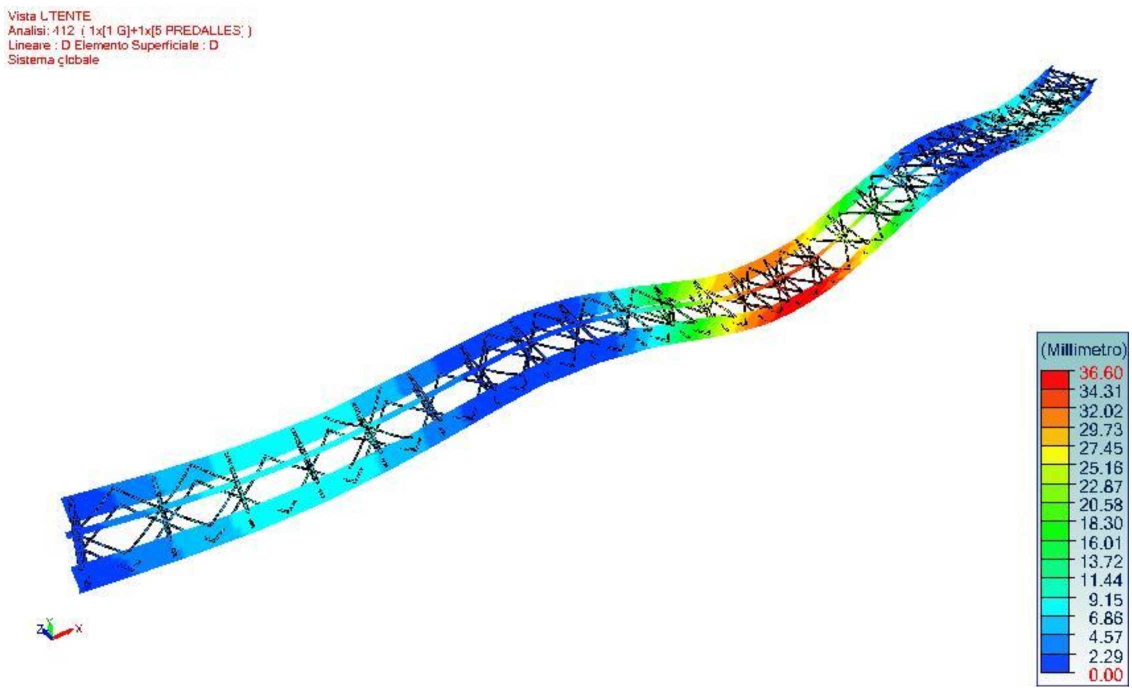

Figure 35: Displacement due to steel deck with predalles

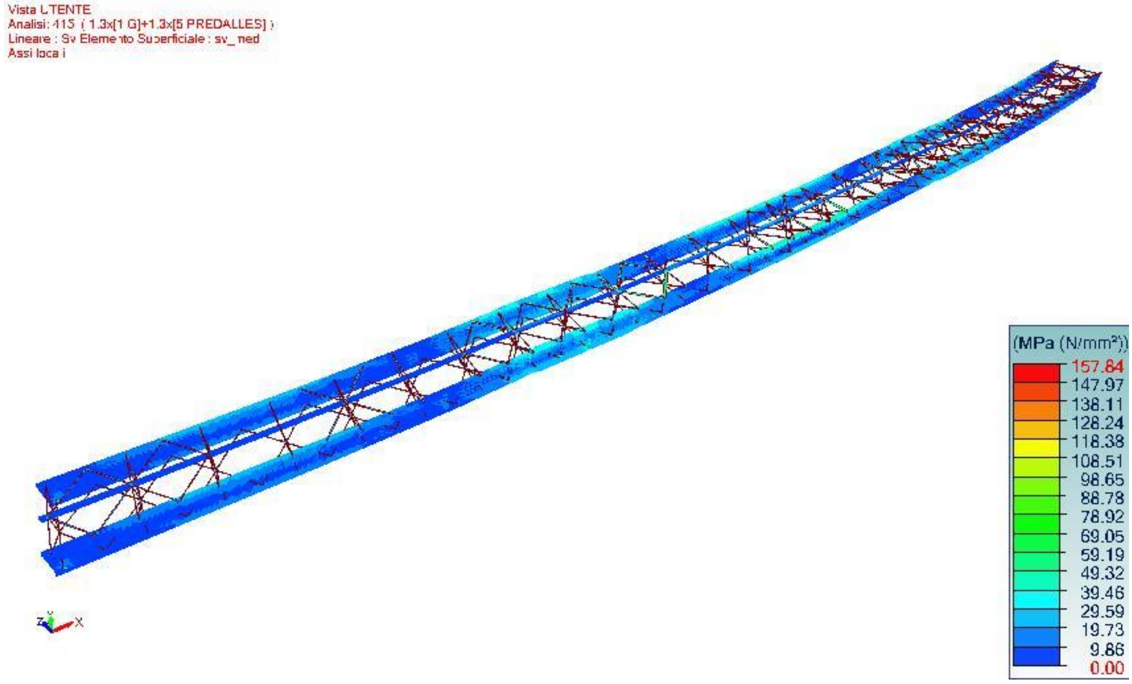

Figure 36: Von Mises tension due to steel deck with predalles

4.1.3. DECK WITH CASTING CONCRETE – PHASE 1

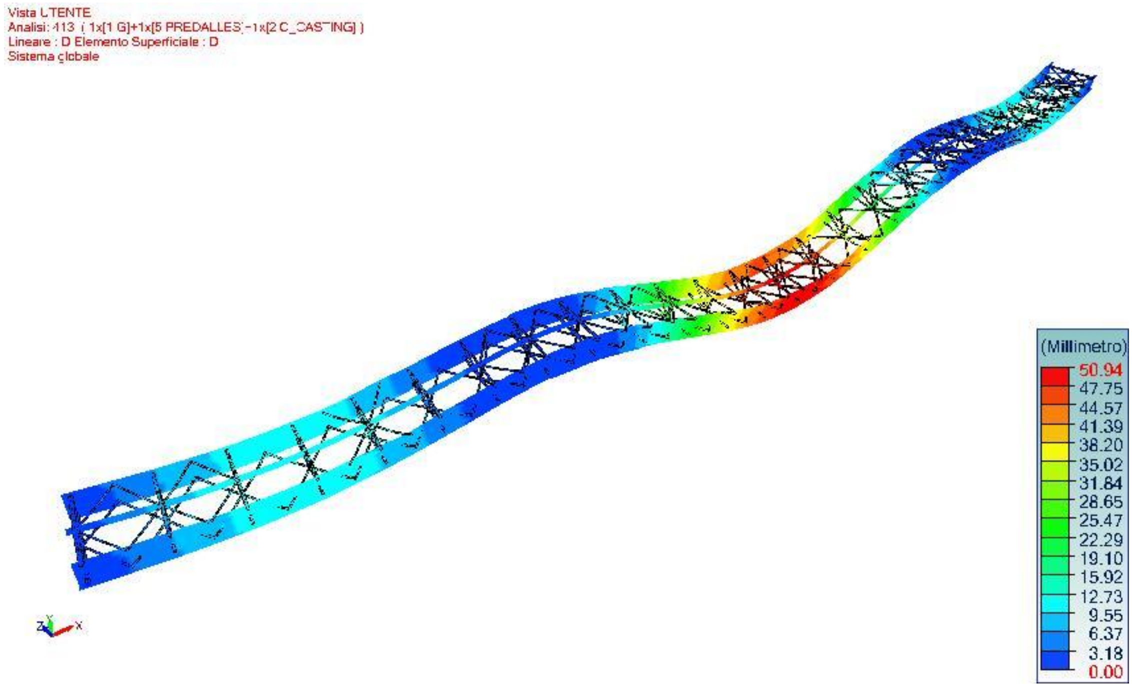

Figure 37: Displacement due to steel deck with predalles and casting concrete

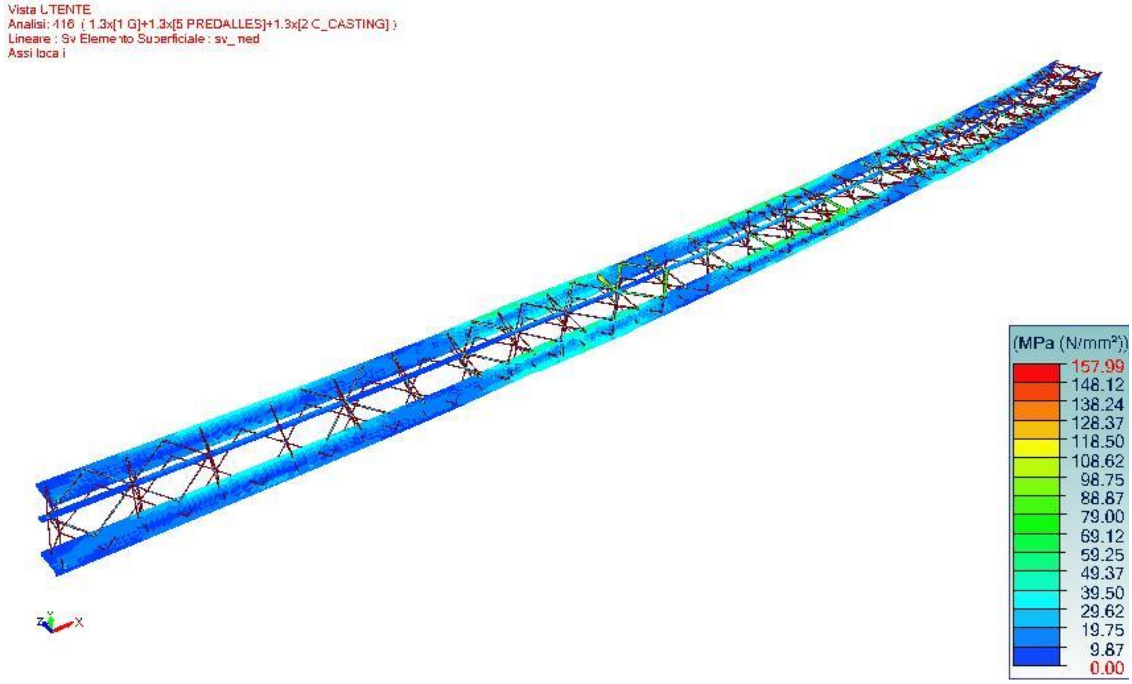

Figure 38: Von Mises tension due to steel deck with predalles and casting concrete

4.1.4. PERMANENT LOADS – PHASE 2A

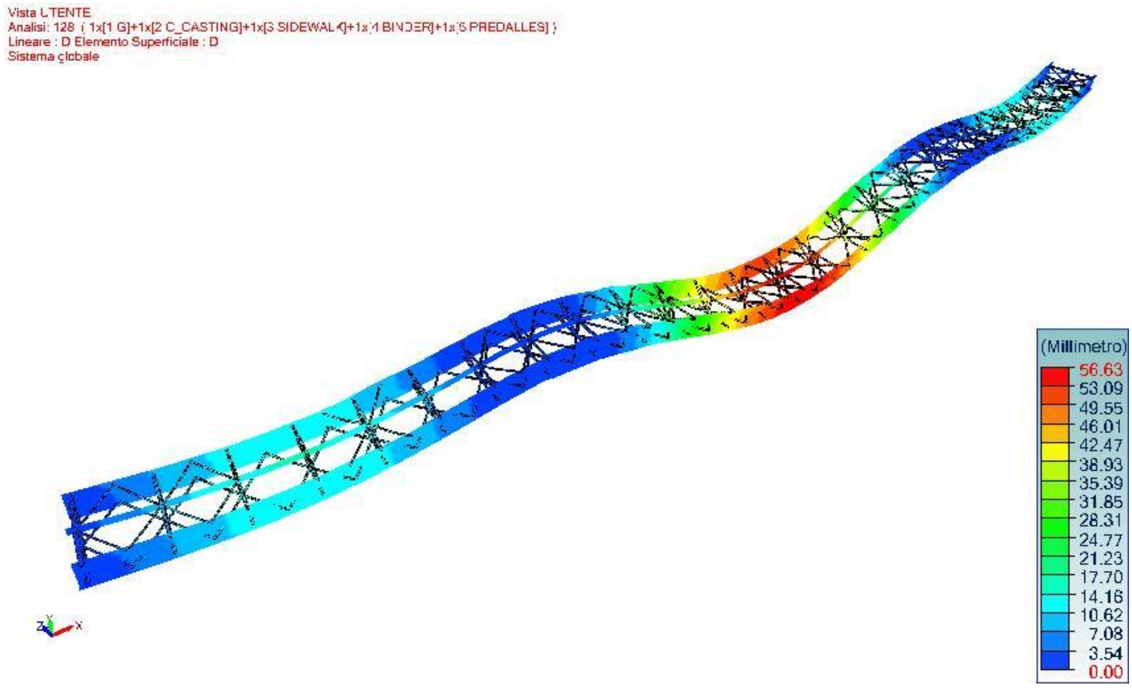

Figure 39: Displacement of the deck

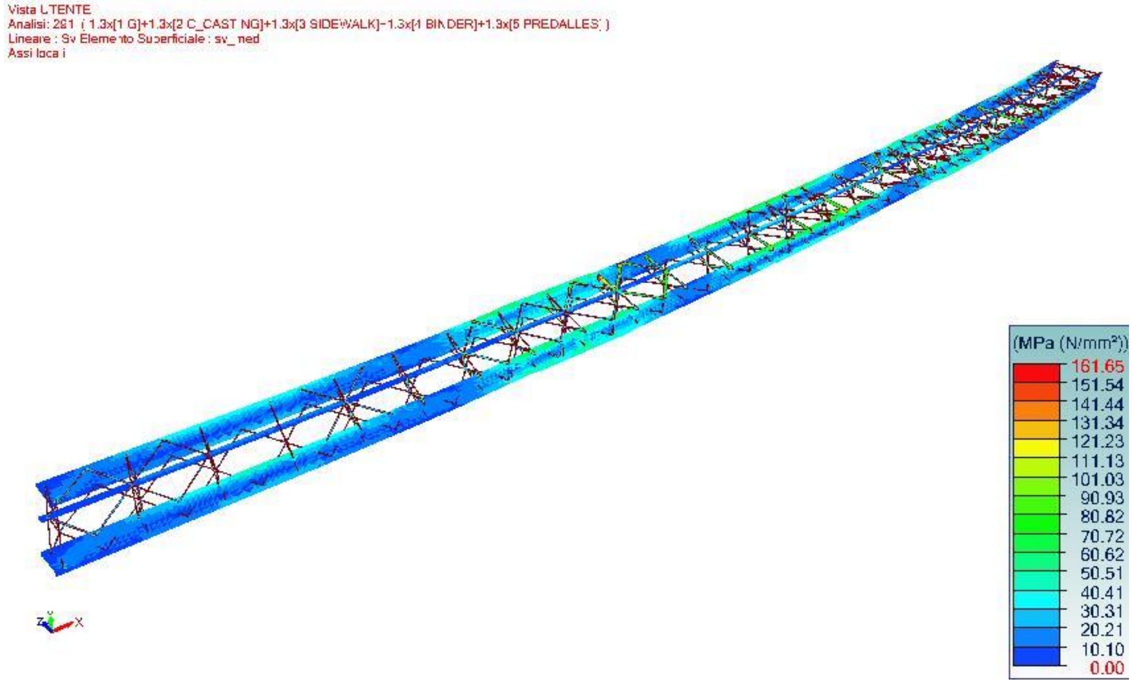

Figure 40: Von Mises tension of the deck

4.1.5. WIND EFFECT – PHASE 3

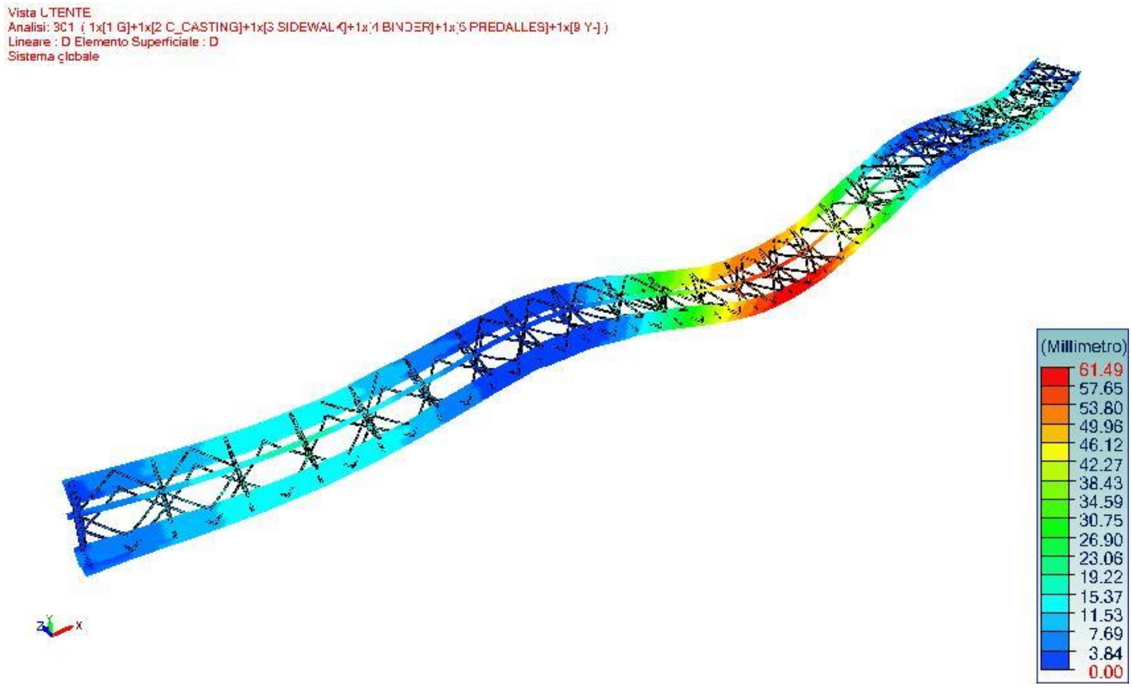

Figure 41: Displacement due wind load

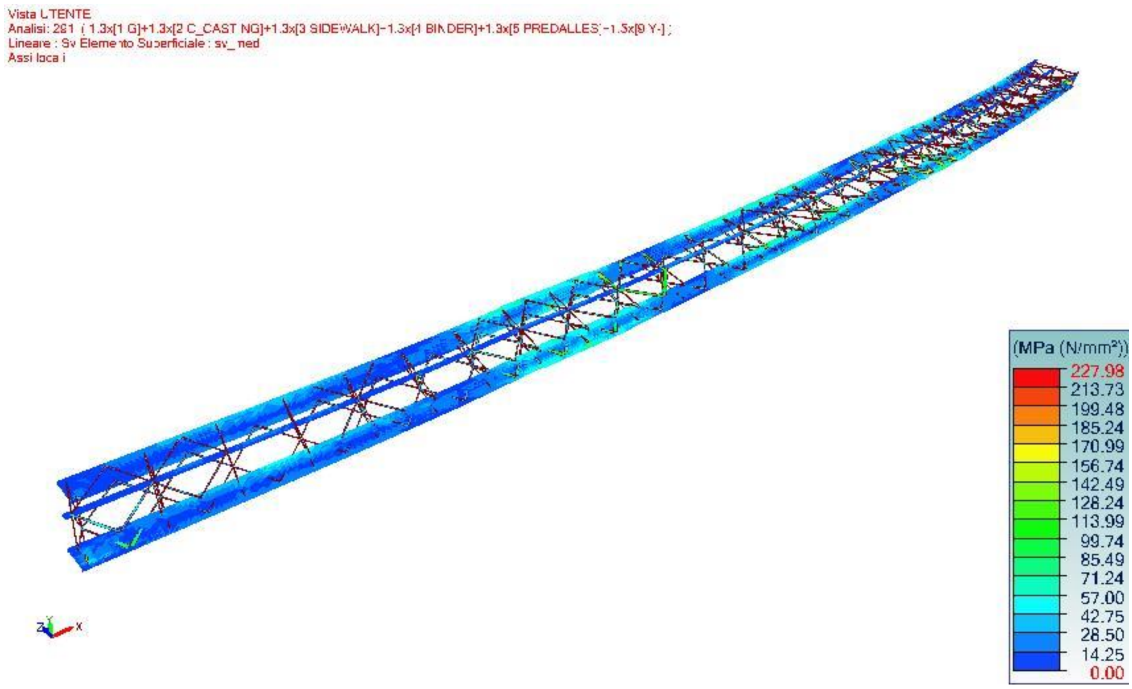

Figure 42: Von Mises tension due wind load

4.2. VERIFICATION OF MAIN BEAM

The main beams have the static function of sustaining the road platform, supporting the reinforced concrete slab to which they are connected by means of Nelson-type shear connectors. Afterwards we will present the verifications referring to the most requested sections, i.e. the intermediate supports and the one in the middle of the second span.

The analysis for the main beams will include two types of approaches: the first considering resistance of membrane and secondly, verify that there is no buckling or instability during the various loading phases.

As mentioned in the Italian Technical Regulations, the cross-sections of structural elements are classified according to their rotational capacity C_θ defined as: $C_\theta = \frac{\theta_r}{\theta_y} - 1$. Being θ_i the rotations corresponding respectively to the ultimate deformation and yield strength. The classification of the cross sections of structural steel element is made according to their ability to deform into plastic field. It is possible distinguish 4 classes of section in order of their rotational capacity. Since the main beams are characterized by single elements welded together, it is essential to also carry out an analysis of the flexural behaviour. The following table, table 26 and 27 are used to establish class of steel element and compression and tensile width.

Table 24:Maximum width to thickness table. Used to establish steel class. From EN 1993-1-1

Internal compression parts

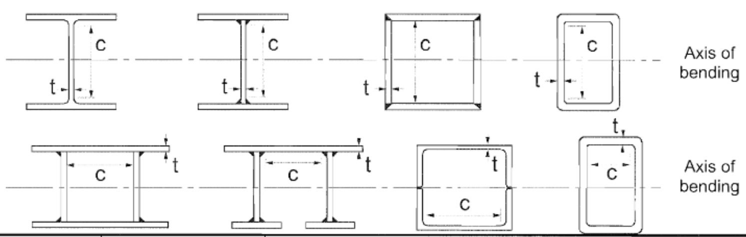

Class	Part subject to bending	Part subject to compression	Part subject to bending and compression
Stress distribution in parts (compression positive)	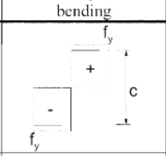	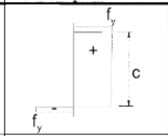	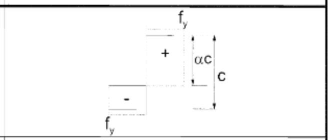
1	$c/t \le 72\varepsilon$	$c/t \le 33\varepsilon$	when $\alpha > 0{,}5$: $c/t \le \frac{396\varepsilon}{13\alpha - 1}$ when $\alpha \le 0{,}5$: $c/t \le \frac{36\varepsilon}{\alpha}$
2	$c/t \le 83\varepsilon$	$c/t \le 38\varepsilon$	when $\alpha > 0{,}5$: $c/t \le \frac{456\varepsilon}{13\alpha - 1}$ when $\alpha \le 0{,}5$: $c/t \le \frac{41{,}5\varepsilon}{\alpha}$
Stress distribution in parts (compression positive)	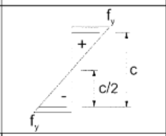	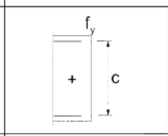	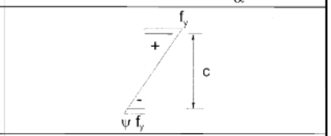
3	$c/t \le 124\varepsilon$	$c/t \le 42\varepsilon$	when $\psi > -1$: $c/t \le \frac{42\varepsilon}{0{,}67 + 0{,}33\psi}$ when $\psi \le -1^{*)}$: $c/t \le 62\varepsilon(1-\psi)\sqrt{(-\psi)}$

$\varepsilon = \sqrt{235/f_y}$	f_y	235	275	355	420	460
	ε	1,00	0,92	0,81	0,75	0,71

*) $\psi \le -1$ applies where either the compression stress $\sigma \le f_y$ or the tensile strain $\varepsilon_y > f_y/E$

Table 25: Used to understand the parts subject to bending and compression. From EN 1993-1-1.

Outstand flanges

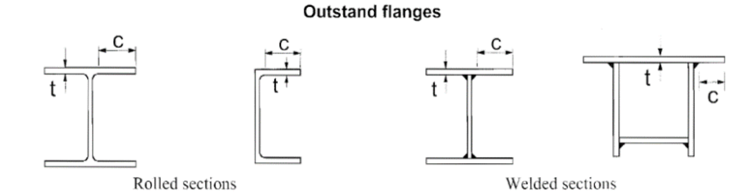

Class	Part subject to compression	Part subject to bending and compression: Tip in compression	Part subject to bending and compression: Tip in tension
Stress distribution in parts (compression positive)	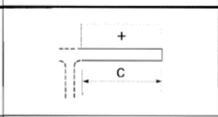	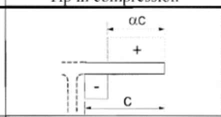	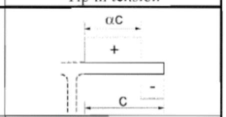
1	$c/t \le 9\varepsilon$	$c/t \le \frac{9\varepsilon}{\alpha}$	$c/t \le \frac{9\varepsilon}{\alpha\sqrt{\alpha}}$
2	$c/t \le 10\varepsilon$	$c/t \le \frac{10\varepsilon}{\alpha}$	$c/t \le \frac{10\varepsilon}{\alpha\sqrt{\alpha}}$
Stress distribution in parts (compression positive)	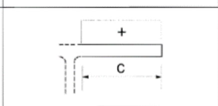	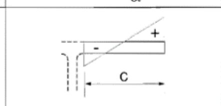	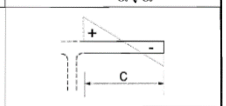
3	$c/t \le 14\varepsilon$	$c/t \le 21\varepsilon\sqrt{k_\sigma}$ For k_σ see EN 1993-1-5	

$\varepsilon = \sqrt{235/f_y}$	f_y	235	275	355	420	460
	ε	1,00	0,92	0,81	0,75	0,71

The partial factors are important to carry out the checks and be applied to one's own combinations of characteristic values. The table below summarizes their values and uses.

Table 26:Partial Factors.

Resistance of cross-section. Class 1-2-3-4	γ_{M0}	1,05
Instability of Membrane	γ_{M1}	1,05
Instability of membrane (bridge)	γ_{M1}	1,1
Tension of cross-section in tension to fracture	γ_{M2}	1,25

4.2.1. MEMBRANE RESISTANCE

For the verification of the beams the design resistance to be considered depends on the classification of the sections. In our case, all longitudinal elements are in class 4.

First Step. It is in the elastic field, where they must respect the following relation:

$$\sigma_{VM} < \frac{f_{yk}}{\gamma_{M0}}$$

$$\sigma_{VM} = \sqrt{\sigma_x^2 - \sigma_x \sigma_y + \sigma_y^2 + 3\tau_{xy}^2}$$

σ_{VM}, is the Von Misses Tension in according Advance Design results.

Second Step. Verification the normal stress.

$$\frac{N_{ed}}{N_{pl,Rd}} < 1$$

Where the resisting normal $N_{pl,Rd} = \frac{A \cdot f_{yk}}{\gamma_{M0}}$.

Third Step. Compression Verification.

$$\frac{N_{ed}}{N_{c,Rd}} < 1$$

Where $N_{pl,Rd} = \frac{A \cdot f_{yk}}{\gamma_{M0}}$.

Fourth Step. Bending moment verification.

$$\frac{M_{ed}}{M_{c,Rd}} < 1$$

Where $M_{c,Rd} = \frac{W_{min} \cdot f_{yk}}{\gamma_{M0}}$.

W_{min}, is calculated by eliminating the parts of the section that are inactive due to local instability, according to the following procedure exposed in UNI EN1993-1-5 and choosing the lesser of the modules thus obtained.

Fifth Step. Shear verification.

$$\frac{V_{ed}}{V_{c,Rd}} < 1$$

Where $V_{c,Rd} = \frac{A_v \cdot f_{yk}}{\sqrt{3} \cdot \gamma_{M0}}$ in the case of zero torsion.

A_v is the resisting area provides from NTC 2018 (§4.2.4.1.2.4).

In the case of torsion, the resisting shear force shall be:

$$V_{c,Rd,red} = V_{c,Rd} \sqrt{1 - \frac{\tau_{t,Ed}}{1{,}25 \cdot f_{yk}/\sqrt{3} \cdot \gamma_{M0}}}$$

$\tau_{t,Ed}$, is the maximum tangential stress along the profile.

4.2.2. MEMBRANE STABILITY

The procedure in this case marked in the membranal analysis and the related stress behaviour.

First Step. Compression verification.

$$\frac{N_{ed}}{N_{b,Rd}} < 1$$

Where $N_{b,Rd} = \frac{\chi \cdot A \cdot f_{yk}}{\gamma_{M1}}$

The coefficient χ depends on type of cross section and kind of steel used.

Other coefficients are considered in this analysis:

$\chi = \frac{1}{\Phi + \sqrt{\Phi^2 + \bar{\lambda}^2}} \leq 1.$

$\Phi = \frac{1}{2}\left[1 + \alpha(\bar{\lambda} - 0{,}2) + \bar{\lambda}^2\right].$

α is a imperfection factor given by the table 4.2 VIII of NTC2018.

$\bar{\lambda} = \sqrt{\frac{A \cdot f_{yk}}{N_{cr}}}$. Normalized slenderness.

$N_{cr} = \frac{\pi^2 \cdot E \cdot J}{l_0^2}$. Eulerian normal force.

Other important check is the slenderness verification. The upper limit is given by the relation: $\lambda = l_0/i$. l_0 is the characteristic length and i is the radius of inertia.

Second Step. Bending verification.

Beams subjected to the compressive banding which is not sufficiently tightened at the sides must be checked against flex-torsional instability.

$$\frac{M_{ed}}{M_{b,Rd}} < 1$$

Where $M_{b,Rd} = \chi_{LT} \cdot W_y \cdot \frac{f_{yk}}{\gamma_{M1}}$.

The χ_{LT} coefficient is a reduction factor of flex-torsion instability. It is evaluated by:

$\chi_{LT} = \frac{1}{f} \cdot \frac{1}{\Phi_{LT} + \sqrt{\Phi_{LT}^2 + \beta \overline{\lambda_{LT}}^2}} \leq K_\chi.$

$\Phi = \frac{1}{2}\left[1 + \alpha_{LT}\left(\overline{\lambda_{LT}} - \lambda_{LT,0}\right) + \beta \cdot \overline{\lambda_{LT}}^2\right].$

$\overline{\lambda_{LT}} = \sqrt{\frac{W_y \cdot f_{yk}}{M_{cr}}}$. Normalized slenderness.

The others coefficient are proposed and defined by the NTC2018 (§4.2.4.1.3.2)

Third Step. Buckling verification.

In calculating longitudinal stresses, account should be taken of the combined effect of shear lag and plate buckling.

During the design procedure the longitudinal stiffening elements that have a great stability function are not taken into consideration. The effective area A_{eff} should be determined assuming that the cross section is subject only to stresses due to uniform axial compression.

At the beginning, the study of the case of plates without longitudinal stiffeners, is a must in order to understand the effect of slender inside the material.

As shown the table below, the fundamental parameter is the ratio between maximum tensile stress and maximum compressive stress. This coefficient ψ cannot assume values higher than 1, which would correspond to the pure compression limit case. On the basis of this parameter, the portions of the cooperating area, the instability coefficient, the reduction coefficient and the relative slimness of the membrane are determined.

Table 27:Internal compression elements. Stress relationship and buckling factor.

Stress distribution (compression positive)	Effective[1] width b_{eff}
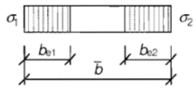	$\psi = 1$: $b_{eff} = \rho\ \bar{b}$ $b_{e1} = 0,5\ b_{eff}$ $b_{e2} = 0,5\ b_{eff}$
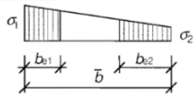	$1 > \psi \geq 0$: $b_{eff} = \rho\ \bar{b}$ $b_{e1} = \frac{2}{5-\psi} b_{eff}$ $b_{e2} = b_{eff} - b_{e1}$
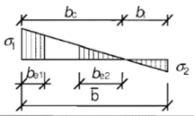	$\psi < 0$: $b_{eff} = \rho\ b_c = \rho\ \bar{b} / (1-\psi)$ $b_{e1} = 0,4\ b_{eff}$ $b_{e2} = 0,6\ b_{eff}$

$\psi = \sigma_2/\sigma_1$	1	$1 > \psi > 0$	0	$0 > \psi > -1$	-1	AC1 $-1 > \psi \geq -3$ AC1
Buckling factor k_σ	4,0	$8,2 / (1,05 + \psi)$	7,81	$7,81 - 6,29\psi + 9,78\psi^2$	23,9	$5,98\ (1-\psi)^2$

All buckling and shear lag phenomena are developed on §3.3 and §4 of EN1993-1-5.

On the other hand, in the case of plates with stiffeners, the effective areas of the compressed areas alone must be taken into account, considering the globular instability of the stiffened panel and the local instability of each sub-panel.

Fourth Step. Shear Verification.

For stiffened or unstiffened webs, the design resistance on shear point of view should be taken as:

$$V_{b,Rd} = V_{bw,Rd} + V_{bf,Rd} \leq \frac{\eta \cdot f_{yw} \cdot h_w \cdot t}{\sqrt{3} \cdot \gamma_{M1}}$$

Where:

$V_{bw,Rd} = \frac{\chi_w \cdot f_{yw} \cdot h_w \cdot t}{\sqrt{3} \cdot \gamma_{M1}}$. Contribution of the web.

$V_{bf,Rd} = \frac{b_f \cdot t_f^2 \cdot f_{yf}}{c \cdot \gamma_{M1}} \left[1 - \left(\frac{M_{Ed}}{M_{f,k} / \gamma_{M0}}\right)^2\right]$. Flange contribution.

The final verification is made by:

$$\frac{V_{Ed}}{V_{b,Rd}} < 1$$

4.3.DIAFRAGMS & BRACES

As did in the main beam, we proceed in the same way in order to very all components inside the model and all cross-section defined in the design procedures.

The deck bracing is inserted in order to guarantee the stability of the transoms at the connection with the main beams and therefore their stability against the phenomena of flex-torsional instability. In order to guarantee this condition of stability, they must be able to withstand the stresses deriving from the tendency of the compressed band to swerve sideways. In order to define these effects, the indications contained in UNI EN 1993-1-1: 2005 are used.

The analysis for the main beams will include two types of approaches: the first considering resistance of membrane and secondly, verify that there is no buckling or instability during the various loading phases.

As mentioned in the Italian Technical Regulations, the cross-sections of structural elements are classified according to their rotational capacity C_θ defined as: $C_\theta = \frac{\theta_r}{\theta_y} - 1$. Being θ_i the rotations corresponding respectively to the ultimate deformation and yield strength. The classification of the cross sections of structural steel element is made according to their ability to deform into plastic field. It is possible distinguish 4 classes of section in order of their rotational capacity. Since the main beams are characterized by single elements welded together, it is essential to also carry out an analysis of the flexural behaviour. The following table, table 26 and 27 are used to establish class of steel element and compression and tensile width.

Table 28:Maximum width to thickness table. Used to establish steel class. From EN 1993-1-1

Internal compression parts

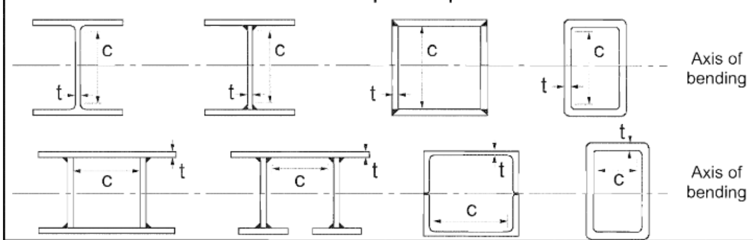

Class	Part subject to bending	Part subject to compression	Part subject to bending and compression
Stress distribution in parts (compression positive)	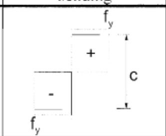	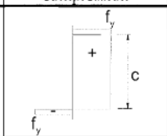	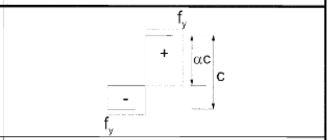
1	$c/t \leq 72\varepsilon$	$c/t \leq 33\varepsilon$	when $\alpha > 0,5$: $c/t \leq \frac{396\varepsilon}{13\alpha - 1}$ when $\alpha \leq 0,5$: $c/t \leq \frac{36\varepsilon}{\alpha}$
2	$c/t \leq 83\varepsilon$	$c/t \leq 38\varepsilon$	when $\alpha > 0,5$: $c/t \leq \frac{456\varepsilon}{13\alpha - 1}$ when $\alpha \leq 0,5$: $c/t \leq \frac{41,5\varepsilon}{\alpha}$
Stress distribution in parts (compression positive)	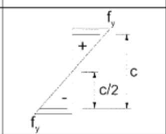	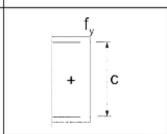	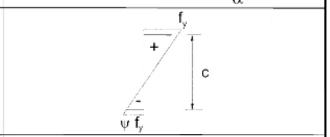
3	$c/t \leq 124\varepsilon$	$c/t \leq 42\varepsilon$	when $\psi > -1$: $c/t \leq \frac{42\varepsilon}{0,67 + 0,33\psi}$ when $\psi \leq -1^{*)}$: $c/t \leq 62\varepsilon(1-\psi)\sqrt{(-\psi)}$

$\varepsilon = \sqrt{235/f_y}$	f_y	235	275	355	420	460
	ε	1,00	0,92	0,81	0,75	0,71

*) $\psi \leq -1$ applies where either the compression stress $\sigma \leq f_y$ or the tensile strain $\varepsilon_y > f_y/E$

Table 29: Used to understand the parts subject to bending and compression. From EN 1993-1-1.

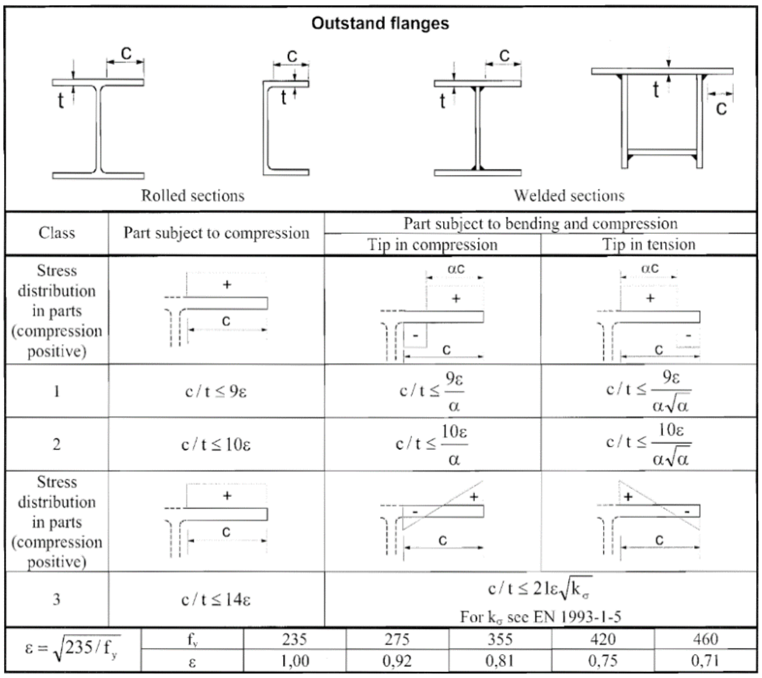

Outstand flanges

Rolled sections — Welded sections

Class	Part subject to compression	Part subject to bending and compression: Tip in compression	Part subject to bending and compression: Tip in tension
Stress distribution in parts (compression positive)			
1	$c/t \le 9\varepsilon$	$c/t \le \frac{9\varepsilon}{\alpha}$	$c/t \le \frac{9\varepsilon}{\alpha\sqrt{\alpha}}$
2	$c/t \le 10\varepsilon$	$c/t \le \frac{10\varepsilon}{\alpha}$	$c/t \le \frac{10\varepsilon}{\alpha\sqrt{\alpha}}$
Stress distribution in parts (compression positive)			
3	$c/t \le 14\varepsilon$	$c/t \le 21\varepsilon\sqrt{k_\sigma}$ For k_σ see EN 1993-1-5	

$\varepsilon = \sqrt{235/f_y}$					
f_y	235	275	355	420	460
ε	1,00	0,92	0,81	0,75	0,71

The partial factors are important to carry out the checks and be applied to one's own combinations of characteristic values. The table below summarizes their values and uses.

Table 30:Partial Factors.

Resistance of cross-section. Class 1-2-3-4	g_{M0}	1,05
Instability of Membrane	g_{M1}	1,05
Instability of membrane (bridge)	g_{M1}	1,1
Tension of cross-section in tension to fracture	g_{M2}	1,25

4.3.1. MEMBRANE RESISTANCE

For the verification of the beams the design resistance to be considered depends on the classification of the sections. In our case, all longitudinal elements are in class 4.

First Step. It is in the elastic field, where they must respect the following relation:

$$\sigma_{VM} < \frac{f_{yk}}{\gamma_{M0}}$$

$$\sigma_{VM} = \sqrt{\sigma_x^2 - \sigma_x\sigma_y + \sigma_y^2 + 3\tau_{xy}^2}$$

σ_{VM}, is the Von Misses Tension in according Advance Design results.

Second Step. Verification the normal stress.

$$\frac{N_{ed}}{N_{pl,Rd}} < 1$$

Where the resisting normal $N_{pl,Rd} = \frac{A \cdot f_{yk}}{\gamma_{M0}}$.

Third Step. Compression Verification.

$$\frac{N_{ed}}{N_{c,Rd}} < 1$$

Where $N_{pl,Rd} = \frac{A \cdot f_{yk}}{\gamma_{M0}}$.

Fourth Step. Bending moment verification.

$$\frac{M_{ed}}{M_{c,Rd}} < 1$$

Where $M_{c,Rd} = \frac{W_{min} \cdot f_{yk}}{\gamma_{M0}}$.

W_{min}, is calculated by eliminating the parts of the section that are inactive due to local instability, according to the following procedure exposed in UNI EN1993-1-5 and choosing the lesser of the modules thus obtained.

4.3.2. MEMBRANE STABILITY

The procedure in this case marked in the membranal analysis and the related stress behaviour.

First Step. Compression verification.

$$\frac{N_{ed}}{N_{b,Rd}} < 1$$

Where $N_{b,Rd} = \frac{\chi \cdot A \cdot f_{yk}}{\gamma_{M1}}$

The coefficient χ depends on type of cross section and kind of steel used.

Other coefficients are considered in this analysis:

$\chi = \frac{1}{\Phi + \sqrt{\Phi^2 + \bar{\lambda}^2}} \leq 1.$

$\Phi = \frac{1}{2}\left[1 + \alpha\left(\bar{\lambda} - 0{,}2\right) + \bar{\lambda}^2\right].$

α is a imperfection factor given by the table 4.2 VIII of NTC2018.

$\bar{\lambda} = \sqrt{\frac{A \cdot f_{yk}}{N_{cr}}}$. Normalized slenderness.

$N_{cr} = \frac{\pi^2 \cdot E \cdot J}{l_0^2}$. Eulerian normal force.

Other important check is the slenderness verification. The upper limit is given by the relation: $\lambda = l_0/i$. l_0 is the characteristic length and i is the radius of inertia.

Second Step. Bending verification.

Beams subjected to the compressive banding which is not sufficiently tightened at the sides must be checked against flex-torsional instability.

$$\frac{M_{ed}}{M_{b,Rd}} < 1$$

Where $M_{b,Rd} = \chi_{LT} \cdot W_y \cdot \frac{f_{yk}}{\gamma_{M1}}$.

The χ_{LT} coefficient is a reduction factor of flex-torsion instability. It is evaluated by:

$\chi_{LT} = \frac{1}{f} \cdot \frac{1}{\Phi_{LT}+\sqrt{\Phi_{LT}^2+\overline{\beta\lambda_{LT}}^2}} \leq K_{\chi}$.

$\Phi = \frac{1}{2}\left[1 + \alpha_{LT}\left(\overline{\lambda_{LT}} - \lambda_{LT,0}\right) + \beta \cdot \overline{\lambda_{LT}}^2\right]$.

$\overline{\lambda_{LT}} = \sqrt{\frac{W_y \cdot f_{yk}}{M_{cr}}}$. Normalized slenderness.

The others coefficient are proposed and defined by the NTC2018 (§4.2.4.1.3.2)

<u>Third Step</u>. Method A of NTC2018

Since we are in a situation of prismatic rods subject to N_{Ed} compression and bending moments $M_{y,Ed}$ and $M_{z,Ed}$ agents in the two main planes of inertia, in the presence of constraints that prevent torsional displacement, it will be necessary to check that this equation proposed by the Italian legislation.

$$\frac{N_{Ed} \cdot \gamma_{M1}}{\chi_{min} \cdot f_{yk} \cdot A} + \frac{M_{y,Ed} \cdot \gamma_{M1}}{W_y \cdot f_{yk} \cdot \left(1 - \frac{N_{Ed}}{N_{cr,y}}\right)} + \frac{M_{z,Ed} \cdot \gamma_{M1}}{W_z \cdot f_{yk} \cdot \left(1 - \frac{N_{Ed}}{N_{cr,z}}\right)} \leq 1$$

Where:

χ_{min}, in the minimum inflection factor related to the main inertial axis.

$N_{cr,y}$ *and* $N_{cr,z}$, Eulerian critic loads related to the own axis.

$M_{y,Ed}$ *and* $M_{z,Ed}$, equivalent mending moment according to the law.

4.4.DEFORMAZION VERIFICATION

From the analysis and with reference to the modelling shown above, the deformation values are obtained, divided by the various load conditions. The values are expressed in mm with positive deformations downwards.

The deformations in the different spans will be evaluated, taking as reference the segments C2-C3 for the first span and C8 for the main span with a length of 70 meters.

Table 31:Deformations values

Deformations in mm	**Span 1**	1/L	**Span 2**	1/L
	C2-C3	[L=49,5m]	**C8**	[L=70,0m]
Dead load steel deck	7,83	1/6322	32,89	1/2128
Dead load predalles	4,46	1/11098	18.38	1/3808
Permanent load	2,06	1/24029	6,37	1/10989
Crowd load	2,45	1/20204	3,38	1/21280
Traffic load	10,56	1/4688	40,75	1/20710
Total	**27,36**	**1/1809**	**101,76**	**1/687**

Looking at the results obtained, the deflection that the both spans will have to be paid for in such a way as not to have an excessive future deformation will be:

Table 32:Final apply deformation to the main beams

Pre - deformations in mm	**Span 1**	**Span 2**
	C2-C3	**C8**
	30	**130**

The values are evaluated taking into account the final service of the structure. This means that are evaluated using the static acceptance from the Italian regulation: “Collaudo statico”. The loads are multiplying times a coefficient in order to considering every agent during the nominal life.

4.5.FORCES ACTING ON SUPPORTS

4.5.1. VERTICAL ACTIONS

The maximum vertical actions transmitted to the supports and to the pier cap are easily identifiable from the shear and bending moment diagrams above.

4.5.2. HORIZONTAL ACTIONS

4.5.2.1. LONGITUDINAL BRAKING ACTION

The braking or acceleration action is a function of the total vertical load acting on the conventional lane no. 1 and is equal to:

$$Q = 0{,}6 \cdot (2 \cdot Q_{1k}) + 0{,}1 \cdot q_{1k} \cdot w_1 . L = 0{,}6 \cdot (2 \cdot 300) + 0{,}1 \cdot 9 \cdot 3{,}00 \cdot 59{,}75 = 197335\ daN$$

The force, applied at pavement level and acting along the lane axis, is uniformly distributed over the loaded length.

4.5.2.2. TRASVERSAL CENTRIFUGAL ACTION

The table 4.3 of the EN1991-1-2 explain the centrifugal forces to apply on the bridge carriageway level and radially to the carriageway axis. The horizontal radius of the carriageway centreline in this case is greater than 1500 meters, so the centrifugal forces must be neglected.

4.5.2.3. WIND ACTION AT UNLOADED DECK

The following table summarized all parameters useful to evaluate the horizontal forces acting on the steel deck during the unloading phase. The Q value represents the total horizontal force on the pier cup.

Table 33:wind action parameters at unloaded deck

h_{beam}	2,5	m
h_i	2,9	m
P	123,309	daN/m^2
μ_1	0,2	-
H_T	431,5814	daN/m
Q	25786,99	daN

Where:

h_{beam} is the height of the main beam.

h_i total heigh loaded.

H_T is the total horizontal forces along the carriageway.

4.5.2.4. *WIND ACTION AT LOADED DECK*

As did before for the unloaded case, now the following table explains the parameters used to calculate the total horizontal load acting at the carriageway and oh pier cap.

Table 34:wind action parameters at loaded deck

$\mathbf{h_{beam}}$	2,5	m
$\mathbf{h_i}$	5,9	m
P	135,7038	daN/m^2
$\mathbf{m_1}$	0,2	-
$\mathbf{H_T}$	882,0744	daN/m
Q	52703,95	daN

4.6.CONCRETE SLAB

The concrete slab has a width of 13.5 m and a thickness of 28 cm in the direction of the width is divided into 2 lateral cantilevers of 285 cm and two central spans of 390 cm.

As defined in the initial description, the first layer of the slab is composed of predalle, suitably shaped in function of the presence of shear connectors.

4.6.1. DEAD LOAD

The trusses of the prefabricated systems react to the weight of the slab as self-supporting. No scaffolding system will be provided for the side configurations as each row of pre-fabricated trusses is properly connected with a corrugated bar.

$q_{predalles} = 0{,}06 \cdot 2500 = 150\ kg/m^2$. Predalles own weight.

$q_{c\_casting} = 0{,}22\ \cdot 2500 = 550\ kg/m^2$. Casting concrete over the predalles.

$q_{tot} = 700\ kg/m^2$.

4.6.2. PERMANENT LOAD

$q_{sidewalk} = 0{,}20 \cdot 2500 = 500\ kg/m^2$. Sidewalk for pedestrian.

$q_{binder} = 0{,}10 \cdot 1750 = 175\ kg/m^2$. Surface finishing layer.

$q_{guardrail} = 150\ kg/m$. Guardrail

$q_{parapet} = 100\ kg/m$. Parapet

4.6.3. ACCIDENTAL CROWD LOAD

The crowd loading should be defined and represented as a uniformly distributed load equal to 5 kN/m^2.

4.6.4. ACCIDENTAL TRUCK LOAD

The loads Q_{1k} and Q_{2k} provided NTC2108 are considered. The footprint load of variable dimensions depending on the scheme under consideration is diffused at slab axis level upper considering that the slab is 28 cm high and the average thickness of the wearing course is 10 cm.

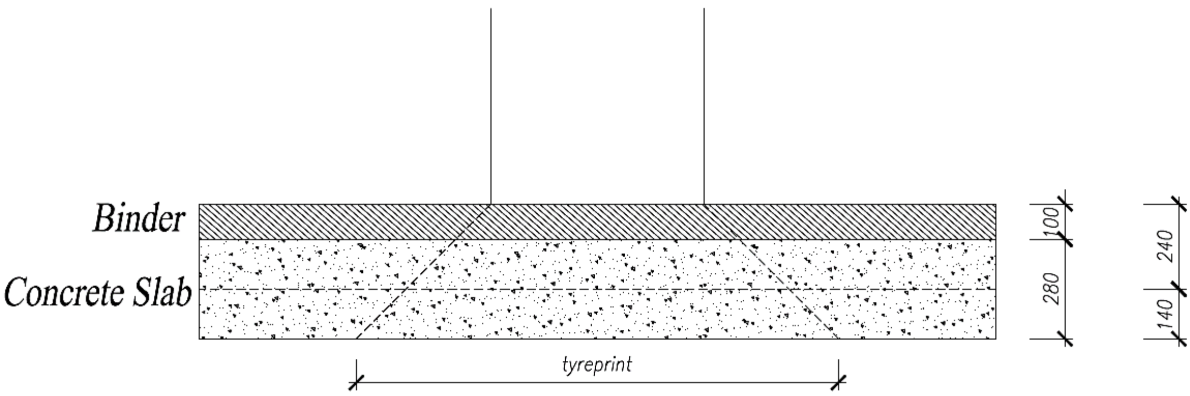

Figure 43: Vertical load diffusion..

4.6.4.1. CANTILEVER ZONE

<u>LOAD MODEL 1</u>

The following picture is taken from the Eurocode 1 where is expressed the guideline to evaluate the local effect of tyres print in the different load models.

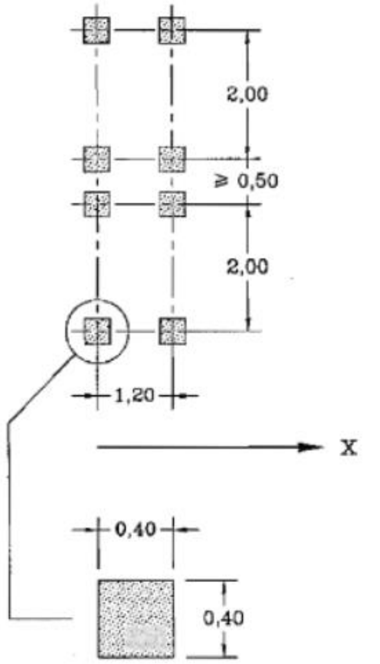

Figure 44: Application of tandem system

The scheme in this case is shown below with each geometrical dimension.

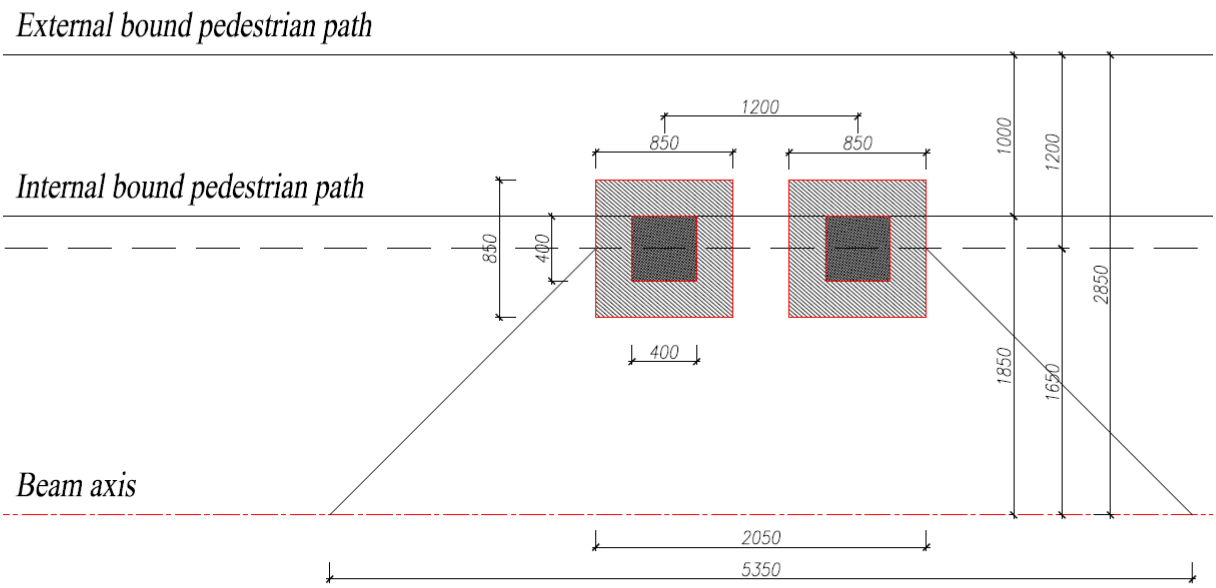

Figure 45:Horizontal diffusion of traffic load.

$$F_{1k} = \frac{Q_{1k}}{l_p + l_t + l_b} = \frac{300}{0,85 + 1,2 + 1,65} = 81,08\ kN = 8108,1\ daN$$

Where:

l_p, is the print width.

l_t, is the tandem distance.

l_b, is the distance between print and main beam.

The bending moment due to concentrated load is expressed as:

$$M_{1k} = F_{1k} \cdot l_b = 8108{,}1 \cdot 1{,}65 = 13378{,}4\ daNm$$

Instead, the bending moment due to distributed load is:

$$M_{1qk} = q_{1k} \cdot \frac{b^2}{2} = 9{,}00 \cdot \frac{1{,}85^2}{2} = 1540{,}1\ daNm$$

<u>LOAD MODEL 2</u>

In this case change the scheme system of applied load.

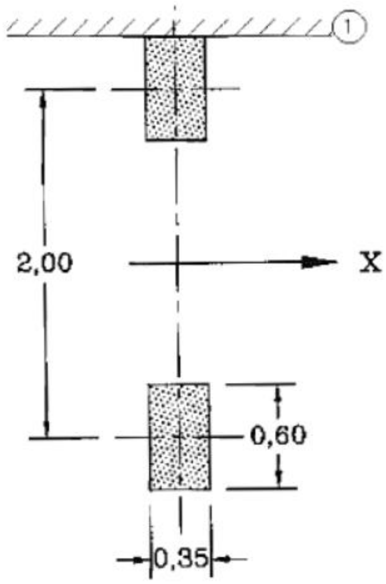

Figure 46: General scheme of load model 2 from Eurocode 1.

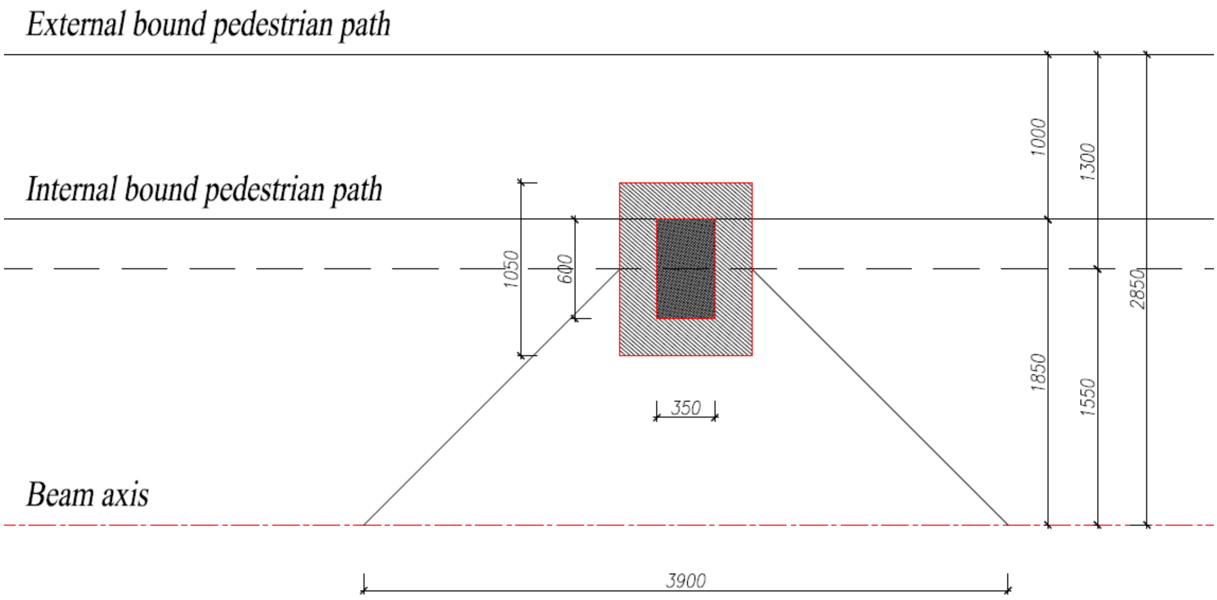

Figure 47:Horizzontal diffusion of load.

$$F_{2k} = \frac{Q_{2k}}{l_p + 2 \cdot l_b} = \frac{200}{0{,}8 + 2 \cdot 1{,}55} = 51{,}28\ kN = 5128{,}2\ daN$$

$$M_{2k} = F_{2k} \cdot l_b = 5128{,}2 \cdot 1{,}55 = 7948{,}7\ daNm$$

4.6.4.2. CENTRAL SPAN

In the following are analysed both configuration of load for lane 1 and 2 in the case of load model 1 because is the worst one.

Lane n_r.°1

$$F_{1k} = \frac{Q_{1k}}{r + l_t + \frac{i_t}{2}} = \frac{300}{0{,}4 + 1{,}2 + \frac{2{,}00}{2}} = 115{,}3kN = 11538{,}5daN$$

Lane n_r.°2

$$F_{1k} = \frac{Q_{1k}}{r + l_t + \frac{i_t}{2}} = \frac{200}{0{,}4 + 1{,}2 + \frac{2{,}00}{2}} = 76{,}9kN = 7692{,}3daN$$

4.6.5. VEHICLES IMPACT

It is considered a local action due to the impact of vehicles in diversion, equal to 100 kN. This horizontal transversal force is applied at 100 cm from the height of the road surface on a line 50 cm long and spreads all the way down to the middle of the slab.

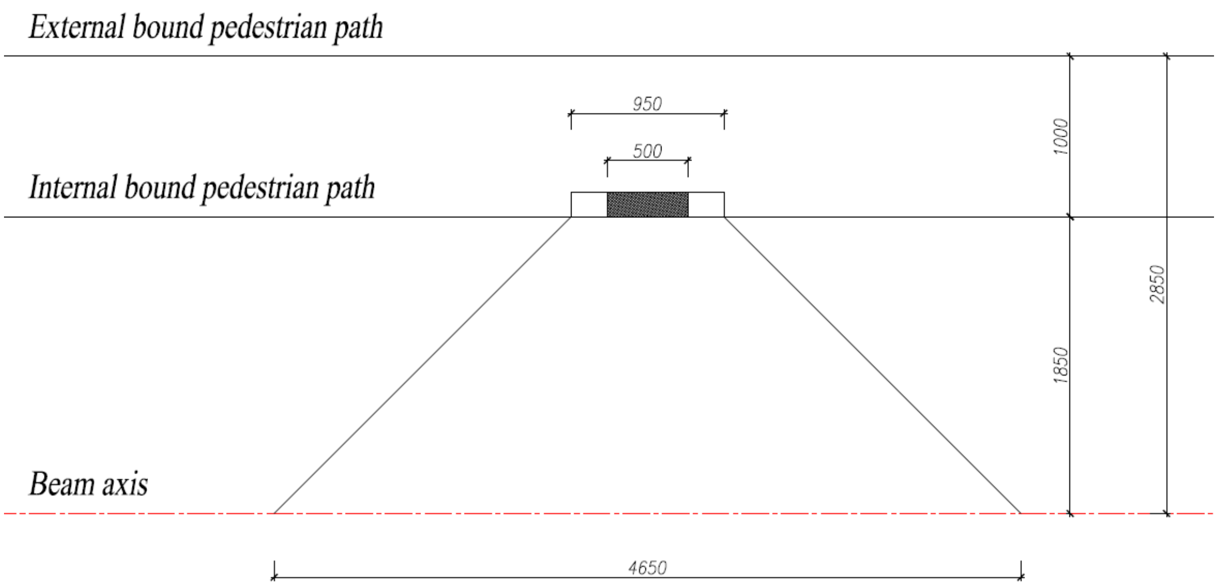

Figure 48:Horizzontal diffusion of vehicle impact

$N = \frac{100}{4,65} = 21,5 \frac{kN}{m} = 2150,5 \; daN/m$.

$M = 21,5 \cdot (1,00 + 0,10 + 0,28/2) = 26,67 \frac{kNm}{m} = 2666,7 \frac{daNm}{m}$.

4.6.6. DIAGRAMS

With reference to the modelling indicated, the following figures and table show the bending moment characteristics distinct by structural element and by load condition.

<u>Concrete Slab.</u>

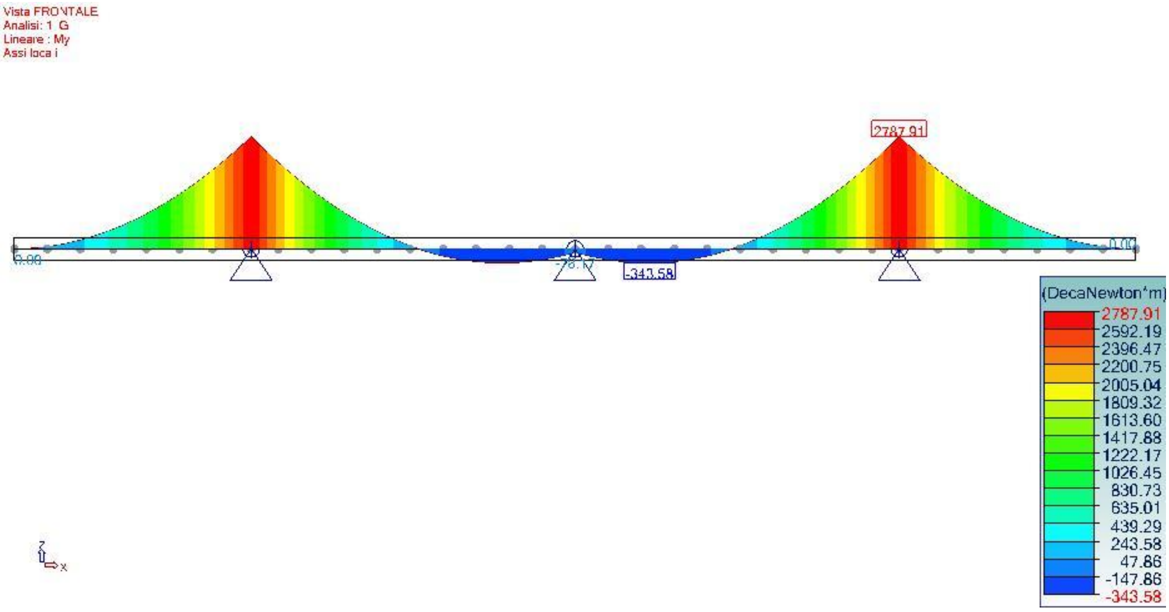

Figure 49: Bending moment of concrete slab.

<u>Permanent load.</u>

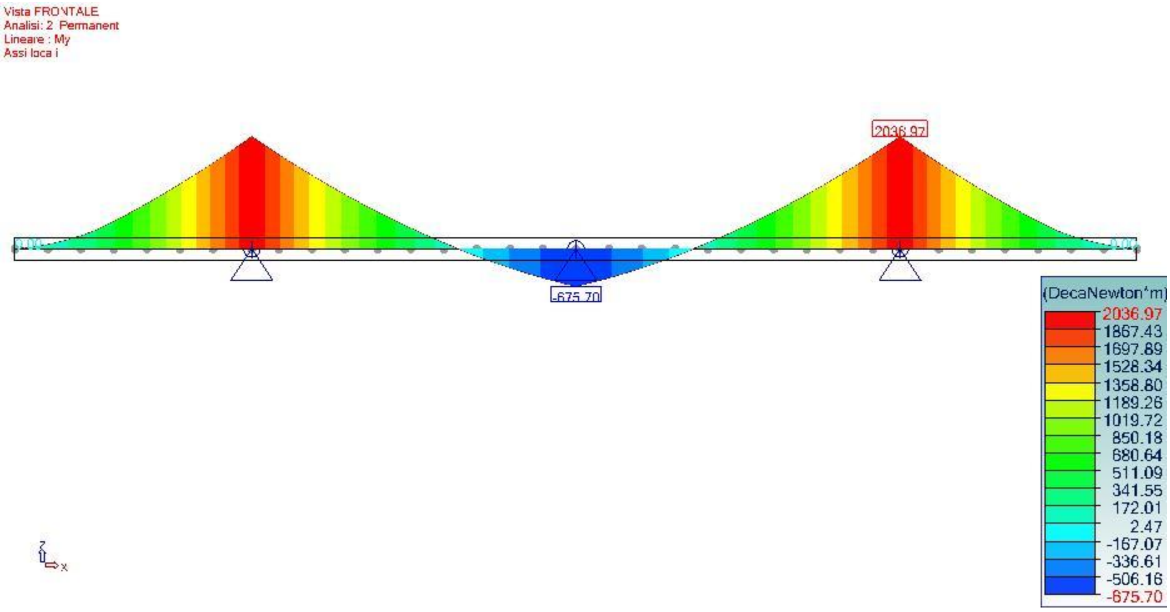

Figure 50:Bending moment of permanent load

Crowd load.

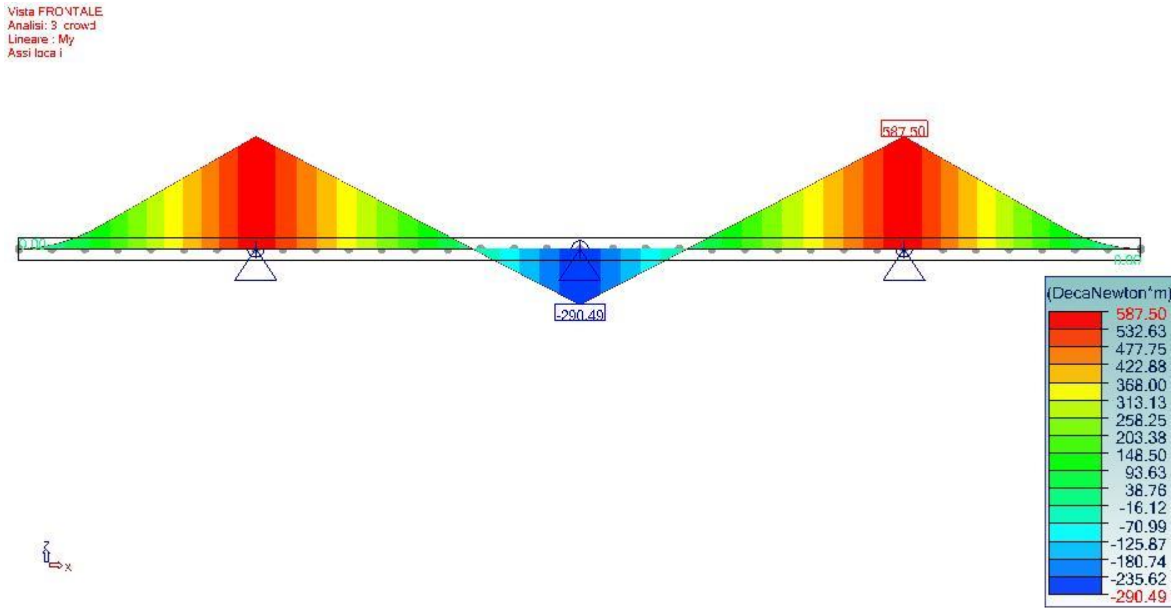

Figure 51: Bending moment of crowd effect.

Traffic load.

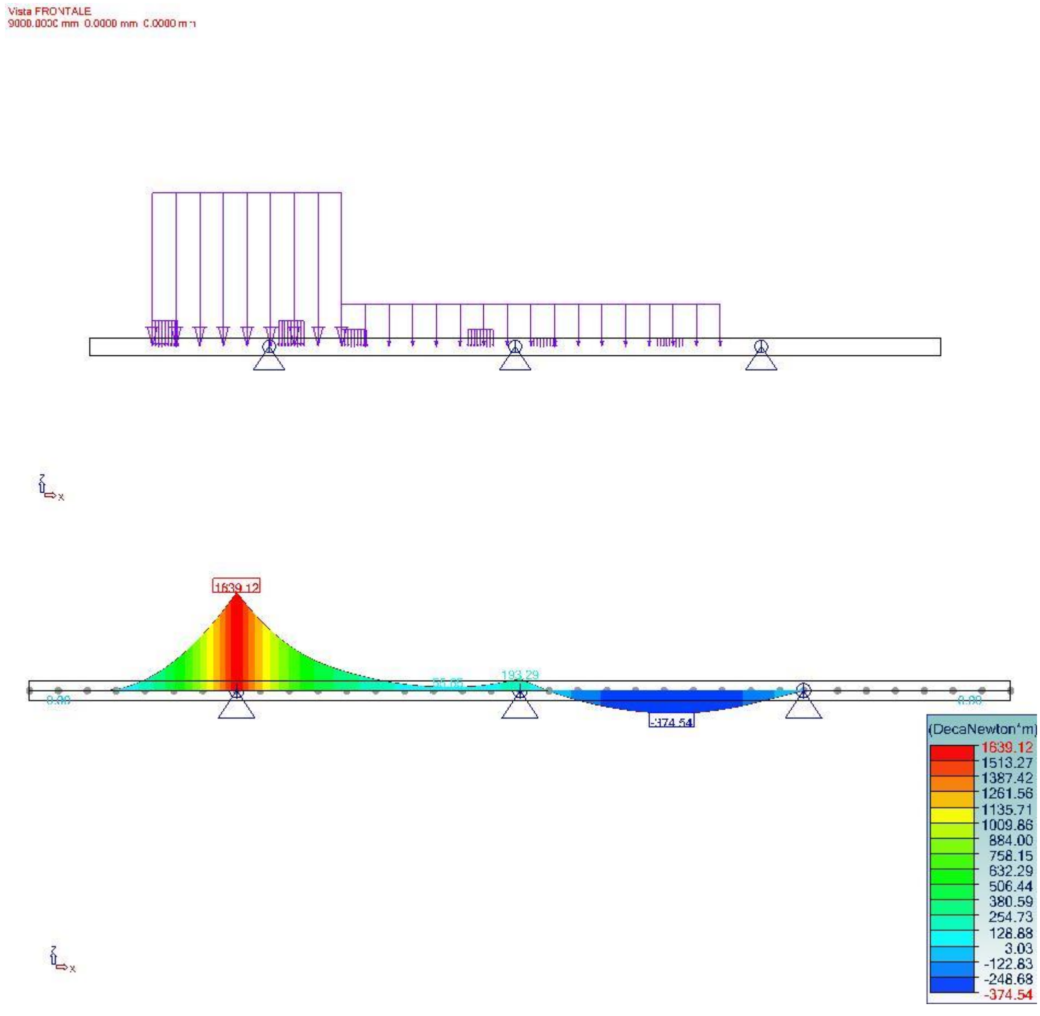

Figure 52:Bending moment of traffic load

In the next table are summarized all bending moment values.

	Concrete Slab [daNm]	Permanent [daNm]	Traffic load [daNm]	Crowd load [daNm]	Impact [daNm]
Cantilever	-2787,91	-2036,97	-1639,12	-587,5	-2666,67
Middle	343,58	-	374,54	-	-
Span	-	675,7	-193,29	290,49	-

4.6.7. REINFORCEMENT

<u>Preliminary phase – casting concrete.</u>

$q_{predalles} = 0{,}06 \cdot 2500 = 150\ \ kg/m/m$. Predalles own weight.

$q_{c\_casting} = 0{,}22\ \cdot 2500 = 550\ \ kg/m/m.$ Casting concrete over the predalles.

$q_{worker} = 100\ \ kg/m/m.$ Own weight of operator.

$q_{tot} = 800\, kg/m/m.$

$$M = -\frac{q_{tot} b^2}{2} = -800 \cdot \frac{2{,}85^2}{2} = -3249 \frac{daNm}{m} = -1353{,}75\ daNm/m$$

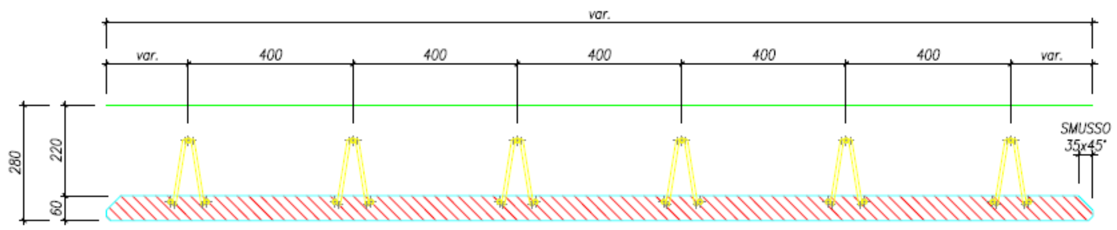

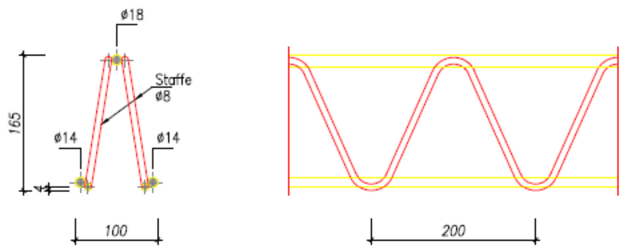

Figure 53:General system of predalle. Unit of major is in cm up and mm the cross-section below.

Upper reinforcement (1Φ18) $\sigma_{sup} = \frac{M}{b} \cdot \frac{1}{A_\phi} = \frac{135375}{16{,}5} \cdot \frac{1}{2{,}54} = 3224{,}18\ daN/cm^2$

Lowe reinforcement (2Φ14) $\sigma_{sup} = \frac{M}{b} \cdot \frac{1}{A_\phi} = \frac{135375}{16{,}5} \cdot \frac{1}{2 \cdot 1{,}54} = 2664{,}89\ daN/cm^2$

<u>Stability of compressed reinforcement.</u>

Moment of inertia $J = \frac{1}{4} \cdot \pi \cdot R^4 = \frac{1}{4} \cdot \pi \cdot 7{,}00^4 = 1886{,}74\ mm^4$

Eulerian critic load $N_{cr} = \frac{\pi^2 \cdot E \cdot J}{l_0^2} = \frac{\pi^2 \cdot 210.000 \cdot 1886,74}{200^2} = 97.710,5\ N$

dimensionless slenderness $\bar{\lambda} = \sqrt{A \cdot \frac{f_{yk}}{N_{cr}}} = \sqrt{\frac{\pi 14^2}{4} \cdot \frac{450}{97762,2}} = 0,84$

Coefficient $\Phi = \frac{1}{2}\left[1 + \alpha\left(\bar{\lambda} - 0,2\right) + \bar{\lambda}^2\right] = \frac{1}{2}\left[1 + 0,49(0,084 - 0,2) + 0,084^2\right] = 1,01$

Reduction factor $\chi = \frac{1}{\Phi + \sqrt{\Phi^2 + \bar{\lambda}^2}} = \frac{1}{1,01 + \sqrt{1,01^2 + 0,84^2}} = 0,43 \leq 1$

Action $N_{Ed} = \frac{\gamma_{G1} M_{Ed}}{b} = 1,35 \cdot \frac{147682}{16,5} 10 = 106659,1\ N$

Resisting force $N_{Rd} = \chi \cdot f_{yk} \cdot \frac{A}{\gamma_{M1}} = 27050,32\ N$

As we can see, the lower reinforcement doesn't satisfy the instability check, so as was defined, will be utilized a pre-cast predalles and not wire frame trusses system of predalles.

4.6.7.1. SLE -CANTILEVER

<u>Rare combination</u>

$$M = M_{c.slab} + M_{perm} + M_{acc.\ traffic} = -2787,91 - 2036,97 - 1639,12 - 587,5 = -7051,5\ \text{daNm}$$

Table 35: Rare combination values

RARE COMBINATION				
M	-7051,5	daNm		
cross section				
Base	100	cm		
Height	28	cm		
Ambietal coondition XF4				
reinforcement set				
upper reinforcement	Φ18/40 + Φ22/40			
lower reinforcement	Φ20/20			
σ_{cls}	62,08	daN/cm2	180	daN/cm2
σ_s	1755	daN/cm2	3600	daN/cm2

$$\sigma_{cls} < 0,6 f_{ck} = 180\ daN/cm^2$$

$$\sigma_s < 0,8 f_{yk} = 360\ daN/cm^2$$

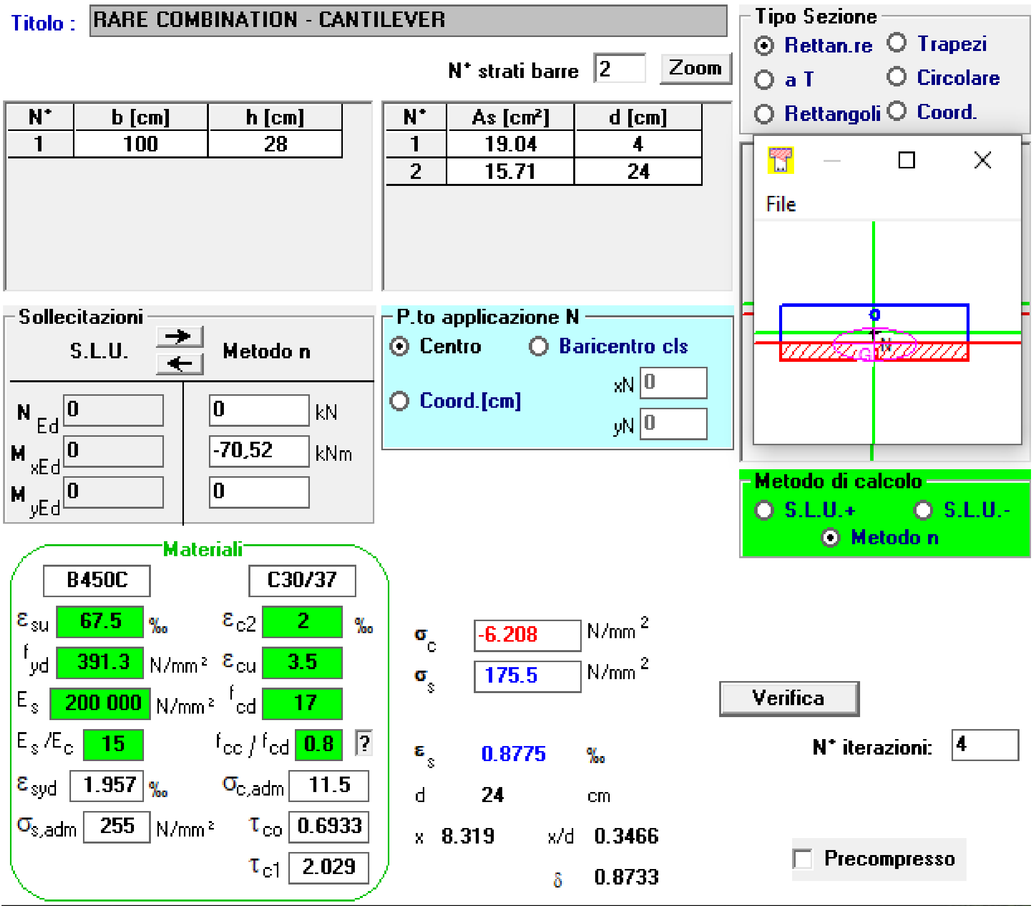

Figure 54:Stress result of rare combination.

Frequent combination

$$M = M_{c.slab} + M_{perm} + \psi_{1,1} \cdot M_{acc.\ traffic} = -2787{,}91 - 2036{,}97 + 0{,}75(-1639{,}12 - 587{,}5) = -6494{,}85 \text{ daNm}$$

Table 36:Frequent combination values

FREQUENT COMBINATION				
M	-6494,845	daNm/m		
cross section				
base	100	cm		
height	28	cm		
Ambietal coondition XF4				
reinforcement set				
upper reinforcement	Φ18/40 + Φ22/40			
lower reinforcement	Φ20/20			
σcls	57,6	daN/cm2	180	daN/cm2
σs	1628	daN/cm2	3600	daN/cm2

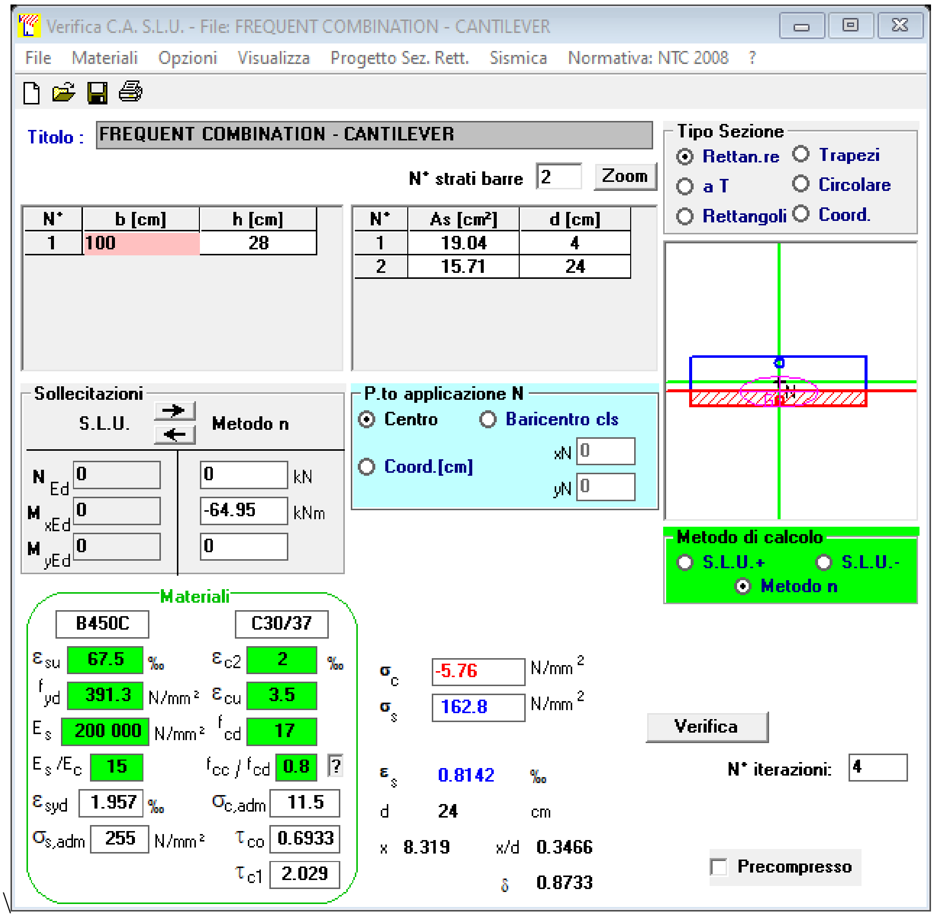

Figure 55:Stress result of frequent combination

Table 37: frequent SLE verification

FREQUENT COMBINATION VERIFICATION			
Concrete 30/37	fck	30	N/mm^2
	Rck	37	N/mm^2

Condizioni ambientali	Classe di esposizione
Ordinarie	X0, XC1, XC2, XC3, XF1
Aggressive	XC4, XD1, XS1, XA1, XA2, XF2, XF3
Molto aggressive	XD2, XD3, XS2, XS3, XA3, XF4

Exposure class XF4

low sensibility of the reinforcement

Gruppi di Esigenze	Condizioni ambientali	Combinazione di azioni	Armatura			
			Sensibile		Poco sensibile	
			Stato limite	w_k	Stato limite	w_k
A	Ordinarie	frequente	apertura fessure	$\leq w_2$	apertura fessure	$\leq w_3$
		quasi permanente	apertura fessure	$\leq w_1$	apertura fessure	$\leq w_2$
B	Aggressive	frequente	apertura fessure	$\leq w_1$	apertura fessure	$\leq w_2$
		quasi permanente	decompressione	-	apertura fessure	$\leq w_1$
C	Molto aggressive	frequente	formazione fessure	-	apertura fessure	$\leq w_1$
		quasi permanente	decompressione	-	apertura fessure	$\leq w_1$

w1	0,2 mm

w2	0,3	mm			
w3	0,4	mm			
σs	162,8	N/mm^2	As	1903,805148	mm^2
kt	0,6		As'	1570,796327	mm^2
b	1000	mm	Base		
h	280	mm	Height		
d	240	mm			
c	40	mm	Steel cover		
x	75,59429824	mm	Neutral axis		
Ecm	34330,80	N/mm^2	Concrete Young modulus		
n	15	-			
ae	6,116956823	-			
hc,eff	68,13523392	mm	effective height		
Ac,eff	68135,23392	mm^2	Effective concrete area		
As	1570,796327	mm^2	Steel Area		
ρeff	0,023054098				
fctm	3,33	N/mm^2			
εsm	0,000304189		Average deformation		
Δsm	140,726732		Average crack distance		
k1	0,8				
k2	0,5				
k3	3,4				
k4	0,425		wk	0,111278658	SATISFY

Quasi-permanent combination

$$M = M_{c.slab} + M_{perm} = -2787{,}91 - 2036{,}97 = -4824{,}88 \text{ daNm}$$

Table 38:Quasi-permanent combination values

QUASI-PERMANENT COMBINATION				
M	-4824,88	daNm/m		
cross section				
base	100	cm		
height	28	cm		
Ambietal coondition XF4				
reinforcement set				
upper reinforcement	Φ18/40 + Φ22/40			
lower reinforcement	Φ20/20			
σ_{cls}	42,79	daN/cm^2	135	daN/cm^2
σ_s	1210	daN/cm^2	3600	daN/cm^2

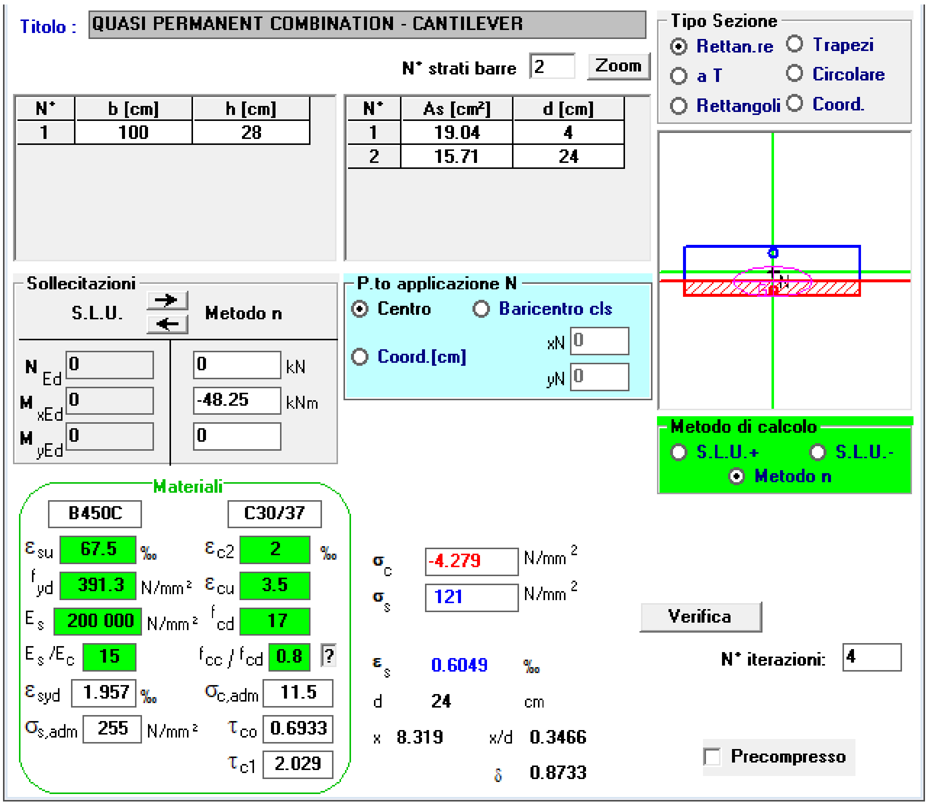

Figure 56:Stress result of frequent combination

Table 39: Quasi-permanent SLE verification

QUASI-PERMANENT COMBINATION VERIFICATION			
Concrete 30/37	fck	30	N/mm^2
	Rck	37	N/mm^2

Condizioni ambientali	Classe di esposizione
Ordinarie	X0, XC1, XC2, XC3, XF1
Aggressive	XC4, XD1, XS1, XA1, XA2, XF2, XF3
Molto aggressive	XD2, XD3, XS2, XS3, XA3, XF4

Exposure class XF4

low sensibility of the reinforcement

Gruppi di Esigenze	Condizioni ambientali	Combinazione di azioni	Armatura			
			Sensibile		Poco sensibile	
			Stato limite	w_k	Stato limite	w_k
A	Ordinarie	frequente	apertura fessure	$\leq w_2$	apertura fessure	$\leq w_3$
		quasi permanente	apertura fessure	$\leq w_1$	apertura fessure	$\leq w_2$
B	Aggressive	frequente	apertura fessure	$\leq w_1$	apertura fessure	$\leq w_2$
		quasi permanente	decompressione	-	apertura fessure	$\leq w_1$
C	Molto aggressive	frequente	formazione fessure	-	apertura fessure	$\leq w_1$
		quasi permanente	decompressione	-	apertura fessure	$\leq w_1$

w1	0,2	mm			
w2	0,3	mm			
w3	0,4	mm			
σs	121	N/mm^2	As	1903,805148	mm^2
kt	0,6		As'	1570,796327	mm^2

b	1000	mm	Base
h	280	mm	Height
d	240	mm	
c	40	mm	Steel cover
x	75,59429824	mm	Neutral axis
Ecm	34330,80	N/mm²	Concrete Young modulus
n	15	-	
ae	6,116956823	-	
hc,eff	68,13523392	mm	effective height
Ac,eff	68135,23392	mm²	Effective concrete area
As	1570,796327	mm²	Steel Area
ρeff	0,023054098		
fctm	3,33	N/mm²	
εsm	0,000105		Average deformation
Δsm	140,726732		Average crack distance
k1	0,8		
k2	0,5		
k3	3,4		
k4	0,425		wk 0,08270711 SATISFY

4.6.7.2. SLE -MIDDLE

<u>Preliminary phase – casting concrete.</u>

$q_{predalles} = 0{,}06 \cdot 2500 = 150\ kg/m/m\,.$ Predalles own weight.

$q_{c\_casting} = 0{,}22\ \cdot 2500 = 550\ kg/m/m.$ Casting concrete over the predalles.

$q_{worker} = 100\ kg/m/m.$ Own weight of operator.

$q_{tot} = 800\, kg/m/m.$

$$M = -\frac{q_{tot} b^2}{2} = -800 \cdot \frac{3{,}9^2}{2} = -6084 \frac{daNm}{m} = -2535\ daNm/m$$

Upper reinforcement (1Φ18) $\sigma_{sup} = \frac{M}{b} \cdot \frac{1}{A_\phi} = \frac{253500}{16{,}5} \cdot \frac{1}{2{,}54} = 6037{,}53\ daN/cm^2$

Lowe reinforcement (2Φ14) $\sigma_{inf} = \frac{M}{b} \cdot \frac{1}{A_\phi} = \frac{253500}{16{,}5} \cdot \frac{1}{2 \cdot 1{,}54} = 4990{,}2\ daN/cm^2$

<u>Rare combination</u>

$$M = M_{c.slab} + M_{perm} + M_{acc.\ traffic} = 343{,}58 + 374{,}54 = 718{,}12\ \text{daNm}$$

Table 40: Rare combination values

RARE COMBINATION		
M	718,12	daNm
cross section		
Base	100	cm
Height	28	cm
Ambietal coondition XF4		

reinforcement set				
upper reinforcement	Φ18/40 + Φ22/40			
lower reinforcement	Φ20/20			
σ_{cls}	6,644	daN/cm^2	180	daN/cm^2
σ_s	216,7	daN/cm^2	3600	daN/cm^2

$$\sigma_{cls} < 0{,}6 f_{ck} = 180\ daN/cm^2$$

$$\sigma_s < 0{,}8 f_{yk} = 360\ daN/cm^2$$

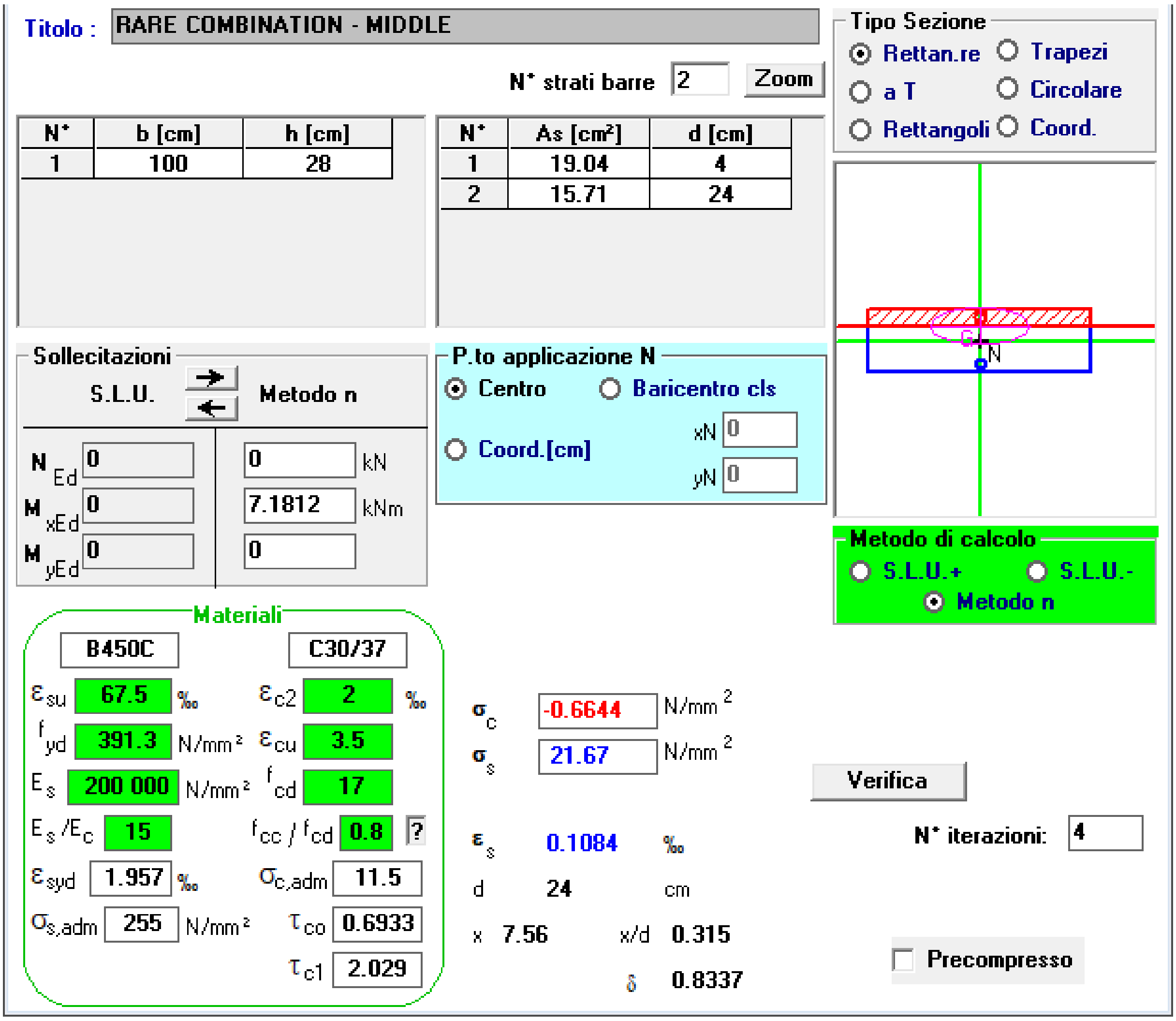

Figure 57:Stress result of rare combination.

Frequent combination

$$M = M_{c.slab} + M_{perm} + \psi_{1,1} \cdot M_{acc.\ traffic} = 343{,}58 + 0{,}75(374{,}54) = 624{,}49\ \text{daNm}$$

Table 41:Frequent combination values

FREQUENT COMBINATION				
M	624,49	daNm/m		
cross section				
base	100	cm		
height	28	cm		
Ambietal coondition XF4				
reinforcement set				
upper reinforcement	Φ18/40 + Φ22/40			
lower reinforcement	Φ20/20			
σcls	5,778	daN/cm2	180	daN/cm2
σs	188,5	daN/cm2	3600	daN/cm2

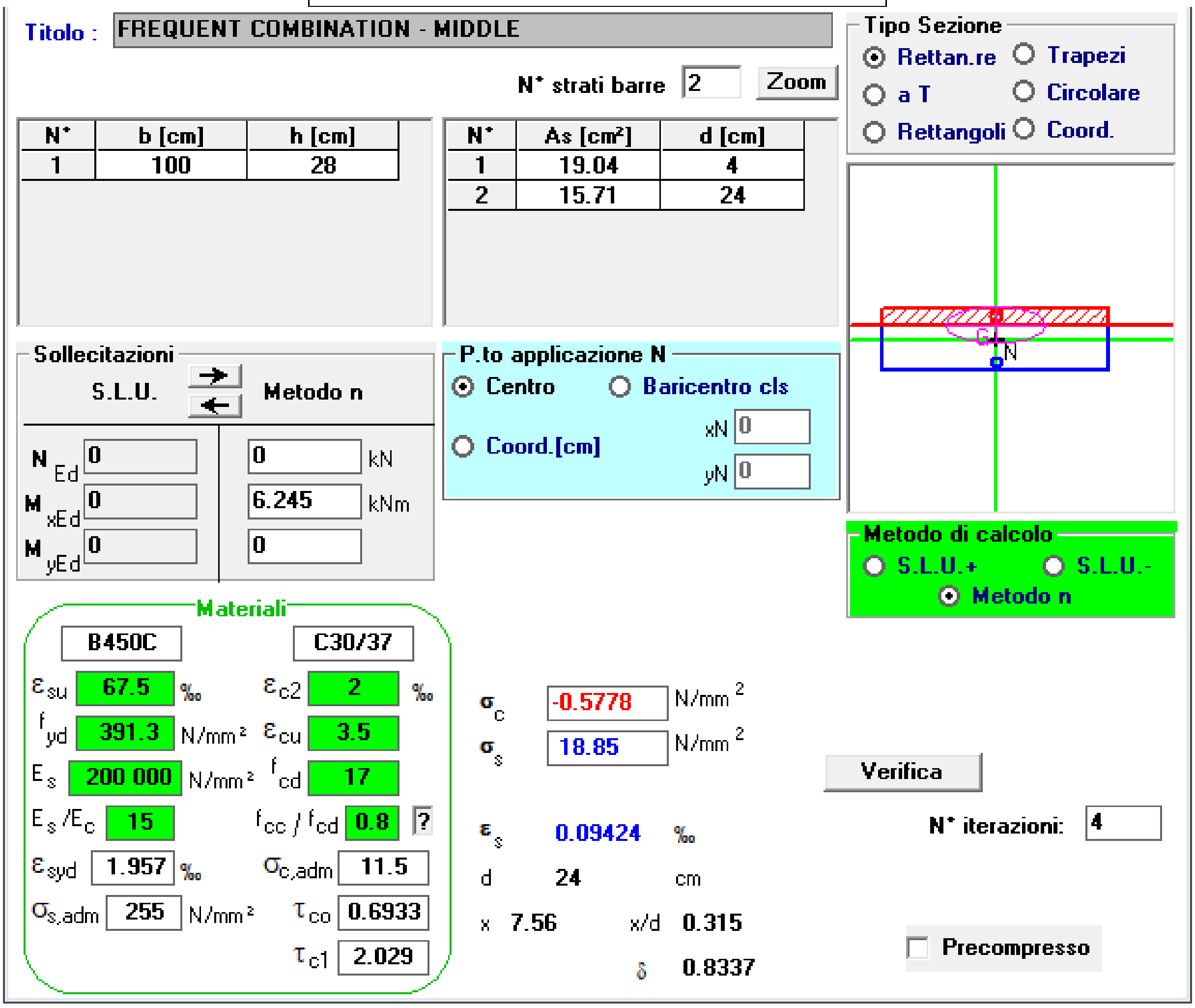

Figure 58:Stress result of frequent combination

Table 42: Frequent SLE verification

FREQUENT COMBINATION VERIFICATION						
Concrete 30/37			fck	30	N/mm^2	
			Rck	37	N/mm^2	

Condizioni ambientali	Classe di esposizione
Ordinarie	X0, XC1, XC2, XC3, XF1
Aggressive	XC4, XD1, XS1, XA1, XA2, XF2, XF3
Molto aggressive	XD2, XD3, XS2, XS3, XA3, XF4

Exposure class XF4

low sensibility of the reinforcement

Gruppi di Esigenze	Condizioni ambientali	Combinazione di azioni	Armatura			
			Sensibile		Poco sensibile	
			Stato limite	w_k	Stato limite	w_k
A	Ordinarie	frequente	apertura fessure	$\leq w_2$	apertura fessure	$\leq w_3$
		quasi permanente	apertura fessure	$\leq w_1$	apertura fessure	$\leq w_2$
B	Aggressive	frequente	apertura fessure	$\leq w_1$	apertura fessure	$\leq w_2$
		quasi permanente	decompressione	-	apertura fessure	$\leq w_1$
C	Molto aggressive	frequente	formazione fessure	-	apertura fessure	$\leq w_1$
		quasi permanente	decompressione	-	apertura fessure	$\leq w_1$

w1	0,2	mm				
w2	0,3	mm				
w3	0,4	mm				
σs	18,85	N/mm^2		As	1903,805148	mm^2
kt	0,6			As'	1570,796327	mm^2
b	1000	mm	Base			
h	280	mm	Height			
d	240	mm				
c	40	mm	Steel cover			
x	75,59429824	mm	Neutral axis			
Ecm	34330,80	N/mm^2	Concrete Young modulus			
n	15	-				
ae	6,116956823	-				
hc,eff	68,13523392	mm	effective height			
Ac,eff	68135,23392	mm^2	Effective concrete area			
As	1570,796327	mm^2	Steel Area			
ρeff	0,023054098					
fctm	3,33	N/mm^2				
εsm	0,000381288		Average deformation			
Δsm	140,726732		Average crack distance			
k1	0,8					
k2	0,5					
k3	3,4					
k4	0,425			wk	0,0912175	SATISFY

Quasi-permanent combination

$$M = M_{c.slab} + M_{perm} = 343{,}58 \text{ daNm}$$

Table 43:Quasi-permanent combination values

QUASI-PERMANENT COMBINATION				
M	343,58	daNm/m		
cross section				
base	100	cm		
height	28	cm		
Ambietal coondition XF4				
reinforcement set				
upper reinforcement	Φ18/40 + Φ22/40			
lower reinforcement	Φ20/20			
σ_{cls}	3,179	daN/cm^2	135	daN/cm^2
σ_s	103,7	daN/cm^2	3600	daN/cm^2

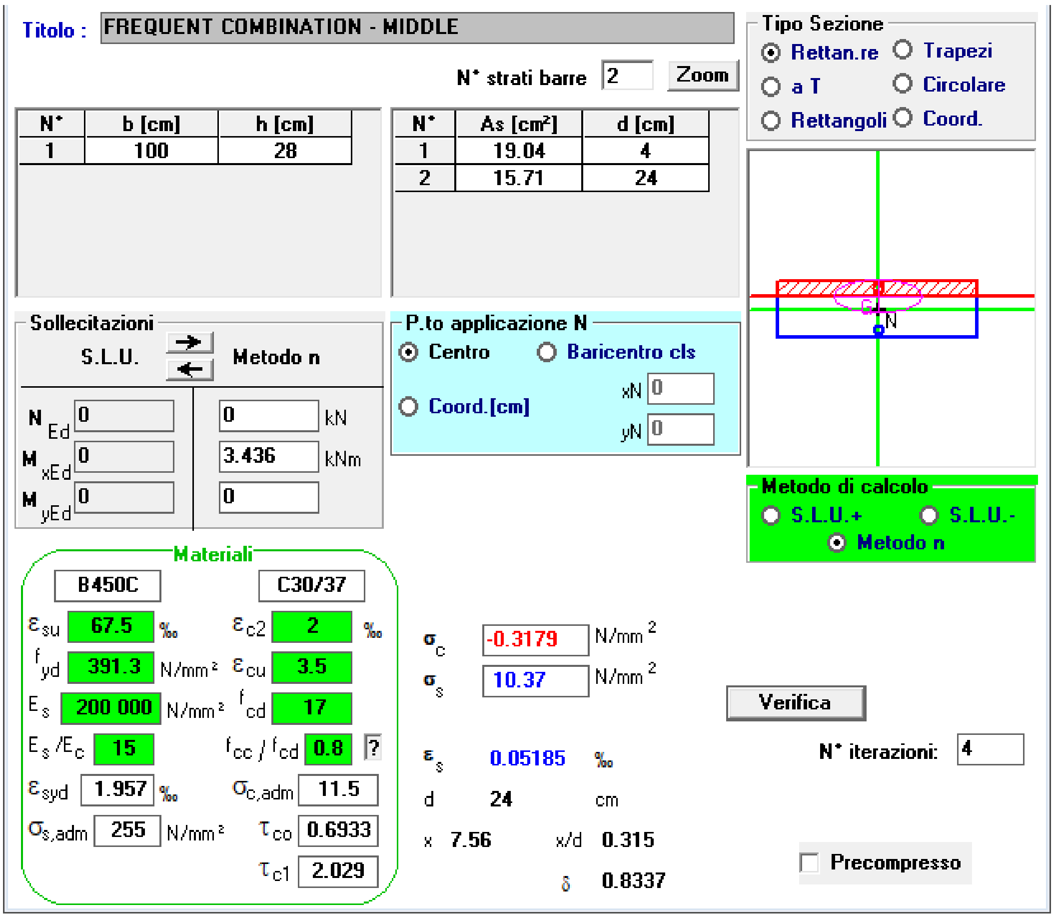

Figure 59:Stress result of frequent combination

Table 44: Quasi-permanent SLE verification

QUASI-PERMANENT COMBINATION VERIFICATION					
Concrete 30/37			fck	30	N/mm^2
			Rck	37	N/mm^2

Condizioni ambientali	Classe di esposizione
Ordinarie	X0, XC1, XC2, XC3, XF1
Aggressive	XC4, XD1, XS1, XA1, XA2, XF2, XF3
Molto aggressive	XD2, XD3, XS2, XS3, XA3, XF4

Exposure class XF4

low sensibility of the reinforcement

Gruppi di Esigenze	Condizioni ambientali	Combinazione di azioni	Armatura			
			Sensibile		Poco sensibile	
			Stato limite	w_k	Stato limite	w_k
A	Ordinarie	frequente	apertura fessure	$\leq w_2$	apertura fessure	$\leq w_3$
		quasi permanente	apertura fessure	$\leq w_1$	apertura fessure	$\leq w_2$
B	Aggressive	frequente	apertura fessure	$\leq w_1$	apertura fessure	$\leq w_2$
		quasi permanente	decompressione	-	apertura fessure	$\leq w_1$
C	Molto aggressive	frequente	formazione fessure	-	apertura fessure	$\leq w_1$
		quasi permanente	decompressione	-	apertura fessure	$\leq w_1$

w1	0,2	mm			
w2	0,3	mm			
w3	0,4	mm			
σs	10,37	N/mm^2	As	1903,805148	mm^2
kt	0,6		As'	1570,796327	mm^2
b	1000	mm	Base		
h	280	mm	Height		
d	240	mm			
c	40	mm	Steel cover		
x	75,59429824	mm	Neutral axis		
Ecm	34330,80	N/mm^2	Concrete Young modulus		
n	15	-			
ae	6,116956823	-			
hc,eff	68,13523392	mm	effective height		
Ac,eff	68135,23392	mm^2	Effective concrete area		
As	1570,796327	mm^2	Steel Area		
ρeff	0,023054098				
fctm	3,33	N/mm^2			
εsm	0,000422		Average deformation		
Δsm	140,726732		Average crack distance		
k1	0,8				
k2	0,5				
k3	3,4				
k4	0,425		wk	0,100878	SATISFY

4.6.7.3. SLE -SPAN

Preliminary phase – casting concrete.

$q_{predalles} = 0{,}06 \cdot 2500 = 150\ kg/m/m$. Predalles own weight.

$q_{c\_casting} = 0{,}22\ \cdot 2500 = 550\ kg/m/m.$ Casting concrete over the predalles.

$q_{worker} = 100\ kg/m/m.$ Own weight of operator.

$q_{tot} = 800\, kg/m/m.$

$$M = -\frac{q_{tot} b^2}{2} = -800 \cdot \frac{3{,}9^2}{2} = -6084 \frac{daNm}{m} = -2535\ daNm/m$$

Upper reinforcement (1Φ18) $\sigma_{sup} = \frac{M}{b} \cdot \frac{1}{A_\phi} = \frac{253500}{16{,}5} \cdot \frac{1}{2{,}54} = 6037{,}53\ daN/cm^2$

Lowe reinforcement (2Φ14) $\sigma_{inf} = \frac{M}{b} \cdot \frac{1}{A_\phi} = \frac{253500}{16{,}5} \cdot \frac{1}{2 \cdot 1{,}54} = 4990{,}2\ daN/cm^2$

Rare combination

$$M = M_{c.slab} + M_{perm} + M_{acc.\ traffic} = 0 + 675{,}7 + 193{,}29 + 290{,}49 = 1159{,}48 \text{ daNm}$$

Table 45: Rare combination values

RARE COMBINATION				
M	1159,48	daNm		
cross section				
Base	100	cm		
Height	28	cm		
Ambietal coondition XF4				
reinforcement set				
upper reinforcement	Φ18/40 + Φ22/40			
lower reinforcement	Φ20/20			
σ_{cls}	10,18	daN/cm²	180	daN/cm²
σ_s	332	daN/cm²	3600	daN/cm²

$$\sigma_{cls} < 0{,}6 f_{ck} = 180\ daN/cm^2$$

$$\sigma_s < 0{,}8 f_{yk} = 360\ daN/cm^2$$

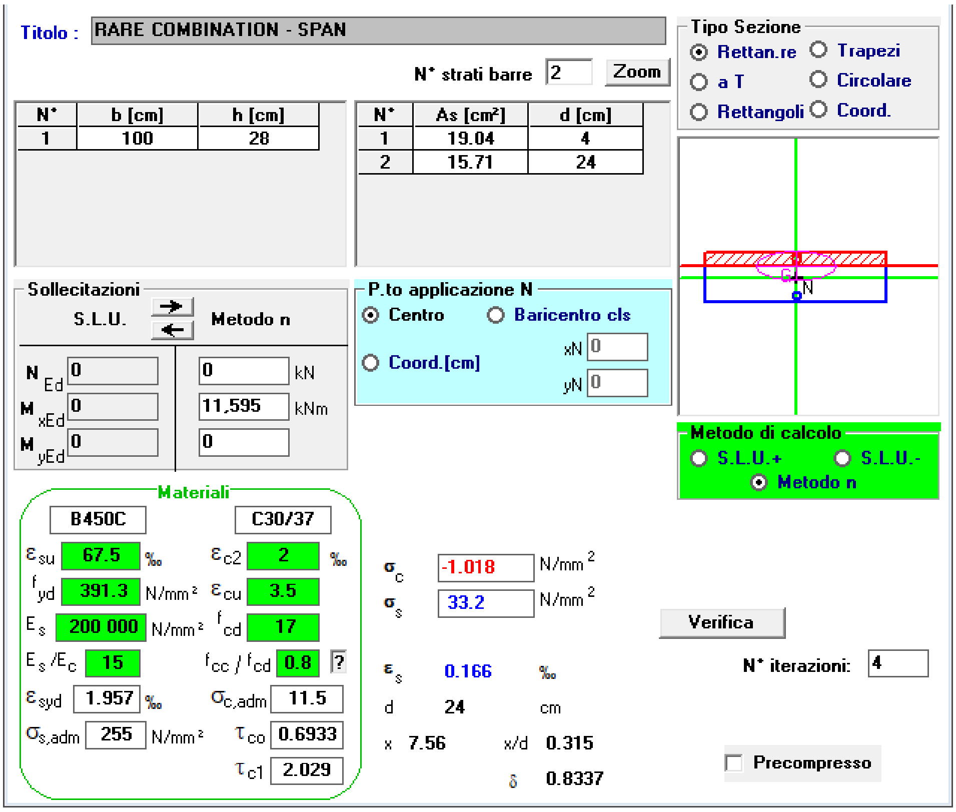

Figure 60:Stress result of rare combination.

Frequent combination

$$M = M_{c.slab} + M_{perm} + \psi_{1,1} \cdot M_{acc.\ traffic} = 0 + 675{,}7 + 0{,}75(193{,}29 + 290{,}49) = 1038{,}535 \text{ daNm}$$

Table 46:Frequent combination values

FREQUENT COMBINATION				
M	1038,535	daNm/m		
cross section				
base	100	cm		
height	28	cm		
Ambietal coondition XF4				
reinforcement set				
upper reinforcement	Φ18/40 + Φ22/40			
lower reinforcement	Φ20/20			
σcls	9,61	daN/cm2	180	daN/cm2
σs	313,4	daN/cm2	3600	daN/cm2

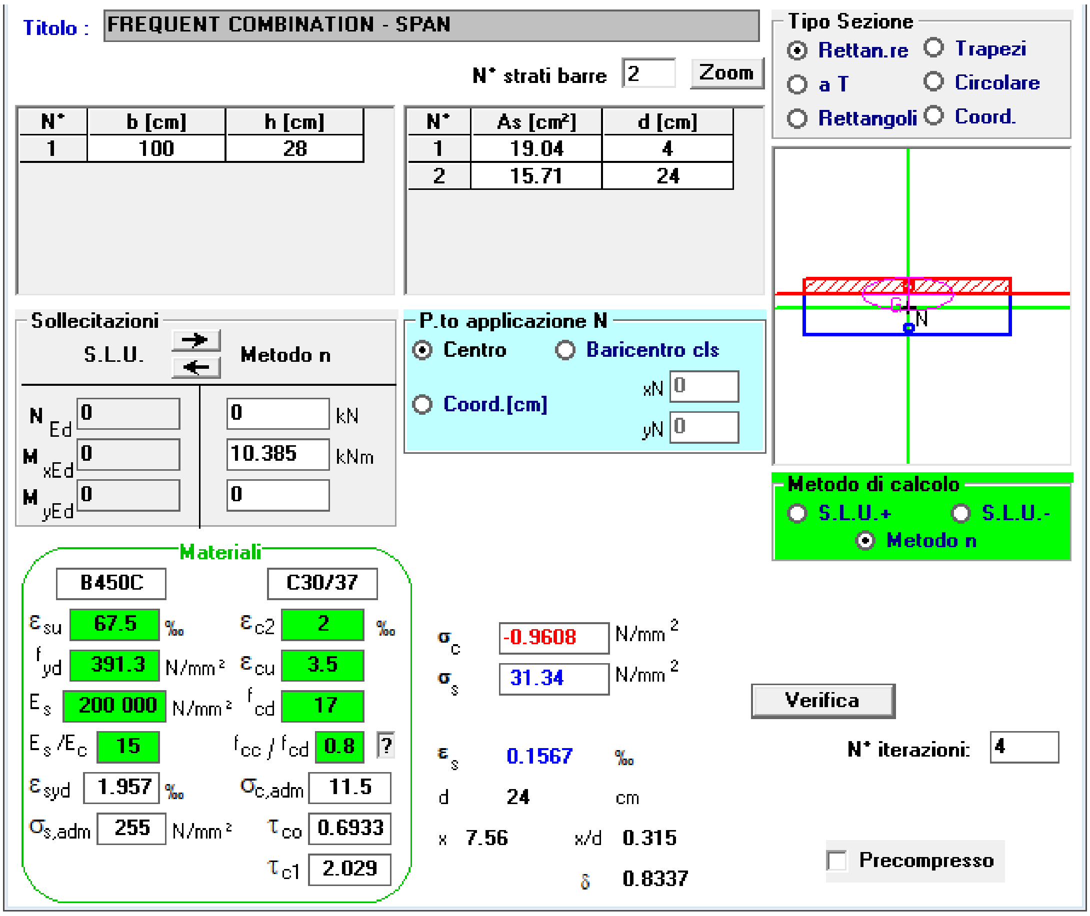

Figure 61:Stress result of frequent combination

Table 47: Frequent SLE verification

FREQUENT COMBINATION VERIFICATION			
Concrete 30/37	fck	30	N/mm²
	Rck	37	N/mm²

Condizioni ambientali	Classe di esposizione
Ordinarie	X0, XC1, XC2, XC3, XF1
Aggressive	XC4, XD1, XS1, XA1, XA2, XF2, XF3
Molto aggressive	XD2, XD3, XS2, XS3, XA3, XF4

Exposure class XF4

low sensibility of the reinforcement

Gruppi di Esigenze	Condizioni ambientali	Combinazione di azioni	Armatura			
			Sensibile		Poco sensibile	
			Stato limite	w_k	Stato limite	w_k
A	Ordinarie	frequente	apertura fessure	$\leq w_2$	apertura fessure	$\leq w_3$
		quasi permanente	apertura fessure	$\leq w_1$	apertura fessure	$\leq w_2$
B	Aggressive	frequente	apertura fessure	$\leq w_1$	apertura fessure	$\leq w_2$
		quasi permanente	decompressione	-	apertura fessure	$\leq w_1$
C	Molto aggressive	frequente	formazione fessure	-	apertura fessure	$\leq w_1$
		quasi permanente	decompressione	-	apertura fessure	$\leq w_1$

w1	0,2	mm
w2	0,3	mm
w3	0,4	mm

σs	18,85	N/mm^2	As	1903,805148	mm^2
kt	0,6		As'	1570,796327	mm^2
b	1000	mm	Base		
h	280	mm	Height		
d	240	mm			
c	40	mm	Steel cover		
x	75,59429824	mm	Neutral axis		
Ecm	34330,80	N/mm^2	Concrete Young modulus		
n	15	-			
ae	6,116956823	-			
hc,eff	68,13523392	mm	effective height		
Ac,eff	68135,23392	mm^2	Effective concrete area		
As	1570,796327	mm^2	Steel Area		
ρeff	0,023054098				
fctm	3,33	N/mm^2			
εsm	0,000381288		Average deformation		
Δsm	140,726732		Average crack distance		
k1	0,8				
k2	0,5				
k3	3,4				
k4	0,425		wk	0,0912175	SATISFY

Quasi-permanent combination

$$M = M_{c.slab} + M_{perm} = 675{,}7 \text{ daNm}$$

Table 48:Quasi-permanent combination values

QUASI-PERMANENT COMBINATION				
M	657,7	daNm/m		
cross section				
base	100	cm		
height	28	cm		
Ambietal coondition XF4				
reinforcement set				
upper reinforcement	Φ18/40 + Φ22/40			
lower reinforcement	Φ20/20			
σ_{cls}	6,251	daN/cm^2	135	daN/cm^2
σ_s	203,9	daN/cm^2	3600	daN/cm^2

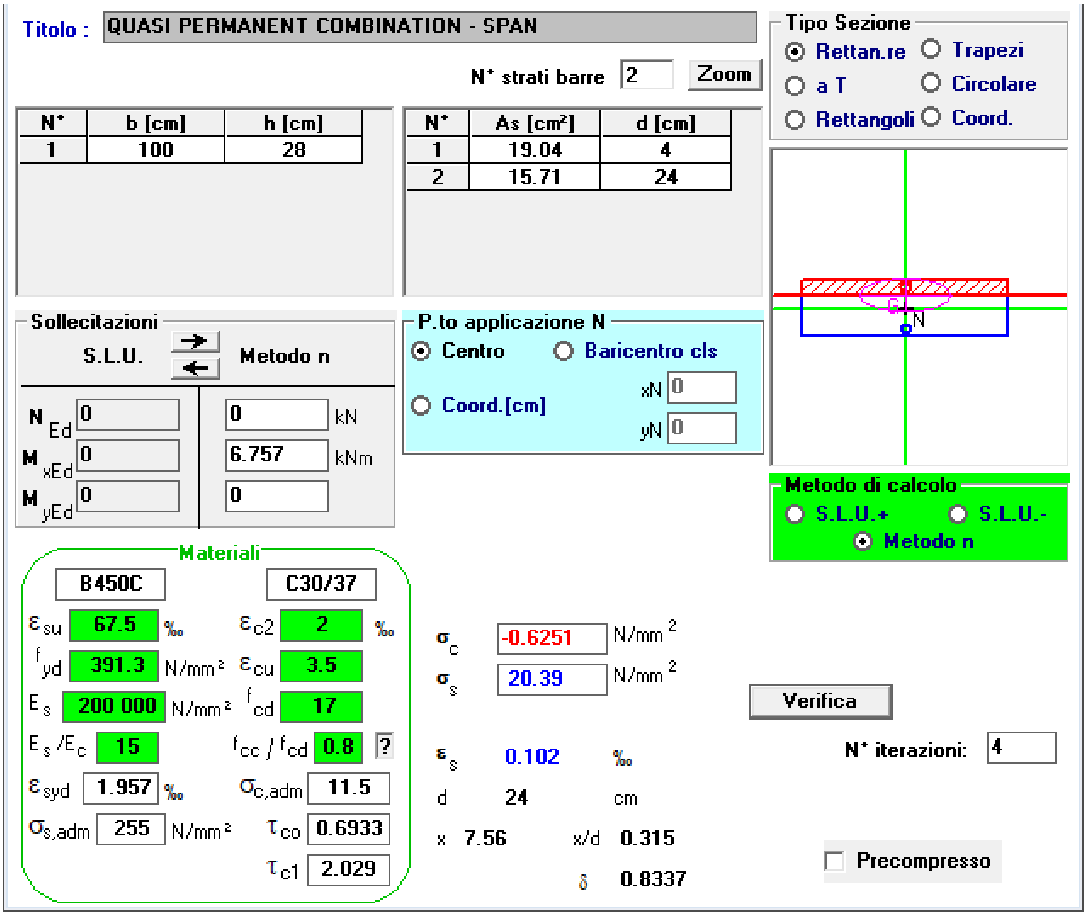

Figure 62:Stress result of frequent combination

Table 49: Quasi-permanent SLE verification

QUASI-PERMANENT COMBINATION VERIFICATION			
Concrete 30/37	fck	30	N/mm^2
	Rck	37	N/mm^2

Condizioni ambientali	Classe di esposizione
Ordinarie	X0, XC1, XC2, XC3, XF1
Aggressive	XC4, XD1, XS1, XA1, XA2, XF2, XF3
Molto aggressive	XD2, XD3, XS2, XS3, XA3, XF4

Exposure class XF4

low sensibility of the reinforcement

Gruppi di Esigenze	Condizioni ambientali	Combinazione di azioni	Armatura			
			Sensibile		Poco sensibile	
			Stato limite	w_k	Stato limite	w_k
A	Ordinarie	frequente	apertura fessure	$\leq w_2$	apertura fessure	$\leq w_3$
		quasi permanente	apertura fessure	$\leq w_1$	apertura fessure	$\leq w_2$
B	Aggressive	frequente	apertura fessure	$\leq w_1$	apertura fessure	$\leq w_2$
		quasi permanente	decompressione	-	apertura fessure	$\leq w_1$
C	Molto aggressive	frequente	formazione fessure	-	apertura fessure	$\leq w_1$
		quasi permanente	decompressione	-	apertura fessure	$\leq w_1$

w1	0,2	mm
w2	0,3	mm
w3	0,4	mm

σs	20,39	N/mm^2		As	1903,805148	mm^2
kt	0,6			As'	1570,796327	mm^2
b	1000	mm	Base			
h	280	mm	Height			
d	240	mm				
c	40	mm	Steel cover			
x	75,59429824	mm	Neutral axis			
Ecm	34330,80	N/mm^2	Concrete Young modulus			
n	15	-				
ae	6,116956823	-				
hc,eff	68,13523392	mm	effective height			
Ac,eff	68135,23392	mm^2	Effective concrete area			
As	1570,796327	mm^2	Steel Area			
ρeff	0,023054098					
fctm	3,33	N/mm^2				
εsm	0,000374		Average deformation			
Δsm	140,726732		Average crack distance			
k1	0,8					
k2	0,5					
k3	3,4					
k4	0,425			wk	0,089463	SATISFY

4.6.7.4. SLU

The general configuration of reinforcement is the following.

Table 50:General set of concrete slab

CROSS SECTION		
Base	100	cm
Height	28	cm
AMBIETAL COONDITION XF4		
REINFORCEMENT SET		
UPPER REINFORCEMENT	Φ18/40 + Φ22/40	
LOWER REINFORCEMENT	Φ20/20	

<u>SLU Combination.</u>

SLU verifications are carried out in the cantilever area as they are more stressed.

$$M = \gamma_{G1} M_{c.slab} + \gamma_{G2} M_{perm} + \gamma_{Q1} M_{acc.\ traffic}$$
$$= -1{,}35 \cdot 2787{,}91 - 1{,}5 \cdot 2036{,}97 - 1{,}3 \cdot (1639{,}12 + 587{,}5) = -9825{,}07 \text{ daNm}$$

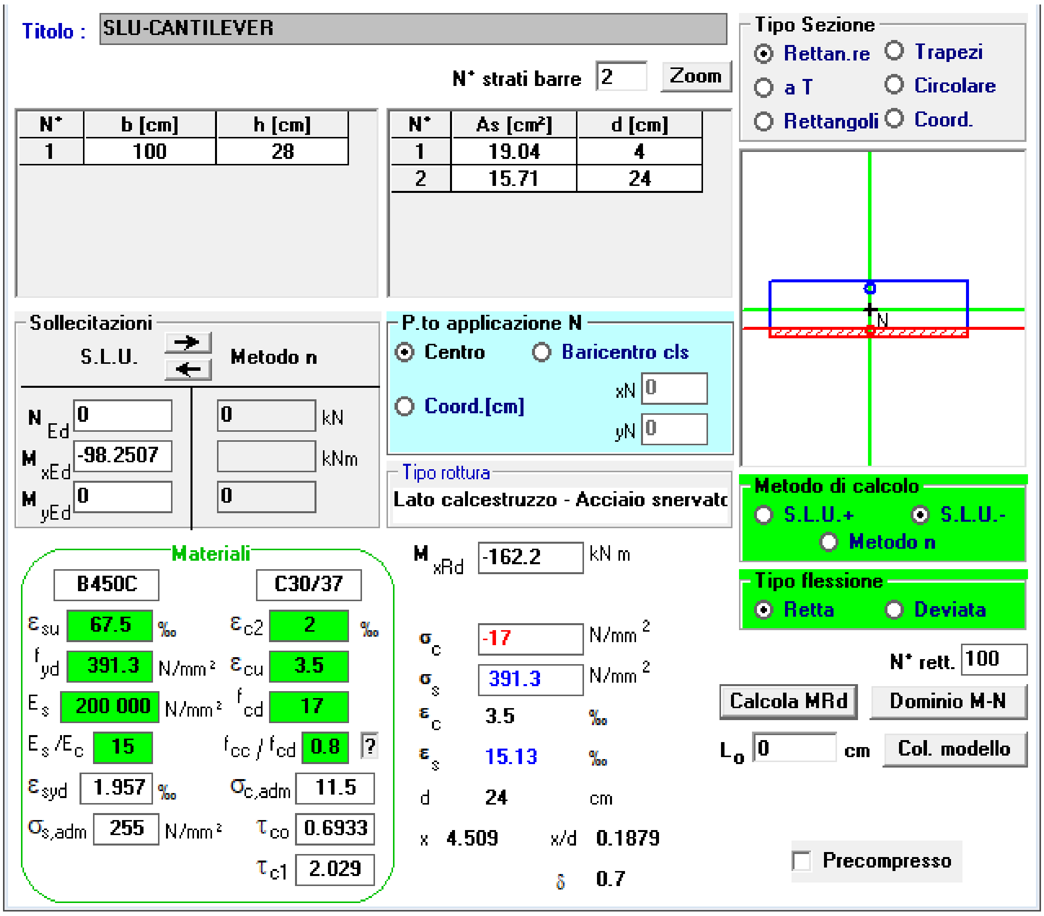

Figure 63:SLU analysis of cantilever zone.

M_{Rd}	-16220	daNm
I_R	1,6508	SATISFY

Accidental Combination.

$M = M_{c.slab} + M_{perm} + M_{acc.\ traffic} + M_{vehicle} = 2787{,}91 - 2036{,}97 - (1639{,}12 + 587{,}5) - 2666{,}67 = -9718{,}17$ daNm.

$N_{vehicle} = 21150\ daN/m.$

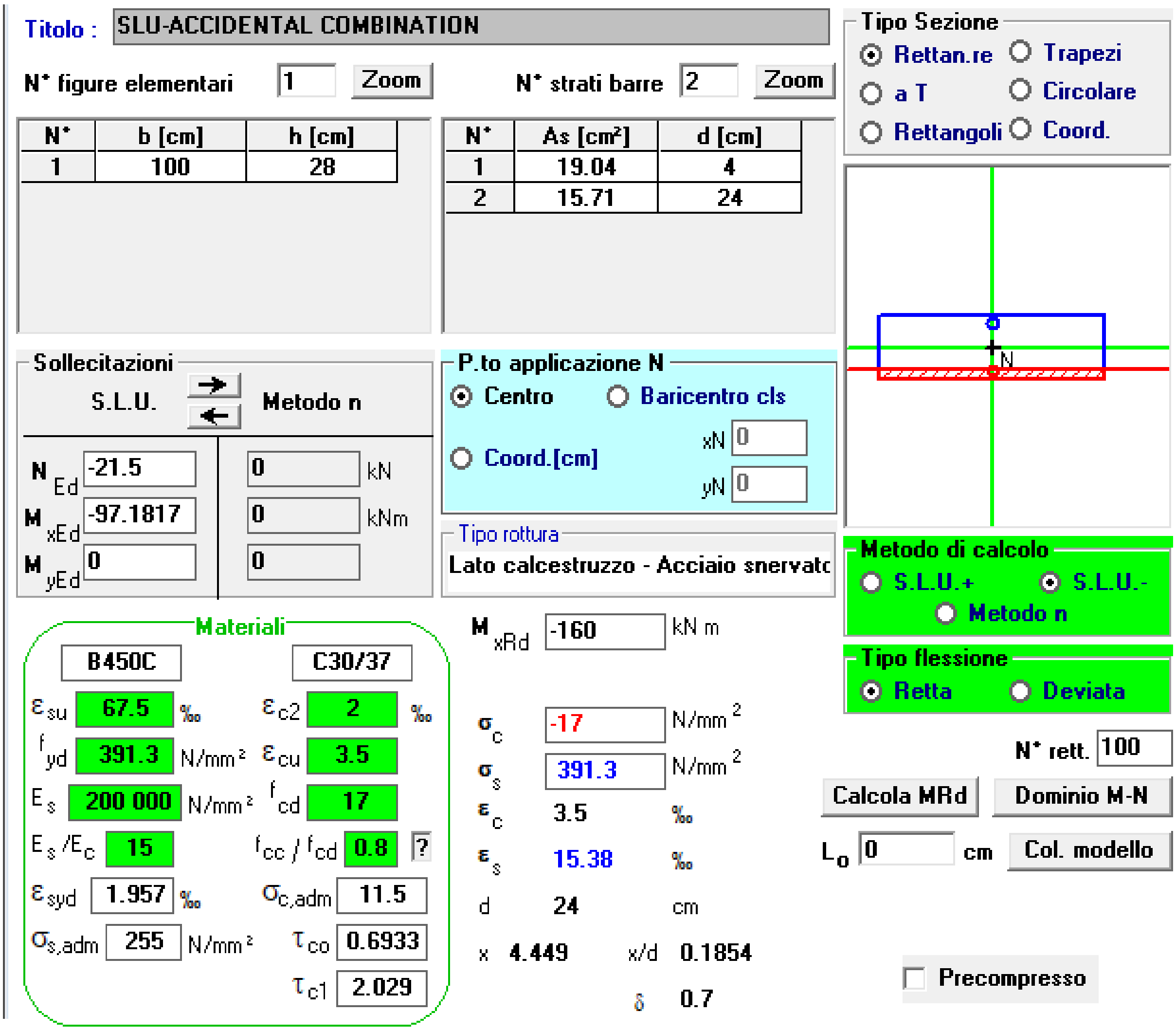

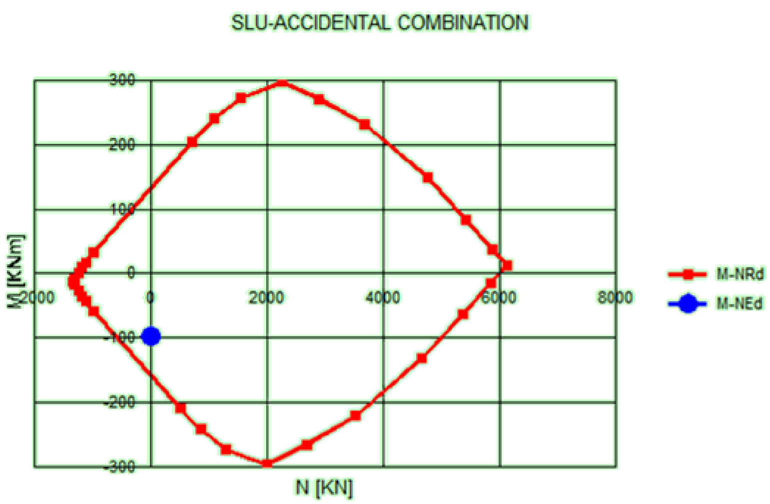

Figure 64:Accidental SLU analysis results.

MRd	-16000	daNm
IR	1,6464	SATISFY

Quasi-Permanent Combination.

$$M = \gamma_{G1} M_{c.slab} + \gamma_{G2} M_{perm} + \gamma_{Q1} M_{acc.\ traffic}$$
$$= +1{,}35 \cdot 0 + 1{,}5 \cdot 675{,}7 + 1{,}3 \cdot (193{,}29 + 290{,}39) = 1666{,}65 \text{ daNm}$$

It is considered the span zone.

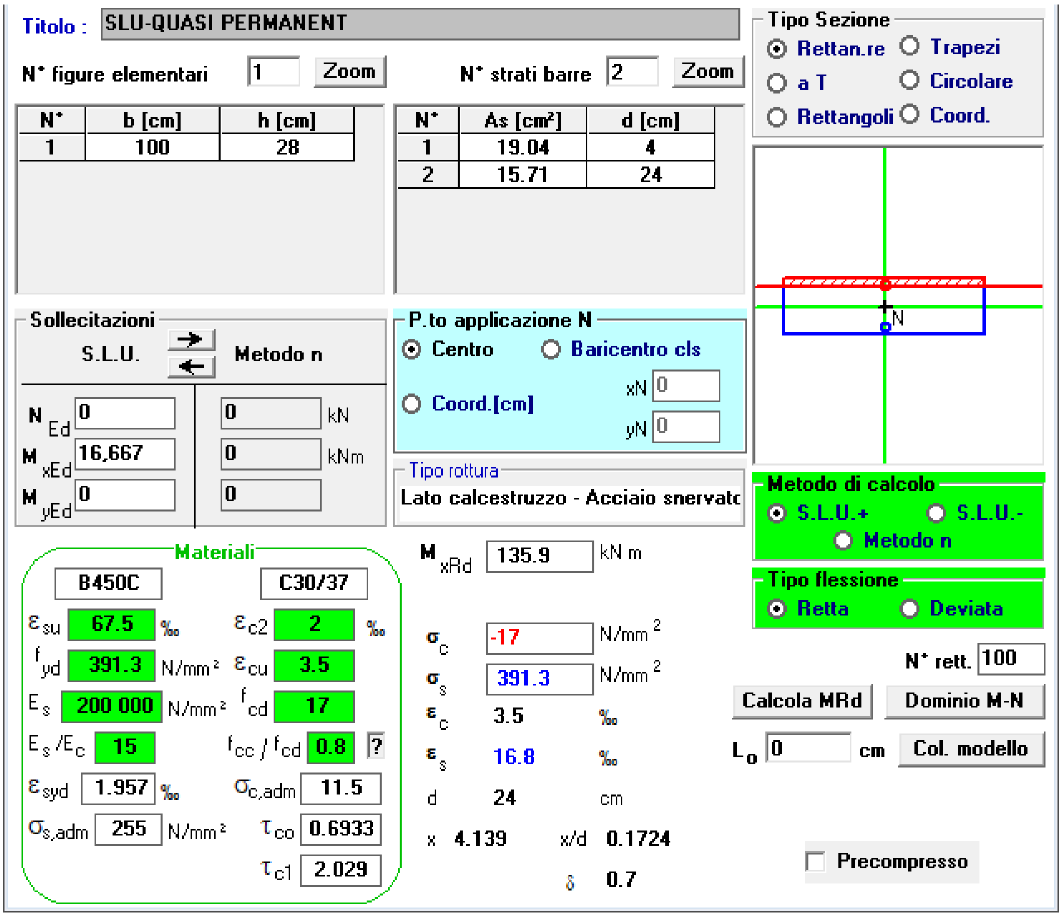

Figure 65:Quasi-permanent SLU combination analysis and results.

M_{Rd}	13500	daNm
I_R	8,100	SATISFY

4.7.SHEAR BOLTS VERIFICATION

It is used in mixed steel-concrete structures to create a collaboration between the steel beam and the concrete itself, creating an existing solid structure.

The pins have a bump at the head to prevent the slab from lifting ("uplifting"). Eurocode 4 prescribes that the connector must be able to resist a tensile force, which tends to pull it out of the concrete, equal to 1/10 of the shear strength.

The connectors can be set at a constant interaxle (if they are sufficiently ductile as "Nelson" rungs generally are); or better following the shear diagram, so that each connector resists the sliding force acting on its spacing. In any case, all connectors must withstand the total sliding force V (longitudinal shear) resulting from the flow of sliding forces between the concrete slab and the steel beam. So, the procedure to design the shear connectors are basically the following.

First is necessary to determine the characteristic of studs.

$\Phi_p = 22mm$. Stud diameter.

$h_{sc} = 200mm$. Stud height.

$f_u = 450\ N/mm^2$. Ultimate tensile pins strength.

After that, the design resistance of the connector must be calculated. It is given by the minimum value between the shear resistance and the crushing resistance of the concrete.

$P_{Rd,1} = \frac{0,8 \cdot f_u \cdot \pi \cdot \phi^2/4}{\gamma_V}$. Shear resistance of connector.

$P_{Rd,2} = \frac{0,29 \cdot \alpha \cdot \phi^2 \sqrt{f_{ck} \cdot E_{cm}}}{\gamma_V}$. Compressive strength of concrete.

For serviceability verification:

$$P_{adm} = \min\left(P_{Rd,1}; P_{Rd,2}\right) \cdot k_t$$

Where k_t is a reduction factor. It is a function if the ribs will be positioned parallelly or transversely to the supporting beams. In this case will be positioned along the main beams.

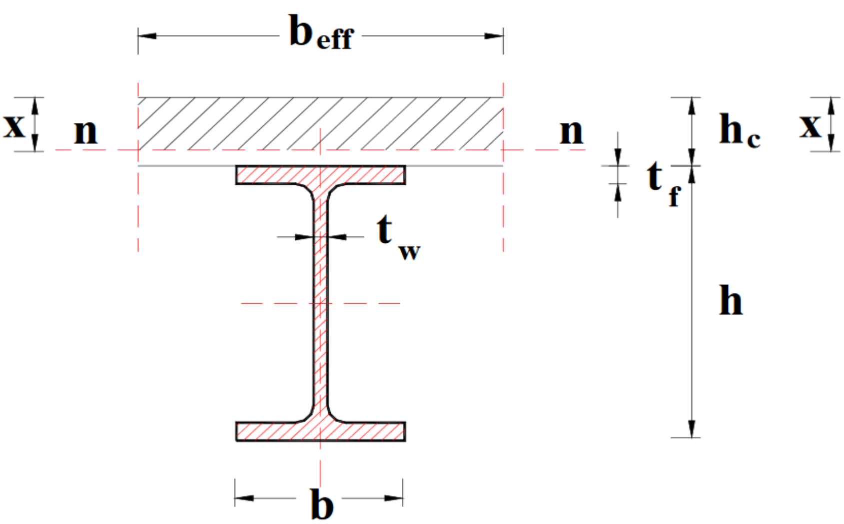

Figure 66:Computation of neutral axis position

The computation of the neutral axis position is basically the equilibrium of bending moment. It is clearly that neutral axis will cut the steel beam. The principal moment of inertia and static moment is that case will express as:

$A_c \cdot \left(x - \frac{h_c}{2}\right) = n \cdot A_a \left(\frac{h}{2} + h_c - x\right)$.

$J_{omo} = J_a + \frac{J_c}{n} + A_a \left(\frac{h}{2} + h_c - x\right)^2 + \frac{A_c}{n}(x - h_c)^2$.

Remember that the n factor is directly dependent of time of apply loading, as did previous in the shrinkage chapter. As EN1994-1 suggests, the shifting forces per unit length proposed by Jouraswki shall be write as: $s = V \cdot \frac{S^*}{J_{omo}}$, where the ratio $\frac{S^*}{J_{omo}}$ is the internal arm that the shear bolts are able to absorb in terms of longitudinal shear. Determining the internal arm, that it is function of "n" factor, it is easily understanding which the maximum action is acting on each pin, $P_{max} = \frac{s}{n_r \cdot i}$. The n_r represents the number of bolts positioned on each raw.

The Eurocode proposes a minimum spacing between connectors: $i = 22 \cdot t_f\sqrt{235/f_{yk}}$.

4.8.BOLTED AND WELDED JOINTS VERIFICATION

4.8.1. BOLTED CONNECTIONS

Bolted connections are one of the most widely used methods for assembling the various steel structural elements. Bolted connections are necessary in order to limit work on site; steel structures thus become pre-assembled structures in which most of the work is carried out in the workshop and the individual structural elements are assembled on site with considerable advantages in terms of time.

The bolted connections can be stressed by shear, traction or shear and traction. If necessary, the bolts can be tightened to produce an initial preload resulting in friction connections; in this case, high strength bolts are used. The operating mechanism of the shear friction union originates from the tangential actions that develop at the interface of the connected elements as a result of pre-stressing applied to the bolts.

Figure 67: Bolt elements.

The verification of bolted connections must be carried out for the ultimate limit state and, if required, for the service limit state; the first corresponds to the collapse of the connection, the second takes into account any limits to deformability such as, for example, the sliding with the resumption of the bolt-hole clearance in the shear unions, the decompression with consequent detachment of the plates in the traction unions.

4.8.1.1. CATEGORIES OF BOLT CONNECTION

Bolted connections are classified according to the type of stress they are subjected to; in particular, there may be shear, tensile or combined stressed connections.

SHEAR LOAD CONNECTIONS.

The design of a shear bolted connection shall comply with one of the following categories:

1) Category A: bearing type:
In this category, ordinary bolts or high-strength bolts must be used. Preload and special requirements for contact surfaces are not required. The ultimate design load must not exceed either the shear strength or the design burr resistance.
2) Category B: frictional connections resistant to SLS:
In this category, preloaded bolts of class 8.8 or 10.9 with controlled tightening torque must be used. There must be no sliding at the SLS. The design shear load at the SLS must not exceed the design shear strength; in addition, the design shear load must not exceed either the design shear strength or the design burr resistance.
3) Category C: frictional high strength connection resistant to ULS
In this category, high-strength bolts of class 8.8 or 10.9 must be used, preloaded with a controlled tightening torque. There must be no sliding at the ULS. The design shear load must not exceed either the design creep resistance or the design burr resistance.

TENSILE STRESS CONNECTIONS.

The design of a tensile bolted connection shall comply with one of the following categories:

1) Category D: connections with non-preloaded bolts
In this category, ordinary bolts or high-strength bolts from class 4.6 to 10.9 inclusive shall be used. Preload is not required. This category must not be used if there are frequent variations in tensile strength. However, they may be used in connections calculated to withstand normal wind loads.
2) Category E: connections with preloaded bolts
In this category, high strength bolts of class 8.8 or 10.9 with controlled tightening torque must be used.

4.8.1.2. FORCE TRANSMISSION AND COLLAPSE MODE IN SHEAR-LOADED CONNECTIONS

CONNECTION WITH SINGLE BOLT

Consider a symmetrical connection between sheet metal with a single bolt. The collapse modes of this elementary connection can be:

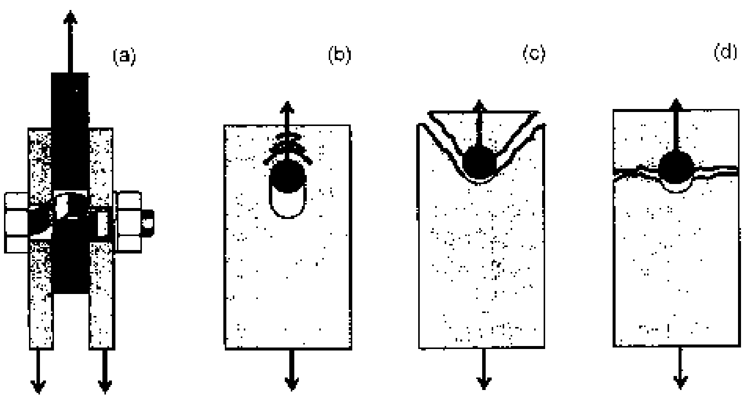

Figure 68: kind of bolt breakage

- Breakage due to bolt cutting (a)
- Breakage due to sheet burring (b)
- Breakage due to sheet cutting (c)
- Breakage due to sheet tensile stressing (d)

For each of these collapse mechanisms, resistance must be determined; the weakest mechanism will be the one that governs the problem. Bolts do not always have sufficient ductility to allow the redistribution of internal action in the structure. Therefore, it is necessary to dimension the bolts so that ductile mechanisms are formed before the bolt collapses by shearing. However, a bolted connection is correctly designed when the resistances associated with the collapse mechanisms are close together.

The analysis in the elastic field of the tensional state, whether stretched or compressed, is complex. In practice, it is advisable to refer to simplified diagrams justified by the plastic redistribution of the stresses.

BREAKAGE DUE TO BOLT CUTTING

To define the design shear strength of each strong section of the bolt [mechanism (a)] it makes no sense to use the Huber Von Mises criterion because the bolt cannot be considered as a deflected beam as it is a stocky element in which the diameter is of the same order of magnitude as the thickness of the connected elements. It is more logical to assume as design resistance a conventional value directly connected to the area of the resistant section, distinguishing whether or not the cutting plane passes through the threaded part of the bolt.

BREAKAGE DUE TO BURRING AND CUTTING OF THE SHEET

The design resistance to rolling or shearing of the sheet metal [mechanisms (b) and (c)] depend on the distance of the bolt from the end of the plate measured in the direction of the force; the behaviour will be different for compressive and tensile stresses. The rolling resistance depends on the type of material of the plates, the diameter of the bolt and the minimum distances imposed by the standard prevent the mode of breaking by shearing of the sheet, as the latter is a break of the fragile type.

BREAKAGE DUE TO SHEET TENSILE STRESSING

The presence of the holes determines a distribution of tensions in the sheet metal which, in the elastic field, is characterized by the presence of particularly expensive local points. The redistribution of the collapsing stresses, following the ductility of the material, allows the use of a conventional average value of tension on the net section.

4.8.2. DESIGN RESISTANCE OF A SINGLE SHEAR BOLT

As suggest the Italian and European law, the design procedure to define if each single bolt is correctly dimensioned is described in the following, taking into account the shear resistance, tensile resistance and other local instability as burring and punching phenomena.

The nodes in the pilot beam, the lower diaphragm joints and especially the main beam joints that will be verified as fully restored bolted joints will be subject to bolting.

As all know, at ULS the design shear force $F_{V,Ed}$ on a bolt must not exceed between:

$$F_{V,Ed} \leq \min(F_{V,Rd}; F_{b,Rd})$$

Where,

- $F_{V,Rd}$, shear design resistance.
- $F_{b,Rd}$, design resistance to burring.

4.8.2.1. SHEAR DESIGN RESISTANCE

The shear strength for each bolt shear plane must be assumed as:

$$F_{V,Rd} = \frac{\alpha_V \, f_{ub} \, A}{\gamma_{M2}}$$

When the cutting plane passes through the threaded portion of the bolt (A=As, the bolt's tensile strength area):

- For strength classes 4.6, 5.6, 8.8 → α_V=0,6.
- For strength classes 6,8 e 10.9 → α_V=0,5.

When the cutting plane passes through the unthreaded portion of the bolt (A= gross section area of the bolt):

- For all strength classes → α_V=0,6.

The function of the coefficient a_v is to transform the tensile strength of the f_{ub} into an equivalent shear strength. According to Von Mises 0.57 or 1/√3

4.8.2.2. DESIGN RESISTANCE TO BURRING

The burring resistance must be assumed:

$$F_{b,Rd} = \frac{k_1 \, \alpha_b \, f_u \, d \, t}{\gamma_{M2}}$$

Where: $\alpha_b = \min\left(\alpha_d; \frac{f_{ub}}{f_u}; 1{,}0\right)$

In the direction of the applied load:

- For end bolts
  - $\alpha_d = \frac{e_1}{3d_0}$
- For internal bolts
  - $\alpha_d = \frac{p_1}{3d_0} - \frac{1}{4}$

Perpendicular to the direction of application of the load:

- For end bolts
  - $k_1 = \min\left(2{,}8\frac{e_2}{d_0} - 1{,}7; 2{,}5\right)$
- For internal bolts
  - $k_1 = \min\left(1{,}4\frac{p_2}{d_0} - 1{,}7; 2{,}5\right)$

The burring coefficient k_1 amplifies the ultimate resistance (k_1>1) because it takes into account the actual phenomenon of plasticization, which does not only concern the contact area conventionally evaluated through its diametric projection (d·t), but which affects, following the diffusion of the tensional flows, a larger area of the plate.

4.8.2.3. FULLY RESTORED BOLTED JOINT

As defined above, the fully restored joints will be arranged in the zones of continuity between the different segments of the longitudinal main beams.

The theory that follows is very simple and does not take into account any external stressing force, but the geometry and the type of bolts chosen by us for the verification at the node comes into consideration.

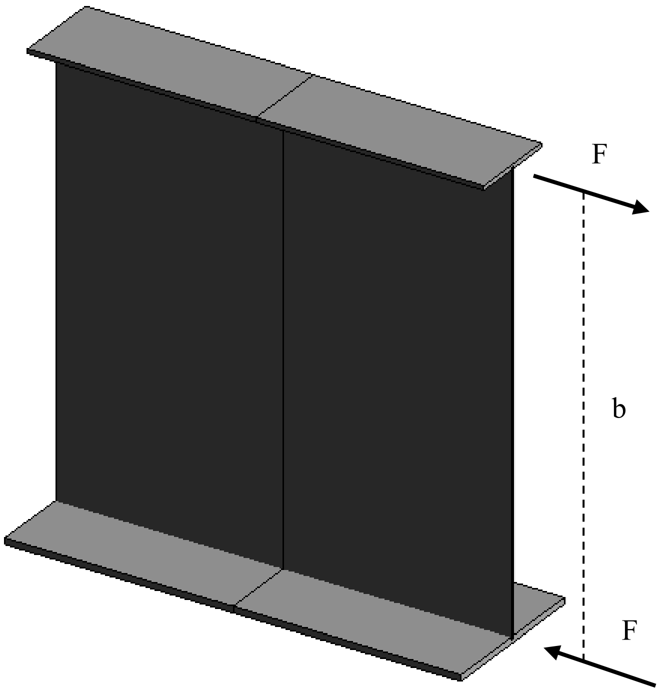

Figure 69:Fully restored bolted joint initial scheme.

Starting from the upper and lower flanges bolted, from the geometrical point of view they are spaced by a certain height called b. The force generated can be summarized according to the equation:

$$F = A \cdot \sigma \rightarrow \ \sigma = \frac{F}{A}$$

Where the A and σ are referred to the bolt conditions used.

Of course, the internal stress can also be described, remaining in a linear elastic regime, according to Navier's equation:

$$\sigma = \frac{M}{W} \rightarrow M = \sigma \cdot W$$

Where the σ express the yielding strength of beam material. In this case was chosen $\sigma = 355/\gamma$.

By imposing the equivalence of bending moments, we obtain the last fundamental equation for the calculation of the number of bolts to be used to complete the complete reset joint.

$$F \cdot b = \sigma \cdot W$$

4.8.2. WELDED CONNECTIONS

Welding is a process by which a permanent union is made between two metallic pieces, with or without the addition of a metallic material, in order to obtain continuity between the pieces in the connecting sections. In addition to the requirement of physical continuity between the pieces, the mechanical properties of the joint must also be suitable in terms of resistance.

Welding is called *heterogeneous* when the filler material is melted, which must necessarily have a lower melting point than the base material and therefore a different composition from that of the pieces to be welded; this is the case of brazing in all its variations.

Welding is called *autogenous* when it involves the fusion of both the base metal and the filler metal, so they must have similar compositions, or the fusion of only the edges to be welded together by pressure. These are the well-known gas or electric arc welds, more traditional procedures still widely used due to their undoubted economic advantages.

Since the study of welding processes requires the knowledge of some particular terms and concepts, some definitions are given below:

- Base metal: it is the metal that constitutes the pieces to be welded and can be the same for both pieces, and different;
- Filler metal: it is the metal that is introduced in the form of rods, wires or ribbons and deposited in the molten state between the edges to be joined.
- Melting bath: is the portion of metal that is in the molten state during the welding operation. The melting bath is the general one consisting partly of the base metal and partly of the filler metal.
- Dilution ratio, R_d: is the ratio between the volume of molten base metal and the volume of the entire fusion bath; it expresses the dilution that the filler metal undergoes by the base metal. Dilution is measured experimentally by examining the section of the joint:

$$R_d = \frac{base\ metal\ melted}{total\ volume\ melted} x\ 100$$

4.8.2.1. CLASSIFICATION OF WELDED JOINTS

The weld seam consists of all the metal, both the base and the filler, solidified by cooling after being melted down in the welding process. The weld seam is the essential and resistant element of the welded joint. Depending on the position of the weld seam, the following weld positions can be distinguished: plane, vertical, frontal, overhead.

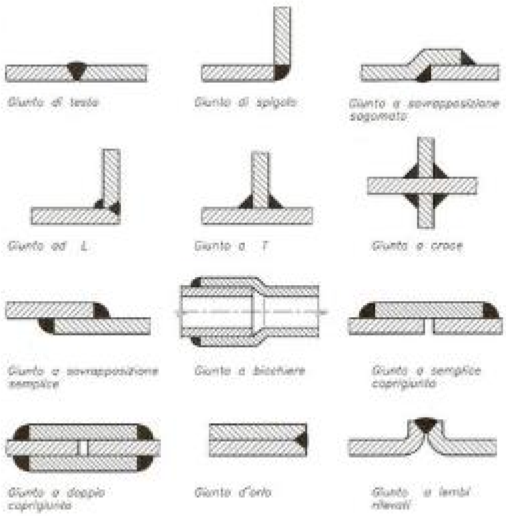

Figure 70:Position of welding

The result of the welding operation is called a welded joint. The type of joint is determined by the number, size and relative orientation of the parts to be joined. According to UNI EN 12345:2000, different types of joints can be distinguished.

The preparation of the flaps, called kerchief, is named after the shape of the cross-section of the compartment to be filled with welding, you will have preparation such as V, U, X, Y, K and J.

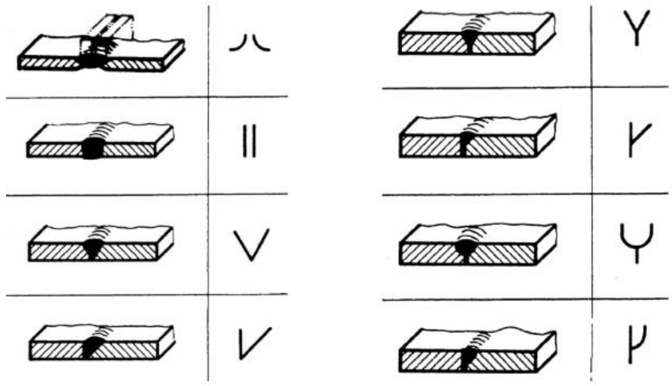

Figure 71:Type of welding

4.8.2.1.1. CORNER BEAD WELDING

GEOMETRY AND DIMENSIONS

Corner bead welds can be used to connect parts with a 60° to 120° waist angle. Angles of less than 60° are allowed, but in this case the weld must be considered as a partially penetrating butt weld. Angles greater than 120° are not to be considered effective for the transmission of forces; alternatively, their resistance must be determined according to the load tests suggested by EN 1990 - Annex D.

Corner weldings must not end at the corners of the parts or elements, but must be made to return continuously, at full section, around the corner for a length equal to twice the side of the cord, whenever this return can be made on the same plane.

EFFECTIVE LENGTH

The effective length of a corner bead weld must be equal to the length of the full-section seam. This can be considered equal to the weld length reduced by twice the groove height (a) of the weld.

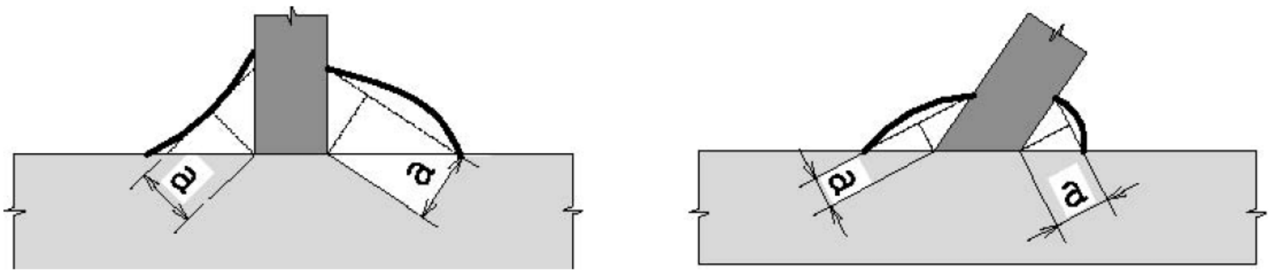

Figure 72:Effective way to calculate the welding length and cross-section.

Welds with an effective length (l) of less than 30 mm or 6 times the height of the groove (a) must be neglected in order to transmit the forces. $l \geq \max(30\ mm; 6a)$.

GROOVE HEIGHT

The groove height (a) of a corner seam weld should be taken as the height of the largest triangle that can be inscribed between the flaps and the surface of the weld, measured perpendicularly to the outer side of this triangle. The throat height of a welding bead shall not be less than 3 mm.

4.8.2.2. DESIGN RESISTANCE PER UNIT LENGTH

The design resistance per unit length of a corner seam weld can be calculated using the following methods:

- directional method;
- simplified method.

4.8.2.2.1. DIRECTIONAL METHOD

In this method, the forces transmitted per unit length are divided into components parallel and transverse to the longitudinal axis of the weld and normal and transverse to the plane of the groove section.

The area of the groove section must be calculated using the following relationship:

$$A_w = \sum a \, l_{eff}$$

An even distribution of tension over the groove section of the weld is assumed, resulting in shear and normal stresses as follows:

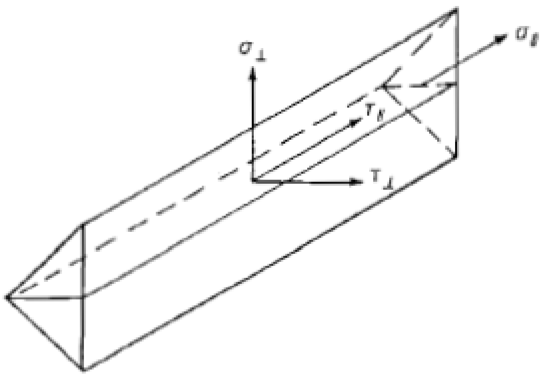

Figure 73:Welding stress

$\sigma_{\perp}$, normal stress perpendicular to the throat section.

σ_{n}, normal stress parallel to the welding axis.

$\tau_{\perp}$, shear stress, in the plane of the throat section, perpendicular to the welding axis.

$\tau_{||}$, shear stress, in the plane of the throat section, parallel to the welding axis.

The normal stress σ_{n}, is not considered

when checking the resistance of the weld. Considering the groove section in its actual position, the resistance of the corner bead weld will be enough if the following conditions:

$$\sqrt{\sigma_{\perp}^{2} + 3\left(\tau_{\perp}^{2} + \tau_{\parallel}^{2}\right)} \leq \frac{f_u}{\beta_w \gamma_{M2}} \ \& \ \sigma_{\perp} \leq 0{,}9 \frac{f_u}{\gamma_{M2}}$$

Where:

f_u, nominal tensile strength at break of the weakest part of the joint

β_w, coefficiente di correlazione.

- $\beta = 0{,}80$ for steel S235
- $\beta = 0{,}85$ for steel S275
- $\beta = 0{,}90$ for steel S355
- $\beta = 1{,}00$ for steel S420 and S460

4.8.2.2.2. SIMPLIFIED METHOD

The strength of a corner seam weld is acceptable if, at each point of its length, the resultant of all design forces per unit length $F_{w,Ed}$,transmitted by the weld does not exceed the design strength $F_{w,Rd}$. Therefore, the verification criterion becomes:

$$F_{w,Ed} \leq F_{w,Rd}$$

Where

$F_{w,Rd} = a\, f_{vw,d}$.

$f_{vw,d} = \frac{f_u/\sqrt{3}}{\beta_w \gamma_{M2}}$.

β_w, is a coefficient given by the Italian regulation. It is suitable from table 4.2XIX of NTC2018.

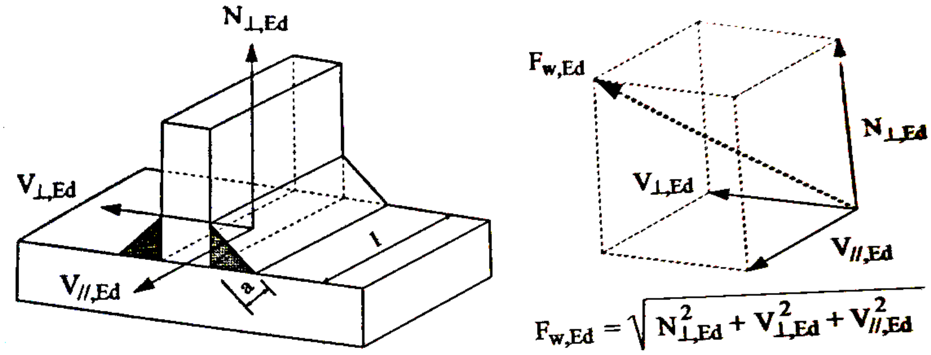

Figure 74:Scheme of welding forces

4.8.3. *WELDING OF SHEAR CONNECTORS*

As defined in the chapter §4.7, the shear connectors are used to control the resist at shear loading acting on the top of the concrete-steel composite structure.

How is composed the welding shear connectors? Basically, it is characterized by the release of very high current peaks voltage in an extremely short time. When the gun is operated by pressing a button, an electric arc is created between the base or head of the pin and the base surface, melting and fixing both materials.

The procedure shall be distinguished in:

- Choose bolt and type of welding.
- Loading the welding gun.
- Place the machine close to the welding base.
- Activation of welding process.
- Get off the gun from the point.

There are different types of guns suitable for different welding processes with specific internal components. they are distinguished by long arc welding, short arc welding or condensation. Each of them has the ability, depending on the voltage transferred to it, to perform welds of different joint thicknesses.

In this thesis, we have taken into consideration the Nelson shear connectors, commercially known as KB, produced in compliance with the European reference standards EN ISO and EN 10025-2 respecting the minimum requirements indicated for the material making up the connector.

5. B.I.M. METHODOLOGY

5.1.GENERAL PURPOSES

In the last few years, BIM has been the subject of great discussions in terms of design and planning, as it represents a process that allows for the disciplinary design of different elements of a model containing various useful information throughout the life cycle of a building. This includes the development of the project itself, starting from the preliminary phase of the entity modelling, i.e. the inputs of the process, up to the phase of data management, and the outputs, from which the analysis can be obtained according to the desired purposes. The gap between the CAD (Computer Aided Design) project and the innovative BIM methodology has been clear now, since in the first case, the design is limited, where all the set of views and data converge in a two-dimensional project whose represented entities do not contain any kind of information. Completely different is the BIM process, whose starting point is given by a multidisciplinary parametric model (architectural, structural and mechanical), giving life to entities that can be created through an automatic process, added value for the optimization of design time required today for speed and performance. This does not mean that BIM is a simple methodology, on the contrary, it is a complex system that must be used.

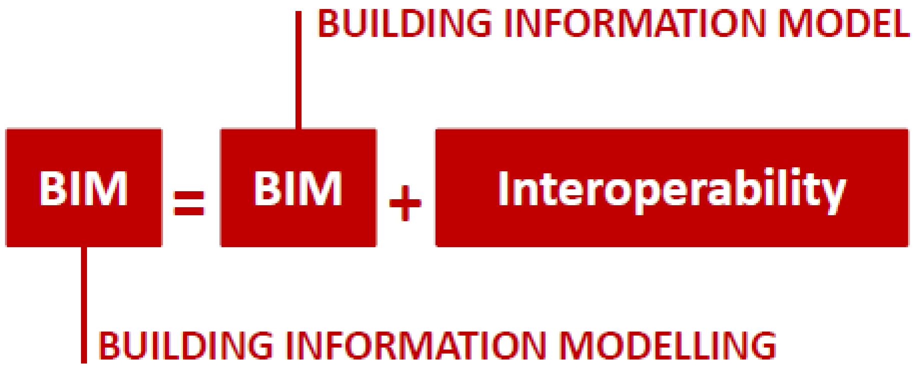

Figure 75:Interoperability concept. Source BIM and InfraBim slides

What has just been described is very advantageous for the project's management, because by updating the BIM model you can update all the information it contains, i.e. the costs of the metric calculation, material involved, cross sections changing and so on, applying interoperability between different software. What distinguishes the BIM methodology is the possibility to include in the Modeling also the working phases prior to the construction of the building itself, but which are part of the building process, such as excavations, temporary works and overall dimensions of the machinery involved in the transport and disassembly of materials; for this reason it is necessary to have a careful planning from the earliest stages to avoid unexpected events on site.

Indeed, what is important to point out is that the "integrated design process" that controls and manages each phase of the project has as its final result innovation, a prerogative of today's market of construction companies, to be able to give an advance to construction processes.

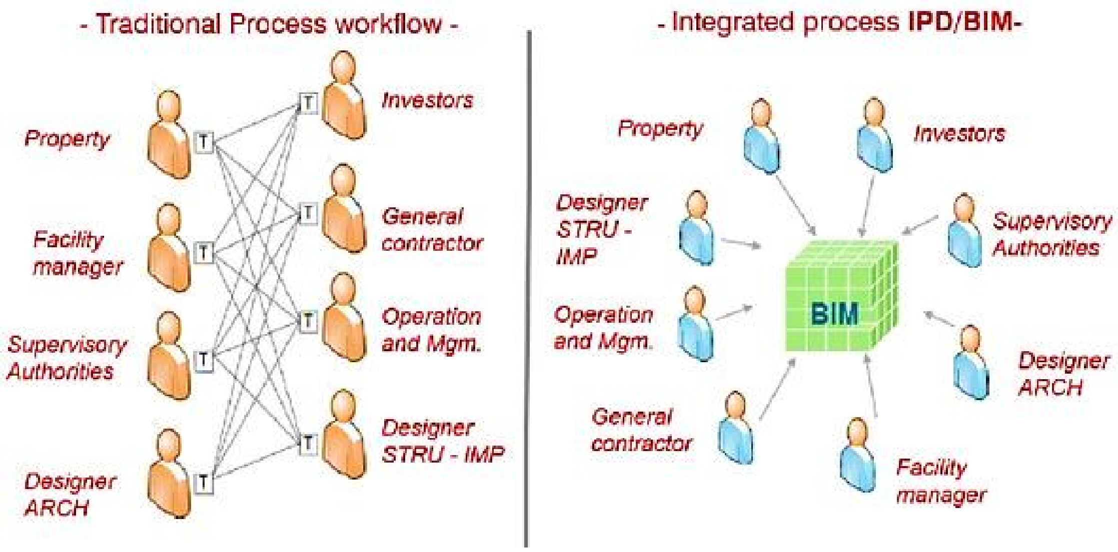

Figure 76:Comparison between traditional and integrated process. Source BIM and InfraBim slides

The use of BIM in structural design simplifies the life of the designer thanks to a continuous exchange between architectural model and structural one. Among the main challenges that professionals and companies must be able to take up and exploit in order to be increasingly competitive and efficient on the Italian and international markets are: compliance with the Technical Regulations for Construction (NTC 2018, Italian rule), the implementation of the Minimum Environmental Criteria (CAM), the adoption of Building Information Modelling (BIM) processes for the optimal management of the entire building cycle, the use of the potential offered by technologically advanced solutions that the digital industry provides at increasingly affordable costs.

Undestrand which is effectly the meaning of the BIM method, now the next step is know the methodology and the effectivness of "interoperability" done. it is used to define and describe the different softwares capability to excange data and information by a common type of exchange format file, i.e. the most used format file is IFC, industry foundation classes, standard format based on "standard for the exchange of product model data". The versions of IFC have evolved and updated over the years, making it properly regulated according to ISO 16739:2013. The current law specifies the cenceptual data schema and proper exchange file format in order to be used to Building.

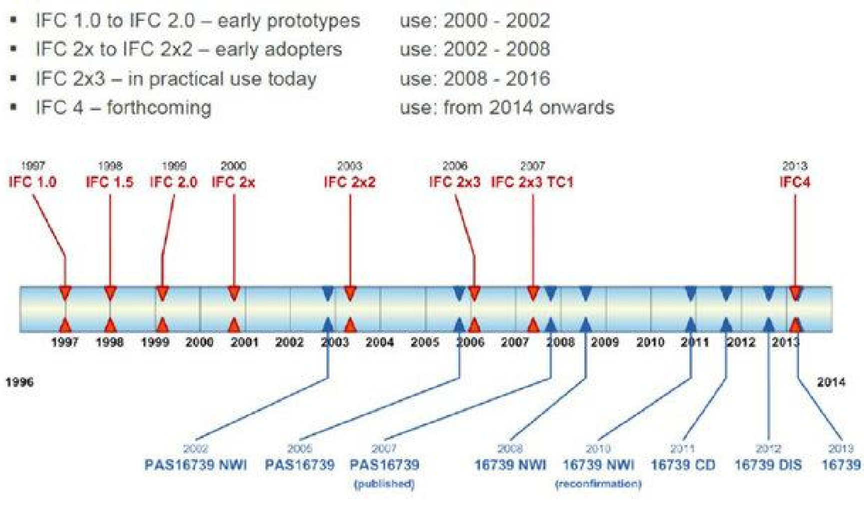

Figure 77:Updating of IFC format during the years. (Acampa, 2018)

Basically IFC is an open source standard for the exchange of construction data models in the design and construction of buildings with different software products. It aims to exchange information within a team or professionals figures and between different software applications at different stages of design, construction, maintenance and installation. IFC extension files support 2D and 3D property and geometry data. Since IFC definitions are regularly updated and developed over the years, as described in Figure 68 above, it is necessary to define what the differences of the extensions used are.

- IFC4: this is used to transfer IFC models in order to import and modify them in a BIM-enabled software; it allows to transfer parametric projects and complex contexts (possible manual adjustments to manage software differences).
- IFC2x3: it is also defined as coordination View Version 2.0. optimized for the coordinated exchange of BIM models between the main disciplines of the building industry; it is currently the most widely used model view definition supported by the BIM market. coordination view also supports an elementary parametric derivation of building components when they are imported into planning tools, which is mostly used for the exchange of architectural models, building technology and engineering.
- IFC2x2: also called CoordinationView. it is only used in isolated cases, for example when exporting MVD definitions for software products that do not support IFC2x3. Each of these operations can be manually adapted to specific workflow needs.

All extension file seen before should be summarized in a generic acrnonymous: MVD. Model View Definition, is used for the targeted exchange of specialized models, taking into account the graphical information and content that the planner needs, as described before for each ot these.

Of course, the IFC extension file was used in this thesis to exchange data e information from softwares in order to loss as less as possible data information. The goal will be test the interoperability between software used and test if parameters are loss and reach an high value of level of detail, LOD, in order to built a detail construction drawing and present it to the steel factory.

In essence, the level of detail should be thought as input to the element in such a way to update the information and detail informations.

- LOD 100: the model must be presented as symbol or generic representation, just conceptual position and possible behaviour.
- LOD 200: the model element may be graphically represented within the model as a generic system or assembly with approximate quantities, size, orientatio and so on.
- LOD 300: the model element within the element as a specific system, object or assembly in term of defined information but not graphic informations attached to the model.
- LOD 400: the model is graphically represented within the model as a specif system, object, quantity, size orientation and other characteristics, with a detailing fabrication installation information.
- LOD 500: the model is a field verified representation in term of size and components quntity.

The figure 68 explains basically the conceptual scheme of LOD, from the conceptual design process until reach the end process of construction , called As-built final scheme.

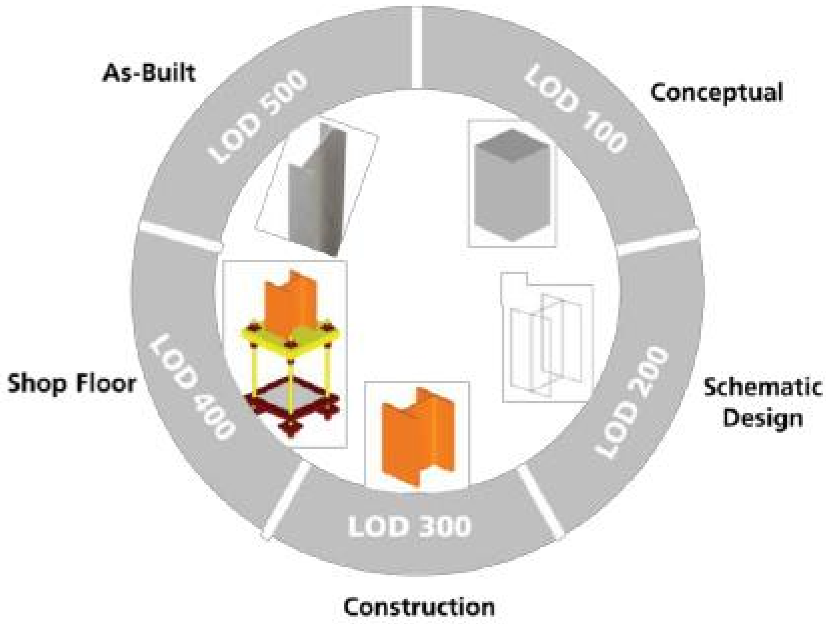

Figure 78: Conceptual scheme of LOD increasing. Source BIM and InfraBim slides

5.2.ADVANCE DESIGN

Advance Design is a software specially developed for designers and professionals looking for the best solution for the analysis and design of reinforced concrete, steel and wood structures according to the latest versions of the Eurocodes and Italian rules.

Advance Design, AD, provides fast and easy modelling, features a powerful FEM solver, wizards to perform full checks, and a post-processor for detailed, automated calculation results and reports, as did and represented in the previews result chapters.

It is part of the GRAITEC Advance Suite and is integrated in a BIM process dedicated to the design of structures. The software supports intuitive model integration, using native objects or families seamlessly, easily interoperability between suite Autodesk by using several tools.

The process used in the use of the software has been that of continuous modelling of the main elements of the deck taking into account that they are elements with different sections, with a discontinuous curved development. The technical characteristics of the surface elements have been defined previously in chapter 1, where the material used has been described in detail. Subsequently, the permanent loads and related traffic function loads were defined as appropriate and the related variable loads. The modelling of the diaphragms and upper and lower braces was chosen as beam elements, De Saint Venant theory, due to problems related to the connections and joints between them. The final result of the modelling is shown in the figure below, figure 69.

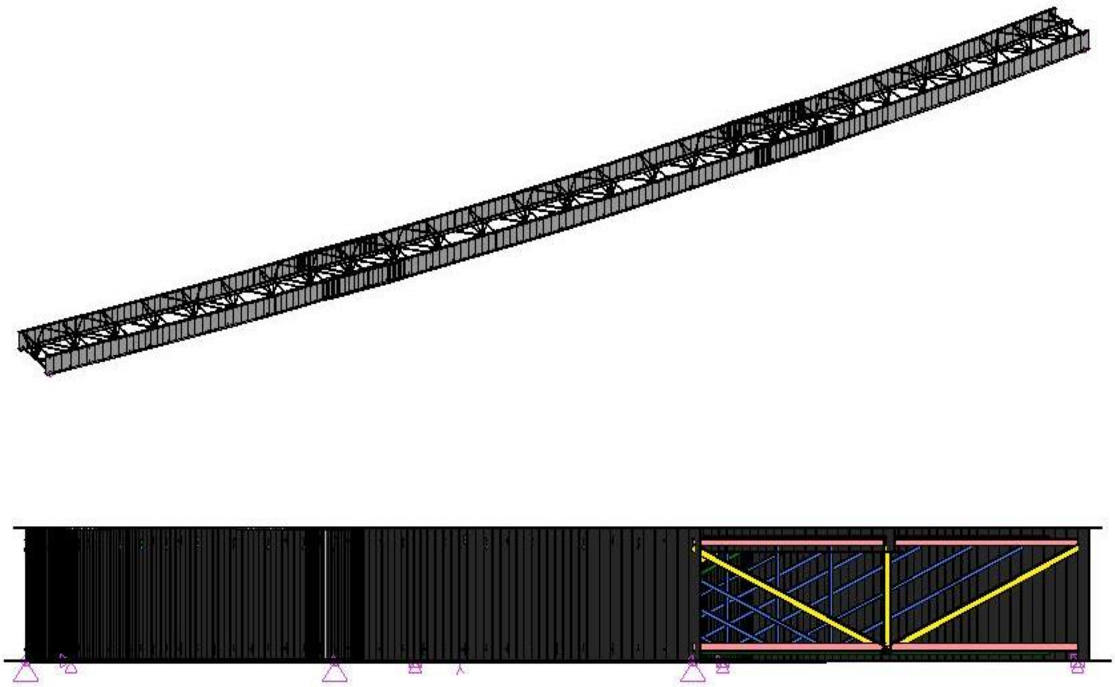

Figure 79: Advance Design model.

As described in the previous chapters, all the necessary conditions required by the regulations have been verified, both at the ultimate limit state and the serviceability limit state as well, comparing the requirements of the Italian technical regulations with the Eurocode prescription.

Being a structural calculation program, and thanks to its BIM philosophy, it has been possible to carry out the direct passage with Advance Steel, to increase the level of detail, and then with Idea Statica to verify the actual feasibility of the joint construction and verification of the resistance in the specific nodes.

5.3.IDEA STATICA

Idea Statica is software designed to save time for structural engineers, builders, consultants and all those who perform or use structural analysis. The principle of the programme is to study the analytical and behavioural behaviour of structures and their members.

Idea Static, IS, could model and build any type of bolted or welded joint of the steel- steel or steel-concrete type. It also provides detailed testing of the stresses, stiffness, buckling and bending moment analysis of the joint under examination. The forces that can be analysed are multiple and, in any direction, taking into account all the interactions and effects.

Thanks to its own characteristics, the program has been used for the achievement of the verification of bolted joints, the fully restrained bolted joints between the main beams and others bolted joints.

The verification and analysis procedure is conceptually divided in: import of the elements and load combinations from the calculation software used to the structural analysis by using a direct link ADC , identify the type of connection and set material properties, type and geometry of connection. At the end, it checks the plates, bolts and any welds present if satisfy the load condition. All checks follow the Italian NTC2018 and Eurocode 1993-1-8 regulations.

On the other hand, interoperability was tested between the software used to improve the level of detail and actual calculation of the joint, to test the double methodology.

5.4.ADVANCE STEEL

Advance Steel (AS) is part of Autodesk and GRAITEC suite, CAD software application for 3D modelling and local detail of steel structures. AS has many functions, among which we can highlight: the creation of 3D models using with ease the pre-set libraries such as beams, metal plates, bolts, welds and others; creation of arrangement and shop drawings, fabrication drawings; modelling of complex structures as spiral stairs or barriers; Automatic determination of lists of elements.

Thanks to its huge potential and vast library, it has been possible to perform all the operations of constraints between the different elements previously modelled with the calculation program. As explained before, this software has been used to increase the level of detail of each single node, going to arrange in a constructively accessible way each single component, previously verified.

Moreover, this programme was used to achieve the final objective of the thesis, which is to produce the construction details and then present them in the workshop and subsequently produce them.

5.5.EFFECTIVE INTEROPERABILITY

The methodological process used for the structural calculation of the deck and subsequent local tests, as described above, was to use *Advance Design* software for general modelling and for the combination of appropriately defined loads by finite element analysis; subsequently the model was imported into the detail program, such as *Advance Steel*, in order to create each joint ad hoc and actually predict the distance between bolts and welds. Finally, interoperability was tested, with both software, with the local analysis program, *Idea Statica* in this specific case.

It should be noted that this thesis did not include the analysis of the supports, columns and abutments, but only the structural part of the deck was calculated.

How was the model created?

Initially, the topography and the environmental issues were discussed and the track to be followed with the central pilot beam was defined. Subsequently, the different profiles and sections to be used were hypothesized and then verified with the application of traffic and variable loads.

Defined as such, continuous modelling was chosen in order to have a greater operability in the tensional checks in each single two-dimensional element, which, as previously defined, was the theory for the construction of the longitudinal main beams. The transverse stiffeners have been designed to maintain the suitable torsional behaviour and to counteract lateral deformations coming from vertical and horizontal loads. Then the lower braces were added all over the deck to neutralize the rotation and torsion and then added on top only in the most critical areas, position of the supports and half of the longest span, the middle one.

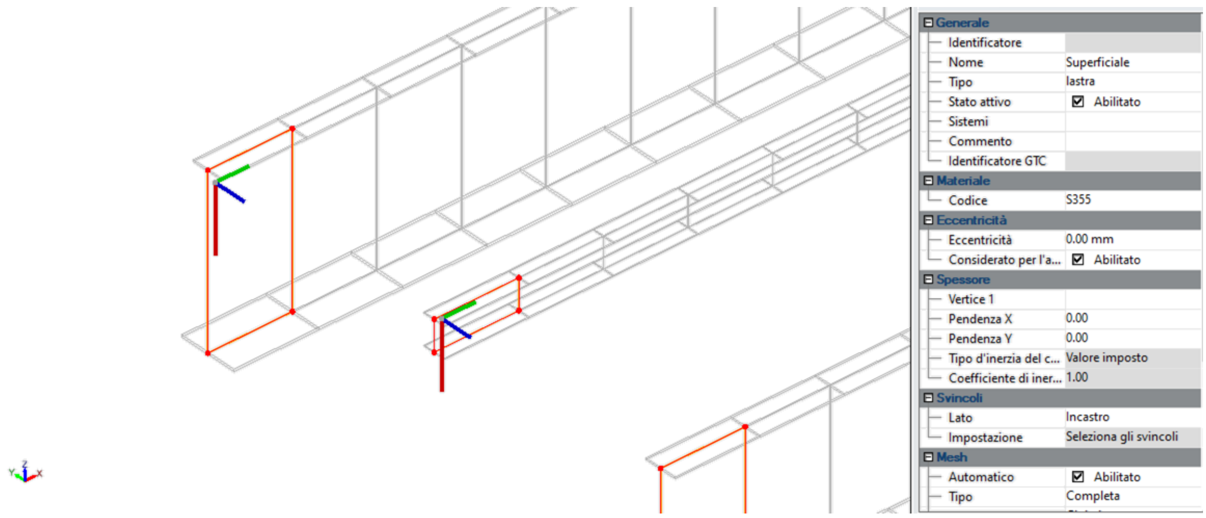

Figure 80: Graphical representation of plate elements.

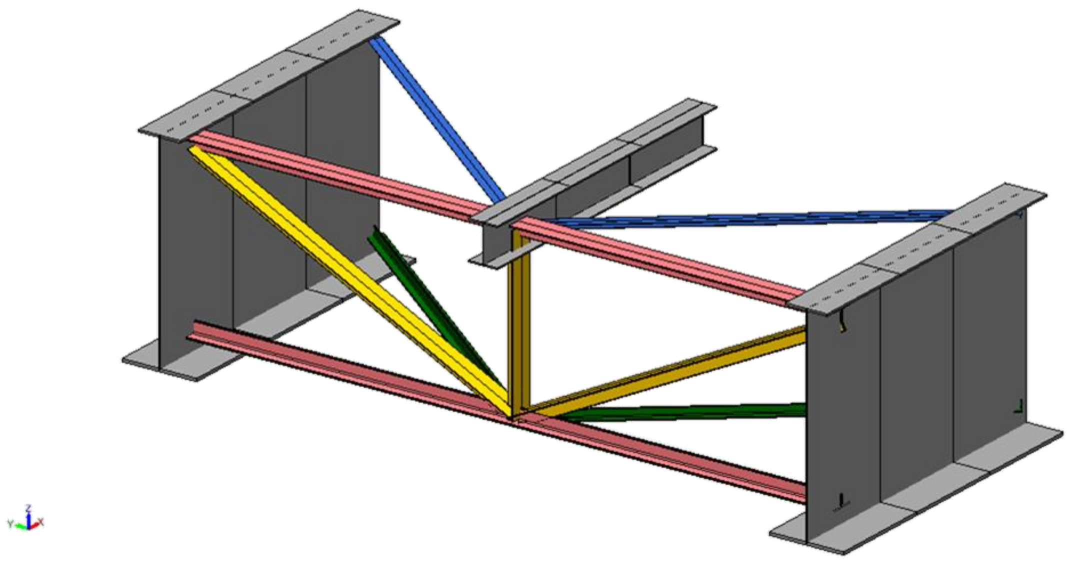

Figure 81: Graphical representation of first deck segment.

As we can see in both figures above represented, every single element within the program has its own well defined characteristics, such as its geometric characteristics, definition of material, section used, orientation, possible initial and final junctions, load transfer capacity and possibility to be tested, such as resistance and fire stability. These are the characteristics that we can define within the Advance Design program during modeling. To be clear, the software works with the Eurocode design criteria, during the steel calculation for both global and local assumptions, in such a way for buckling and lateral torsional phenomenon.

The supports designed are simple hinges where, each one of them, has variations of movement allowed in the direction depending on the device used.

At the end of the showing the deck, the program provides us with its very important verification tools: the geometric verification 

and global verification 

that includes all the features listed above considering the mesh factor defined.

After completing the modeling it is essential to define the mesh to be used to make the final calculation.

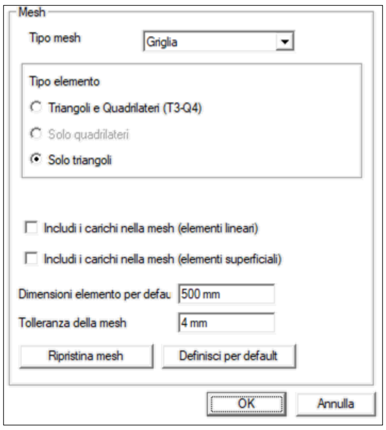

Figure 82:Mesh used for modelling

Within the calculation software, the mesh definition can be defined in two different ways: the first one defines a general unique mesh for all as represented in Figure 72, the second one, the most laborious one, is to define for each element the subdivision of the mesh in geometric and tolerance terms. In this case it was decided to mesh the whole deck with a general mesh equal for all in order to have a final equipotential match. Furthermore, the Grid type algorithm has been defined in this case, based on the *Graitec Effel* meshing algorithm, combining it with the triangular geometry of planar elements and plates. The T3 mesh type, triangular meshes with a node on each vertex, doesn't take into account the loads applied on the structure elements, in this case the loads do not affect the meshing of the elements.

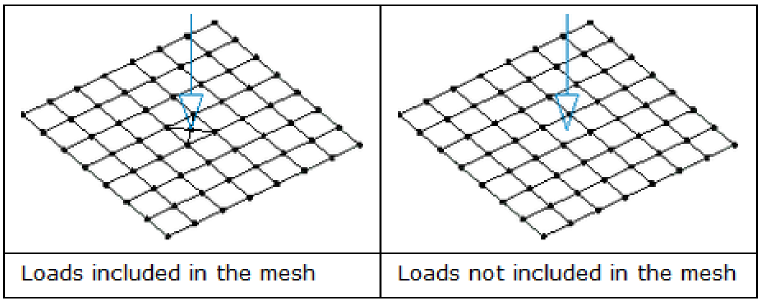

Figure 83:Effect of load on mesh. Source Graitec website.

The tolerance defines the minimal distance required for two nodes to be distinct. If the distance between two nodes is smaller than this value, the corresponding nodes are merged into a single node, otherwise will be display a computational error should be solved as soon as possible because it causes an inability of the programme to carry out the FEM analysis.

Until now, the actual modelling process of the deck has been described, taking into account all operational issues.

Afterwards the interoperability between the above listed software was tested. first of all the direct passage between Advance Design and Idea Statica was verified, in order to design the structural nodes that we will describe later on. The switch is very easy thanks to the ADC direct tool. Basically, it consists in selecting the nodes and elements we are interested in, go to the BIM section and click the keyword 

.

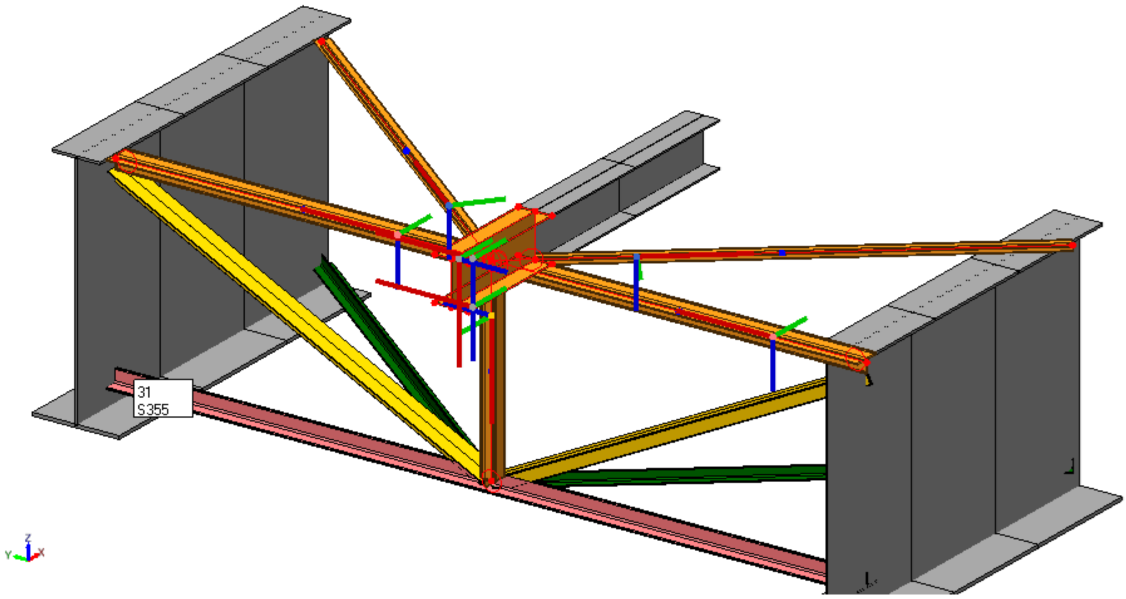

Figure 84: Selection of prop. elements in Advance Design.

As we can see in the list of elements connected in the node previously selected in figure 74, the pilot beam does not appear. Figure 75 explains the problem of interoperability. The main element in question, the pilot beam, has been created using two-dimensional elements with continuous theory. Static idea works only with elements that follow the concept of De Saint Venant's theory, i.e. beam elements.

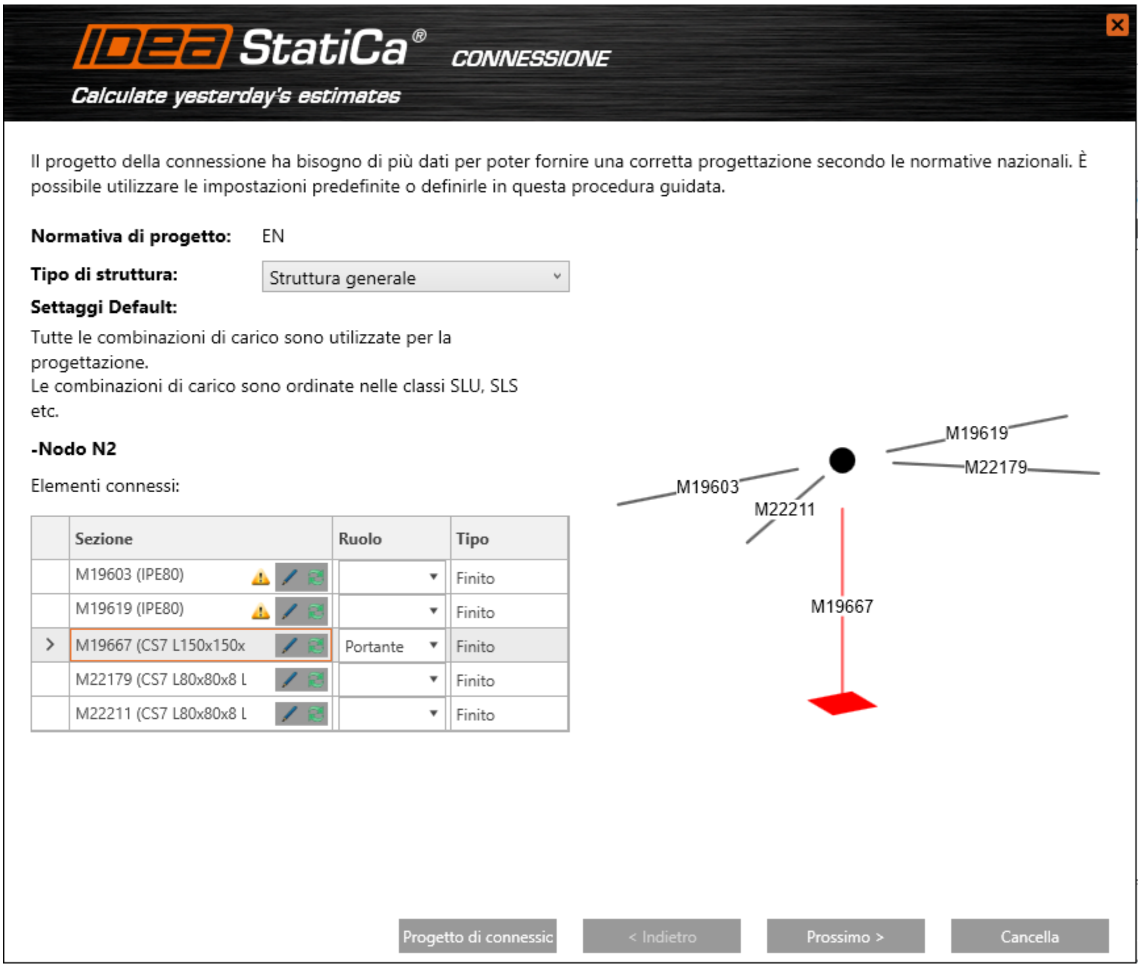

Figure 85: Step 1 of interoperability with Idea Statica connection.

Idea Statica allows to change the profile or the kind of the element, but the superficial type doesn't work. The figure 76 below shows the partial interoperability between the software. In fact, as far as the linear elements are concerned, the passage has been directed without any recognizable problems. instead, as said before, the pilot beam has been replaced with the first profile present in the software library.

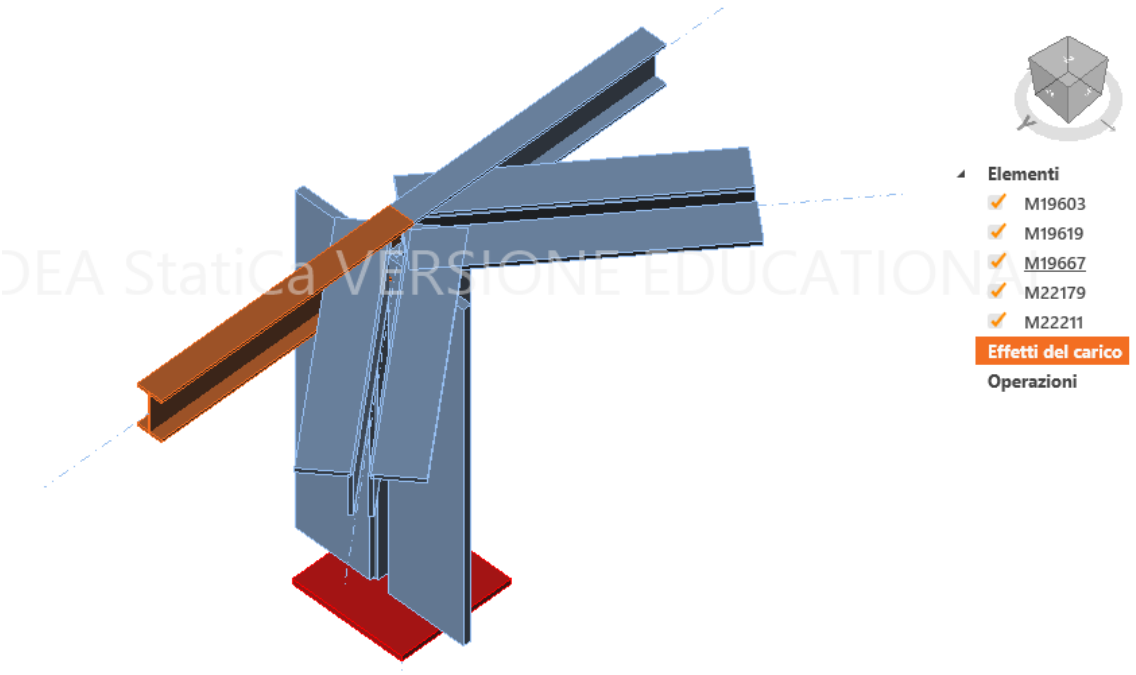

Figure 86:Idea Statica representation of elements.

In this case, the only remedy to overcome this problem was to introduce a new compound profle, welded section with mixed structure.

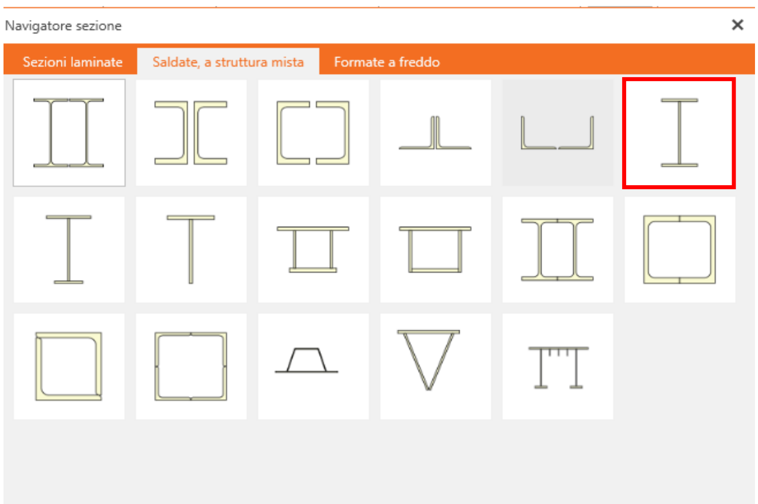

Figure 87: Choose of cross-section type

Once you have defined the type of section and its geometrical characteristics for the missing section, can proceed with the operations necessary to define the joint in this case.

The Idea Statica software allows you to perform the following non-linear analyses:

- **EPS** – Stress/strain design (joint code-check, optional buckling analysis).
- **ST** – Connection stiffness (rotational/axial stiffness of selected member connection).
- **MC** – Member capacity design (code-check of non-dissipative connections for seismic design).
- **DR** – Joint design resistance (maximum possible loading, reserve in joint capacity)

The structural analysis in this enviroment is done on non-linear and nonlinearities type of behaviour, always following the european design code, e.g. EN1993-1-8. The base of solving joint is with the Component method CM, has the ability to solve the joint as a system of interconnected items in FEM approach. The elastic-plastic analysis in this case is requested, by done two type of analysis in the background: Geometrically linear analysis, in terms of material and contact nonlinearities for stress and strain analysis, and Eigenvalue analysis, useful to determine the possibility of buckling.

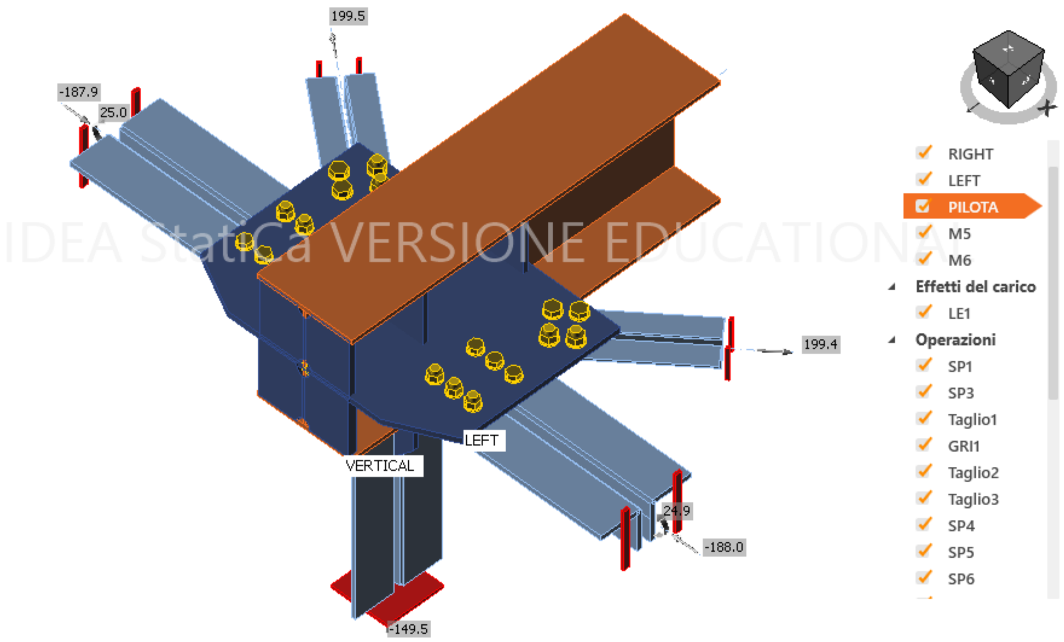

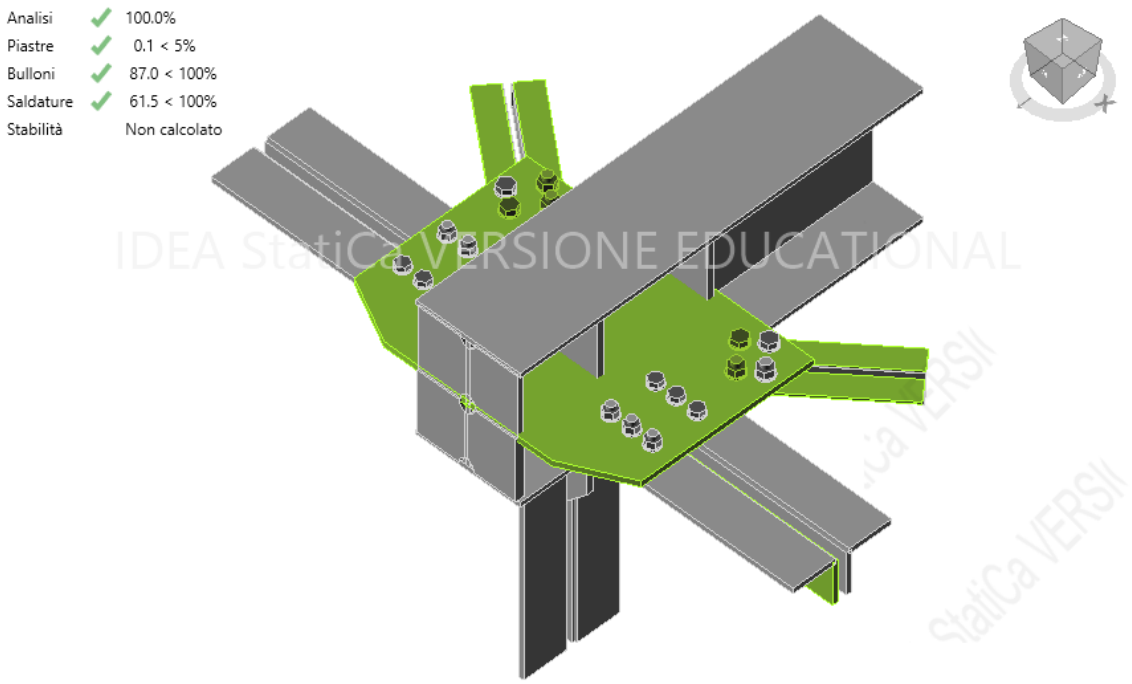

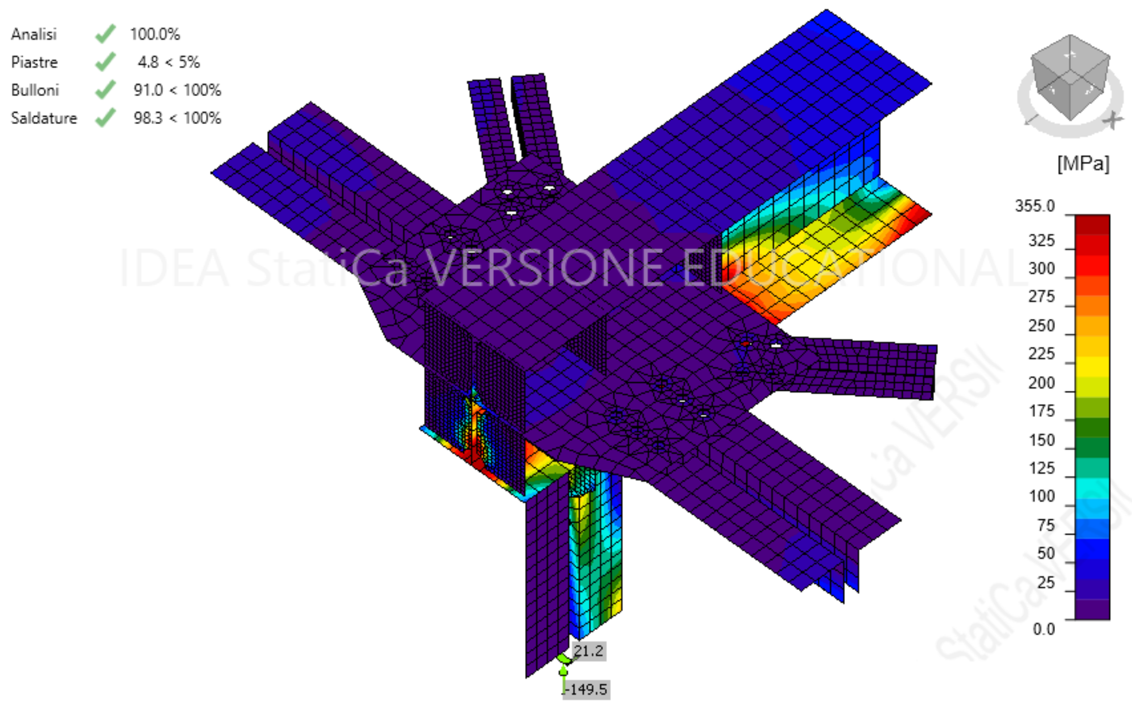

Figure 88: Final geometrical and FEM result.

The images shown in figure 78 represent the 3 operating phases that have been used by this software. the first represents the design configuration of the entire node, bolts, plates and welds. The second is the result of the EPS analysis; finally, the third image expresses the results in terms of connection stiffness, ST, with output the bending moment and flexural stiffness graph of the node itself.

Concluded with the local analysis of each joint under consideration in the deck, the interoperability between the calculation and graphic software was tested. Using Advance Steel, as graphic software to increase the level of detail, it was possible to create the final construction of details of the nodes and beam elements, plate used for the bridge in question.

Initially, the Advance Design model was exported to Advance Steel using ".smlx", steel markup language. Thanks to the BIM Graitec tool is very easy export the structural model into a steel language. The result of final exportation is shown in the following picture.

Figure 89: Assonometric view of importation steel deck from Advance Design to Advance Steel.

As we can see, the main longitudinal beam, where in the Advance Design was defined as plate steel element with own material characteristic, when it is exported into Advance Steel environment they are recognized as always as steel elements, but with different geometrical shape, in particular the web thickness was changed.

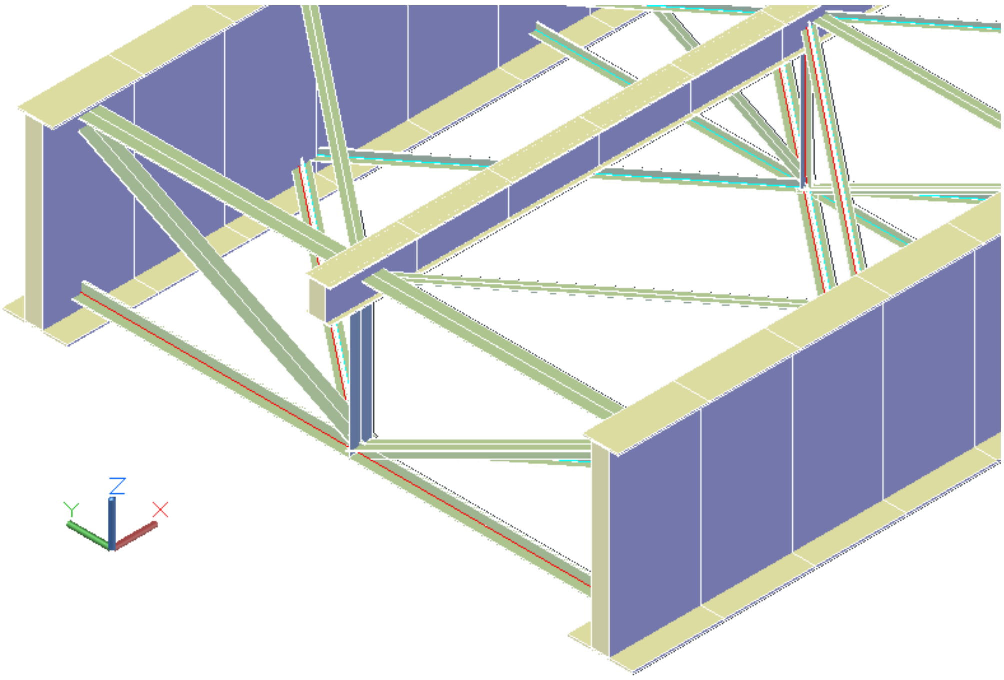

Figure 90:Local view of exportation in assonometric visualisation.

Instead, as we can see in the figure 80, the beam elements placed in transversal and horizontal plane are placed and they have been exported correctly, following the previously set sections and according to the general geometric configuration.

Starting from this good base, there was need to replace the position of the upper and lower flange, to form all the sections that the deck has in each segment of the deck.

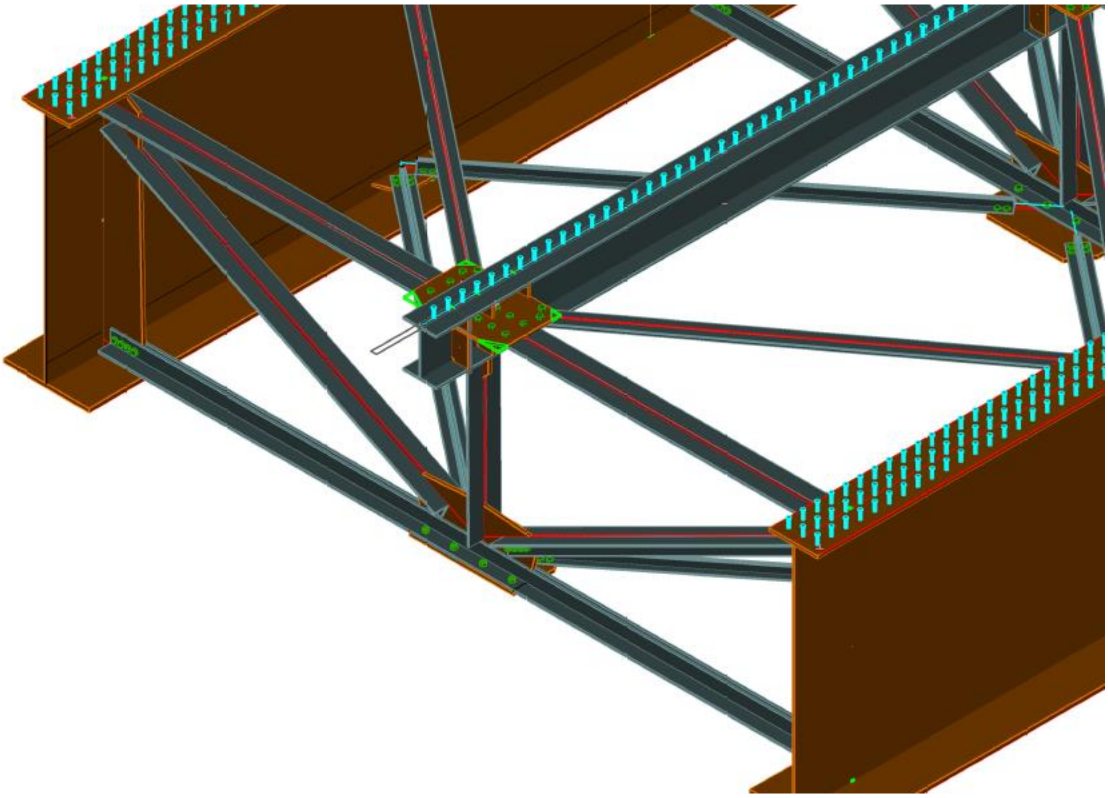

Figure 91: Final Assonometric view of detailed drawing from Advance Steel.

Having done so, the kerb welding between the plates was arranged. Once the main beams had been rebuilt, it was possible to replicate the construction detail previously verified with the local verification programme. As is represented in the previous figure 81, it is shown the shear connectors, bolts, welds and other plates useful to complete the node.

The following image shows the progressive evolution of the previously analysed node. In conclusion, it was appropriate to create the construction detail drawing of each element involved in this node.

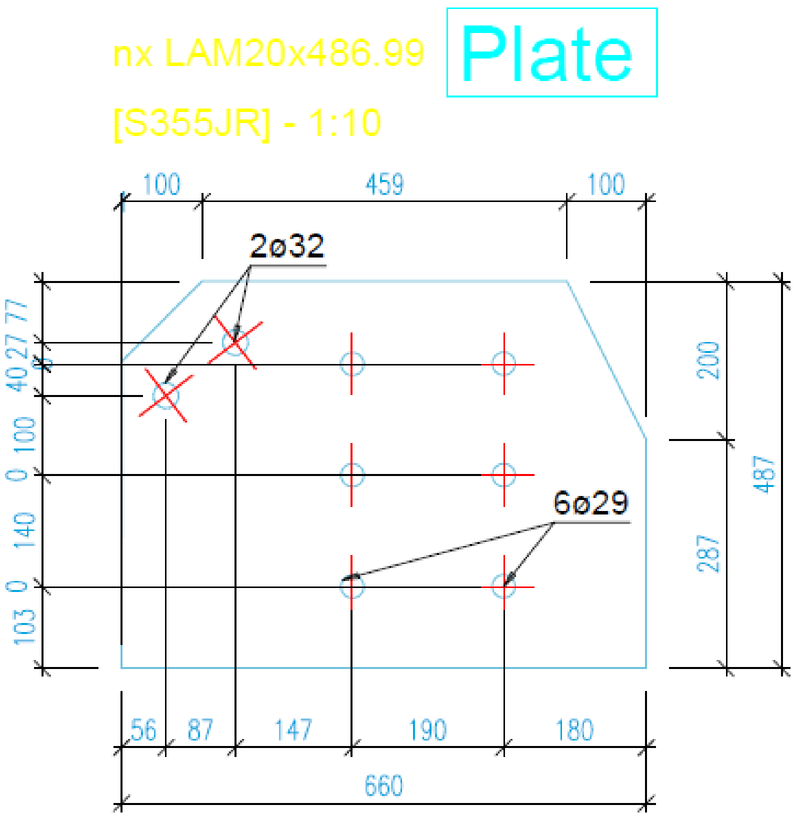

Figure 92: Detailed drawing of single plate used

Now it is interesting to test the interoperability between Advance Steel with Idea Statica. in this case there can be two ways to test the path, i.e. through 2 commands: "*CONUI*" or "*CONCHECK*". The first command couldn't be used because my pc system didn't allow it, considering that all "student" license versions were used. Instead with the second command, it was possible to open the local verification workspace in the following program.

Once the procedure that follows the command has been carried out, the result is as shown in Figure 83. As you can see the export did not take place, not saving the plates using and not recognizing the profiles previously used and verified in the previous interoperability step.

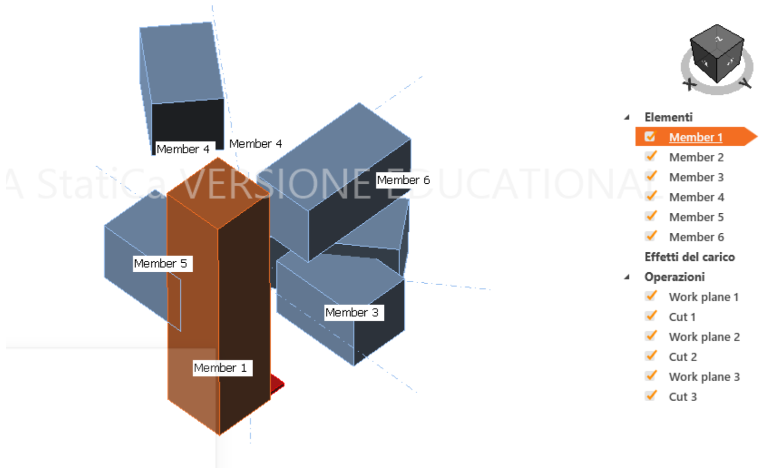

Figure 93:Exportation into Idea Statica environmental.

CONCLUSION

Basically, the case study analysed was made to understand the use of B.I.M. methodology in the structural field, application for long deck steel bridge. A bridge with deck in mixed steel-concrete structure was calculated from a static and dynamic point of view. The slab, beams and secondary structures were calculated with static loads, considering traffic loads as static action in different sections, based on the influence line.

The checks on the structural elements were carried out in accordance with the regulatory requirements imposed by DM 17/01/2018 and according to the Eurocode, all of which were satisfied both at the ultimate limit state and the serviceability limit state by using an Advance Design software environment. It constitutes an intuitive interface, easy to use and has several design commands, where was performed the global structural calculations.

The next step was exploiting the interoperability between Idea Statica and Advance Steel to check the local effects and increase the level of detail until drawing the final details.

Interoperability through software is not yet optimal, as problems are still displayed in the export of surface elements. In the first case, switching between Advance design and Idea Statica, it is clearly observed that the local verification program does not clearly recognize section and properties of the continuous two-dimensional element, vice versa it is optimal for the local control of elements that follow the theory of de Saint Venant. In the second case, switching between Advance Design and Advance steel, the switchover and interoperability is 90% satisfied, still challenging the recognition of surface elements but saving all the beam sections previously used for structural calculations.

By verifying the actual interoperability between the software, the final objective of the thesis was to properly carry out the local checks of the described nodes and then to reach a high level of detail. The achievement of a high level of detail allowed me to understand at a constructive level how each single beam and plate element could be connected, taking into consideration operating distances, welds and bolts. Important has been the realization of the beam-to-beam joints by means of the theory of fully restored bolted joints, which without taking into account the external loads, there is the possibility to arrange the bolts only through the internal characteristics of the materials that are part of them. The level of detail reached is that corresponding to the workshop construction drawings, marked each single element with a specific nomenclature and giving the appropriate distances in the articles.

I can conclude the thesis, how fundamental is the use of BIM methodology today. It gives the possibility to make any transition from one software to another, even if they are different in principle and use. Approaching with this new method of thinking and designing will make the life of all the professionals who work together in a single project much easier, having the possibility to modify and understand the single model even if they have a different background.

This type of thesis has been fundamental to me and my educational background. I was able to improve my processing skills in the case of structural analysis by taking into account all the legislation that was part of it. I also faced a sort of challenge to myself, because by choosing a thesis based on a steel material I had never faced before I understood what problems could arise and how to solve them.

Moreover, by entering into the BIM methodology I had the opportunity to use multiple software such as those listed in this document, giving me the opportunity to better understand the context with the 3D visualization of each element under consideration and analysis.

ACKNOWLEDGEMENTS

At the end of this work I would like to express my thanks to all those who have helped me, in one way or another, to achieve this important goal.

I thank my parents with great affection and gratitude for their daily moral and economic support in this path of my life.

A special thanks to my brother and sister-in-law, capable with the carefreeness of my nephew Daniele, to make me live moments of serenity, peacefulness and to distract me from everyday life.

I would like to sincerely thank Giulia for having always been there for me, for having shared with me positive and negative moments, having endured and supported us in this journey of our life together, reaching important goals.

To my fellow students that I met at the Polytechnic of Turin. With them I shared everything, from studying to everyday life, facing challenges and travelling together, giving me each of them important advice in any situation.

Thanks to Linda, for having shared this two year of life together, helping us in every academic difficulty and solving every problem we faced.

Thanks to the "Magnifici 4 of Casa Vespucci", Gianluigi, Matia, Alberto, Albertino and Gino. Buddies of a thousand adventures and misadventures, traumatic awakenings and dinners based on "frico and polenta".

I would like to thank my friends, for believing in me and for the beautiful relationship that binds us constantly, especially sharing smart aperitifs in this tricky period.

A sincere thanks to the company LGA Engineering from Savigliano (CN), especially to Engineer Andrea Alberto and his team for helping and teaching me important knowledge during this period of writing my thesis.

BIBLIOGRAPHY

- Acampa, G. (2018). Test for interoperability: from theory to practice. *3D modelling & BIM*, 48-61.
- Ballio G., Bernuzzi C. (2004). Progettare costruzioni in acciaio. Ulrico Hoepli Editore S.p.A., Milano, Italy.
- Belluzzi O. (1989). Scienza delle costruzioni. Vol.2. Zanichelli Editore, Milano, Italy.
- Carpinteri A. (1992). Scienza delle costruzioni 1. Pitagora Editrice, Bologna, Italy.
- Carpinteri A. (1992). Scienza delle costruzioni 2. Pitagora Editrice, Bologna, Italy.
- Commissione di studio per la predisposizione e l'analisi di norme tecniche relative alle costruzioni, CNR-DT 207/2008, (2009). Istruzioni per la valutazione delle azioni e degli effetti del vento sulle costruzioni.
- Cordova B. (2013). Costruzioni in acciaio. Manuale pratico per l'impiego delle norme tecniche per le costruzioni e dell'Eurocodice 3 (UNI EN 1993). Ulrico Hoepli Editore S.p.A., Milano, Italy.
- Ren R and Zhang JModel Information Checking to Support Interoperable BIM Usage in Structural Analysis Computing in Civil Engineering 2019, (361-368).

Technical regulations consulted

- "Norme Tecniche per le costruzioni" adottate con il D.M. of 17 January 2018.
- UNI EN 1991, Actions on structures.
- UNI EN 1992, Design of concrete structures.
- UNI EN 1993, Design of steel structures.
- UNI EN 1994, Design of composite steel and concrete structures.
- UNI EN 1998, Design of structures for earthquake resistance.

User's guide:

- Advance design user guide.
- Idea Statica theoretical background.
- Advance Steel user guide.
- Workbook di implementazione pilota del BIM, Autodesk.
- Pilota BIM. Manuale introduttivo, Autodesk.
- Guida all'interoperabilità, Autodesk.

WEBSITE CITATIONS

www.buildingsmart.org

https://www.buildingsmart.org/standards/bsi-standards/industry-foundation-classes/

https://www.autodesk.com/solutions/bim/hub/bim-interoperability

https://www.autodesk.com/solutions/bim

https://knowledge.autodesk.com/support/revit-products/learn-explore/caas/simplecontent/content/useful-useful-ifc-links.html

https://www.ideastatica.com/it/idea-statica-and-graitec/

https://www.ideastatica.com/idea-statica-and-trimble/

https://www.ideastatica.com/steel/?gclid=EAIaIQobChMItM2Tt_-M6AIVSsKyCh0J2gerEAAYASAAEgK9qfD_BwE

https://www.steelconstruction.info/Bridges

esse1-gis.mi.ingv.it

https://it.graitec.com/advance-design/

http://www.ibimi.it/lod-livello-di-dettaglio-per-il-bim/

http://www.nelsonsaldaturaperni.it

https://www.promozioneacciaio.it/

ANNEX A – MODEL CALIBRATION

CALIBRATION OF SAINT VENANT AND CONTINUOUS MODELS

Model calibration gives us the possibility to compare the behaviour of the elements in a more detailed way and closer to the real tensional development. Therefore, our aim in this chapter is to study what the differences are from the De Saint Venant model to the continuous one in term of displacement, forces and tension, in order to understand in a better way how the program works. All analytical tests are conducted by Advance Design Software

As the first analysis, the general static system is composed of beam **IPE 300 (S355),** placed on pinned and rolled supports and loaded with a concentrated load of 1000 daN on different position and direction.

The meshes used for the FEM analysis are [dimension/tolerance]: De Saint Venant element [150mm/50mm], Continuous element [50mm/10mm].

The following images explain the general characteristics in order to compare the methodologies (firstly is shown the continuous result then the De Saint Venant).

De Saint Venant element are kept in consideration as linear element which has own cross-section, type of material, orientation, constraint and mesh. We must remember that there are some limitations on Saint-Venant principle's: constraints, volume forces, apply forces only at the end-sections and decay region around twice the main dimension of cross-section, constant cross section along all straight beam axis.

Instead of DSV (De Saint Venant) theory element, continuous one is created as superficial type, properly defined as thin walled element. Even in this case, the element has own thickness, length, deep, material, constraint, orientation and mesh.

BEAM LOADED ON Z-DIRECTION

STATIC SCHEME

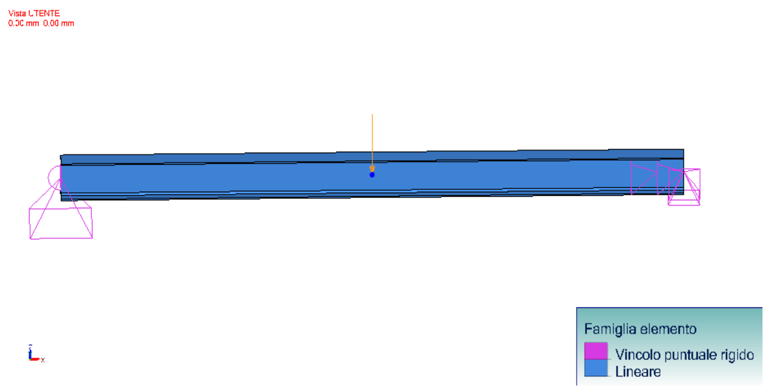

Figure 94: General scheme. Beam loaded on z direction.

DISPLACEMENT – G

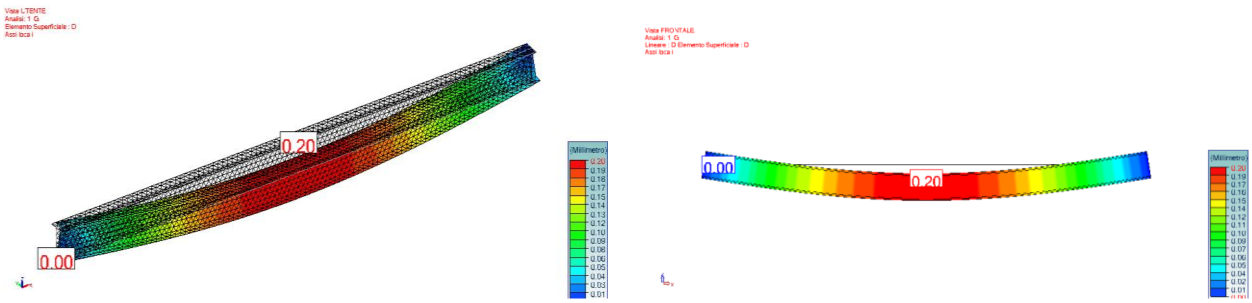

Figure 95:Dead load effect. left is expressed the continuous behaviour.

DISPLACEMENT – Q

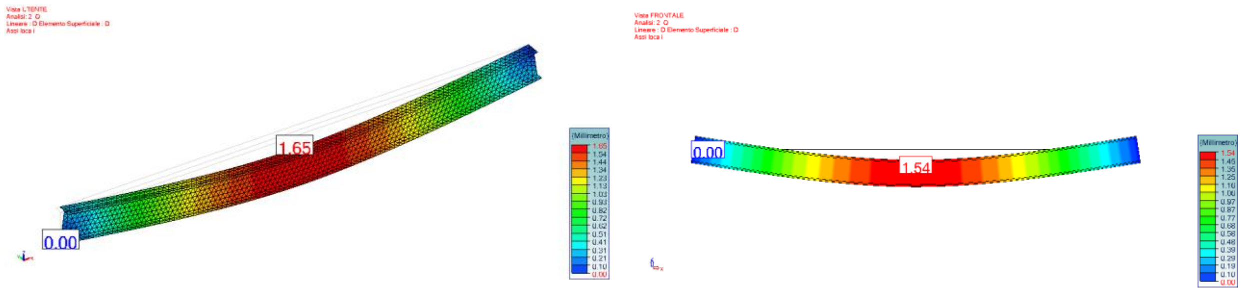

Figure 96: Variable load effect. Left is expressed the continuous behaviour.

DISPLACEMENT – LC SLU

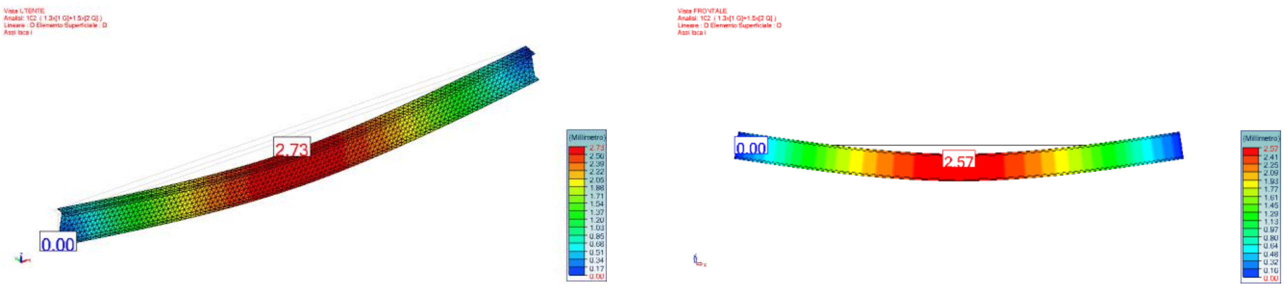

Figure 97: load combination effect. Left is expressed the continuous behaviour.

Table 51:Displacement values. Beam loaded on z direction.

DISPLACEMENT [MAX]			
	D S V	CONTINUOUS	%
G	0,20 mm	0,20 mm	-
Q	1,54 mm	1,65 mm	7
L.C.	2,57 mm	2,73 mm	6

STRESS ANALYSIS – σ_{xx} – G

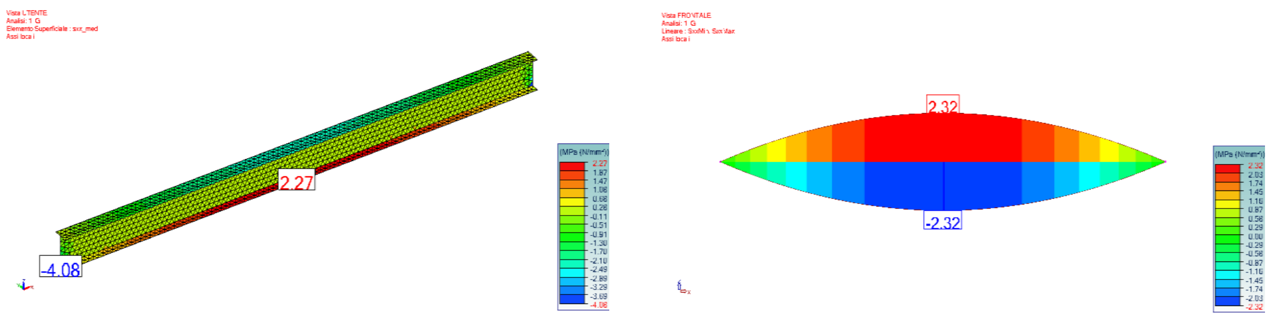

Figure 98: Dead load stress effect. left is expressed the continuous behaviour.

STRESS – σ_{xx} – Q

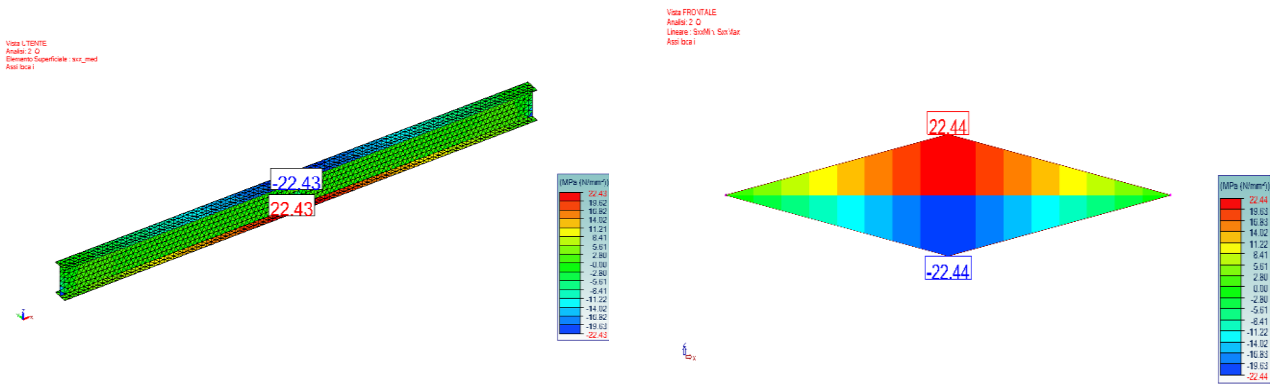

Figure 99: Variable load stress effect. left is expressed the continuous behaviour.

TENSION –σ_{xx} – LC SLU

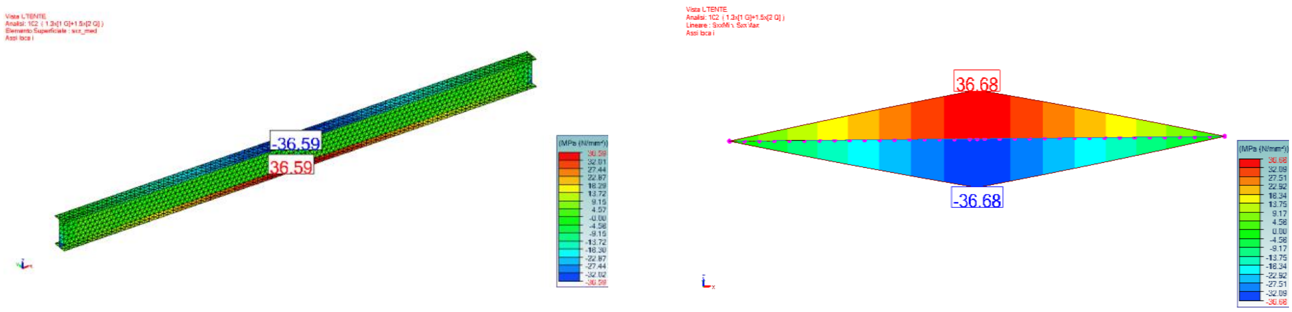

Figure 100: Load combination stress effect. left is expressed the continuous behaviour

Table 52:Stress values. Beam loaded on z direction.

STRESS σ_{xx}			
	D S V	CONTINUOUS	%
G	2,32 MPa	2,27 MPa	2
Q	22,44 MPa	22,43 MPa	0,5
L.C.	36,68 MPa	36,59 MPa	0,3

TENSION – σ_{VM} LC SLU

$$\sigma_{VM} = \sqrt{\sigma_x^2 - \sigma_x\sigma_y + \sigma_y^2 + 3\tau_{xy}^2}.$$

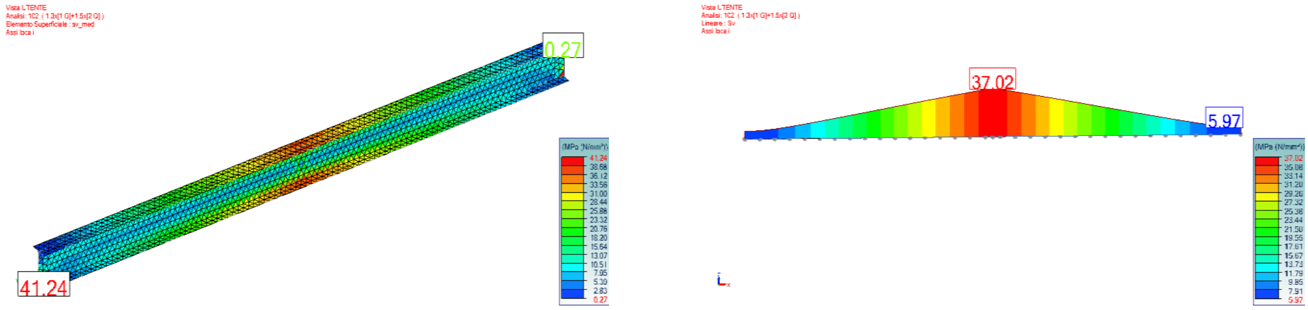

Figure 101: Load combination Von Mises stress effect. left is expressed the continuous behaviour

Table 53: Von Mises values. Bema loaded on z direction

STRESS σ_{VM}			
	D S V	CONTINUOUS	%
L.C.	37,02 MPa	41,24 MPa	11,4

BEAM LOADED ON Y-DIRECTION

In this case, we have rotated the concentrated load of 90° in order to study the resisting cross-section on y direction.

STATICH SCHEME

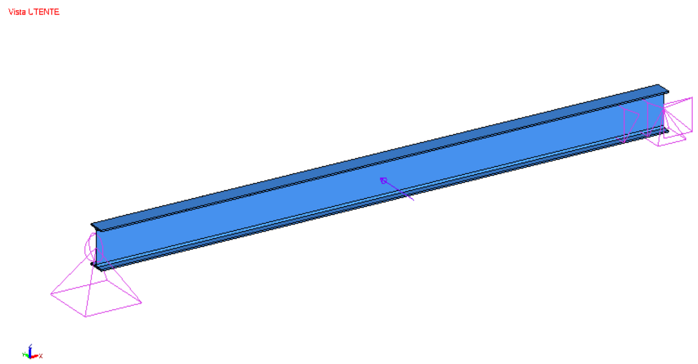

Figure 102:General scheme. Beam loaded on y direction.

DISPLACEMENT – G

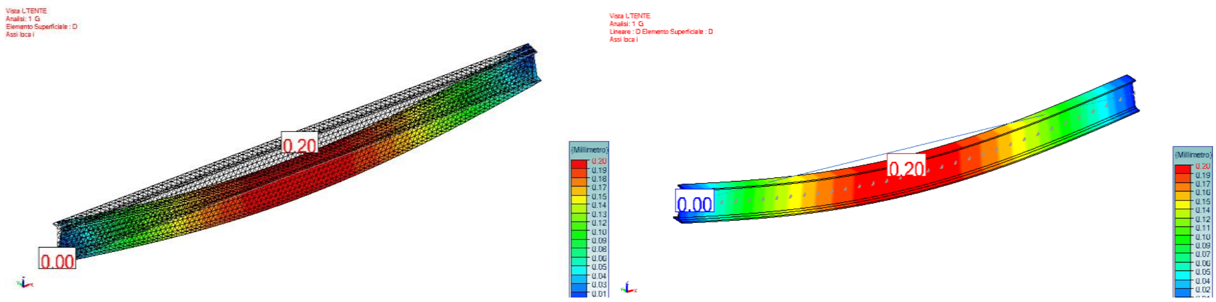

Figure 103:Dead load effect. left is expressed the continuous behaviour

DISPLACEMENT – Q

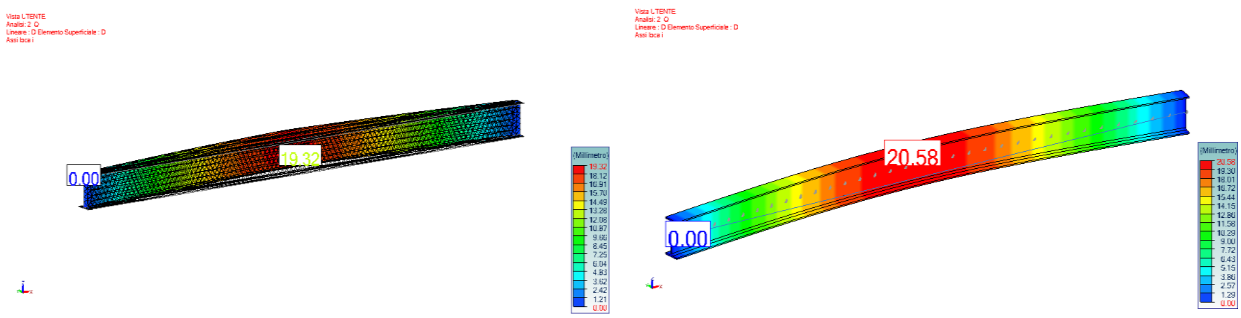

Figure 104: Variable load effect. Left is expressed the continuous behaviour.

DISPLACEMENT – LC SLU

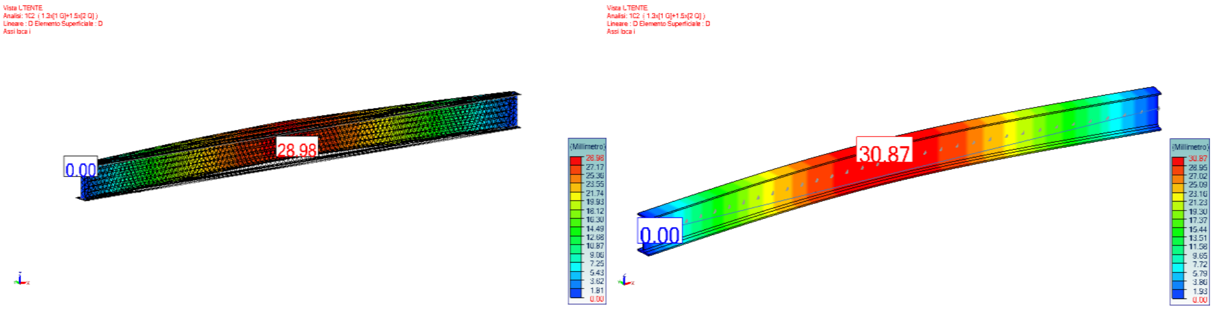

Figure 105: Load combination displacement effect. Left is expressed the continuous behaviour.

Table 54:Displacement values. Beam loaded on y direction.

DISPLACEMENT [MAX]			
	D S V	CONTINUOUS	%
G	0,20 mm	0,20 mm	-
Q	20,58 mm	19,32 mm	6,5
L.C.	30,87 mm	28,98 mm	6,5

STRESS – σ_{xx} – LC SLU

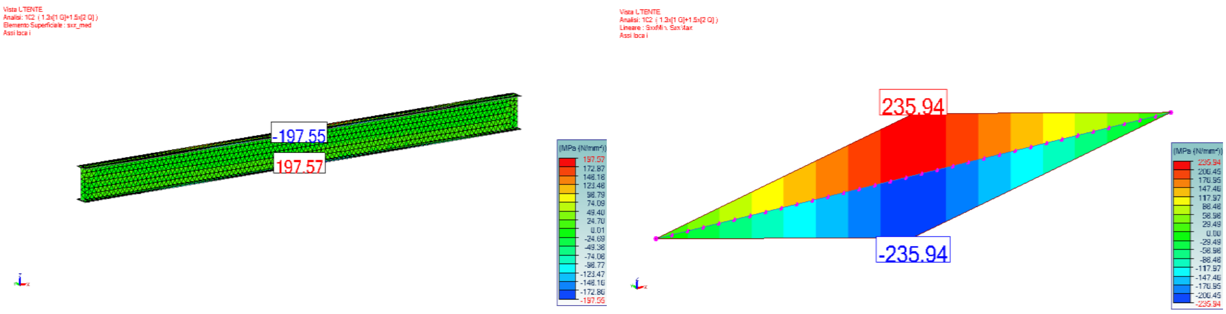

Figure 106:Load combination stress effect, Left is expressed the continuous behaviour.

Table 55: Stress values. Beam loaded on y direction.

STRESS σ_{xx}			
	D S V	CONTINUOUS	%
L.C.	235,94 MPa	197,57 MPa	19

STRESS– σ_{VM} – LC SLU

$$\sigma_{VM} = \sqrt{\sigma_x^2 - \sigma_x\sigma_y + \sigma_y^2 + 3\tau_{xy}^2}.$$

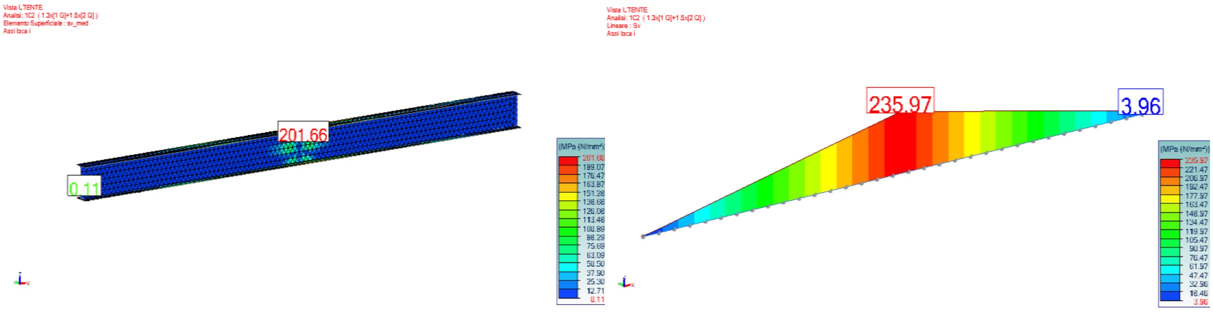

Figure 107: Load combination Von Mises stress effect. Left is expressed the continuous behaviour.

Table 56: Von Mises values. Beam loaded on y direction.

STRESS σ_{VM}			
	D S V	**CONTINUOUS**	**%**
L.C.	**235,97 MPa**	**201,66 MPa**	**17**

BEAM LOADED ON Z-DIRECTION WITH TRANSVERSAL ELEMENT TORSION ANALISYS

Differently what was done, we now analyse the general behaviour obtained by adding a transverse element. This new approach wants to be a practical example to the analogy between the beams-shear connectors.

The transversal element has 0,5m of length and is placed on half of the main one. The cross-section used is the same of before calibration and mesh as well.

In order to study the torsion effect of all system, we decide to shift the concentrated load at the end of the transversal beam, as shown the below image; the concentrated load is 1000 daN.

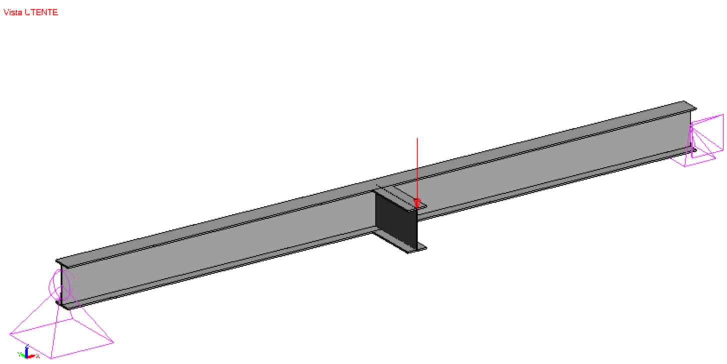

Figure 108:General scheme of torsional analysis.

As we did before for bending analysis, we'll display displacement, bending moment and tension for several cases. In order to calculate the displacements, it was assumed that the rotations in the x-direction would be blocked, in order to obtain an accurate result.

DISPLACEMENT – G

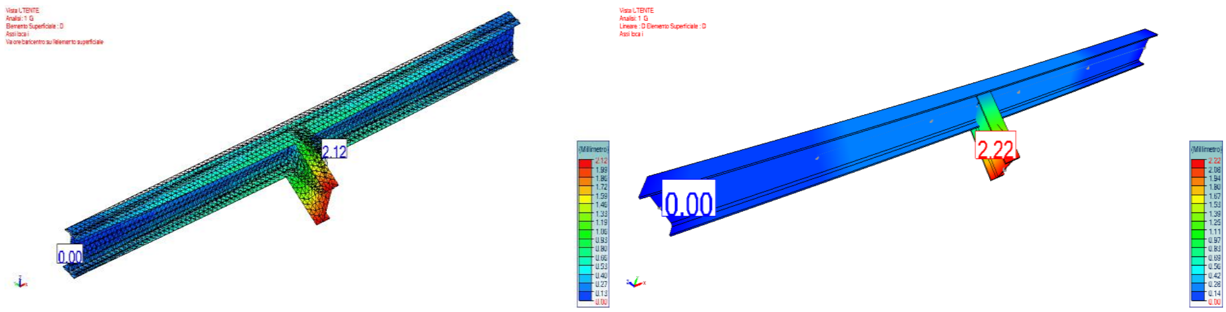

Figure 109:Dead load effect. Left is expressed the continuous behaviour.

DISPLACEMENT – Q

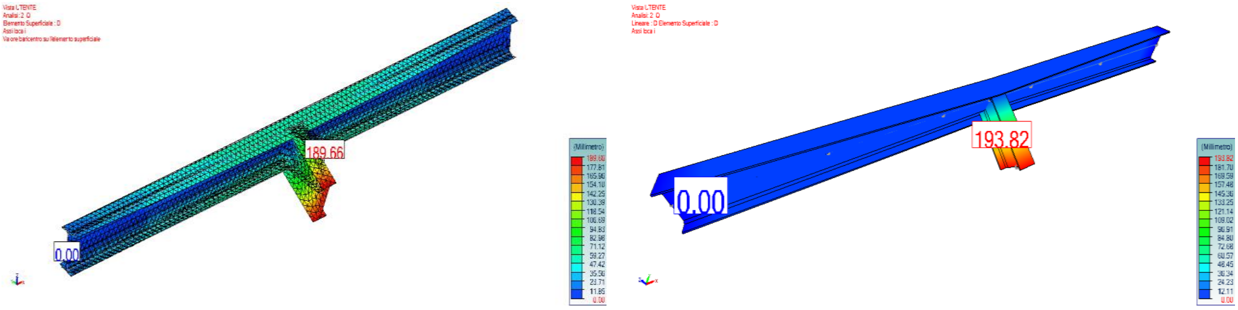

Figure 110: Variable load effect. Left is expressed the continuous behaviour.

DISPLACEMENT – LC SLU

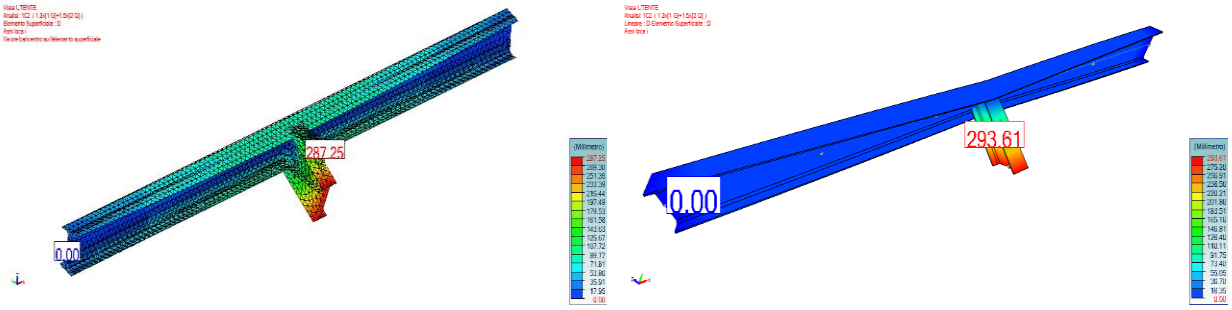

Figure 111:Load combination effect. left is expressed the continuous behaviour.

Table 57: Displacement values. Torsional analysis

DISPLACEMENT [MAX]			
	LINEAR	**CONTINUOUS**	**%**
G	**2.22 mm**	**2,12 mm**	**4,7**
Q	**193,82 mm**	**189,66mm**	**2,3**
L.C.	**293,61 mm**	**287,25 mm**	**2.2**

For the stress analysis, i have returned to the initial binding condition, i.e. pinned-rolled supports.

STRESS – σ_{xx} – LC

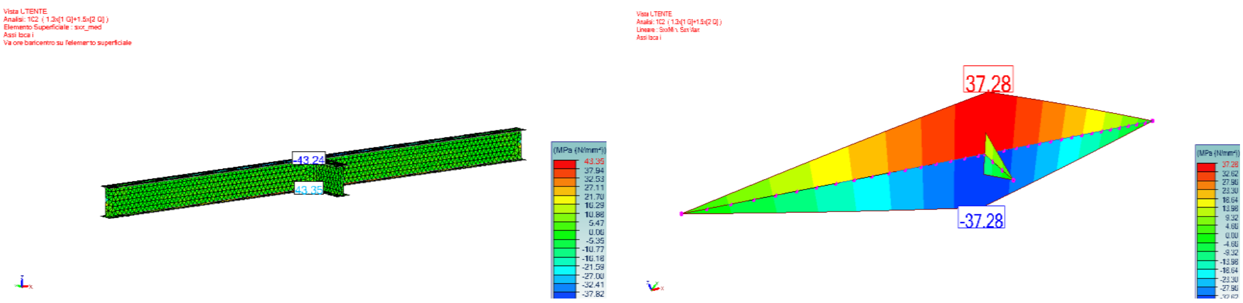

Figure 112: Load combination stress effect. Left is expressed the continuous behaviour.

Table 58:Stress values. Torsional analysis

STRESS σ_{xx}			
	LINEAR	**CONTINUOUS**	**%**
L.C.	**37,28 MPa**	**43,35 MPa**	**16**

STRESS – σ_{VM} – LC SLU

$$\sigma_{VM} = \sqrt{\sigma_x^2 - \sigma_x\sigma_y + \sigma_y^2 + 3\tau_{xy}^2}.$$

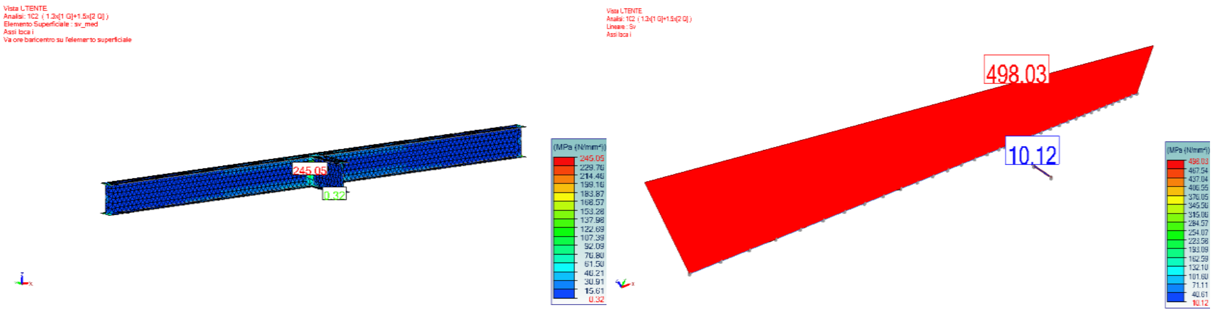

Figure 113: Load combination Von Mises stress effect. Left is expressed the continuous behaviour.

Table 59:Von mises values. Torsional analysis.

STRESS σ_{VM}			
	LINEAR	**CONTINUOUS**	**%**
L.C.	**498,03 MPa**	**245,05 MPa**	**-**

For the study of continuous elements, we rely on thin plates. Thin plates have usually dimension as h/L=1/50 - 1/10. They have characteristics as flexural stiffness that carry two-dimensional load distributions mainly through bending moments, torques and shearing in a manner similar to beams. The study of the plates is usually carried out with reference to its middle plane, which is the plane perpendicular to the thickness that cuts the plate into two portions of equal size. The theory behind the analysis of the plates is called Kirchhoff's theory. As we know, the tensional state governing the plates are second order differential equations, which are difficult to solve manually.

An important analysis to be carried out is that of shear and bending shear. Since we are in the case of a longitudinal beam and a transverse element positioned in the middle, as if it were a cantilever fixed to the main beam.

As a first analysis shear verification was done. The law suggests applying shear forces must be lower than resisting on. In this case we have:

$$\frac{V_{Sd}}{V_{c,Rd}} \leq 1$$

$$V_{c,Rd} = \frac{A_v\, f_{yk}}{\sqrt{3}\,\gamma_{M0}}$$

$$A_v = A - 2\, b\, t_f + (t_w + 2\, r)\, t_f$$

in our case we are in a situation of torsion due to the load condition, so the resisting shear of the cross-section is reduced by:

$$V_{c,Rd,red} = \frac{A_v\, f_{yk}}{\sqrt{3}\,\gamma_{M0}} \sqrt{1 - \frac{\tau_{t,Sd}}{1{,}25\, f_{yk}/\sqrt{3}\gamma_{M0}}}$$

$$\tau_{t,Sd} = \frac{M_t b_{max}}{I_t} = \frac{3\, M_t\, b_{max}}{\sum_{i=1}^{n}\left(a_1\, b_i^3\right)}$$

In our case the shear check was not satisfied, because the resisting shear in lower than applied one. So, starting from shear check on stress point of view we can define which will be the max concentrated load acting on the edge of the beam.

$$\frac{\tau_{t,Sd}}{f_{yk}/\sqrt{3}\,\gamma_{M0}} \leq 1{,}0$$

Going backwards the maximum load will be **P = 568,24 daN** instead of 1000 daN applied.

The second step analysis is the bending shear check. NTC 2018 says that a beam I or H, subjected to bending on the plane of the core, has a flange (flat band) stretched and a compressed. This, if it is slender and not sufficiently bound laterally, tends to warp, undergoing a twist. Once the geometrical limits have been exceeded it is necessary to carry out a torsional instability test.

$$\frac{M_{Sd}}{M_{b,Rd}} \leq 1$$

Where,

M_{Sd}, maximum bending moment;

$M_{b,Rd}$, resisting bending moment due to instability.

$$M_{b,Rd} = \chi_{LT}\, W_y \frac{f_{yk}}{\gamma_{M1}}$$

W_y, resisting modulus, equal to the plastic modulus for class 1 and 2;

χ_{LT}, reduction factor for bending-shear instability;

$$\chi_{LT} = \frac{1}{f} \frac{1}{\phi_{LT} + \sqrt{\phi_{LT}^2 - \lambda_{LT}^2}} \leq K\chi$$

$$f = 1 - 0{,}5(1 - k_c)\,[1 - 2{,}0\,(\lambda_{LT} - 0{,}8)^2]$$

$$\phi_{LT} = \frac{1}{2}\left[1 + \alpha_{LT}\left(\lambda_{LT} - \lambda_{LT,0}\right) + \lambda_{LT}\right]$$

Where α_{LT} is a geometrical coefficient function of cross-section (H/B), available on NTC 2018.

$$\lambda_{LT} = \sqrt{\frac{W_{y,Pl}\, f_{yk}}{M_{cr}}}$$

$$M_{cr} = C_1 \frac{\pi^2\, E\, I_z}{(k\, L)^2} \sqrt{\left(\frac{k}{k_w}\right)^2 \frac{I_w}{I_z} \frac{(kL)^2\, G\, I_t}{E\, I_z}}$$

I_t, torsion constant. It is evaluated as:

$$I_t = \frac{1}{3} \sum a_i\, b_i^3$$

I_w, swallowing constant. It is expressed as:

$$I_w = \frac{1}{4}\frac{t_f\, b^3}{6} h_a^2 \approx \frac{1}{6}\, t_f\, b^3$$

$$h_a = H - t_f$$

We can neglect the instability torsion because we are in the case of $\lambda_{LT} \leq 0{,}4$ and it is satisfied.

Now, we'll demonstrate the effects, in terms of torsion, of the new maximum load found before, $P = 568{,}24 daN$, by using Advance Design and the calculation in order to show all passages towards the final results.

	P	**L**	**P**	**L**
	daN	**m**	**daN**	**m**
	1000	**0,5**	**568,2**	**0,5**
M_t	500,0	daNm	284,1	daNm
M_t	5000000,0	Nmm	2841196,3	Nmm
τ_{max}	343,5	N/mm^2	195,2	N/mm^2
Av	2568,0	mm^2	2568,0	mm^2
γ_{M0}	1,1	-	1,1	-
$V_{c,Rd}$	501266,1	N	501266,1	N
$V_{c,Rd}$	50126,6	daN	50126,6	daN
d	NOT SAT.	-	0,4	-
$V_{c,Rd,red}$	NOT SAT.	N	224173,0	N
SHEAR VERIFICATION				
$\dfrac{\tau_{t,Sd}}{f_{yk}/\sqrt{3}\,\gamma_{M0}}$	1,72	**>1**	0,98	**<1**
	NOT SATISFIED		**SATISFIED**	

LOAD P=568,2 daN VERIFICATION

DISPLACEMENT – G

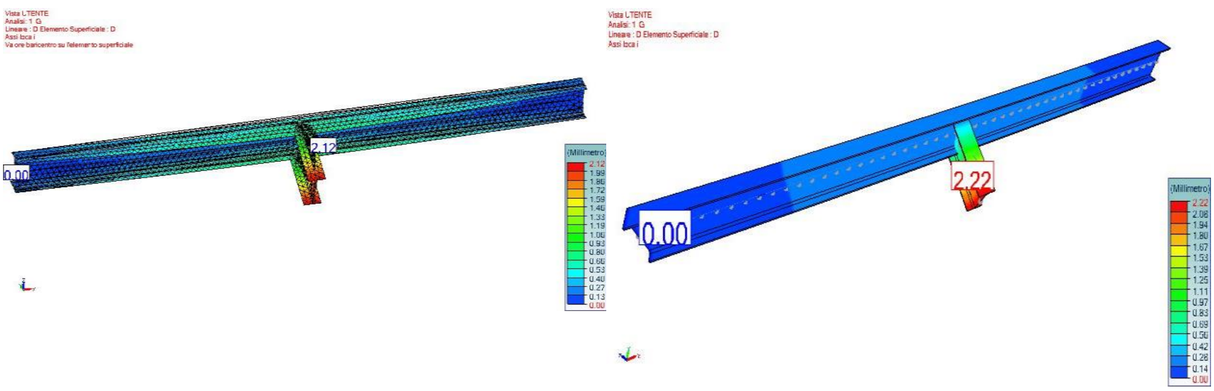

Figure 114:Dead load effect. Left is expressed the continuous behaviour.

DISPLACEMENT – Q

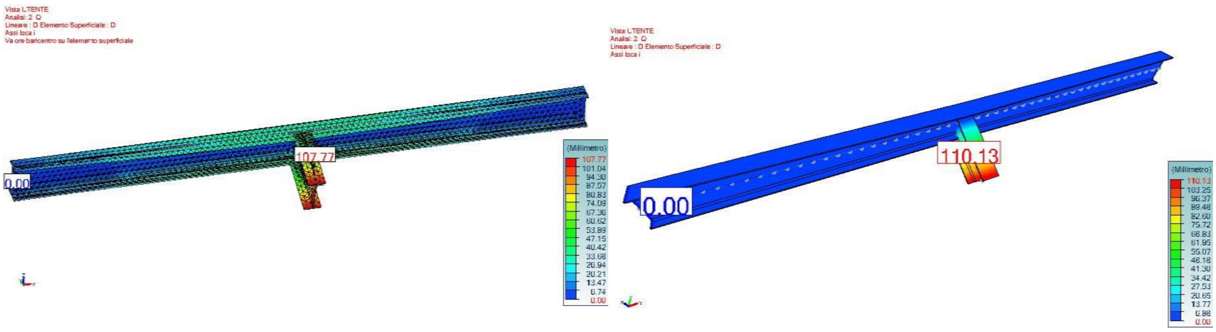

Figure 115:Variable load effect. Left is expressed the continuous behaviour.

DISPLACEMENT – LC SLU

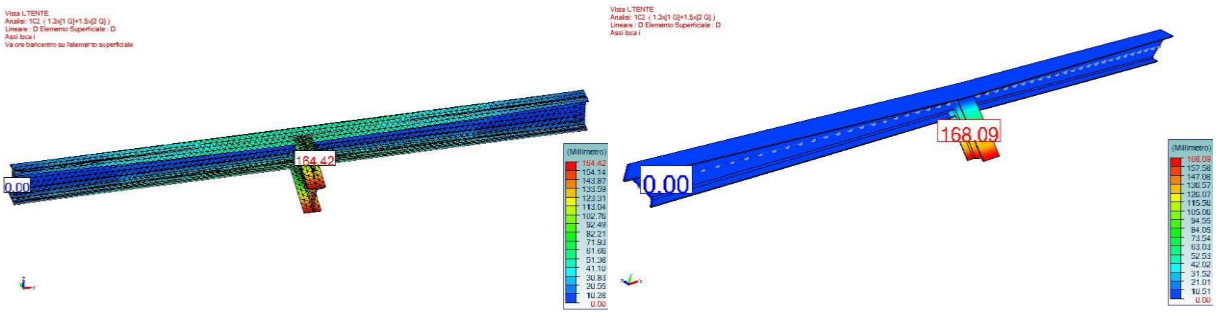

Figure 116:Load combination effect. Left is expressed the continuous behaviour.

Table 60:Displacement values. Torsional analysis with the max concentrated apply load

DISPLACEMENT [MAX]			
	LINEAR	**CONTINUOUS**	**%**
G	**2.22 mm**	**2,12 mm**	**4,7**
Q	**110,13 mm**	**107,77 mm**	**2,2**
L.C.	**168,09 mm**	**164,42 mm**	**2.2**

STRESS – σ_{xx} – LC

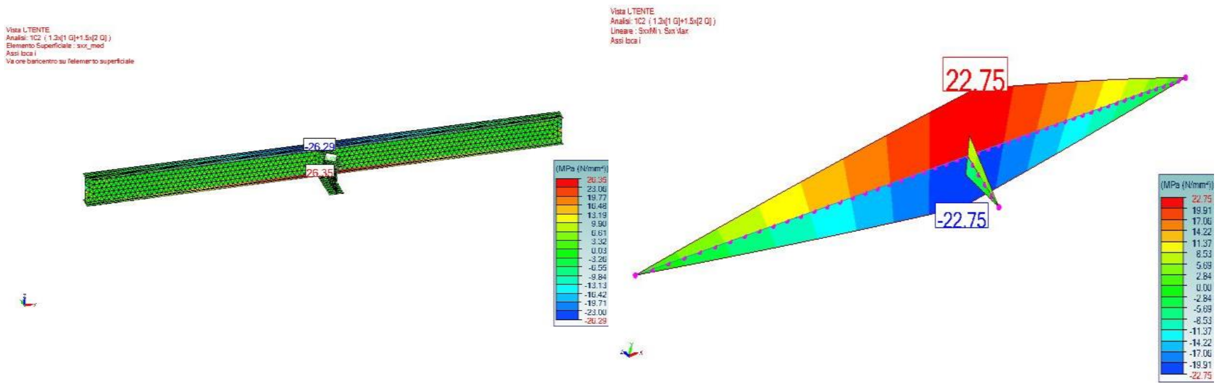

Figure 117:Load combination stress effect. Left is expressed the continuous behaviour.

Table 61:Stress values. Torsional analysis with the max concentrated apply load

TENSION σ_{xx}			
	LINEAR	**CONTINUOUS**	**%**
L.C.	**22,75 MPa**	**26,35 MPa**	**15,8**

STRESS– σ_{VM} – LC SLU

$$\sigma_{VM} = \sqrt{\sigma_x^2 - \sigma_x\sigma_y + \sigma_y^2 + 3\tau_{xy}^2}.$$

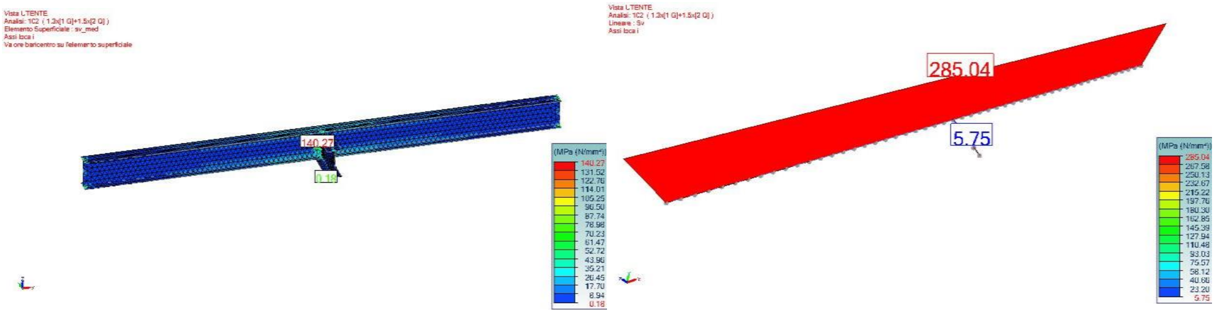

Figure 118: Load combination Von Mises stress effect. Left is expressed the continuous behaviour.

Table 62: Von mises Stress values. Torsional analysis with the max concentrated apply load

STRESS σ_{VM}			
	LINEAR	**CONTINUOUS**	**%**
L.C.	**285,04 MPa**	**140,27 MPa**	**-**

ANNEX B – INTEROPERABILITY CALIBRATION

To study the effective interoperability that there are between the 3 programs chosen to address during the thesis, we chose as a case study a scenic scale. It is an emergency staircase, developed vertically for about 20 meters, with a width of 9 meters and a depth of about 3.5 meters. The structure is made of steel carpentry with curved plate elements in the landings, having rigidity as main function.

The loop used for the calculation and future design is to start from Advance Design with the structural model, first choosing the sections for each single element: column, beam, floor, plate, etc.; then going to export it in advance steel to increase the level of detail, from LOD 2 to reach LOD 5.

Idea Statica instead has the function of importing the joint elements that you want to perform the local verification. The connections can be multiple as described above.

In this case instead we wanted to study how it was the passage or the interoperability from a drawing of Advance Steel and importing it later on Advance design.

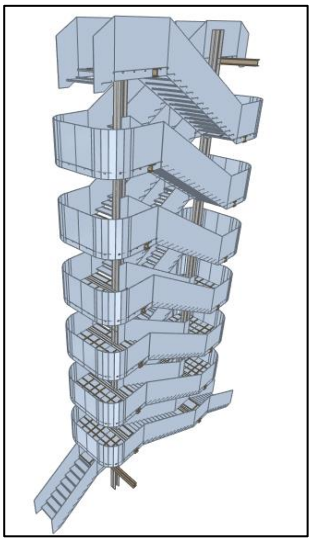

Figure 119: IFC result of Advance Steel modelling

So, the *smlx* format, Steel Markup Language Document, is an extension of the model description, giving the ability to save each type of element with its own mechanical, geometric and parametric characteristics of each element.

By testing the passage, i.e. importing the same file in Advance Design, we realize that the interoperability takes place in an optimal way, i.e. all the elements with their own characteristics are saved, or rather almost all of them.

The problem we see is concentrated on the curved plates; in fact, during the Advance Design import, in addition to creating some large elements in smaller elements, we observe in particular that the plate elements with curvature are also discretized in elements with smaller size but separated with a clearly visible tolerance. Another problem is always found in the curvature elements, they are not imported, perhaps because they have different reference systems from the default one.

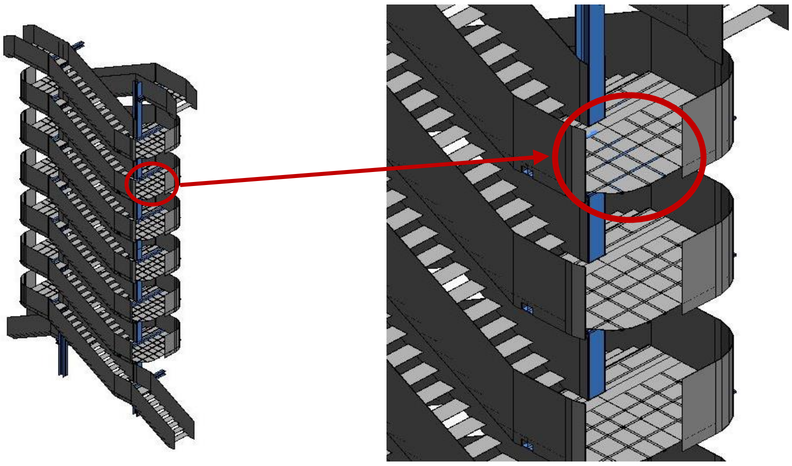

Figure 120:Import File in Advance Design; Highlighting interoperability

Observed what are the advantages and the small problems, which will be solved in the next releases, now we are going to test the switch between Advance Design and Idea Statica. The interoperability in this environment is very fast and immediate. Thanks to the tool  installed in AD allows, after selecting the predefined elements and nodes, to easily export and proceeds with the design phase of the connection chosen. For example, we have chosen the connection between the beam and the column, as shown in the figure below.

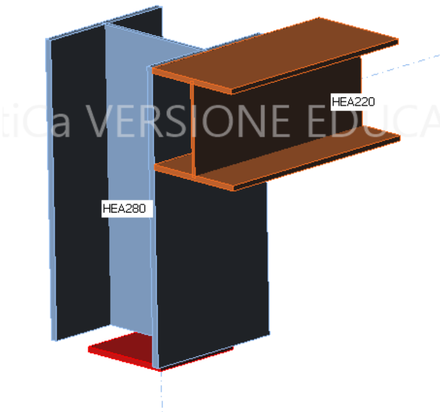

Figure 121:Interoperability check between Advance design and Idea Statica.

After which processes and inputs chosen for the node in matter, we can view the one hypothetic result:

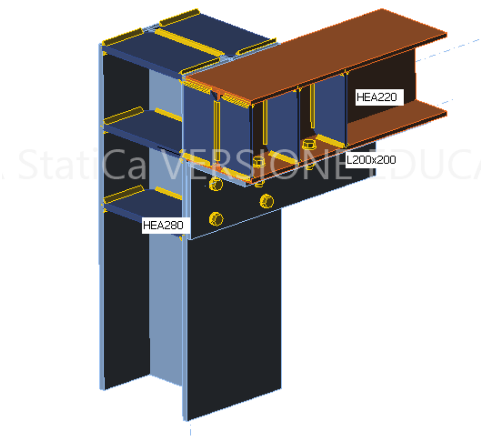

Figure 122:Final result of Idea Statica manipulations

ANNEX C – ELEMENT RESULTS

MAIN BEAMS ANALYSIS

PROFILE		
	Height [mm]	2500
	thickness upper flange [mm]	25
	width upper flange [mm]	500
	thickness added uuper flange [mm]	0
	width added upper flange [mm]	0
	web thickness [mm]	18
	thickness lower flange [mm]	35
	width lower flange [mm]	900
	thickness added lower flange [mm]	0
	width added lower flange [mm]	0
	As [mm^2]	87920,00
	Iy [mm^4]	2,39E+09
	Yg [mm]	969,37

Reference lenght [mm]	12744	C1
Number of beams	2	

Type of steel S	355	JR

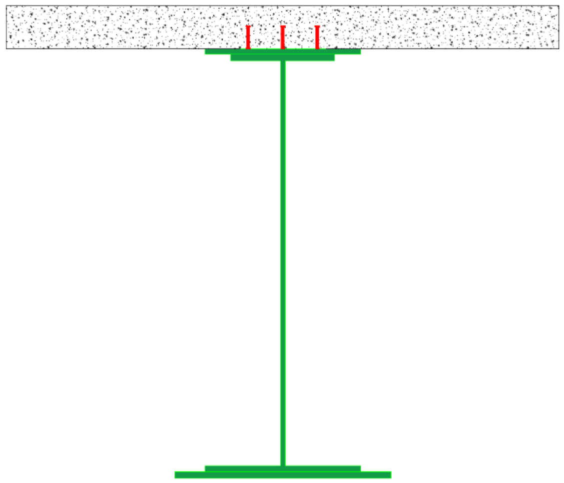

CONCRETE		
	Rck [N/mm^2]	37
	Thickness [mm]	280
	Thickness predalles [mm]	60
	Effective width [mm]	3375

COEFFICIENTS		
	Permanent loads	18,40
	Accidental loads	6,12
	Shrinkage	16,19
	Seattlement	22,86

SHEAR BOLTS		
	Resistence [N/mm²]	450
	Safity factor	1,25
	Diameter [mm]	22
	number on set	3
	span [mm]	110,00

	n	**A [mm²]**	**$Y_{G,i}$ [mm]**	**$Y_{n,i}$ [mm]**	**J [mm⁴]**	**J_{tor} [mm⁴]**
Steel element	0	87920,00	969,37	969,37	2,39E+09	20210026,7
Steel element + phase 2a	18,40	17474348,46	2497,80	1099,84376	6,59E+10	4,5439E+11
Steel element + phase 3	6,12	5868444,20	2497,80	670,771985	1,06E+11	1,5108E+11
Steel element + phase 2b	16,19	15384282,08	2497,80	1047,24231	7,04E+10	3,9977E+11
Steel element + phase 2c	22,86	21694677,28	2497,80	1187,50045	5,86E+10	5,6468E+11

ACTIONS				
	M [daNm]	N [daN]	T [daN]	Mt [daNm]
Dead load Steel	128525,08	5634,23	15894,89	3,46
Dead load concrete	76486,64	197343,43	59476,48	12,8
Permanent	76144,73	74706	29933,06	18,16
Accidental load + crowd	46096	75911,66	49069	24,07
Wind	10215,5	9088,41	4523,81	11,87

Compression verification		
λ	1,05943396	
L [mm]	12744	$\frac{N_{ed}}{N_{b,Rd}} < 1$
N_{cr} [daN]	27807903,82	
α	0,49	
ϕ	1,271761478	$N_{b,Rd} = \frac{\chi \cdot A \cdot f_{yk}}{\gamma_{M1}}$
χ	0,506250304	
γ_{M1}	1,1	
$N_{b,Rd}$ [daN]	1436443,818	
N_{ed} [daN]	353595,32	SATISFY

Shear verification		
ε	0,813616513	
η	1,2	
hw/t	135,5555556	
a [mm]	12744	
a/hw	5,22295082	
k_t	5,486631784	
σ_E [N/mm2]	7643101202	
λ_w	0,000163792	
0,83/h	0,691666667	
χ_w	1,2	
$V_{bw,Rd}$ [daN]	982016,1226	
$M_{f,red}$ [daNm]	304260,8736	
$V_{bf,Rd}$ [daN]	8162,601982	
$V_{b,Rd}$ [daN]	990178,7246	
Ved [daN]	1543734,3	SATISFY

Bending verification		
ψ	1	
G [N/mm^2]	80769,2308	$M_{b,Rd} = \chi_{LT} \cdot W_y \cdot \frac{f_{yk}}{\gamma_{M1}}$
M_{cr} [N/mm]	5,9567E+12	
J_T [mm^4]	4,6875E+10	
J_w [mm^6]	9,7019E+18	
J_x [mm^4]	2,179E+10	
E [N/mm^2]	210000	
λ_{LT}	40,289851	
$\lambda_{LT,0}$	0,2	
α_{LT}	0,49	
ϕ	1	
κc	1	
Kc	0,00061604	
ϕ_{LT}	821,958062	$\frac{M_{ed}}{M_{b,Rd}} < 1$
χ_{LT}	0,00060867	
$M_{b,rd}$ [daNm]	560520177	
M_{ed} [daNm]	32725245	SATISFY

$$V_{b,Rd} = V_{bw,Rd} + V_{bf,Rd} \leq \frac{\eta \cdot f_{yw} \cdot h_w \cdot t}{\sqrt{3} \cdot \gamma_{M1}}$$

$$V_{bw,Rd} = \frac{\chi_w \cdot f_{yw} \cdot h_w \cdot t}{\sqrt{3} \cdot \gamma_{M1}}$$

$$V_{bf,Rd} = \frac{b_f \cdot t_f^2 \cdot f_{yf}}{c \cdot \gamma_{M1}} \left[1 - \left(\frac{M_{Ed}}{M_{f,k}/\gamma_{M0}}\right)^2\right]$$

PROFILE		
	Height [mm]	2500
	thickness upper flange [mm]	25
	width upper flange [mm]	500
	thickness added uuper flange [mm]	0
	width added upper flange [mm]	0
	web thickness [mm]	16
	thickness lower flange [mm]	35
	width lower flange [mm]	900
	thickness added lower flange [mm]	0
	width added lower flange [mm]	0
	As [mm^2]	83040,00
	Iy [mm^4]	2,39E+09
	Yg [mm]	954,65

CONCRETE		
	Rck [N/mm^2]	37
	Thickness [mm]	280
	Thickness predalles [mm]	60
	Effective width [mm]	3375

COEFFICIENTS		
	Permanent loads	18,40
	Accidental loads	6,12
	Shrinkage	16,19
	Seattlement	22,86

Reference lenght [mm]	9501	C2
Number of beams	2	

Type of steel S	355	JR

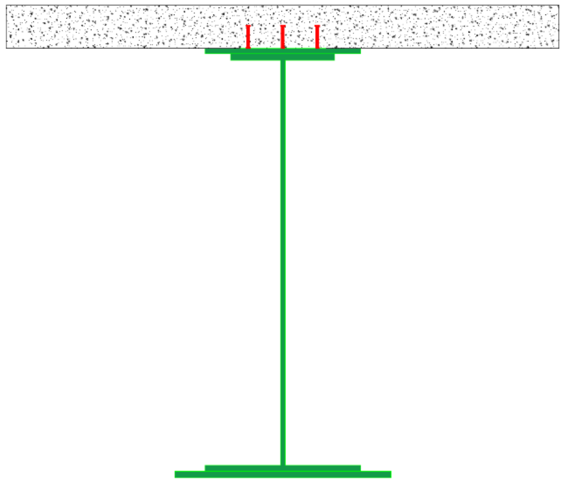

SHEAR BOLTS		
	Resistence [N/mm^2]	450
	Safity factor	1,25
	Diameter [mm]	22
	number on set	2
	span [mm]	110,00

	n	**A [mm^2]**	**$Y_{G,i}$ [mm]**	**$Y_{n,i}$ [mm]**	**J [mm^4]**	**J_{tor} [mm^4]**
Steel element	0	83040,00	954,65	954,65	2,39E+09	15497593,33
Steel element + phase 2a	18,40	17469468,46	2503,87	1076,439773	6,43E+10	4,54381E+11
Steel element + phase 3	6,12	5863564,20	2503,87	651,8259424	1,02E+11	1,5108E+11
Steel element + phase 2b	16,19	15379402,08	2503,87	1023,705861	6,85E+10	3,9976E+11
Steel element + phase 2c	22,86	21689797,28	2503,87	1164,74632	5,73E+10	5,64672E+11

ACTIONS				
	M [daNm]	N [daN]	T [daN]	Mt [daNm]
Dead load Steel	132949,08	5626,03	5436,88	0,89
Dead load concrete	224841,4	242948,46	18828,64	14,85
Permanent	84006,64	90105,46	7075,18	2,26
Accidental load + crowd	105672,87	107078,48	14541,76	8,08
Wind	10863,97	9468,44	949,85	2,21

Compression verification		
λ	0,814167078	
L [mm]	9501	$\frac{N_{ed}}{N_{b,Rd}} < 1$
N_{cr} [daN]	44472200,56	
α	0,49	
ϕ	0,981904949	$N_{b,Rd} = \frac{\chi \cdot A \cdot f_{yk}}{\gamma_{M1}}$
χ	0,653259606	
γ_{M1}	1,1	
$N_{b,Rd}$ [daN]	1750688,235	
N_{ed} [daN]	445758,43	SATISFY

Shear verification		
ε	0,813616513	
η	1,2	
hw/t	152,5	
a [mm]	9501	
a/hw	3,893852459	
k_t	5,603815925	
σ_E [N/mm2]	6793867735	
λ_w	0,000173728	
0,83/h	0,691666667	
χ_w	1,2	
$V_{bw,Rd}$ [daN]	872903,2201	
$M_{f,red}$ [daNm]	505776,4717	$\frac{V_{Ed}}{V_{b,Rd}} < 1$
$V_{bf,Rd}$ [daN]	11944,07014	
$V_{b,Rd}$ [daN]	884847,2902	
Ved [daN]	458824,6	SATISFY

Bending verification		
ψ	1	
G [N/mm^2]	80769,23077	$M_{b,Rd} = \chi_{LT} \cdot W_y \cdot \frac{f_{yk}}{\gamma_{M1}}$
M_{cr} [N/mm]	6,16328E+12	
J_T [mm^4]	41666666667	
J_w [mm^6]	3,57352E+18	
J_x [mm^4]	19369045333	
E [N/mm^2]	210000	
λ_{LT}	37,34371015	
$\lambda_{LT,0}$	0,2	
α_{LT}	0,49	
ϕ	1	
κc	1	
Kc	0,000717076	
ϕ_{LT}	706,8765528	$\frac{M_{ed}}{M_{b,Rd}} < 1$
χ_{LT}	0,000707831	
$M_{b,rd}$ [daNm]	579411417,5	
M_{ed} [daNm]	54746999	SATISFY

$$V_{b,Rd} = V_{bw,Rd} + V_{bf,Rd} \leq \frac{\eta \cdot f_{yw} \cdot h_w \cdot t}{\sqrt{3} \cdot \gamma_{M1}}$$

$$V_{bw,Rd} = \frac{\chi_w \cdot f_{yw} \cdot h_w \cdot t}{\sqrt{3} \cdot \gamma_{M1}}$$

$$V_{bf,Rd} = \frac{b_f \cdot t_f^2 . f_{yf}}{c \cdot \gamma_{M1}}\left[1 - \left(\frac{M_{Ed}}{M_{f,k}/\gamma_{M0}}\right)^2\right]$$

PROFILE		
	Height [mm]	2500
	thickness upper flange [mm]	25
	width upper flange [mm]	500
	thickness added uuper flange [mm]	0
	width added upper flange [mm]	0
	web thickness [mm]	16
	thickness lower flange [mm]	35
	width lower flange [mm]	900
	thickness added lower flange [mm]	0
	width added lower flange [mm]	0
	As [mm^2]	83040,00
	Iy [mm^4]	2,39E+09
	Yg [mm]	954,65

CONCRETE		
	Rck [N/mm^2]	37
	Thickness [mm]	280
	Thickness predalles [mm]	60
	Effective width [mm]	3375

COEFFICIENTS		
	Permanent loads	18,40
	Accidental loads	6,12
	Shrinkage	16,19
	Seattlement	22,86

Reference lenght [mm]	12002	C3
Number of beams	2	

Type of steel S	355	JR

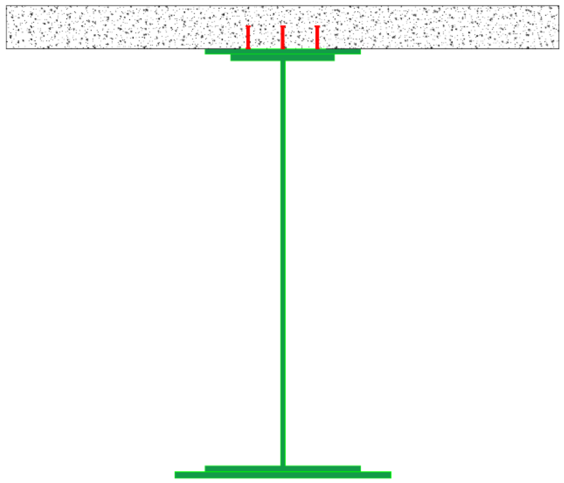

SHEAR BOLTS		
	Resistence [N/mm^2]	450
	Safity factor	1,25
	Diameter [mm]	22
	number on set	2
	span [mm]	110,00

	n	**A [mm^2]**	**$Y_{G,i}$ [mm]**	**$Y_{n,i}$ [mm]**	**J [mm^4]**	**J_{tor} [mm^4]**
Steel element	0	83040,00	954,65	954,65	2,39E+09	15497593,33
Steel element + phase 2a	18,40	17469468,46	2503,87	1076,439773	6,43E+10	4,54381E+11
Steel element + phase 3	6,12	5863564,20	2503,87	651,8259424	1,02E+11	1,5108E+11
Steel element + phase 2b	16,19	15379402,08	2503,87	1023,705861	6,85E+10	3,9976E+11
Steel element + phase 2c	22,86	21689797,28	2503,87	1164,74632	5,73E+10	5,64672E+11

ACTIONS				
	M [daNm]	N [daN]	T [daN]	Mt [daNm]
Dead load Steel	115971,85	4961,64	17471,02	1,15
Dead load concrete	216107,89	220652,85	64231,65	14,55
Permanent	80732,6	82076,25	24120,78	7,53
Accidental load + crowd	101145,85	104099,5	29587,4	14,02
Wind	10852,15	8861,89	6823,67	3,62

Compression verification		
λ	1,028484714	
L [mm]	12002	$\frac{N_{ed}}{N_{b,Rd}} < 1$
N_{cr} [daN]	27868911,79	
α	0,49	
ϕ	1,231869158	$N_{b,Rd} = \frac{\chi \cdot A \cdot f_{yk}}{\gamma_{M1}}$
χ	0,523588634	
γ_{M1}	1,1	
$N_{b,Rd}$ [daN]	1403179,461	
N_{ed} [daN]	411790,24	SATISFY

Bending verification		
ψ	1	
G [N/mm^2]	80769,23077	$M_{b,Rd} = \chi_{LT} \cdot W_y \cdot \frac{f_{yk}}{\gamma_{M1}}$
M_{cr} [N/mm]	5,46109E+12	
J_T [mm^4]	41666666667	
J_w [mm^6]	7,2036E+18	
J_x [mm^4]	19369045333	
E [N/mm^2]	210000	
λ_{LT}	39,67195872	
$\lambda_{LT,0}$	0,2	
α_{LT}	0,49	
ϕ	1	
κc	1	
Kc	0,000635379	
ϕ_{LT}	797,1027841	$\frac{M_{ed}}{M_{b,Rd}} < 1$
χ_{LT}	0,000627661	
$M_{b,rd}$ [daNm]	513785869,4	
M_{ed} [daNm]	51395819	SATISFY

Shear verification		
ε	0,813616513	
η	1,2	
hw/t	152,5	
a [mm]	12002	
a/hw	4,918852459	
k_t	5,505322666	
σ_E [N/mm2]	6793867735	
λ_w	0,000173728	
0,83/h	0,691666667	
χ_w	1,2	
$V_{bw,Rd}$ [daN]	872903,2201	
$M_{f,red}$ [daNm]	475934,5048	$\frac{V_{Ed}}{V_{b,Rd}} < 1$
$V_{bf,Rd}$ [daN]	9163,579092	
$V_{b,Rd}$ [daN]	882066,7992	
Ved [daN]	135410,85	SATISFY

$$V_{b,Rd} = V_{bw,Rd} + V_{bf,Rd} \leq \frac{\eta \cdot f_{yw} \cdot h_w \cdot t}{\sqrt{3} \cdot \gamma_{M1}}$$

$$V_{bw,Rd} = \frac{\chi_w \cdot f_{yw} \cdot h_w \cdot t}{\sqrt{3} \cdot \gamma_{M1}}$$

$$V_{bf,Rd} = \frac{b_f \cdot t_f^2 \cdot f_{yf}}{c \cdot \gamma_{M1}} \left[1 - \left(\frac{M_{Ed}}{M_{f,k}/\gamma_{M0}}\right)^2\right]$$

PROFILE		
	Height [mm]	2500
	thickness upper flange [mm]	30
	width upper flange [mm]	500
	thickness added uuper flange [mm]	0
	width added upper flange [mm]	0
	web thickness [mm]	22
	thickness lower flange [mm]	35
	width lower flange [mm]	900
	thickness added lower flange [mm]	20
	width added lower flange [mm]	400
	As [mm^2]	107630,00
	Iy [mm^4]	2,55E+09
	Yg [mm]	947,51

CONCRETE		
	Rck [N/mm^2]	37
	Thickness [mm]	280
	Thickness predalles [mm]	60
	Effective width [mm]	3375

COEFFICIENTS		
	Permanent loads	18,40
	Accidental loads	6,12
	Shrinkage	16,19
	Seattlement	22,86

Reference lenght [mm]	9501	C4
Number of beams	2	

Type of steel S	355	JR

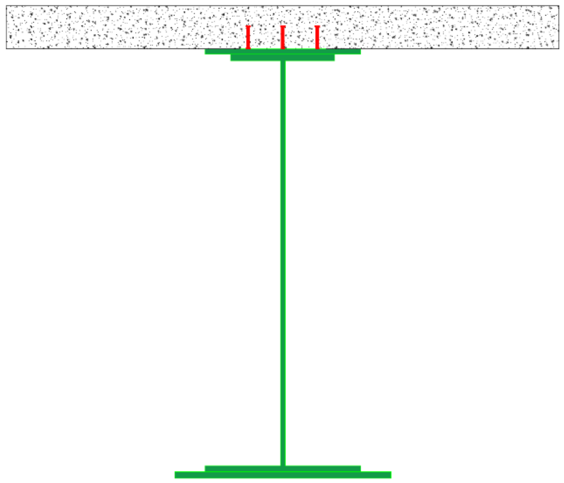

SHEAR BOLTS		
	Resistence [N/mm^2]	450
	Safity factor	1,25
	Diameter [mm]	22
	number on set	3
	span [mm]	110,00

	n	**A [mm^2]**	**$Y_{G,i}$ [mm]**	**$Y_{n,i}$ [mm]**	**J [mm^4]**	**J_{tor} [mm^4]**
Steel element	0	107630,00	947,51	947,51	2,55E+09	20708393,33
Steel element + phase 2a	18,40	17494058,46	2445,37	1181,529247	7,20E+10	4,54386E+11
Steel element + phase 3	6,12	5888154,20	2445,37	741,5627364	1,20E+11	1,51085E+11
Steel element + phase 2b	16,19	15403992,08	2445,37	1130,067901	7,72E+10	3,99766E+11
Steel element + phase 2c	22,86	21714387,28	2445,37	1265,844183	6,35E+10	5,64677E+11

ACTIONS				
	M [daNm]	N [daN]	T [daN]	Mt [daNm]
Dead load Steel	264294,77	2042,33	29788,59	38,38
Dead load concrete	433687,1	503061,41	117592	14,32
Permanent	159215,81	186326,75	43516,2	11,12
Accidental load + crowd	185264,92	195180,46	57047,37	32,98
Wind	19758,23	18706,73	5534,88	9,48

Compression verification		
λ	0,802775712	
L [mm]	9501	$\frac{N_{ed}}{N_{b,Rd}} < 1$
N_{cr} [daN]	59288879,67	
α	0,49	
ϕ	0,969904472	$N_{b,Rd} = \frac{\chi \cdot A \cdot f_{yk}}{\gamma_{M1}}$
χ	0,660411448	
γ_{M1}	1,1	
$N_{b,Rd}$ [daN]	2293948,17	
N_{ed} [daN]	886610,95	SATISFY

Shear verification		
ε	0,813616513	
η	1,2	
hw/t	110,2777778	
a [mm]	9501	
a/hw	3,916143806	
k_t	5,600821104	
σ_E [N/mm2]	9288394364	
λ_w	0,000148579	
0,83/h	0,691666667	
χ_w	1,2	
$V_{bw,Rd}$ [daN]	1193409,949	
$M_{f,red}$ [daNm]	945050,0414	$\frac{V_{Ed}}{V_{b,Rd}} < 1$
$V_{bf,Rd}$ [daN]	17247,01138	
$V_{b,Rd}$ [daN]	1210656,961	
Ved [daN]	247944,17	SATISFY

Bending verification		
ψ	1	
G [N/mm^2]	80769,23077	
M_{cr} [N/mm]	8,3446E+12	$M_{b,Rd} = \chi_{LT} \cdot W_y \cdot \frac{f_{yk}}{\gamma_{M1}}$
J_T [mm^4]	57291666667	
J_w [mm^6]	4,9136E+18	
J_x [mm^4]	25822176188	
E [N/mm^2]	210000	
λ_{LT}	37,05637606	
$\lambda_{LT,0}$	0,2	
α_{LT}	0,49	
ϕ	1	
κc	1	
Kc	0,000728239	
ϕ_{LT}	696,1173154	$\frac{M_{ed}}{M_{b,Rd}} < 1$
χ_{LT}	0,000718779	
$M_{b,rd}$ [daNm]	784399796,5	
M_{ed} [daNm]	10424626	SATISFY

$$V_{b,Rd} = V_{bw,Rd} + V_{bf,Rd} \leq \frac{\eta \cdot f_{yw} \cdot h_w \cdot t}{\sqrt{3} \cdot \gamma_{M1}}$$

$$V_{bw,Rd} = \frac{\chi_w \cdot f_{yw} \cdot h_w \cdot t}{\sqrt{3} \cdot \gamma_{M1}}$$

$$V_{bf,Rd} = \frac{b_f \cdot t_f^2 \cdot f_{yf}}{c \cdot \gamma_{M1}} \left[1 - \left(\frac{M_{Ed}}{M_{f,k} / \gamma_{M0}}\right)^2\right]$$

PROFILE		
	Height [mm]	2500
	thickness upper flange [mm]	30
	width upper flange [mm]	900
	thickness added uuper flange [mm]	0
	width added upper flange [mm]	0
	web thickness [mm]	28
	thickness lower flange [mm]	35
	width lower flange [mm]	1250
	thickness added lower flange [mm]	25
	width added lower flange [mm]	400
	As [mm^2]	148230,00
	Iy [mm^4]	7,66E+09
	Yg [mm]	1006,37

CONCRETE		
	Rck [N/mm^2]	37
	Thickness [mm]	280
	Thickness predalles [mm]	60
	Effective width [mm]	3375

COEFFICIENTS		
	Permanent loads	18,40
	Accidental loads	6,12
	Shrinkage	16,19
	Seattlement	22,86

Reference lenght [mm]	2800	C5
Number of beams	4	

Type of steel S	355	JR

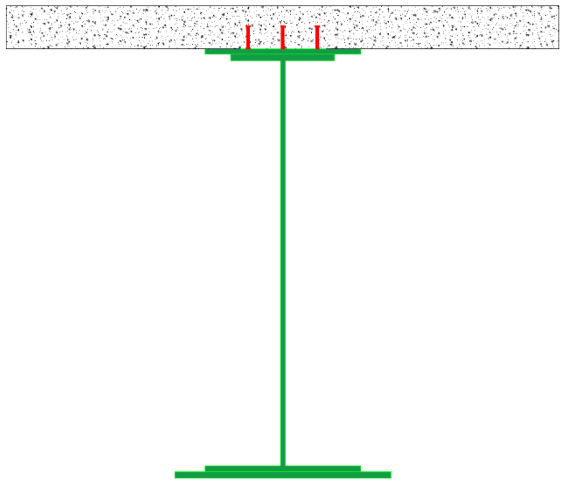

SHEAR BOLTS		
	Resistence [N/mm²]	450
	Safity factor	1,25
	Diameter [mm]	22
	number on set	2
	span [mm]	110,00

	n	A [mm²]	$Y_{G,i}$ [mm]	$Y_{n,i}$ [mm]	J [mm⁴]	J_{tor} [mm⁴]
Steel element	0	148230,00	1006,37	1006,37	7,66E+09	16264905208
Steel element + phase 2a	18,40	17534658,46	2375,33	1303,998351	8,63E+10	4,7063E+11
Steel element + phase 3	6,12	5928754,20	2375,33	863,5446831	1,50E+11	1,67329E+11
Steel element + phase 2b	16,19	15444592,08	2375,33	1256,256079	9,29E+10	4,1601E+11
Steel element + phase 2c	22,86	21754987,28	2375,33	1380,266266	7,60E+10	5,80921E+11

ACTIONS				
	M [daNm]	N [daN]	T [daN]	Mt [daNm]
Dead load Steel	358077,35	837,88	35670,31	5,73
Dead load concrete	640151,59	634988,06	139147,53	21,11
Permanent	234365,26	234954,45	50749,61	9,29
Accidental load + crowd	291683,53	258949,82	68956,01	35,1
Wind	31287,99	23739,1	6380,94	16,78

Compression verification		
λ	0,246957297	$\frac{N_{ed}}{N_{b,Rd}} < 1$
L [mm]	2801	
N_{cr} [daN]	862821057,1	
α	0,49	$N_{b,Rd} = \frac{\chi \cdot A \cdot f_{yk}}{\gamma_{M1}}$
ϕ	0,541998491	
χ	0,976118724	
γ_{M1}	1,1	
$N_{b,Rd}$ [daN]	4669543,44	
N_{ed} [daN]	1129730,21	SATISFY

Shear verification		
ε	0,813616513	
η	1,2	
hw/t	86,67857143	
a [mm]	2801	
a/hw	1,154099712	
k_t	8,343124426	
σ_E [N/mm2]	11825924072	
λ_w	0,000131677	
0,83/h	0,691666667	
χ_w	1,2	
$V_{bw,Rd}$ [daN]	1519441,886	$\frac{V_{Ed}}{V_{b,Rd}} < 1$
$M_{f,red}$ [daNm]	1391621,647	
$V_{bf,Rd}$ [daN]	75803,4342	
$V_{b,Rd}$ [daN]	1595245,32	
Ved [daN]	294523,46	SATISFY

Bending verification		
ψ	1	$M_{b,Rd} = \chi_{LT} \cdot W_y \cdot \frac{f_{yk}}{\gamma_{M1}}$
G [N/mm^2]	80769,23077	
M_{cr} [N/mm]	2,03975E+13	
J_T [mm^4]	72916666667	
J_w [mm^6]	1,60238E+17	
J_x [mm^4]	32660882333	
E [N/mm^2]	210000	
λ_{LT}	26,65600785	
$\lambda_{LT,0}$	0,2	
α_{LT}	0,49	
ϕ	1	
κc	1	
Kc	0,001407375	$\frac{M_{ed}}{M_{b,Rd}} < 1$
ϕ_{LT}	362,2530992	
χ_{LT}	0,001382124	
$M_{b,rd}$ [daNm]	1907760946	
M_{ed} [daNm]	152427773	SATISFY

$$V_{b,Rd} = V_{bw,Rd} + V_{bf,Rd} \leq \frac{\eta \cdot f_{yw} \cdot h_w \cdot t}{\sqrt{3} \cdot \gamma_{M1}}$$

$$V_{bw,Rd} = \frac{\chi_w \cdot f_{yw} \cdot h_w \cdot t}{\sqrt{3} \cdot \gamma_{M1}}$$

$$V_{bf,Rd} = \frac{b_f \cdot t_f^2 \cdot f_{yf}}{c \cdot \gamma_{M1}} \left[1 - \left(\frac{M_{Ed}}{M_{f,k}/\gamma_{M0}}\right)^2\right]$$

PROFILE		
	Height [mm]	2500
	thickness upper flange [mm]	30
	width upper flange [mm]	900
	thickness added uuper flange [mm]	40
	width added upper flange [mm]	600
	web thickness [mm]	28
	thickness lower flange [mm]	35
	width lower flange [mm]	1250
	thickness added lower flange [mm]	35
	width added lower flange [mm]	900
	As [mm^2]	148230,00
	Iy [mm^4]	1,04E+10
	Yg [mm]	1006,37

CONCRETE		
	Rck [N/mm^2]	37
	Thickness [mm]	280
	Thickness predalles [mm]	60
	Effective width [mm]	3375

COEFFICIENTS		
	Permanent loads	18,40
	Accidental loads	6,12
	Shrinkage	16,19
	Seattlement	22,86

Reference lenght [mm]	2800	C5a
Number of beams	4	

Type of steel S	355	JR

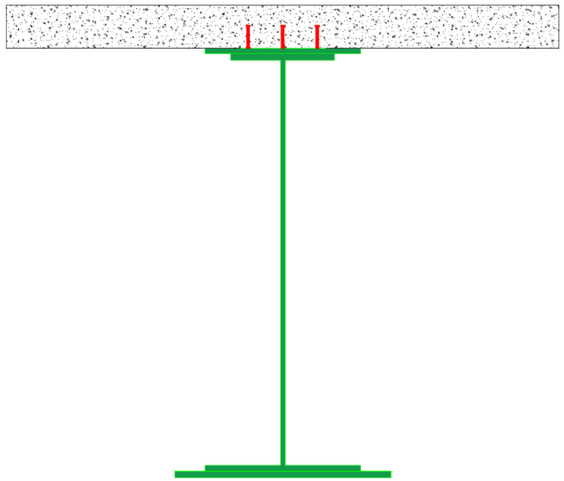

SHEAR BOLTS		
	Resistence [N/mm^2]	450
	Safity factor	1,25
	Diameter [mm]	22
	number on set	3
	span [mm]	110,00

	n	**A [mm^2]**	**$Y_{G,i}$ [mm]**	**$Y_{n,i}$ [mm]**	**J [mm^4]**	**J_{tor} [mm^4]**
Steel element	0	148230,00	1006,37	1006,37	1,04E+10	24802318125
Steel element + phase 2a	18,40	17534658,46	2282,04	1394,619771	9,65E+10	4,79168E+11
Steel element + phase 3	6,12	5928754,20	2282,04	968,8709124	1,74E+11	1,75867E+11
Steel element + phase 2b	16,19	15444592,08	2282,04	1351,218178	1,04E+11	4,24547E+11
Steel element + phase 2c	22,86	21754987,28	2282,04	1462,674372	8,46E+10	5,89459E+11

ACTIONS				
	M [daNm]	N [daN]	T [daN]	Mt [daNm]
Dead load Steel	503361,9	13967,18	46552,05	62,23
Dead load concrete	1108978,78	818834,63	165948,03	45,58
Permanent	402124,58	295974,65	59377,98	38,92
Accidental load + crowd	547641,56	403977,11	86827,49	141,95
Wind	56046,77	30606,71	7331,48	59,64

Compression verification		
λ	0,747934078	
L [mm]	7401	$\frac{N_{ed}}{N_{b,Rd}} < 1$
N_{cr} [daN]	122053079,7	
α	0,49	
ϕ	0,913946541	$N_{b,Rd} = \frac{\chi \cdot A \cdot f_{yk}}{\gamma_{M1}}$
χ	0,69482968	
γ_{M1}	1,1	
$N_{b,Rd}$ [daN]	4312817,299	
N_{ed} [daN]	1532753,57	SATISFY

Shear verification		
ε	0,813616513	
η	1,2	
hw/t	85,11190476	
a [mm]	7401	
a/hw	3,105575293	
k_t	5,754739945	
σ_E [N/mm2]	11612177114	
λ_w	0,000132883	
0,83/h	0,691666667	
χ_w	1,2	
$V_{bw,Rd}$ [daN]	1491978,824	
$M_{f,red}$ [daNm]	2352480,406	$\frac{V_{Ed}}{V_{b,Rd}} < 1$
$V_{bf,Rd}$ [daN]	39244,28795	
$V_{b,Rd}$ [daN]	1531223,112	
Ved [daN]	358705,55	SATISFY

Bending verification		
ψ	1	
G [N/mm^2]	80769,23077	$M_{b,Rd} = \chi_{LT} \cdot W_y \cdot \frac{f_{yk}}{\gamma_{M1}}$
M_{cr} [N/mm]	1,19877E+13	
J_T [mm^4]	72916666667	
J_w [mm^6]	2,95596E+18	
J_x [mm^4]	32256000000	
E [N/mm^2]	210000	
λ_{LT}	34,55466719	
$\lambda_{LT,0}$	0,2	
α_{LT}	0,49	
ϕ	1	
κc	1	
Kc	0,000837503	
ϕ_{LT}	605,9294057	$\frac{M_{ed}}{M_{b,Rd}} < 1$
χ_{LT}	0,000825851	
$M_{b,rd}$ [daNm]	1125799576	
M_{ed} [daNm]	256210682	SATISFY

$$V_{b,Rd} = V_{bw,Rd} + V_{bf,Rd} \leq \frac{\eta \cdot f_{yw} \cdot h_w \cdot t}{\sqrt{3} \cdot \gamma_{M1}}$$

$$V_{bw,Rd} = \frac{\chi_w \cdot f_{yw} \cdot h_w \cdot t}{\sqrt{3} \cdot \gamma_{M1}}$$

$$V_{bf,Rd} = \frac{b_f \cdot t_f^2 . f_{yf}}{c \cdot \gamma_{M1}} \left[1 - \left(\frac{M_{Ed}}{M_{f,k} / \gamma_{M0}}\right)^2\right]$$

PROFILE		
	Height [mm]	2500
	thickness upper flange [mm]	40
	width upper flange [mm]	500
	thickness added uuper flange [mm]	0
	width added upper flange [mm]	0
	web thickness [mm]	22
	thickness lower flange [mm]	35
	width lower flange [mm]	900
	thickness added lower flange [mm]	25
	width added lower flange [mm]	400
	As [mm^2]	114300,00
	Iy [mm^4]	2,68E+09
	Yg [mm]	993,10

CONCRETE		
	Rck [N/mm^2]	37
	Thickness [mm]	280
	Thickness predalles [mm]	60
	Effective width [mm]	3375

COEFFICIENTS		
	Permanent loads	18,40
	Accidental loads	6,12
	Shrinkage	16,19
	Seattlement	22,86

Reference lenght [mm]	11501	C6
Number of beams	2	

Type of steel S	355	JR

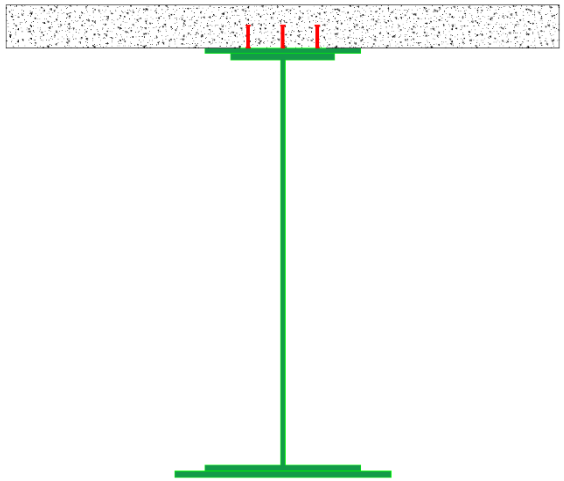

SHEAR BOLTS		
	Resistence [N/mm^2]	450
	Safity factor	1,25
	Diameter [mm]	22
	number on set	2
	span [mm]	110,00

	n	A [mm^2]	$Y_{G,i}$ [mm]	$Y_{n,i}$ [mm]	J [mm^4]	J_{tor} [mm^4]
Steel element	0	114300,00	993,10	993,10	2,68E+09	6079584375
Steel element + phase 2a	18,40	17500728,46	2355,14	1205,287	7,38E+10	4,60445E+11
Steel element + phase 3	6,12	5894824,20	2355,14	763,6324	1,25E+11	1,57144E+11
Steel element + phase 2b	16,19	15410662,08	2355,14	1154,357	7,93E+10	4,05825E+11
Steel element + phase 2c	22,86	21721057,28	2355,14	1288,322	6,50E+10	5,70736E+11

ACTIONS				
	M [daNm]	N [daN]	T [daN]	Mt [daNm]
Dead load Steel	503361,9	13967,18	46552,05	62,23
Dead load concrete	453584,65	494085,65	130091,1	18,35
Permanent	165004,82	179346,36	47482,15	8,2
Accidental load + crowd	215475,82	226879,45	67036,96	42,7
Wind	20815,6	18817,77	6253,7	11,64

Compression verification		
λ	1,010824583	
L [mm]	11501	$\frac{N_{ed}}{N_{b,Rd}} < 1$
N_{cr} [daN]	39712112,77	
α	0,49	
ϕ	1,209535191	$N_{b,Rd} = \frac{\chi \cdot A \cdot f_{yk}}{\gamma_{M1}}$
χ	0,533683181	
γ_{M1}	1,1	
$N_{b,Rd}$ [daN]	4312817,299	
N_{ed} [daN]	914278,64	SATISFY

Shear verification		
ε	0,813616513	
η	1,2	
hw/t	110,3090909	
a [mm]	11501	
a/hw	4,739162683	
k_t	5,518097063	
σ_E [N/mm2]	9291031783	
λ_w	0,000148558	
0,83/h	0,691666667	
χ_w	1,2	
$V_{bw,Rd}$ [daN]	1193748,816	
$M_{f,red}$ [daNm]	1217732,801	
$V_{bf,Rd}$ [daN]	22621,47056	
$V_{b,Rd}$ [daN]	1216370,286	
Ved [daN]	291162,24	SATISFY

Bending verification		
ψ	1	
G [N/mm^2]	80769,23077	
M_{cr} [N/mm]	7,48808E+12	$M_{b,Rd} = \chi_{LT} \cdot W_y \cdot \frac{f_{yk}}{\gamma_{M1}}$
J_T [mm^4]	57291666667	
J_w [mm^6]	8,71562E+18	
J_x [mm^4]	25344000000	
E [N/mm^2]	210000	
λ_{LT}	38,75444874	
$\lambda_{LT,0}$	0,2	
α_{LT}	0,49	
ϕ	1	
κc	1	
Kc	0,00066582	$\frac{M_{ed}}{M_{b,Rd}} < 1$
ϕ_{LT}	760,8994886	
χ_{LT}	0,000657544	
$M_{b,rd}$ [daNm]	704285691,8	
M_{ed} [daNm]	133742719	SATISFY

$$V_{b,Rd} = V_{bw,Rd} + V_{bf,Rd} \leq \frac{\eta \cdot f_{yw} \cdot h_w \cdot t}{\sqrt{3} \cdot \gamma_{M1}}$$

$$V_{bw,Rd} = \frac{\chi_w \cdot f_{yw} \cdot h_w \cdot t}{\sqrt{3} \cdot \gamma_{M1}}$$

$$V_{bf,Rd} = \frac{b_f \cdot t_f^2 . f_{yf}}{c \cdot \gamma_{M1}} \left[1 - \left(\frac{M_{Ed}}{M_{f,k} / \gamma_{M0}}\right)^2\right]$$

PROFILE		
	Height [mm]	2500
	thickness upper flange [mm]	30
	width upper flange [mm]	500
	thickness added uuper flange [mm]	0
	width added upper flange [mm]	0
	web thickness [mm]	16
	thickness lower flange [mm]	35
	width lower flange [mm]	900
	thickness added lower flange [mm]	35
	width added lower flange [mm]	400
	As [mm^2]	98900,00
	Iy [mm^4]	2,63E+09
	Yg [mm]	848,39

CONCRETE		
	Rck [N/mm^2]	37
	Thickness [mm]	280
	Thickness predalles [mm]	60
	Effective width [mm]	3375

COEFFICIENTS		
	Permanent loads	18,40
	Accidental loads	6,12
	Shrinkage	16,19
	Seattlement	22,86

Reference lenght [mm]	11002	C7
Number of beams	2	

Type of steel S	355	JR

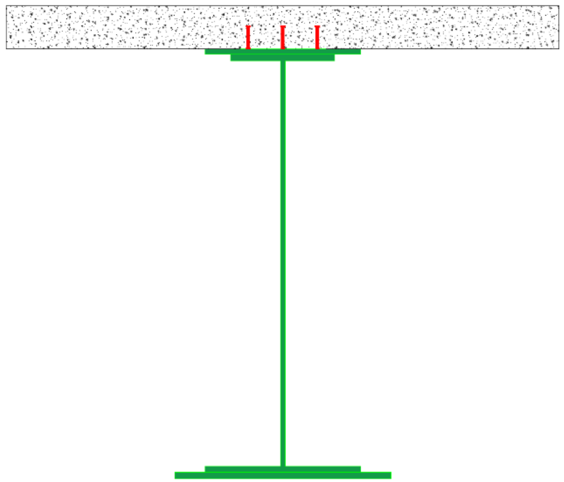

SHEAR BOLTS		
	Resistence [N/mm^2]	450
	Safity factor	1,25
	Diameter [mm]	22
	number on set	2
	span [mm]	110,00

	n	A [mm^2]	$Y_{G,i}$ [mm]	$Y_{n,i}$ [mm]	J [mm^4]	J_{tor} [mm^4]
Steel element	0	98900,00	848,39	848,39	2,63E+09	8513074792
Steel element + phase 2a	18,40	17485328,46	2389,88	1147,654865	6,96E+10	4,62878E+11
Steel element + phase 3	6,12	5879424,20	2389,88	711,2851439	1,14E+11	1,59577E+11
Steel element + phase 2b	16,19	15395262,08	2389,88	1095,592136	7,45E+10	4,08258E+11
Steel element + phase 2c	22,86	21705657,28	2389,88	1233,556287	6,16E+10	5,7317E+11

ACTIONS				
	M [daNm]	N [daN]	T [daN]	Mt [daNm]
Dead load Steel	503361,9	13967,18	46552,05	62,23
Dead load concrete	378517,95	400011,11	70774,27	40,23
Permanent	135830,96	144577,14	25640,02	12,47
Accidental load + crowd	161766,08	178396,12	35018,86	46,58
Wind	17185,44	15013,8	3078,6	7,9

Compression verification		
λ	1,054722503	
L [mm]	11002	$\frac{N_{ed}}{N_{b,Rd}} < 1$
N_{cr} [daN]	31560815,81	
α	0,49	
ϕ	1,265626792	$N_{b,Rd} = \frac{\chi \cdot A \cdot f_{yk}}{\gamma_{M1}}$
χ	0,508859808	
γ_{M1}	1,1	
$N_{b,Rd}$ [daN]	1624164,856	
N_{ed} [daN]	736951,55	SATISFY

Bending verification		
ψ	1	
G [N/mm^2]	80769,23077	
M_{cr} [N/mm]	5,57214E+12	$M_{b,Rd} = \chi_{LT} \cdot W_y \cdot \frac{f_{yk}}{\gamma_{M1}}$
J_T [mm^4]	41666666667	
J_w [mm^6]	5,54886E+18	
J_x [mm^4]	18432000000	
E [N/mm^2]	210000	
λ_{LT}	38,31283632	
$\lambda_{LT,0}$	0,2	
α_{LT}	0,49	
ϕ	1	
κc	1	
Kc	0,000681258	
ϕ_{LT}	743,7743584	$\frac{M_{ed}}{M_{b,Rd}} < 1$
χ_{LT}	0,000672693	
$M_{b,rd}$ [daNm]	524008956	
M_{ed} [daNm]	117947689	SATISFY

Shear verification		
ε	0,813616513	
η	1,2	
hw/t	151,2152778	
a [mm]	11002	
a/hw	4,547324914	
k_t	5,533440773	
σ_E [N/mm2]	6736633421	
λ_w	0,000174464	
0,83/h	0,691666667	
χ_w	1,2	
$V_{bw,Rd}$ [daN]	865549,5272	
$M_{f,red}$ [daNm]	1082840,258	
$V_{bf,Rd}$ [daN]	16264,44725	
$V_{b,Rd}$ [daN]	881813,9745	
Ved [daN]	177985,2	SATISFY

$$V_{b,Rd} = V_{bw,Rd} + V_{bf,Rd} \leq \frac{\eta \cdot f_{yw} \cdot h_w \cdot t}{\sqrt{3} \cdot \gamma_{M1}}$$

$$V_{bw,Rd} = \frac{\chi_w \cdot f_{yw} \cdot h_w \cdot t}{\sqrt{3} \cdot \gamma_{M1}}$$

$$V_{bf,Rd} = \frac{b_f \cdot t_f^2 \cdot f_{yf}}{c \cdot \gamma_{M1}} \left[1 - \left(\frac{M_{Ed}}{M_{f,k} / \gamma_{M0}} \right)^2 \right]$$

PROFILE		
	Height [mm]	2500
	thickness upper flange [mm]	30
	width upper flange [mm]	600
	thickness added uuper flange [mm]	0
	width added upper flange [mm]	0
	web thickness [mm]	16
	thickness lower flange [mm]	35
	width lower flange [mm]	900
	thickness added lower flange [mm]	35
	width added lower flange [mm]	600
	As [mm^2]	108509,37
	Iy [mm^4]	3,27E+09
	Yg [mm]	838,95

CONCRETE		
	Rck [N/mm^2]	37
	Thickness [mm]	280
	Thickness predalles [mm]	60
	Effective width [mm]	3375

COEFFICIENTS		
	Permanent loads	18,40
	Accidental loads	6,12
	Shrinkage	16,19
	Seattlement	22,86

Reference lenght [mm]	12295	C8
Number of beams	1	

Type of steel S	355	JR

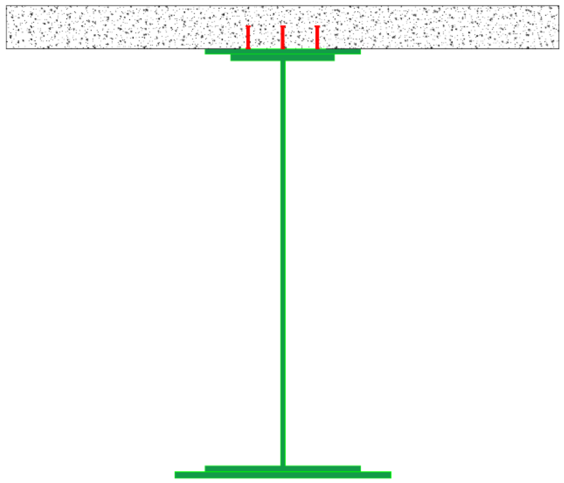

SHEAR BOLTS		
	Resistence [N/mm^2]	450
	Safity factor	1,25
	Diameter [mm]	22
	number on set	3
	span [mm]	110,00

	n	**A [mm^2]**	**$Y_{G,i}$ [mm]**	**$Y_{n,i}$ [mm]**	**J [mm^4]**	**J_{tor} [mm^4]**
Steel element	0	108509,37	838,95	838,95	3,27E+09	8514503958
Steel element + phase 2a	18,40	17494937,82	2368,09	1184,761117	7,29E+10	4,6288E+11
Steel element + phase 3	6,12	5889033,56	2368,09	744,5235524	1,21E+11	1,59579E+11
Steel element + phase 2b	16,19	15404871,45	2368,09	1133,366734	7,82E+10	4,08259E+11
Steel element + phase 2c	22,86	21715266,64	2368,09	1268,909993	6,44E+10	5,73171E+11

ACTIONS				
	M [daNm]	N [daN]	T [daN]	Mt [daNm]
Dead load Steel	503361,9	13967,18	46552,05	62,23
Dead load concrete	417790,58	438275,87	24446,82	45,46
Permanent	150286,51	158492,4	8955,49	18,04
Accidental load + crowd	182466,02	197967,11	12947,18	29,01
Wind	18734,58	16434,71	1060,28	7,33

Compression verification		
λ	1,010824583	
L [mm]	11501	$\frac{N_{ed}}{N_{b,Rd}} < 1$
N_{cr} [daN]	39712112,77	
α	0,49	
ϕ	1,209535191	$N_{b,Rd} = \frac{\chi \cdot A \cdot f_{yk}}{\gamma_{M1}}$
χ	0,533683181	
γ_{M1}	1,1	
$N_{b,Rd}$ [daN]	1968635,962	
N_{ed} [daN]	808702,56	SATISFY

Shear verification		
ε	0,813616513	
η	1,2	
hw/t	110,3090909	
a [mm]	11501	
a/hw	4,739162683	
k_t	5,518097063	
σ_E [N/mm2]	9291031783	
λ_w	0,000148558	
0,83/h	0,691666667	
χ_w	1,2	
$V_{bw,Rd}$ [daN]	1193748,816	
$M_{f,red}$ [daNm]	1153678,369	
$V_{bf,Rd}$ [daN]	16285,7285	
$V_{b,Rd}$ [daN]	1210034,544	
Ved [daN]	929015,4	SATISFY

Bending verification		
ψ	1	
G [N/mm^2]	80769,23077	
M_{cr} [N/mm]	7,48808E+12	$M_{b,Rd} = \chi_{LT} \cdot W_y \cdot \frac{f_{yk}}{\gamma_{M1}}$
J_T [mm^4]	57291666667	
J_w [mm^6]	8,71562E+18	
J_x [mm^4]	25344000000	
E [N/mm^2]	210000	
λ_{LT}	38,75444874	
$\lambda_{LT,0}$	0,2	
α_{LT}	0,49	
ϕ	1	
κc	1	
Kc	0,00066582	
ϕ_{LT}	760,8994886	$\frac{M_{ed}}{M_{b,Rd}} < 1$
χ_{LT}	0,000657544	
$M_{b,rd}$ [daNm]	704285691,8	
M_{ed} [daNm]	125390501	SATISFY

$$V_{b,Rd} = V_{bw,Rd} + V_{bf,Rd} \leq \frac{\eta \cdot f_{yw} \cdot h_w \cdot t}{\sqrt{3} \cdot \gamma_{M1}}$$

$$V_{bw,Rd} = \frac{\chi_w \cdot f_{yw} \cdot h_w \cdot t}{\sqrt{3} \cdot \gamma_{M1}}$$

$$V_{bf,Rd} = \frac{b_f \cdot t_f^2 \cdot f_{yf}}{c \cdot \gamma_{M1}} \left[1 - \left(\frac{M_{Ed}}{M_{f,k} / \gamma_{M0}} \right)^2 \right]$$

DIAPHRAGMS ANALYSIS

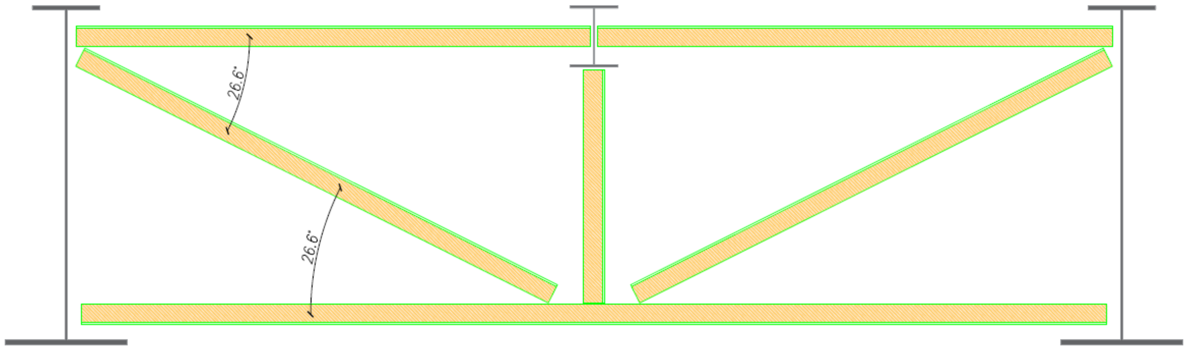

TYPE A

Geometrical conditions						
2L 80x8		Diagonal Element				
Length [mm] L3	3905,5	Class profile	3		γ_{M0}	1,05
A single element [mm2]	1230	fyk [N/mm2]	355		γ_{M1}	1,1
d [mm]	18	α_m brace factor	1,290994		Wel single element [mm3]	12600
e [mm]	22,5506	L system length [mm]	7581,5			
I_x [mm4]	2692592,745	e_0 imperfectio factor	19,57535		ϕx	1,24843
i_x [mm]	33,08398247	e_0/L analysis	0,005		ϕy	1,033899
λx	118,0480616	Ncr,y [daN]	52820,63		χx	0,343956
I_y [mm4]	3887208,17	Ncr,x [daN]	36587,81		χy	0,414815
i_y	39,75130089	$\lambda y'$	0,909212		χmin	0,343956
λy	98,24835697	$\lambda x'$	1,092442		χLT	1

Action		
	M [daNm]	N [daN]
Dead load Steel	35,63	774,87
Dead load concrete	23,44	1313,1
Permanent	10,29	375,77
Accidental load + crowd	248,594	919,6136
Wind	56,26	224,15

Method A (C4.2.4.1.3.3.1)		
Ned [daN]	4114,143	
Meq [daNm]	338,6285	
Utilization Coefficient	0,90611	<1

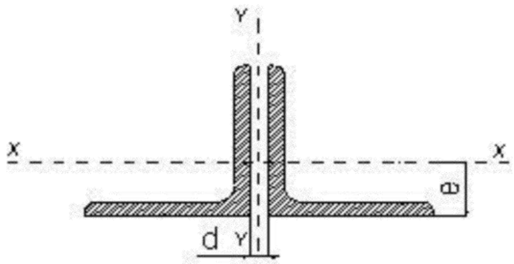

Geometrical conditions					
2L 80x8		Vertical Element			
Length [mm] L4	1720	Class profile	3	γ_{M0}	1,05
A single element [mm2]	1230	fyk [N/mm2]	355	γ_{M1}	1,1
d [mm]	18	α_m brace factor	1,290994	Wel single element [mm3]	12600
e [mm]	22,5506	L system length [mm]	2500		
I_x [mm4]	2692592,745	e_0 imperfectio factor	6,454972	ϕx	0,663526
i_x [mm]	33,08398247	e_0/L analysis	0,004	ϕy	0,61424
λx	51,98890434	Ncr,y [daN]	272332,8	χx	0,674252
I_y [mm4]	3887208,17	Ncr,x [daN]	188639,6	χy	0,742131
i_y	39,75130089	$\lambda y'$	0,400421	χmin	0,674252
λy	43,26902419	$\lambda x'$	0,481117	χLT	1

Action		
	M [daNm]	N [daN]
Dead load Steel	25,02	1126,31
Dead load concrete	16,01	1861,31
Permanent	5,25	587,33
Accidental load + crowd	248,594	6743,833
Wind	16,94	343,47

Method A (C4.2.4.1.3.3.1)	
Ned [daN]	11364,45
Meq [daNm]	309,2345
Utilization Coefficient	0,797832

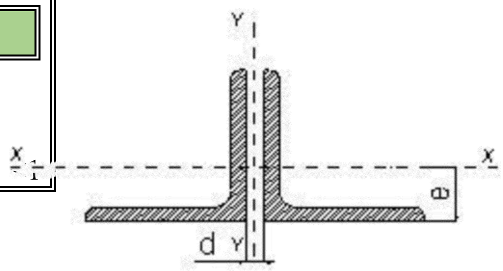

Geometrical conditions

2L 100x10		Up Element			
Length [mm] L2	3805,5	Class profile	3	γ_{M0}	1,05
A single element [mm2]	1920	fyk [N/mm2]	355	γ_{M1}	1,1
d [mm]	18	α_m brace factor	1,290994	Wel single element [mm3]	24620
e [mm]	28,22	L system length [mm]	7581,5		
I_x [mm4]	65853201,208	e_0 imperfectio factor	19,57535	ϕx	0,547877
i_x [mm]	130,9552257	e_0/L analysis	0,005	ϕy	0,860079
λx	29,05955053	Ncr,y [daN]	126543,6	χx	0,863412
I_y [mm4]	8841881,997	Ncr,x [daN]	942480,7	χy	0,502329
i_y	47,98513766	$\lambda y'$	0,733913	χmin	0,502329
λy	79,30580561	$\lambda x'$	0,268923	χLT	1

Action		
	M [daNm]	N [daN]
Dead load Steel	34,04	769,93
Dead load concrete	27,97	1196,91
Permanent	13,79	286,1
Accidental load + crowd	248,594	10115,75
Wind	59,59	350,18

Method A (C4.2.4.1.3.3.1)		
Ned [daN]	13057,08	
Meq [daNm]	346,0975	
Utilization Coefficient	0,489898	<1

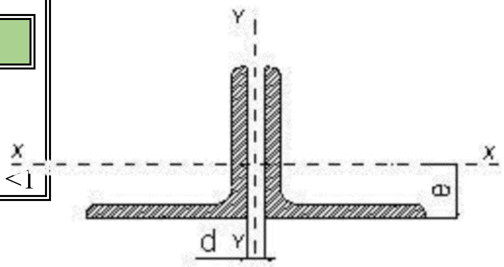

Geometrical conditions	
2L 100x10	low Element

Length [mm] L1	7581,5
A single element [mm2]	1920
d [mm]	18
e [mm]	28,22
I_x [mm4]	65853201,208
i_x [mm]	130,9552257
λx	57,89383323
I_y [mm4]	8841881,997
i_y	47,98513766
λy	157,9968375

Class profile	3
fyk [N/mm2]	355
α_m brace factor	1,290994
L system length [mm]	7581,5
e_0 imperfectio factor	19,57535
e_0/L analysis	0,003
Ncr,y [daN]	31882,58
Ncr,x [daN]	237457,4
λy'	1,462137
λx'	0,535762

γ_{M0}	1,05
γ_{M1}	1,1
Wel single element [mm3]	24620
ϕx	0,7006
ϕy	1,783486
χx	0,631881
χy	0,244516
χmin	0,244516
χLT	1

Action		
	M [daNm]	N [daN]
Dead load Steel	55,88	1321,86
Dead load concrete	22,18	821,3
Permanent	9,62	274,74
Accidental load + crowd	248,594	6743,833
Wind	84,53	439,03

Method A (C4.2.4.1.3.3.1)		
Ned [daN]	9911,839	
Meq [daNm]	363,595	
Utilization Coefficient	0,670595	<1

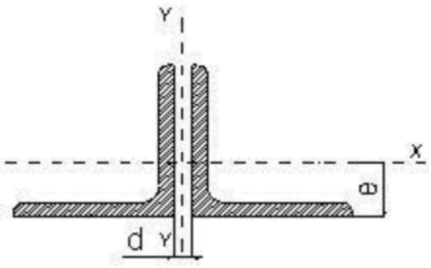

TYPE B

Geometrical conditions					
2L 100x10		Diagonal Element			
Length [mm] L3	3905,5	Class profile	3	γ_{M0}	1,05
A single element [mm2]	1920	fyk [N/mm2]	355	γ_{M1}	1,1
d [mm]	18	α_m brace factor	1,290994	Wel single element [mm3]	24620
e [mm]	28,22	L system length [mm]	7581,5		
I_x [mm4]	65853201,208	e_0 imperfectio factor	19,57535	ϕx	0,551004
i_x [mm]	130,9552257	e_0/L analysis	0,005	ϕy	0,877698
λx	29,82317031	Ncr,y [daN]	120146,3	χx	0,856705
I_y [mm4]	8841881,997	Ncr,x [daN]	894834,4	χy	0,491577
i_y	59,95215571	$\lambda y'$	0,753199	χmin	0,491577
λy	65,1436125	$\lambda x'$	0,27599	χLT	1

Action		
	M [daNm]	N [daN]
Dead load Steel	34,15	624,56
Dead load concrete	15,82	300,21
Permanent	3,89	95,43
Accidental load + crowd	211,952	2814,792
Wind	82,83	2216,65

Method A (C4.2.4.1.3.3.1)		
Ned [daN]	4158,662	
Meq [daNm]	283,3015	
Utilization Coefficient	0,370703	<1

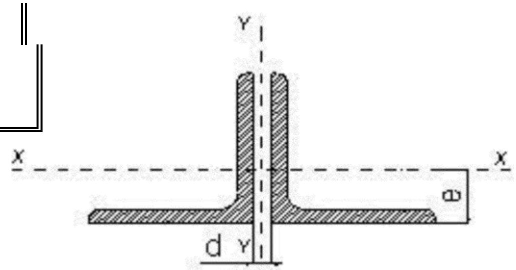

Geometrical conditions	
2L 100x10	Vertical Element

Length [mm] L4	1720	Class profile	3	γ_{M0}	1,05
A single element [mm2]	1920	fyk [N/mm2]	355	γ_{M1}	1,1
d [mm]	18	α_m brace factor	1,290994	Wel single element [mm3]	24620
e [mm]	28,22	L system length [mm]	2500		
I_x [mm4]	65853201,208	e_0 imperfectio factor	6,454972	ϕx	0,49405
i_x [mm]	130,9552257	e_0/L analysis	0,004	ϕy	0,577408
λx	13,13426013	Ncr,y [daN]	619450,9	χx	0,997176
I_y [mm4]	8841881,997	Ncr,x [daN]	4613590	χy	0,804302
i_y	47,98513766	λy'	0,331712	χmin	0,804302
λy	35,84443192	λx'	0,121547	χLT	1

Action		
	M [daNm]	N [daN]
Dead load Steel	45,17	1145,24
Dead load concrete	22,72	1424,2
Permanent	8,66	310,86
Accidental load + crowd	211,952	2814,792
Wind	72,99	285,77

Method A (C4.2.4.1.3.3.1)		
Ned [daN]	6594,396	
Meq [daNm]	312,2635	
Utilization Coefficient	0,398556	<1

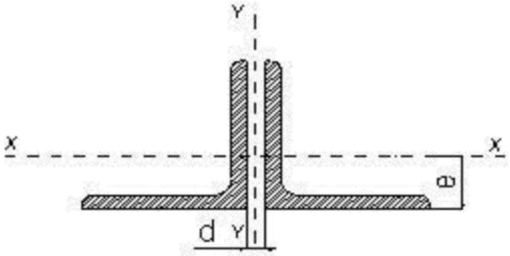

Geometrical conditions					
2L 120x10		Up Element			
Length [mm] L2	3805,5	Class profile	3	γ_{M0}	1,05

A single element [mm2]	2318
d [mm]	18
e [mm]	33,1368
I_x [mm4]	11349616,182
i_x [mm]	49,4787676
λx	76,91177822
I_y [mm4]	14490516,13
i_y	55,90751818
λy	68,06776841

fyk [N/mm2]	355
α_m brace factor	1,290994
L system length [mm]	7581,5
e_0 imperfectio factor	19,57535
e_0/L analysis	0,005
Ncr,y [daN]	207386
Ncr,x [daN]	162433,9
λy'	0,629914
λx'	0,711758

γ_{M1}	1,1
Wel single element [mm3]	36030
ϕx	0,840299
ϕy	0,771481
χx	0,515059
χy	0,565784
χmin	0,515059
χLT	1

Action		
	M [daNm]	N [daN]
Dead load Steel	61,71	1749,83
Dead load concrete	3,44	1893,18
Permanent	4,99	470,71
Accidental load + crowd	211,952	2814,792
Wind	73,39	1150,84

Method A (C4.2.4.1.3.3.1)		
Ned [daN]	8203,566	
Meq [daNm]	304,8945	
Utilization Coefficient	0,275139	<1

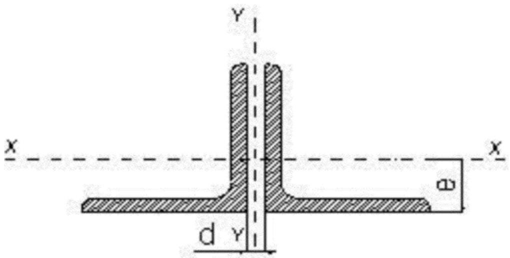

Geometrical conditions					
2L 120x10		low Element			
Length [mm] L1	7581,5		Class profile	3	γ_{M0}	1,05

A single element [mm2]	2318
d [mm]	18
e [mm]	33,1368
I_x [mm4]	11349616,182
i_x [mm]	49,4787676
λx	153,2273411
I_y [mm4]	14490516,13
i_y	55,90751818
λy	135,6078797

fyk [N/mm2]	355
α_m brace factor	1,290994
L system length [mm]	7581,5
e_0 imperfectio factor	19,57535
e_0/L analysis	0,003
Ncr,y [daN]	52250,76
Ncr,x [daN]	40925,12
λy'	1,254945
λx'	1,417999

γ_{M1}	1,1
Wel single element [mm3]	36030
ϕx	1,71242
ϕy	1,466784
χx	0,254082
χy	0,294364
χmin	0,254082
χLT	1

Action		
	M [daNm]	N [daN]
Dead load Steel	114,04	2177,5
Dead load concrete	49,21	1317,93
Permanent	19,89	524,19
Accidental load + crowd	211,952	2814,792
Wind	336,84	2579,31

Method A (C4.2.4.1.3.3.1)		
Ned [daN]	8057,813	
Meq [daNm]	452,2295	
Utilization Coefficient	0,464071	<1

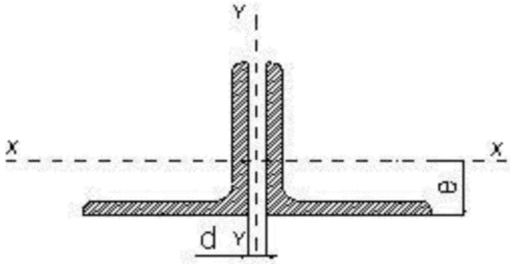

TYPE ABUTMENT

Geometrical conditions					
2L 150x15		Diagonal Element			
Length [mm] L3	3905,5	Class profile	3	γ_{M0}	1,05
A single element [mm2]	4302	fyk [N/mm2]	355	γ_{M1}	1,1
d [mm]	18	α_m brace factor	1,290994	Wel single element [mm3]	83520
e [mm]	42,4735	L system length [mm]	7581,5		
I_x [mm4]	33484310,429	e_0 imperfectio factor	19,57535	ϕx	0,732318
i_x [mm]	62,38360657	e_0/L analysis	0,005	ϕy	0,693138
λx	62,6045882	Ncr,y [daN]	553859,6	χx	0,600205
I_y [mm4]	40759979,35	Ncr,x [daN]	454995,5	χy	0,639908
i_y	68,82825781	λy'	0,525109	χmin	0,600205
λy	56,74268279	λx'	0,579356	χLT	1

Action		
	M [daNm]	N [daN]
Dead load Steel	180,52	2745,89
Dead load concrete	125,77	1898,3
Permanent	28,04	951,41
Accidental load + crowd	2096,276	12070,36
Wind	161,59	3435,8

Method A (C4.2.4.1.3.3.1)		
Ned [daN]	19291,43	
Meq [daNm]	2537,808	
Utilization Coefficient	0,977819	<1

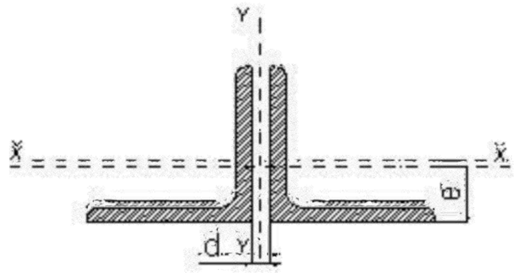

Geometrical conditions	
2L 150x15	Vertical Element

Length [mm] L4	1720
A single element [mm2]	4302
d [mm]	18
e [mm]	42,4735
I_x [mm4]	33484310,429
i_x [mm]	62,38360657
λx	27,57134598
I_y [mm4]	40759979,35
i_y	68,82825781
λy	24,98973612

Class profile	3
fyk [N/mm2]	355
α_m brace factor	1,290994
L system length [mm]	2500
e_0 imperfectio factor	6,454972
e_0/L analysis	0,004
Ncr,y [daN]	2855592
Ncr,x [daN]	2345868
λy'	0,23126
λx'	0,255151

γ_{M0}	1,05
γ_{M1}	1,1
Wel single element [mm3]	83520
ϕx	0,541927
ϕy	0,532055
χx	0,87649
χy	0,899122
χmin	0,87649
χLT	1

Action		
	M [daNm]	N [daN]
Dead load Steel	3,93	1084,29
Dead load concrete	7,66	878,86
Permanent	2,31	223,22
Accidental load + crowd	2096,276	12070,36
Wind	428,86	201,65

Method A (C4.2.4.1.3.3.1)		
Ned [daN]	14943,83	
Meq [daNm]	2114,233	
Utilization Coefficient	0,789735	<1

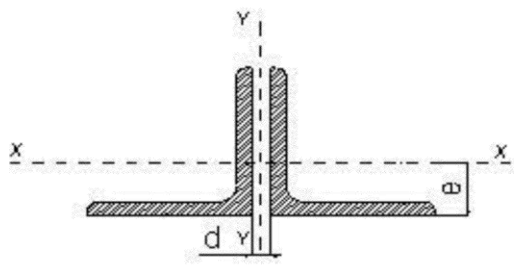

Geometrical conditions	
2L 150x18	Up Element

Length [mm] L2	3805,5
A single element [mm2]	5103
d [mm]	18
e [mm]	43,2687
I_x [mm4]	38123220,899
i_x [mm]	61,11770118
λx	62,26510367
I_y [mm4]	46443804,47
i_y	67,45841177
λy	56,41253478

Class profile	3
fyk [N/mm2]	355
α_m brace factor	1,290994
L system length [mm]	7581,5
e_0 imperfectio factor	19,57535
e_0/L analysis	0,005
Ncr,y [daN]	664696,5
Ncr,x [daN]	545613,6
λy'	0,522054
λx'	0,576215

γ_{M0}	1,05
γ_{M1}	1,1
Wel single element [mm3]	98740
φx	0,729968
φy	0,691019
χx	0,602426
χy	0,642231
χmin	0,602426
χLT	1

Action		
	M [daNm]	N [daN]
Dead load Steel	118,78	1898,27
Dead load concrete	114,7	1781
Permanent	113	1760
Accidental load + crowd	2096,276	12070,36
Wind	180,52	2745,89

Method A (C4.2.4.1.3.3.1)		
Ned [daN]	18797,37	
Meq [daNm]	2524,474	
Utilization Coefficient	0,817163	<1

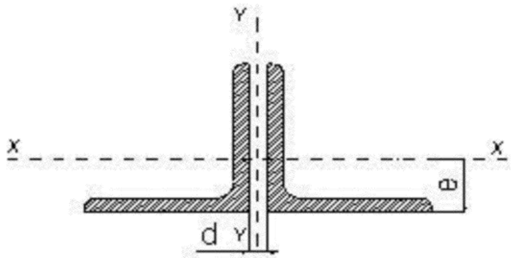

Geometrical conditions					
2L 150x18		low Element			
Length [mm] L1	7581,5	Class profile	3	γ_{M0}	1,05

A single element [mm2]	5103
d [mm]	18
e [mm]	43,2687
I_x [mm4]	38123220,899
i_x [mm]	61,11770118
λx	124,0475321
I_y [mm4]	46443804,47
i_y	67,45841177
λy	112,3877631

fyk [N/mm2]	355
α_m brace factor	1,290994
L system length [mm]	7581,5
e_0 imperfectio factor	19,57535
e_0/L analysis	0,003
Ncr,y [daN]	167469,8
Ncr,x [daN]	137467
λy'	1,040061
λx'	1,147963

γ_{M1}	1,1
Wel single element [mm3]	98740
ϕx	1,320063
ϕy	1,183673
χx	0,32579
χy	0,362402
χmin	0,32579
χLT	1

Action		
	M [daNm]	N [daN]
Dead load Steel	128,05	69,58
Dead load concrete	65,97	347,52
Permanent	2,95	13,44
Accidental load + crowd	2096,276	12070,36
Wind	240,745	1316,61

Method A (C4.2.4.1.3.3.1)		
Ned [daN]	12646,89	
Meq [daNm]	2361,153	
Utilization Coefficient	0,803844	<1

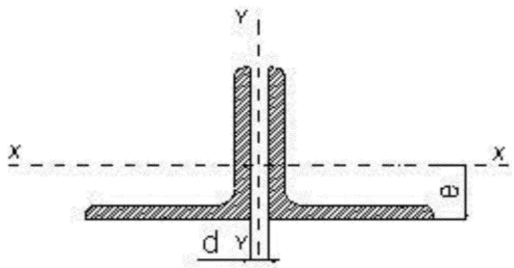

TYPE PIER

Geometrical conditions					
2L 150x15		Diagonal Element			
Length [mm] L3	3905,5	Class profile	3	γ_{M0}	1,05
A single element [mm2]	4302	fyk [N/mm2]	355	γ_{M1}	1,1
d [mm]	18	α_m brace factor	1,290994	Wel single element [mm3]	83520
e [mm]	42,4735	L system length [mm]	7581,5		
I_x [mm4]	33484310,429	e_0 imperfectio factor	19,57535	ϕx	0,732318
i_x [mm]	62,38360657	e_0/L analysis	0,005	ϕy	0,693138
λx	62,6045882	Ncr,y [daN]	553859,6	χx	0,600205
I_y [mm4]	40759979,35	Ncr,x [daN]	454995,5	χy	0,639908
i_y	68,82825781	λy'	0,525109	χmin	0,600205
λy	56,74268279	λx'	0,579356	χLT	1

Action		
	M [daNm]	N [daN]
Dead load Steel	122,53	2168,45
Dead load concrete	209,92	2523,4
Permanent	60,04	721,85
Accidental load + crowd	182466,02	197967,1
Wind	213,45	7430,43

Method A (C4.2.4.1.3.3.1)		
Ned [daN]	205023	
Meq [daNm]	182974,9	
Utilization Coefficient	107,8058	<1

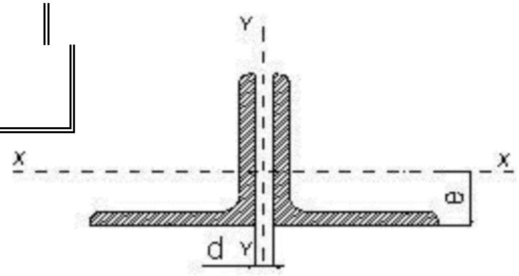

Geometrical conditions					
2L 150x15		Vertical Element			
Length [mm] L4	1720	Class profile	3	γ_{M0}	1,05
A single element [mm2]	4302	fyk [N/mm2]	355	γ_{M1}	1,1
d [mm]	18	α_m brace factor	1,290994	Wel single element [mm3]	83520
e [mm]	42,4735	L system length [mm]	2500		
I_x [mm4]	33484310,429	e_0 imperfectio factor	6,454972	ϕx	0,541927
i_x [mm]	62,38360657	e_0/L analysis	0,004	ϕy	0,532055
λx	27,57134598	Ncr,y [daN]	2855592	χx	0,87649
I_y [mm4]	40759979,35	Ncr,x [daN]	2345868	χy	0,899122
i_y	68,82825781	$\lambda y'$	0,23126	χmin	0,87649
λy	24,98973612	$\lambda x'$	0,255151	χLT	1

Action		
	M [daNm]	N [daN]
Dead load Steel	6,55	1428,01
Dead load concrete	45,66	1918,08
Permanent	13,92	530,34
Accidental load + crowd	1250,5	10135,5
Wind	108,98	367,95

Method A (C4.2.4.1.3.3.1)		
Ned [daN]	15183,06	
Meq [daNm]	1334,904	
Utilization Coefficient	0,499144	<1

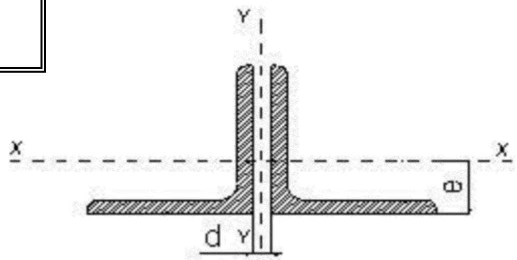

Geometrical conditions					
2L 180x18		Up Element			
Length [mm] L2	3805,5	Class profile	3	γ_{M0}	1,05
A single element [mm2]	6191	fyk [N/mm2]	355	γ_{M1}	1,1
d [mm]	18	α_m brace factor	1,290994	Wel single element [mm3]	144700
e [mm]	43,8996	L system length [mm]	7581,5		
I_x [mm4]	40299092,941	e_0 imperfectio factor	19,57535	ϕx	0,761474
i_x [mm]	57,04955165	e_0/L analysis	0,005	ϕy	0,718203
λx	66,70516927	Ncr,y [daN]	700135,5	χx	0,574141
I_y [mm4]	48920007,6	Ncr,x [daN]	576754,3	χy	0,613837
i_y	62,8561618	$\lambda y'$	0,560278	χmin	0,574141
λy	60,54299039	$\lambda x'$	0,617304	χLT	1

Action		
	M [daNm]	N [daN]
Dead load Steel	47,62	1778,13
Dead load concrete	63,37	1416,54
Permanent	18,11	412,38
Accidental load + crowd	1250,5	10135,5
Wind	19,69	3129,97

Method A (C4.2.4.1.3.3.1)		
Ned [daN]	14860,68	
Meq [daNm]	1418,447	
Utilization Coefficient	0,311627	<1

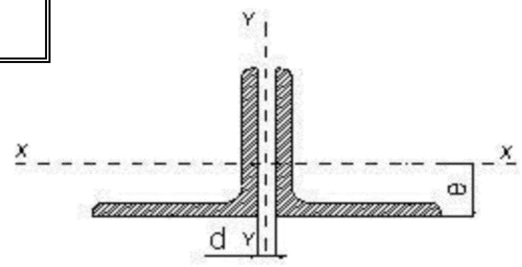

Geometrical conditions					
2L 180x18		low Element			
Length [mm] L1	7581,5	Class profile	3	γ_{M0}	1,05
A single element [mm2]	6191	fyk [N/mm2]	355	γ_{M1}	1,1
d [mm]	18	α_m brace factor	1,290994	Wel single element [mm3]	144700
e [mm]	43,8996	L system length [mm]	7581,5		
I_x [mm4]	40299092,941	e_0 imperfectio factor	19,57535	ϕx	1,431302
i_x [mm]	57,04955165	e_0/L analysis	0,003	ϕy	1,278721
λx	132,8932442	Ncr,y [daN]	176398,7	χx	0,301351
I_y [mm4]	48920007,6	Ncr,x [daN]	145312,9	χy	0,336011
i_y	62,8561618	$\lambda y'$	1,116213	χmin	0,301351
λy	120,6166553	$\lambda x'$	1,229823	χLT	1

Action		
	M [daNm]	N [daN]
Dead load Steel	59,63	579,99
Dead load concrete	23,47	129,45
Permanent	6,93	11,68
Accidental load + crowd	1250,5	10135,5
Wind	374,89	8364,04

Method A (C4.2.4.1.3.3.1)		
Ned [daN]	11104,92	
Meq [daNm]	1369,615	
Utilization Coefficient	0,314836	<1

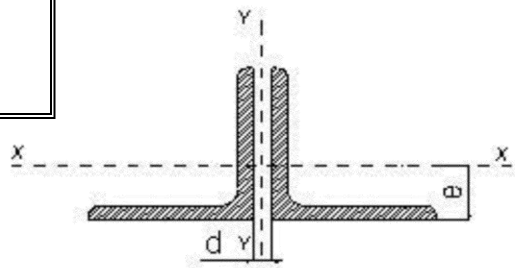

BRACES RESULTS

Geometrical conditions					
2L 80x8		Diagonal Element			
Length [mm] L3	3905,5	Class profile	3	γ_{M0}	1,25
A single element [mm2]	1230	fyk [N/mm2]	355	γ_{M1}	1,1
d [mm]	18	α_m brace factor	1,290994449	Wel single element [mm3]	12600
e [mm]	22,5506	L system length [mm]	7581,5		
I_x [mm4]	2692592,745	e_0 imperfectio factor	19,57534883	φx	1,248430315
i_x [mm]	33,08398247	e_0/L analysis	0,005	φy	1,033898809
λx	118,0480616	Ncr,y [daN]	52820,6273	χx	0,343956051
I_y [mm4]	3887208,17	Ncr,x [daN]	36587,81101	χy	0,414815341
i_y	39,75130089	λy'	0,909211573	χmin	0,343956051
λy	98,24835697	λx'	1,092442327	χLT	1

Action		
	M [daNm]	N [daN]
Dead load Steel	0	2220,3
Dead load concrete	0	1671,63
Permanent	0	613,39
Accidental load + crowd	199,56	9342,995
Wind	0	1455,23

Method A (C4.2.4.1.3.3.1)		
Ned [daN]	15210,4905	
Meq [daNm]	199,56	
Utilization Coefficient	0,700373146	<1

N_{Rd}[daN]	62877,6

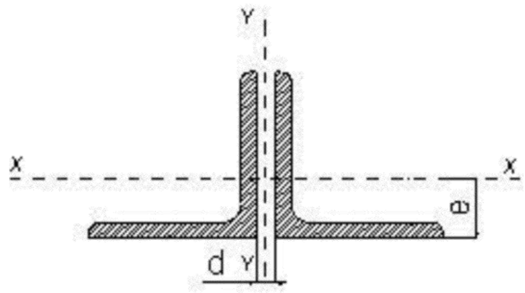

Geometrical conditions					
2L 100x10					
Length [mm] L2	3805,5	Class profile	3	γ_{M0}	1,25
A single element [mm2]	1920	fyk [N/mm2]	355	γ_{M1}	1,1
d [mm]	18	α_m brace factor	1,290994449	Wel single element [mm3]	24620
e [mm]	28,22	L system length [mm]	7581,5		
I_x [mm4]	65853201,208	e_0 imperfectio factor	19,57534883	φx	0,498270343
i_x [mm]	91,81954298	e_0/L analysis	0,005	φy	0,59750303
λx	20,9105811	Ncr,y [daN]	497120,0702	χx	0,985528951
I_y [mm4]	8841881,997	Ncr,x [daN]	3702486,419	χy	0,768970831
i_y	33,64488424	λy'	0,370283314	χmin	0,768970831
λy	57,06662524	λx'	0,135680693	χLT	1

Action		
	M [daNm]	N [daN]
Dead load Steel	0	1408,22
Dead load concrete	0	1192,14
Permanent	0	339,6
Accidental load + crowd	199,56	9342,995
Wind	0	2496,9

Method A (C4.2.4.1.3.3.1)		
Ned [daN]	13193,081	
Meq [daNm]	199,56	
Utilization Coefficient	0,260775698	<1

N_{Rd}[daN]	98150,4

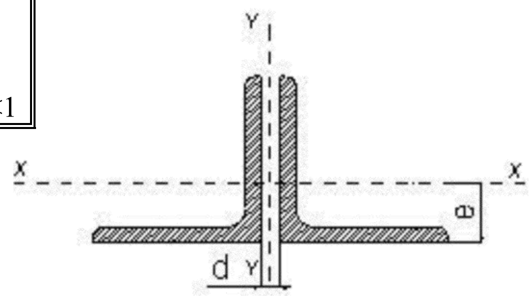

SHEAR CONNECTORS

BEAM SEGMENT		C1
b_eff	mm	3375
h_c	mm	400
h_t	mm	2500
h_predalle	mm	60
h_pins	mm	135
d_pins	mm	22
b_0	mm	250
fu	N/mm2	450
f_ck	N/mm2	30
Ecm	N/mm2	34330,80
g_v	-	1,25
a	-	1
P_Rd1	daN	10947,82208
P_Rd2	daN	11395,56634
P_Rd	daN	10947,82208
n_r	**-**	**3**
k_t	**-**	**0,6**
P_Rd,new	**daN**	**6568,693248**
Ac	mm2	1350000
A	mm2	87920,00
f_yk	N/mm2	355
Rc	daN	2295000
Ra	daN	2972533,333
		neutral axis cut steel beam
x	mm	518,0885984
Mpl	daNm	4134662,186
Ja	mm4	2387852509,00
Jc	mm4	18000000000,00

ACCIDENTAL LOADS		
n	-	6,12
x	mm	670,7719852
Jomo	mm4	1,06E+11
S	mm3	447846519
S/J	mm-1	4,23E-03
SHRINKAGE		
n	-	16,19
x	mm	1047,242307
Jomo	mm4	7,04E+10
S	mm3	137843600,7
S/J	mm-1	1,96E-03
PERMANENT		
n	-	18,40
x	mm	1099,843759
Jomo	mm4	6,59E+10
S	mm3	117413379,6
S/J	mm-1	1,78E-03
SEATTLEMENT		
n	-	22,86
x	mm	1187,500446
Jomo	mm4	5,86E+10
S	mm3	89304067,31
S/J	mm-1	1,52E-03
SHEAR FORCES		
V_permanent	daN	448499
V_truck	daN	720238,5
V_wind	daN	3046,68
s_shear	daN/m	801,96
i_min	mm	150,00
P_max	daN	1782,13
CHECK		OK

BEAM SEGMENT		**C2**
b_eff	mm	3375
h_c	mm	400
h_t	mm	2500
h_predalle	mm	60
h_pins	mm	135
d_pins	mm	22
b_0	mm	250
fu	N/mm2	450
f_ck	N/mm2	30
Ecm	N/mm2	34330,80
g_v	-	1,25
a	-	1
P_Rd1	daN	10947,82208
P_Rd2	daN	11395,56634
P_Rd	daN	10947,82208
n_r	**-**	**2**
k_t	**-**	**0,6**
P_Rd,new	**daN**	**6568,693248**
Ac	mm2	1350000
A	mm2	83040,00
f_yk	N/mm2	355
Rc	daN	2295000
Ra	daN	2807542,857
		neutral axis cut steel beam
x	mm	489,3320884
Mpl	daNm	3945535,31
Ja	mm4	2387499521,00
Jc	mm4	18000000000,00

ACCIDENTAL LOADS		
n	-	6,12
x	mm	651,8259424
Jomo	mm4	1,02E+11
S	mm3	452027872,3
S/J	mm-1	4,43E-03
SHRINKAGE		
n	-	16,19
x	mm	1023,705861
Jomo	mm4	6,85E+10
S	mm3	139806591,7
S/J	mm-1	2,04E-03
PERMANENT		
n	-	18,40
x	mm	1076,439773
Jomo	mm4	6,43E+10
S	mm3	119130675,1
S/J	mm-1	1,85E-03
SEATTLEMENT		
n	-	22,86
x	mm	1164,74632
Jomo	mm4	5,73E+10
S	mm3	90647562,55
S/J	mm-1	1,58E-03
SHEAR FORCES		
V_permanent	daN	258749
V_truck	daN	864682,5
V_wind	daN	3029,95
s_shear	daN/m	483,55
i_min	mm	150,00
P_max	daN	1611,82
CHECK		OK

BEAM SEGMENT		C3
b_eff	mm	3375
h_c	mm	400
h_t	mm	2500
h_predalle	mm	60
h_pins	mm	135
d_pins	mm	22
b_0	mm	250
fu	N/mm2	450
f_ck	N/mm2	30
Ecm	N/mm2	34330,80
g_v	-	1,25
a	-	1
P_Rd1	daN	10947,82208
P_Rd2	daN	11395,56634
P_Rd	daN	10947,82208
n_r	**-**	**2**
k_t	**-**	**0,6**
P_Rd,new	**daN**	**6568,693248**
Ac	mm2	1350000
A	mm2	83040,00
f_yk	N/mm2	355
Rc	daN	2295000
Ra	daN	2807542,857
		neutral axis cut steel beam
x	mm	489,3320884
Mpl	daNm	3945535,31
Ja	mm4	2387499520,00
Jc	mm4	18000000000,00

ACCIDENTAL LOADS		
n	-	6,12
x	mm	651,8259424
Jomo	mm4	1,02E+11
S	mm3	452027872,3
S/J	mm-1	4,43E-03
SHRINKAGE		
n	-	16,19
x	mm	1023,705861
Jomo	mm4	6,85E+10
S	mm3	139806591,7
S/J	mm-1	2,04E-03
PERMANENT		
n	-	18,40
x	mm	1076,439773
Jomo	mm4	6,43E+10
S	mm3	119130675,1
S/J	mm-1	1,85E-03
SEATTLEMENT		
n	-	22,86
x	mm	1164,74632
Jomo	mm4	5,73E+10
S	mm3	90647562,55
S/J	mm-1	1,58E-03
SHEAR FORCES		
V_permanent	daN	213009
V_truck	daN	943575
V_wind	daN	2422,29
s_shear	daN/m	399,09
i_min	mm	150,00
P_max	daN	1330,31
CHECK		OK

BEAM SEGMENT		**C4**
b_eff	mm	3375
h_c	mm	400
h_t	mm	2500
h_predalle	mm	60
h_pins	mm	135
d_pins	mm	22
b_0	mm	250
fu	N/mm2	450
f_ck	N/mm2	30
Ecm	N/mm2	34330,80
g_v	-	1,25
a	-	1
P_Rd1	daN	10947,82208
P_Rd2	daN	11395,56634
P_Rd	daN	10947,82208
n_r	**-**	**2**
k_t	**-**	**0,6**
P_Rd,new	**daN**	**6568,693248**
Ac	mm2	1350000
A	mm2	107630,00
f_yk	N/mm2	355
Rc	daN	2295000
Ra	daN	3638919,048
		neutral axis cut steel beam
x	mm	634,2342567
Mpl	daNm	4850252,87
Ja	mm4	2547559577,00
Jc	mm4	18000000000,00

ACCIDENTAL LOADS		
n	-	6,12
x	mm	741,5627364
Jomo	mm4	1,20E+11
S	mm3	432223143,3
S/J	mm-1	3,60E-03
SHRINKAGE		
n	-	16,19
x	mm	1130,067901
Jomo	mm4	7,72E+10
S	mm3	130935765,3
S/J	mm-1	1,70E-03
PERMANENT		
n	-	18,40
x	mm	1181,529247
Jomo	mm4	7,20E+10
S	mm3	111419609,2
S/J	mm-1	1,55E-03
SEATTLEMENT		
n	-	22,86
x	mm	1265,844183
Jomo	mm4	6,35E+10
S	mm3	84678337,47
S/J	mm-1	1,33E-03
SHEAR FORCES		
V_permanent	daN	370261
V_truck	daN	1013082
V_wind	daN	3637,62
s_shear	daN/m	576,92
i_min	mm	150,00
P_max	daN	1923,07
CHECK		OK

BEAM SEGMENT		C5
b_eff	mm	3375
h_c	mm	400
h_t	mm	2500
h_predalle	mm	60
h_pins	mm	135
d_pins	mm	22
b_0	mm	200
fu	N/mm2	450
f_ck	N/mm2	30
Ecm	N/mm2	34330,80
g_v	-	1,25
a	-	1
P_Rd1	daN	10947,82208
P_Rd2	daN	11395,56634
P_Rd	daN	10947,82208
n_r	**-**	**3**
k_t	**-**	**0,6**
P_Rd,new	**daN**	**6568,693248**
Ac	mm2	1350000
A	mm2	148230,00
f_yk	N/mm2	355
Rc	daN	2295000
Ra	daN	5011585,714
		neutral axis cut steel beam
x	mm	873,4789916
Mpl	daNm	6080359,011
Ja	mm4	7656856608,00
Jc	mm4	18000000000,00

ACCIDENTAL LOADS		
n	-	6,12
x	mm	863,5446831
Jomo	mm4	1,50E+11
S	mm3	405301974,4
S/J	mm-1	2,71E-03
SHRINKAGE		
n	-	16,19
x	mm	1256,256079
Jomo	mm4	9,29E+10
S	mm3	120411395,7
S/J	mm-1	1,30E-03
PERMANENT		
n	-	18,40
x	mm	1303,998351
Jomo	mm4	8,63E+10
S	mm3	102433292
S/J	mm-1	1,19E-03
SEATTLEMENT		
n	-	22,86
x	mm	1380,266266
Jomo	mm4	7,60E+10
S	mm3	77922396,68
S/J	mm-1	1,03E-03
SHEAR FORCES		
V_permanent	daN	558693
V_truck	daN	1153569
V_wind	daN	4852,94
s_shear	daN/m	665,93
i_min	mm	150,00
P_max	daN	1479,84
CHECK		OK

BEAM SEGMENT		C5a
b_eff	mm	3375
h_c	mm	400
h_t	mm	2500
h_predalle	mm	60
h_pins	mm	135
d_pins	mm	22
b_0	mm	200
fu	N/mm2	450
f_ck	N/mm2	30
Ecm	N/mm2	34330,80
g_v	-	1,25
a	-	1
P_Rd1	daN	10947,82208
P_Rd2	daN	11395,56634
P_Rd	daN	10947,82208
n_r	**-**	**3**
k_t	**-**	**0,6**
P_Rd,new	**daN**	**6568,693248**
Ac	mm2	1350000
A	mm2	192330,00
f_yk	N/mm2	355
Rc	daN	2295000
Ra	daN	6502585,714
		neutral axis cut steel beam
x	mm	1133,348273
Mpl	daNm	7044419,285
Ja	mm4	10369681812,00
Jc	mm4	18000000000,00

ACCIDENTAL LOADS		
n	-	6,12
x	mm	968,8709124
Jomo	mm4	1,74E+11
S	mm3	382056688,6
S/J	mm-1	2,20E-03
SHRINKAGE		
n	-	16,19
x	mm	1351,218178
Jomo	mm4	1,04E+11
S	mm3	112491349,3
S/J	mm-1	1,08E-03
PERMANENT		
n	-	18,40
x	mm	1394,619771
Jomo	mm4	9,65E+10
S	mm3	95783836,9
S/J	mm-1	9,93E-04
SEATTLEMENT		
n	-	22,86
x	mm	1462,674372
Jomo	mm4	8,46E+10
S	mm3	73056690,08
S/J	mm-1	8,64E-04
SHEAR FORCES		
V_permanent	daN	563529
V_truck	daN	1157524,5
V_wind	daN	4869,67
s_shear	daN/m	562,01
i_min	mm	150,00
P_max	daN	1248,92
CHECK		OK

BEAM SEGMENT		C6
b_eff	mm	3375
h_c	mm	400
h_t	mm	2500
h_predalle	mm	60
h_pins	mm	135
d_pins	mm	22
b_0	mm	250
fu	N/mm2	450
f_ck	N/mm2	30
Ecm	N/mm2	34330,80
g_v	-	1,25
a	-	1
P_Rd1	daN	10947,82208
P_Rd2	daN	11395,56634
P_Rd	daN	10947,82208
n_r	**-**	**2**
k_t	**-**	**0,6**
P_Rd,new	**daN**	**6568,693248**
Ac	mm2	1350000
A	mm2	114300,00
f_yk	N/mm2	355
Rc	daN	2295000
Ra	daN	3864428,571
		neutral axis cut steel beam
x	mm	673,5387488
Mpl	daNm	5074885,95
Ja	mm4	2678379600,00
Jc	mm4	18000000000,00

ACCIDENTAL LOADS		
n	-	6,12
x	mm	763,6323518
Jomo	mm4	1,25E+11
S	mm3	427352423,8
S/J	mm-1	3,43E-03
SHRINKAGE		
n	-	16,19
x	mm	1154,356693
Jomo	mm4	7,93E+10
S	mm3	128910027
S/J	mm-1	1,62E-03
PERMANENT		
n	-	18,40
x	mm	1205,286654
Jomo	mm4	7,38E+10
S	mm3	109676381
S/J	mm-1	1,49E-03
SEATTLEMENT		
n	-	22,86
x	mm	1288,321561
Jomo	mm4	6,50E+10
S	mm3	83351182,5
S/J	mm-1	1,28E-03
SHEAR FORCES		
V_permanent	daN	337375
V_truck	daN	1269729,44
V_wind	daN	4262,01
s_shear	daN/m	505,44
i_min	mm	150,00
P_max	daN	1684,82
CHECK		OK

BEAM SEGMENT		**C7**			
b_eff	mm	3375	**ACCIDENTAL LOADS**		
h_c	mm	400	**n**	-	6,12
h_t	mm	2500	**x**	mm	711,2851439
h_predalle	mm	60	**Jomo**	mm4	1,14E+11
			S	mm3	438905346,8
h_pins	mm	135	**S/J**	mm-1	3,85E-03
d_pins	mm	22	**SHRINKAGE**		
b_0	mm	250	**n**	-	16,19
			x	mm	1095,592136
fu	N/mm2	450	**Jomo**	mm4	7,45E+10
f_ck	N/mm2	30	**S**	mm3	133811119,4
Ecm	N/mm2	34330,80	**S/J**	mm-1	1,80E-03
g_v	-	1,25	**PERMANENT**		
a	-	1	**n**	-	18,40
			x	mm	1147,654865
P_Rd1	daN	10947,82208	**Jomo**	mm4	6,96E+10
P_Rd2	daN	11395,56634	**S**	mm3	113905182,5
P_Rd	daN	10947,82208	**S/J**	mm-1	1,64E-03
			SEATTLEMENT		
n_r	**-**	**2**	**n**	-	22,86
k_t	**-**	**0,6**	**x**	mm	1233,556287
P_Rd,new	**daN**	**6568,693248**	**Jomo**	mm4	6,16E+10
			S	mm3	86584744,9
Ac	mm2	1350000	**S/J**	mm-1	1,41E-03
A	mm2	98900,00	**SHEAR FORCES**		
f_yk	N/mm2	355	**V_permanent**	daN	448499
Rc	daN	2295000	**V_truck**	daN	868638
Ra	daN	3343761,905	**V_wind**	daN	3654,34
		neutral axis cut steel beam			
x	mm	582,7907459	**s_shear**	daN/m	737,58
Mpl	daNm	4542850,396	**i_min**	mm	150,00
			P_max	daN	2458,61
			CHECK		OK
Ja	mm4	2626235869,00			
Jc	mm4	18000000000,00			

BEAM SEGMENT		C8
b_eff	mm	3375
h_c	mm	600
h_t	mm	2500
h_predalle	mm	60
h_pins	mm	135
d_pins	mm	22
b_0	mm	200
fu	N/mm2	450
f_ck	N/mm2	30
Ecm	N/mm2	34330,80
g_v	-	1,25
a	-	1
P_Rd1	daN	10947,82208
P_Rd2	daN	11395,56634
P_Rd	daN	10947,82208
n_r	**-**	**3**
k_t	**-**	**0,6**
P_Rd,new	**daN**	**6568,693248**
Ac	mm2	2025000
A	mm2	108509,37
f_yk	N/mm2	355
Rc	daN	3442500
Ra	daN	3668650,003
		neutral axis cut steel beam
x	mm	639,4161226
Mpl	daNm	5614105,526
Ja	mm4	3273457880,50
Jc	mm4	60750000000,00

C8		
ACCIDENTAL LOADS		
n	-	6,12
x	mm	757,4462012
Jomo	mm4	1,51E+11
S	mm3	676181238,8
S/J	mm-1	4,48E-03
SHRINKAGE		
n	-	16,19
x	mm	1159,831169
Jomo	mm4	9,79E+10
S	mm3	205190493,2
S/J	mm-1	2,10E-03
PERMANENT		
n	-	18,40
x	mm	1218,923123
Jomo	mm4	9,20E+10
S	mm3	174020112,7
S/J	mm-1	1,89E-03
SEATTLEMENT		
n	-	22,86
x	mm	1319,056077
Jomo	mm4	8,23E+10
S	mm3	131161343,6
S/J	mm-1	1,59E-03
SHEAR FORCES		
V_permanent	daN	494627
V_truck	daN	724194
V_wind	daN	4245,28
s_shear	daN/m	852,05
i_min	mm	150,00
P_max	daN	1893,45
CHECK		OK

FULLY RESTORED BOLTED JOINT OF MAIN BEAMS

BEAM		
h	mm	2500
b_up	mm	500
b_low	mm	900
tf_up	mm	25
tf_low	mm	35
tw	mm	18
hw	mm	2440
A	mm2	87920
Ix	mm4	1,6832E+11
Iy	mm4	2387852509
Wy	mm3	1910282,007
Wpl	mm3	170454800
c/t	-	135,5555556
e	-	0,813616513
x	mm	1747,777778
		752,2222222
Yg	mm	969,37
f_yk	N/mm2	355
PLATE GEOMETRY		
t_1	mm	18
t_2	mm	20
e_1	mm	200
		ok
e_2	mm	200
		ok
p_1	mm	100
		ok
p_2	mm	100
		ok
Free web	mm	2440
		OK
Heigth plate	mm	900
Ftk	N/mm2	510

C1		
FULLY RESTRAINED BOLTED JOINT		
	Nmm	6458572501
b	mm	2440
F	N	2646955,943
	Atot	5098,143187
	n	10
BOLT CHARACTERISTICS		
class		8,8
f_{yb}	[N/mm2]	649
f_{tb}	[N/mm2]	800
Type		**M30**
f_b	mm	30
Ares	mm2	561
column	-	4
raw	-	6
n_b	-	48
SHEAR TEST		
F_vRd	daN	13733,28
F_v,Ed	daN	154373,43
	daN	3216,113125
		SATISFY
TENSILE TEST		
F_t,Rd	daN	32313,6
F_t,Ed	daN	353595,32
F_t,Ed	daN	7366,569167
		SATISFY
COMBINED ACTION - SHEAR AND TENSILE		
	0,397020453	
	SATISFY	

BEAM		
h	mm	2500
b_up	mm	500
b_low	mm	900
tf_up	mm	25
tf_low	mm	35
tw	mm	16
hw	mm	2440
A	mm2	83040
Ix	mm4	1,5822E+11
Iy	mm4	2387499521
Wy	mm3	1909999,617
Wpl	mm3	158547600
c/t	-	152,5
e	-	0,813616513
x	mm	1813,75
		686,25
Yg	mm	954,65
f_yk	N/mm2	355
PLATE GEOMETRY		
t_1	mm	16
t_2	mm	20
e_1	mm	200
		ok
e_2	mm	200
		ok
p_1	mm	100
		ok
p_2	mm	100
		ok
Free web	mm	2440
		OK
Heigth plate	mm	900
Ftk	N/mm2	510

C2		
FULLY RESTRAINED BOLTED JOINT		
	Nmm	6457617752
b	mm	2440
F	N	2646564,652
	Atot	5097,389546
	n	10
BOLT CHARACTERISTICS		
class		8,8
f_{yb}	[N/mm2]	649
f_{tb}	[N/mm2]	800
Type		**M30**
f_b	mm	30
Ares	mm2	561
column	-	4
raw	-	6
n_b	-	48
SHEAR TEST		
F_vRd	daN	13733,28
F_v,Ed	daN	154373,43
	daN	955,8845833
		SATISFY
TENSILE TEST		
F_t,Rd	daN	32313,6
F_t,Ed	daN	445758,43
F_t,Ed	daN	9286,633958
		SATISFY
COMBINED ACTION - SHEAR AND TENSILE		
	0,274882717	
	SATISFY	

BEAM		
h	mm	2500
b_up	mm	500
b_low	mm	900
tf_up	mm	25
tf_low	mm	35
tw	mm	16
hw	mm	2440
A	mm2	83040
Ix	mm4	1,5822E+11
Iy	mm4	2387499520
Wy	mm3	1909999,616
Wpl	mm3	158547600
c/t	-	152,5
e	-	0,813616513
x	mm	1813,75
		686,25
Yg	mm	954,65
f_yk	N/mm2	355
PLATE GEOMETRY		
t_1	mm	16
t_2	mm	20
e_1	mm	200
		ok
e_2	mm	200
		ok
p_1	mm	100
		ok
p_2	mm	100
		ok
Free web	mm	2440
		OK
Heigth plate	mm	900
Ftk	N/mm2	510

C3		
FULLY RESTRAINED BOLTED JOINT		
	Nmm	6457617749
b	mm	2440
F	N	2646564,651
	Atot	5097,389544
	n	10
BOLT CHARACTERISTICS		
class		8,8
f_{yb}	[N/mm2]	649
f_{tb}	[N/mm2]	800
Type		**M30**
f_b	mm	30
Ares	mm2	561
column	-	4
raw	-	6
n_b	-	48
SHEAR TEST		
F_vRd	daN	13733,28
F_v,Ed	daN	154373,43
	daN	2821,059375
		SATISFY
TENSILE TEST		
F_t,Rd	daN	32313,6
F_t,Ed	daN	411790,24
F_t,Ed	daN	8578,963333
		SATISFY
COMBINED ACTION - SHEAR AND TENSILE		
	0,395054024	
	SATISFY	

BEAM		
h	mm	2500
b_up	mm	500
b_low	mm	900
tf_up	mm	30
tf_low	mm	55
tw	mm	22
hw	mm	2415
A	mm2	107630
Ix	mm4	2,0317E+11
Iy	mm4	2547559577
Wy	mm3	2038047,662
Wpl	mm3	203961450
c/t	-	110,2777778
e	-	0,813616513
x	mm	1764,318182
		735,6818182
Yg	mm	947,51
f_yk	N/mm2	355
PLATE GEOMETRY		
t_1	mm	22
t_2	mm	20
e_1	mm	200
		ok
e_2	mm	200
		ok
p_1	mm	100
		ok
p_2	mm	100
		ok
Free web	mm	2415
		OK
Heigth plate	mm	900
Ftk	N/mm2	510

C4		
FULLY RESTRAINED BOLTED JOINT		
	Nmm	6890542094
b	mm	2415
F	N	2853226,54
	Atot	5495,428621
	n	10
BOLT CHARACTERISTICS		
class		8,8
f_{yb}	[N/mm2]	649
f_{tb}	[N/mm2]	800
Type		**M30**
f_b	mm	30
Ares	mm2	561
column	-	4
raw	-	6
n_b	-	48
SHEAR TEST		
F_vRd	daN	13733,28
F_v,Ed	daN	154373,43
	daN	5165,503542
		SATISFY
TENSILE TEST		
F_t,Rd	daN	32313,6
F_t,Ed	daN	886610,95
F_t,Ed	daN	18471,06146
		SATISFY
COMBINED ACTION - SHEAR AND TENSILE		
	0,784429507	
	SATISFY	

BEAM		
h	mm	2500
b_up	mm	900
b_low	mm	1250
tf_up	mm	30
tf_low	mm	60
tw	mm	28
hw	mm	2410
A	mm2	148230
Ix	mm4	3,0742E+11
Iy	mm4	7656856608
Wy	mm3	6125485,286
Wpl	mm3	298348050
c/t	-	86,67857143
e	-	0,813616513
x	mm	1682,678571
		817,3214286
Yg	mm	1006,37
f_yk	N/mm2	355
PLATE GEOMETRY		
t_1	mm	28
t_2	mm	20
e_1	mm	200
		ok
e_2	mm	200
		ok
p_1	mm	100
		ok
p_2	mm	100
		ok
Free web	mm	2410
		OK
Heigth plate	mm	900
Ftk	N/mm2	510

C5		
FULLY RESTRAINED BOLTED JOINT		
	Nmm	20709974064
b	mm	2410
F	N	8593350,234
	Atot	16551,13681
	n	30
BOLT CHARACTERISTICS		
class		8,8
f_{yb}	[N/mm2]	649
f_{tb}	[N/mm2]	800
Type		**M30**
f_{b}	mm	30
Ares	mm2	561
column	-	4
raw	-	6
n_b	-	48
SHEAR TEST		
F_vRd	daN	13733,28
F_v,Ed	daN	154373,43
	daN	6135,905417
		SATISFY
TENSILE TEST		
F_t,Rd	daN	32313,6
F_t,Ed	daN	1129730,21
F_t,Ed	daN	23536,04604
		SATISFY
COMBINED ACTION - SHEAR AND TENSILE		
	0,967050591	
	SATISFY	

BEAM			C5a		
h	mm	2500			
			FULLY RESTRAINED BOLTED JOINT		
b_up	mm	900		Nmm	28047520330
b_low	mm	1250	b	mm	2360
tf_up	mm	70	F	N	11884542,51
tf_low	mm	70		Atot	22890,10499
tw	mm	28		n	41
hw	mm	2360	BOLT CHARACTERISTICS		
A	mm2	192330	class		8,8
Ix	mm4	4,4482E+11	f_{yb}	[N/mm2]	649
Iy	mm4	10369681812	f_{tb}	[N/mm2]	800
Wy	mm3	8295745,45	Type		**M30**
Wpl	mm3	414601250	f_b	mm	30
c/t	-	85,11190476	Ares	mm2	561
e	-	0,813616513	column	-	4
x	mm	1184,464286	raw	-	8
		1315,535714	n_b	-	64
Yg	mm	1071,60	SHEAR TEST		
f_yk	N/mm2	355	F_vRd	daN	13733,28
PLATE GEOMETRY			F_v,Ed	daN	154373,43
t_1	mm	28		daN	5604,774219
t_2	mm	28			SATISFY
e_1	mm	100	TENSILE TEST		
		ok	F_t,Rd	daN	32313,6
e_2	mm	100	F_t,Ed	daN	1532753,57
		ok	F_t,Ed	daN	23949,27453
p_1	mm	70			SATISFY
		ok	COMBINED ACTION - SHEAR AND TENSILE		
p_2	mm	100		0,937510172	
		ok		SATISFY	
Free web	mm	2360			
		OK			
Heigth plate	mm	900			
Ftk	N/mm2	510			

BEAM			C6		
h	mm	2500	FULLY RESTRAINED BOLTED JOINT		
b_up	mm	500		Nmm	7244379109
b_low	mm	1250	b	mm	2400
tf_up	mm	40	F	N	3018491,295
tf_low	mm	60		Atot	5813,73516
tw	mm	22		n	11
hw	mm	2400	BOLT CHARACTERISTICS		
A	mm2	114300	class		8,8
Ix	mm4	2,3222E+11	f_{yb}	[N/mm2]	649
Iy	mm4	2678379600	f_{tb}	[N/mm2]	800
Wy	mm3	2142703,68	Type		**M30**
Wpl	mm3	227022500	f_b	mm	30
c/t	-	110,3090909	Ares	mm2	561
e	-	0,813616513	column	-	4
x	mm	1688,636364	raw	-	6
		811,3636364	n_b	-	48
Yg	mm	993,10	SHEAR TEST		
f_yk	N/mm2	355	F_vRd	daN	13733,28
PLATE GEOMETRY			F_v,Ed	daN	154373,43
t_1	mm	22		daN	6065,88
t_2	mm	20			SATISFY
e_1	mm	100	TENSILE TEST		
		ok	F_t,Rd	daN	32313,6
e_2	mm	100	F_t,Ed	daN	914278,64
		ok	F_t,Ed	daN	19047,47167
p_1	mm	100			SATISFY
		ok	COMBINED ACTION - SHEAR AND TENSILE		
p_2	mm	100		0,862732587	
		ok		SATISFY	
Free web	mm	2400			
		OK			
Heigth plate	mm	700			
Ftk	N/mm2	510			

BEAM		
h	mm	2500
b_up	mm	500
b_low	mm	900
tf_up	mm	30
tf_low	mm	70
tw	mm	16
hw	mm	2400
A	mm2	98900
Ix	mm4	1,7305E+11
Iy	mm4	2626235869
Wy	mm3	2100988,695
Wpl	mm3	167812500
c/t	-	151,2152778
e	-	0,813616513
x	mm	2153,125
		346,875
Yg	mm	848,39
f_yk	N/mm2	355
PLATE GEOMETRY		
t_1	mm	16
t_2	mm	20
e_1	mm	100
		ok
e_2	mm	100
		ok
p_1	mm	100
		ok
p_2	mm	100
		ok
Free web	mm	2400
		OK
Heigth plate	mm	700
Ftk	N/mm2	510

C7		
FULLY RESTRAINED BOLTED JOINT		
	Nmm	7103342731
b	mm	2400
F	N	2959726,138
	Atot	5700,551113
	n	11
BOLT CHARACTERISTICS		
class		8,8
f_{yb}	[N/mm2]	649
f_{tb}	[N/mm2]	800
Type		**M30**
f_b	mm	30
Ares	mm2	561
column	-	4
raw	-	6
n_b	-	48
SHEAR TEST		
F_vRd	daN	13733,28
F_v,Ed	daN	154373,43
	daN	3708,025
		SATISFY
TENSILE TEST		
F_t,Rd	daN	32313,6
F_t,Ed	daN	736951,55
F_t,Ed	daN	15353,15729
		SATISFY
COMBINED ACTION - SHEAR AND TENSILE		
	0,609381364	
	SATISFY	

BEAM		
h	mm	2500
b_up	mm	600
b_low	mm	900
tf_up	mm	30
tf_low	mm	70
tw	mm	16
hw	mm	2400
A	mm2	108509,3663
Ix	mm4	1,9022E+11
Iy	mm4	3273457881
Wy	mm3	2618766,304
Wpl	mm3	182722500
c/t	-	150,7291667
e	-	0,813616513
x	mm	2265,917697
		234,0823031
Yg	mm	838,95
f_yk	N/mm2	355
PLATE GEOMETRY		
t_1	mm	16
t_2	mm	20
e_1	mm	100
		ok
e_2	mm	100
		ok
p_1	mm	100
		ok
p_2	mm	100
		ok
Free web	mm	2400
		OK
Heigth plate	mm	700
Ftk	N/mm2	510

C8		
FULLY RESTRAINED BOLTED JOINT		
	Nmm	8853924172
b	mm	2400
F	N	3689135,072
	Atot	7105,421941
	n	13
BOLT CHARACTERISTICS		
class		8,8
f_{yb}	[N/mm2]	649
f_{tb}	[N/mm2]	800
Type		**M30**
f_b	mm	30
Ares	mm2	561
column	-	4
raw	-	6
n_b	-	48
SHEAR TEST		
F_vRd	daN	13733,28
F_v,Ed	daN	154373,43
	daN	1935,44875
		SATISFY
TENSILE TEST		
F_t,Rd	daN	32313,6
F_t,Ed	daN	808702,56
F_t,Ed	daN	16847,97
		SATISFY
COMBINED ACTION - SHEAR AND TENSILE		
	0,513352314	
	SATISFY	

SEISMIC ANALYSIS

Modo N°	Pulsazione (Rad/s)	Periodo (s)	frequenza (Hz)	Energia (J)	Masse modali		
					X kg (%)	Y kg (%)	Z kg (%)
1	**11,37**	**0,55**	**1,81**	**13,83**	**132.02 (0.02)**	**2614.54 (0.41)**	**32128.07 (5.01)**
2	**14,35**	**0,44**	**2,28**	**44,32**	**81.75 (0.01)**	**90361.44 (14.10)**	**6356.42 (0.99)**
3	18,48	0,34	2,94	96,76	1296.93 (0.20)	210566.78 (32.86)	243.51 (0.04)
4	19,51	0,32	3,11	51,05	28.83 (0.00)	41381.65 (6.46)	3513.83 (0.55)
5	21,51	0,29	3,42	227,2	51.19 (0.01)	2111.00 (0.33)	1593.13 (0.25)
6	21,66	0,29	3,45	143,07	1266.80 (0.20)	60835.28 (9.49)	50111.03 (7.82)
7	22,03	0,29	3,51	102,95	602.47 (0.09)	14908.09 (2.33)	89952.39 (14.04)
8	23,8	0,26	3,79	94,03	115.30 (0.02)	55297.10 (8.63)	211451.87 (32.99)
9	26,84	0,23	4,27	161,89	188.30 (0.03)	144.50 (0.02)	2671.76 (0.42)
10	29,51	0,21	4,7	180,61	131.60 (0.02)	63085.22 (9.84)	485.75 (0.08)
11	32,51	0,19	5,17	321,25	3.53 (0.00)	13761.55 (2.15)	363.51 (0.06)
12	36,05	0,17	5,74	313,37	3188.08 (0.50)	3468.28 (0.54)	611.77 (0.10)
13	36,39	0,17	5,79	174,47	5595.68 (0.87)	120.87 (0.02)	367.54 (0.06)
14	38,18	0,16	6,08	408,08	31.31 (0.00)	13414.23 (2.09)	83.61 (0.01)
15	38,61	0,16	6,15	428,77	404.66 (0.06)	379.02 (0.06)	9.99 (0.00)
16	42,56	0,15	6,77	396,02	195.44 (0.03)	1046.32 (0.16)	1306.33 (0.20)
17	45,32	0,14	7,21	452,54	223.53 (0.03)	42.78 (0.01)	3.21 (0.00)
18	46,01	0,14	7,32	481,26	531.84 (0.08)	225.28 (0.04)	1438.06 (0.22)
19	46,68	0,13	7,43	445,77	121.36 (0.02)	1010.19 (0.16)	248.46 (0.04)
20	48,28	0,13	7,68	565,51	129.08 (0.02)	1669.45 (0.26)	191.08 (0.03)
residual					626572.67 (97.77)	64448.77 (10.06)	237761.04 (37.10)
Total				5102,76	640892.36 (100.00)	640892.36 (100.00)	640892.36 (100.00)

As we can see from the table above, the number of modes represented are not satisfied for the achievement of 85% of the total mass in all three directions. this makes us reflect a lot, as the deck is very rigid and its oscillation frequency is very far from that obtained by dynamic analysis.

The figures that will be arranged next represent the modal results of the first modes of reference.

- 1^{ST} MODE

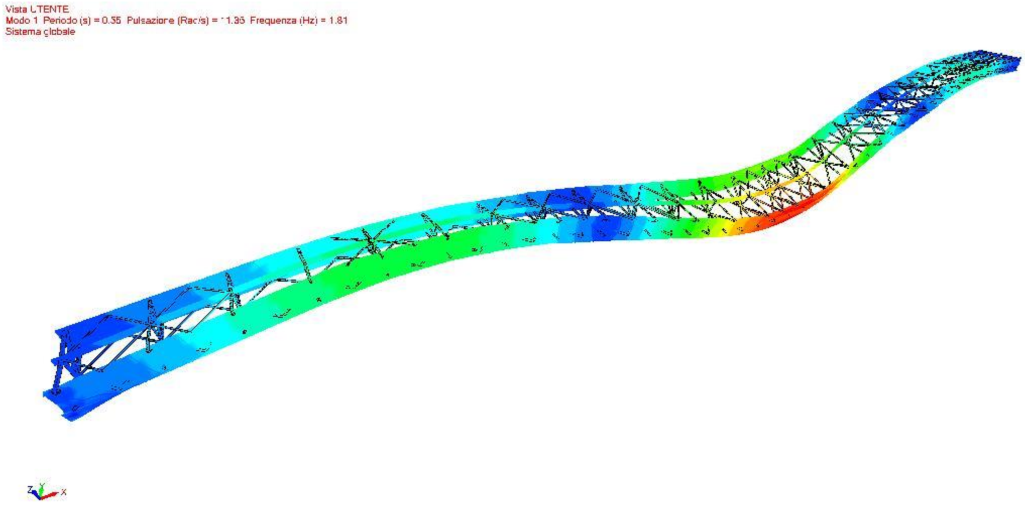

- 2^{nd} MODE

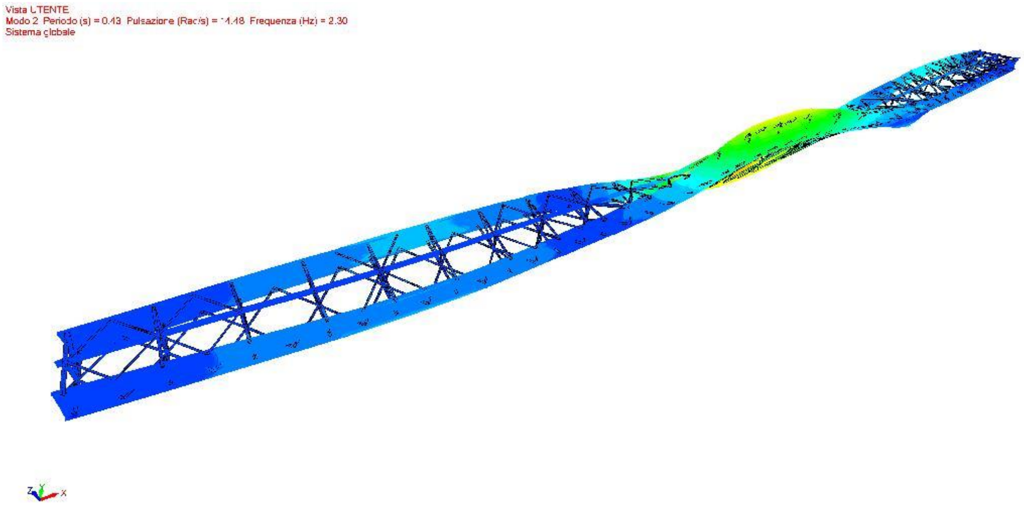

- 3^{RD} MODE

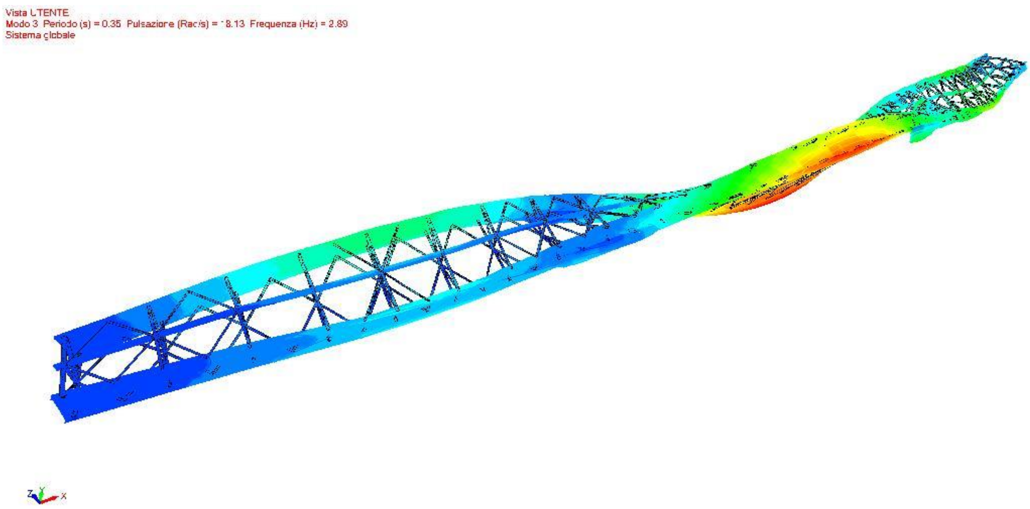

- 4^{TH} MODE

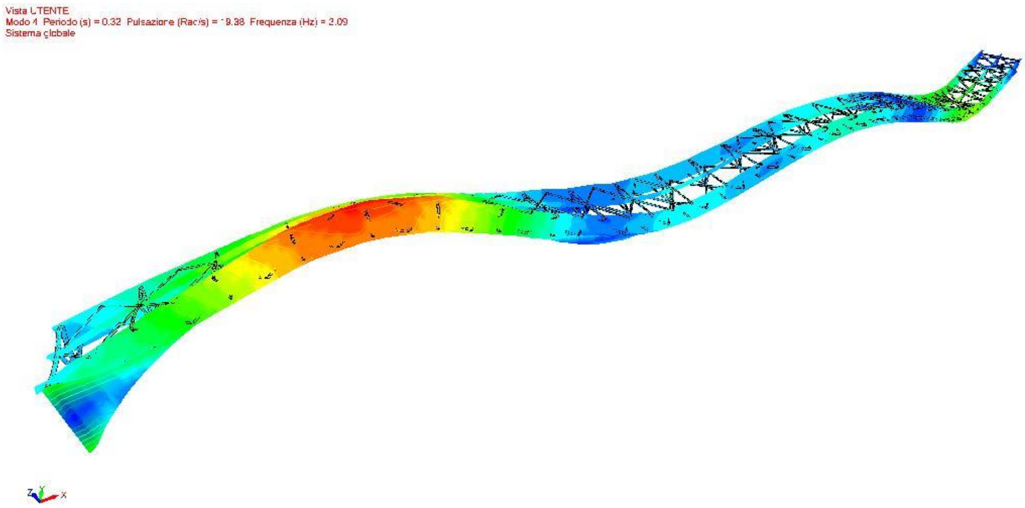
Vista UTENTE
Modo 4 Periodo (s) = 0.32 Pulsazione (Rad/s) = 9.38 Frequenza (Hz) = 2.09
Sistema globale
Z
Y
X

ANNEX D – LOCAL ANALYSIS with IDEA STATICA OUTPUT

FULLY RESTORED BOLTED JOINT

1ST JOINT SEGMENT: C1-C2

ST ANALYSIS

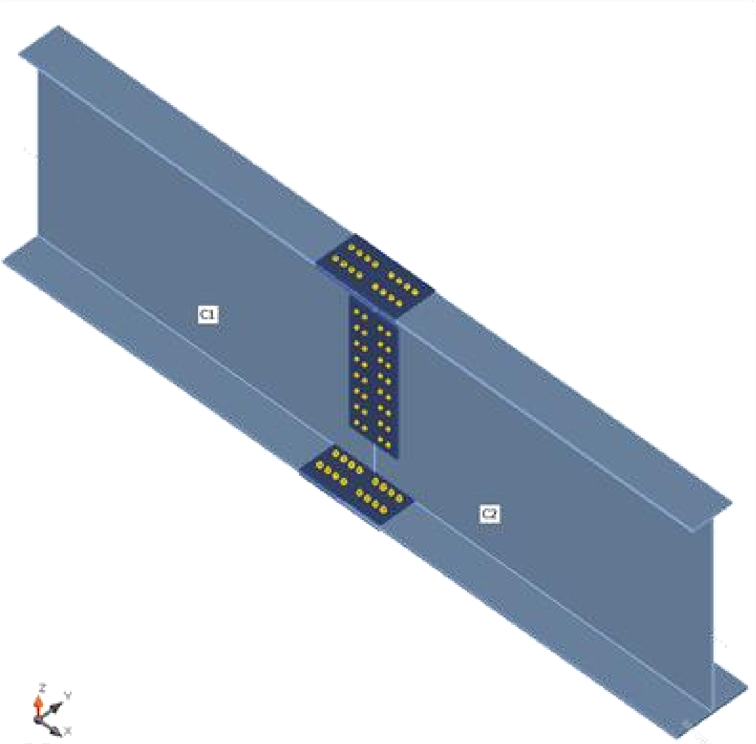

VERIFICATION

Rotational stiffnes- Moment curvature

Mj,Rd [kNm]	**Sj,ini** [MNm/rad]	**Φc** [mrad]	**L** [m]	**Sj,R** [MNm/rad]	**Sj,P** [MNm/rad]	**Class**
-7534.2	4459.4	-2.9	6.00	72362.6	1447.3	Semi-rigid

Tangential rotational rigidity

M [kNm]	**Sjs** [MNm/rad]	**Φ** [mrad]
-3272.5	4494.7	-0.7

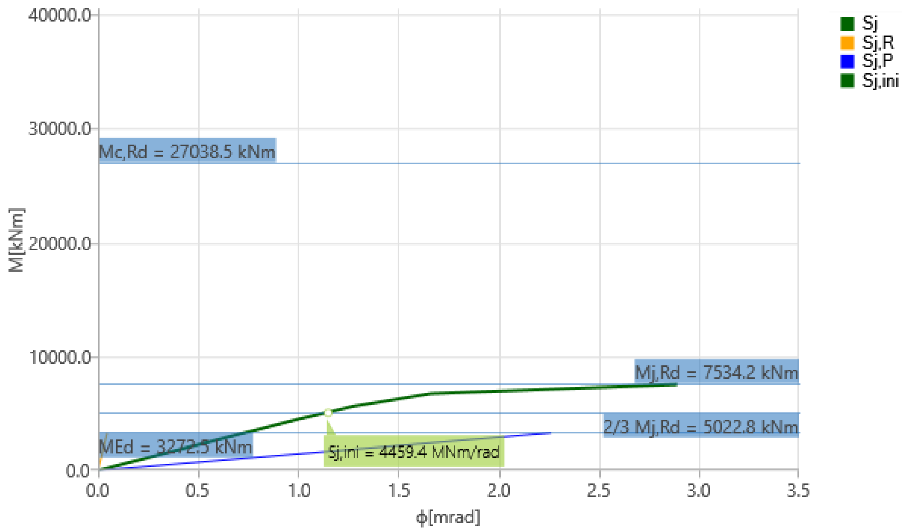

2nd JOINT SEGMENT: C2-C3

ST ANALYSIS

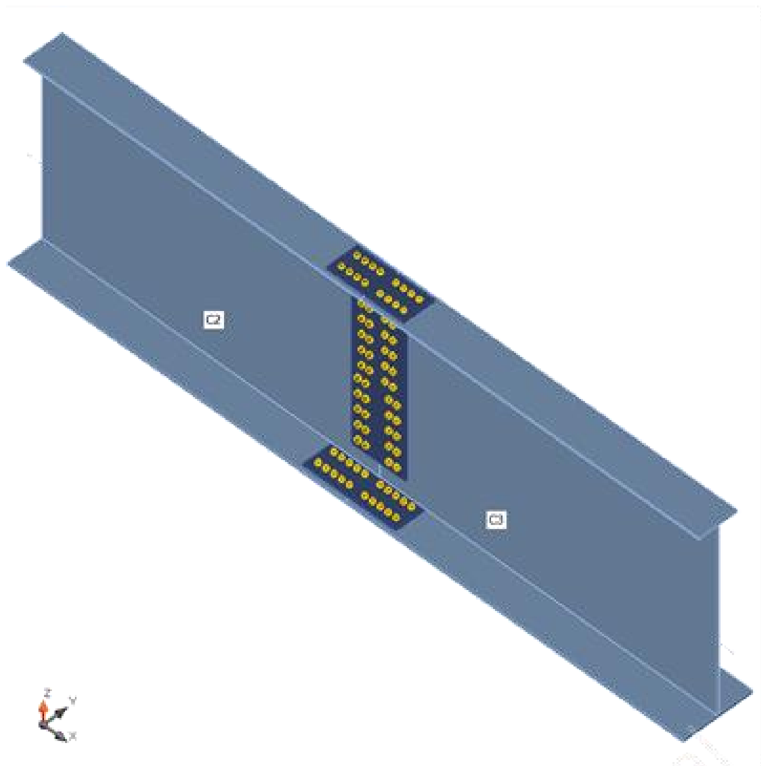

VERIFICATION

Rotational stiffnes- Moment curvature

Mj,Rd [kNm]	**Sj,ini** [MNm/rad]	**Φc** [mrad]	**L** [m]	**Sj,R** [MNm/rad]	**Sj,P** [MNm/rad]	**Class**
-16468.5	6988.6	-61.2	6.00	69919.0	1398.4	Semi-rigid

Tangential rotational rigidity

M [kNm]	**Sjs** [MNm/rad]	**Φ** [mrad]
-5474.7	7032.6	-0.8

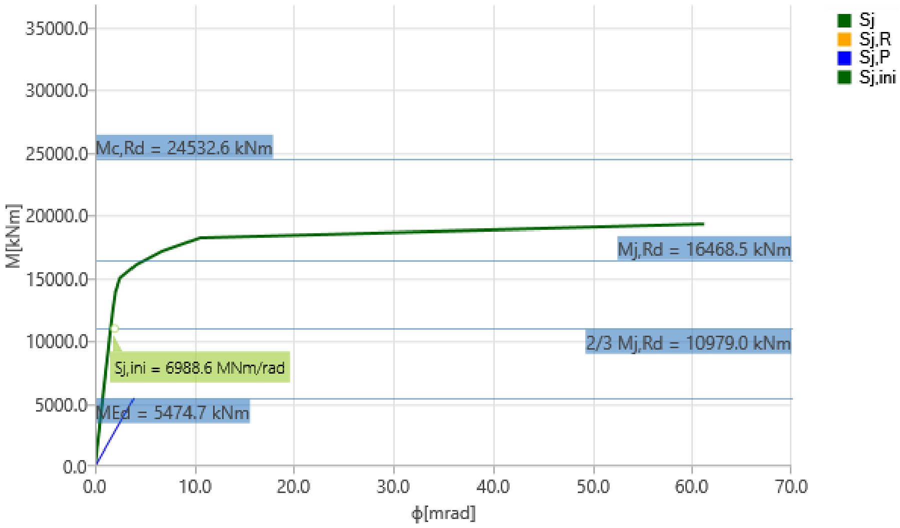

3rd JOINT SEGMENT: C3-C4

ST ANALYSIS

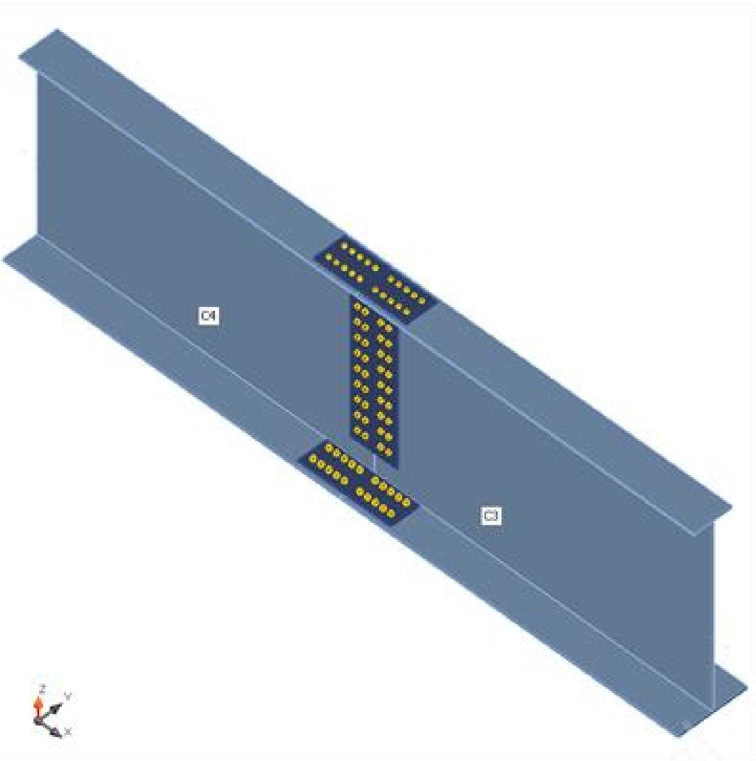

VERIFICATION

Rotational stiffnes- Moment curvature

Mj,Rd [kNm]	**Sj,ini** [MNm/rad]	**Φc** [mrad]	**L** [m]	**Sj,R** [MNm/rad]	**Sj,P** [MNm/rad]	**Class**
-8754.1	6191.4	-17.4	1.00	419514.3	8390.3	Semi-rigid

Tangential rotational rigidity

M [kNm]	**Sjs** [MNm/rad]	**Φ** [mrad]
-5139.6	6236.0	-0.8

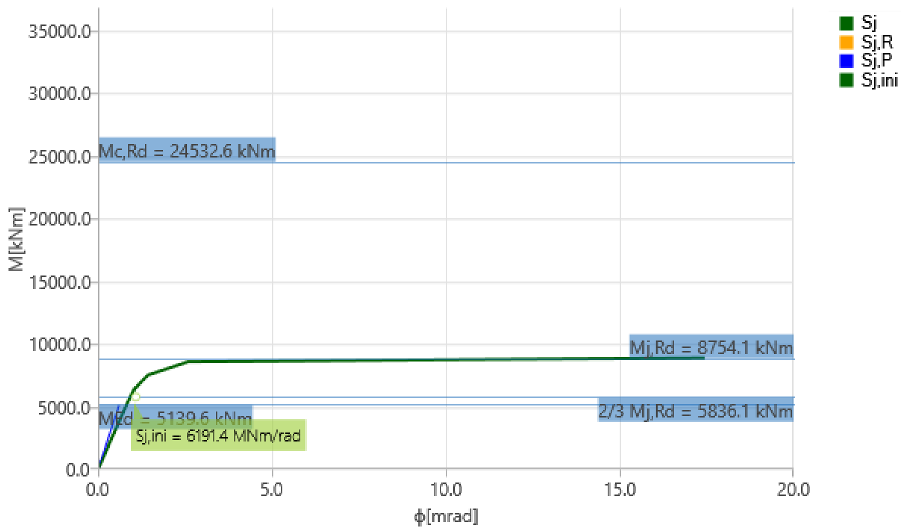

PILOT NODE - ABUTMENT POSITION

ST ANALYSIS

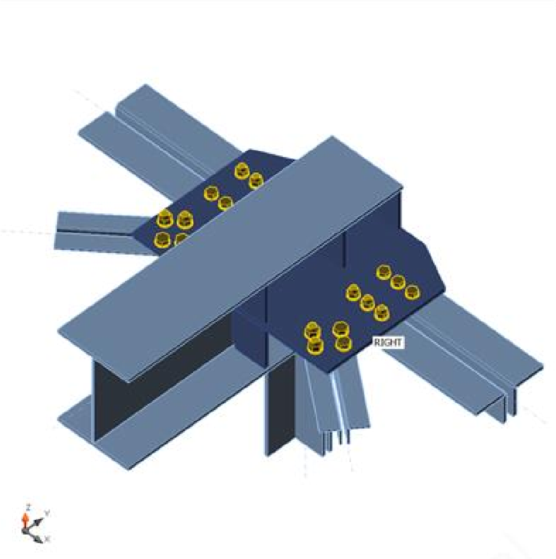

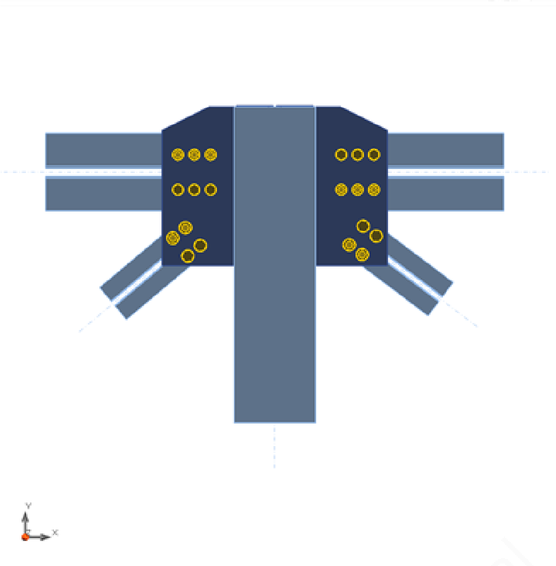

VERIFICATION

Rotational stiffnes- Moment curvature

Mj,Rd [kNm]	**Sj,ini** [MNm/rad]	**Φc** [mrad]	**L** [m]	**Sj,R** [MNm/rad]	**Sj,P** [MNm/rad]	**Class**
22.1	0.2	357.2	1.00	94.5	1.9	Semi-rigid

Tangential rotational rigidity

M [kNm]	**Sjs** [MNm/rad]	**Φ** [mrad]
21.2	0.1	144.0

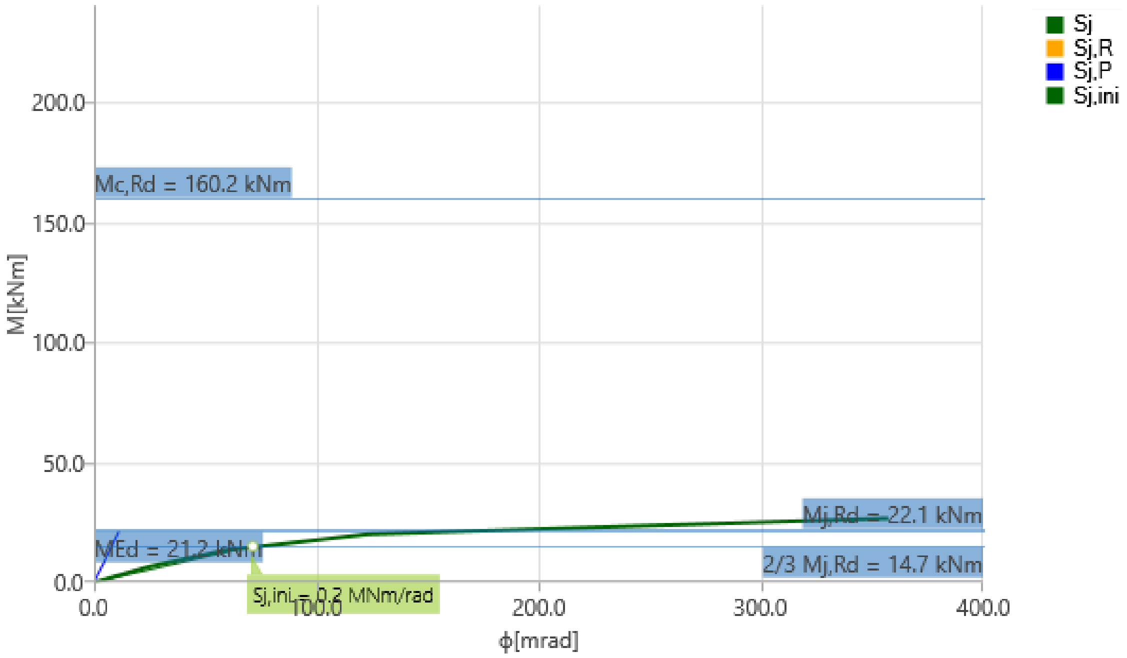

EPS ANALYSIS

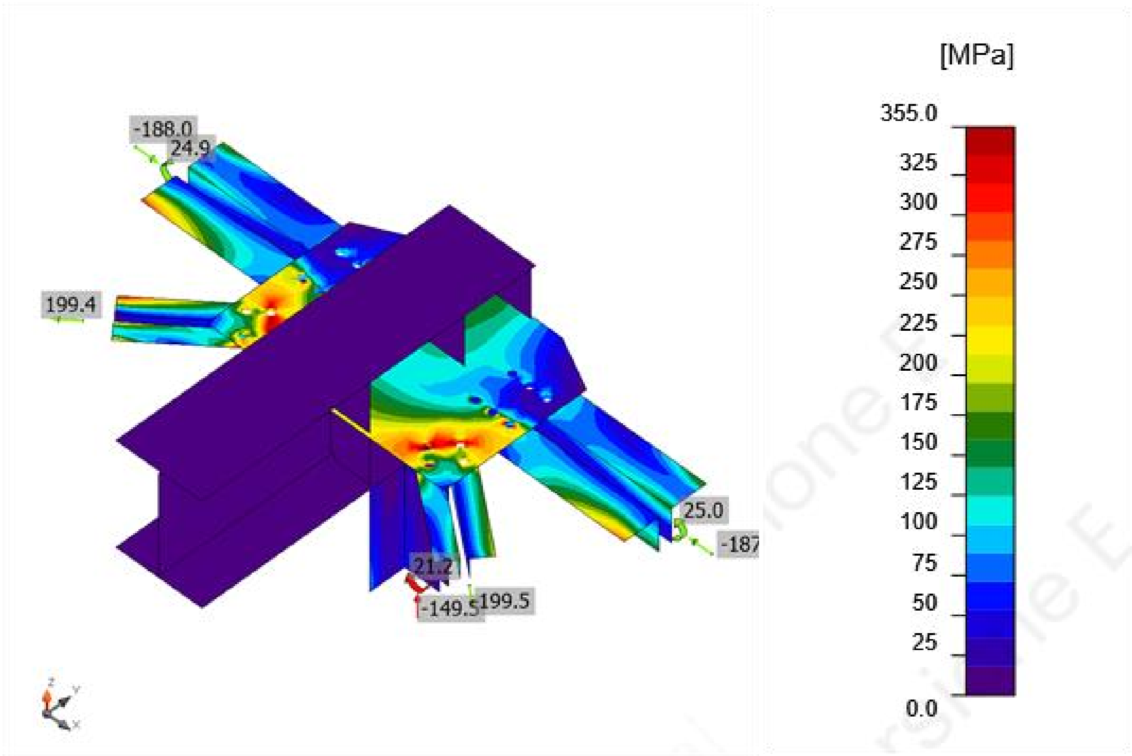

PILOT NODE - MIDDLE POSITION

ST ANALYSIS

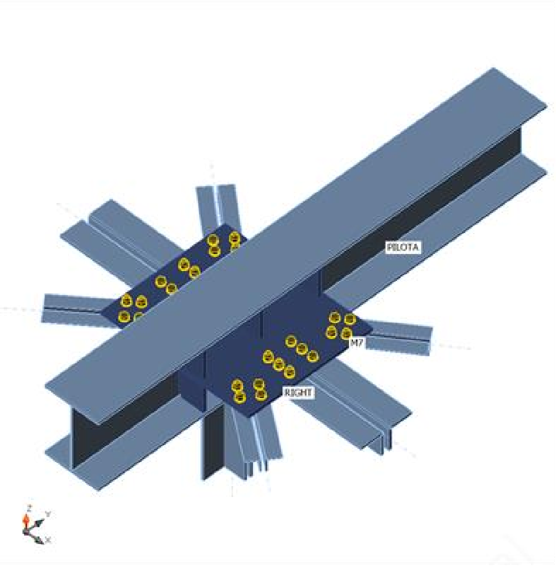

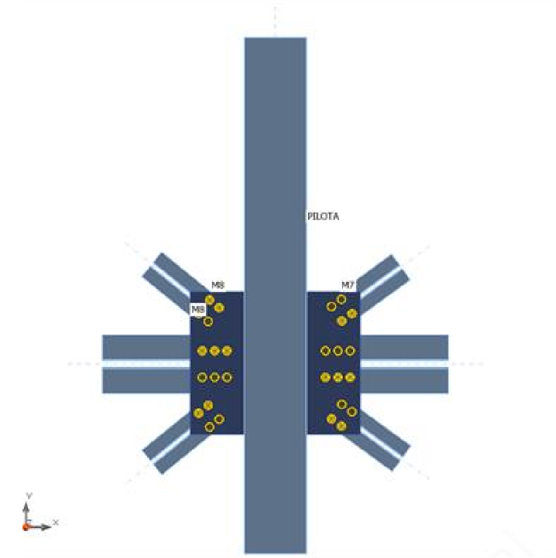

VERIFICATION

Rotational stiffnes- Moment curvature

Mj,Rd [kNm]	**Sj,ini** [MNm/rad]	**Φc** [mrad]	**L** [m]	**Sj,R** [MNm/rad]	**Sj,P** [MNm/rad]	**Class**
29.8	0.2	1367.4	6.00	15.8	0.3	Semi-rigid

Tangential rotational rigidity

M [kNm]	**Sjs** [MNm/rad]	**Φ** [mrad]
21.2	0.2	100.7

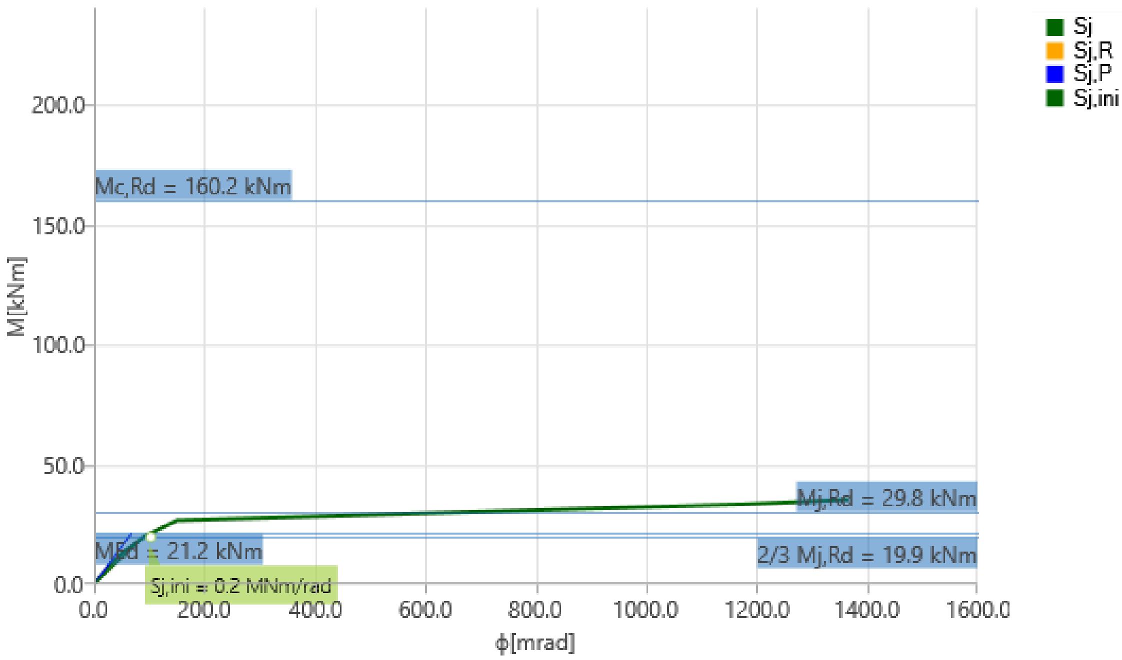

EPS ANALYSIS

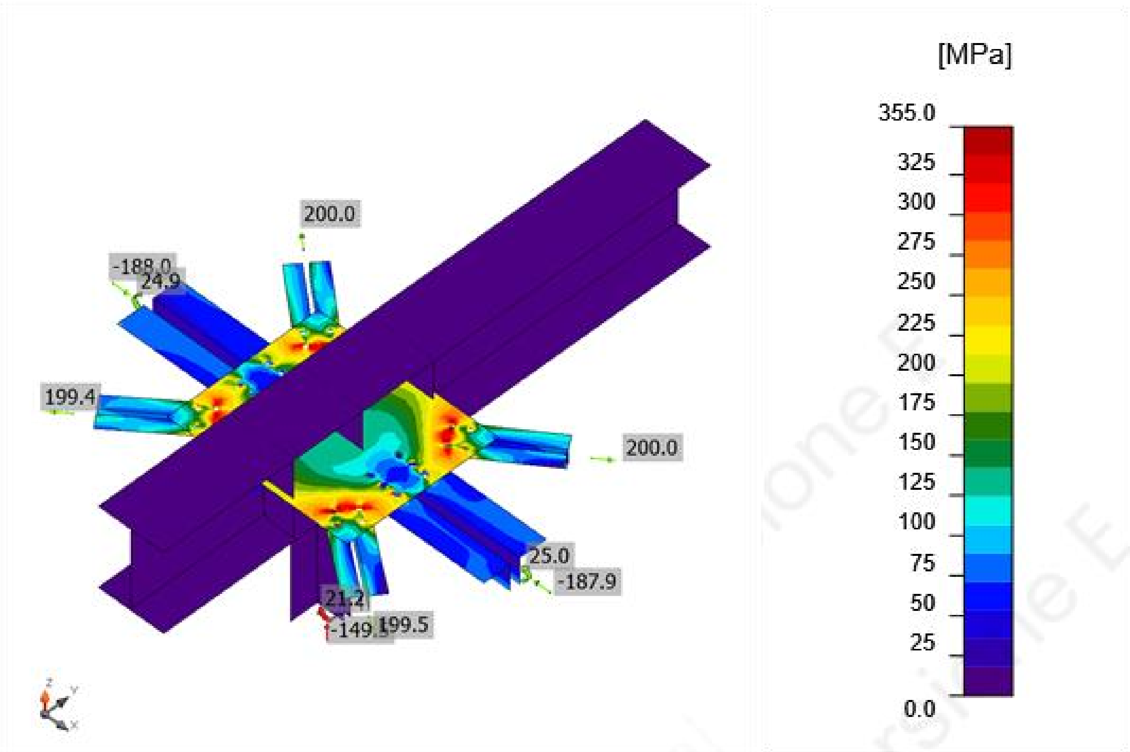

DIAPHRAGM NODE – TYPE A

ST ANALYSIS

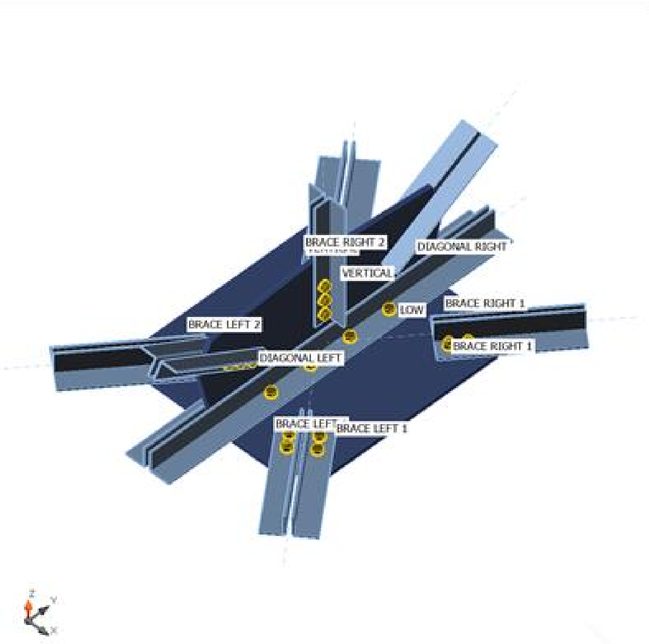

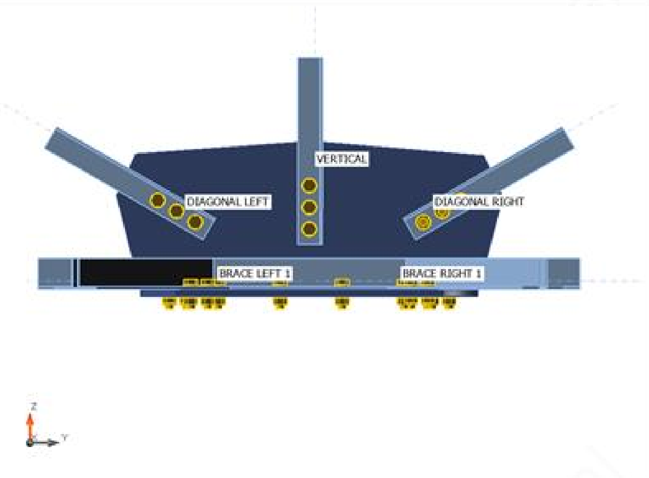

VERIFICATION

Axial stiffnes

N [kN]	Nj,Rd [kN]	dx [mm]	St [MN/m]
-114.0	-771.8	0	355

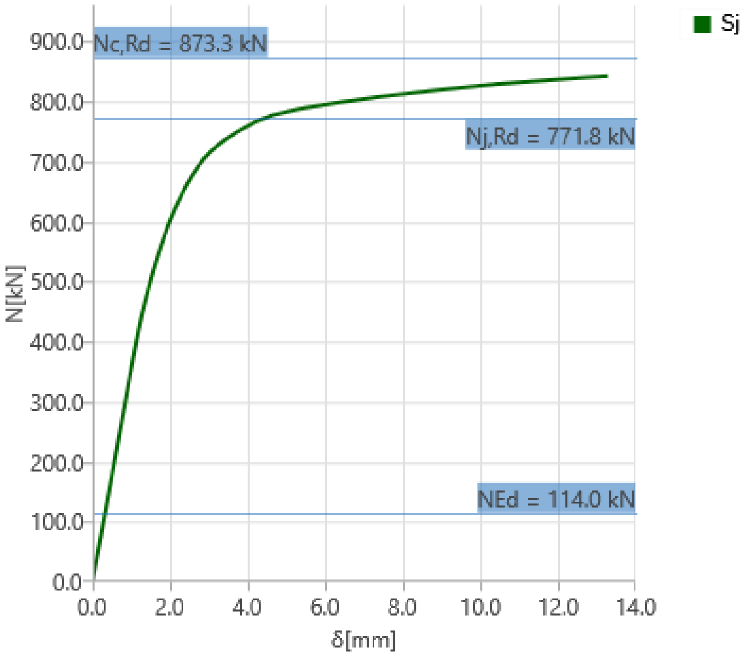

EPS ANALYSIS

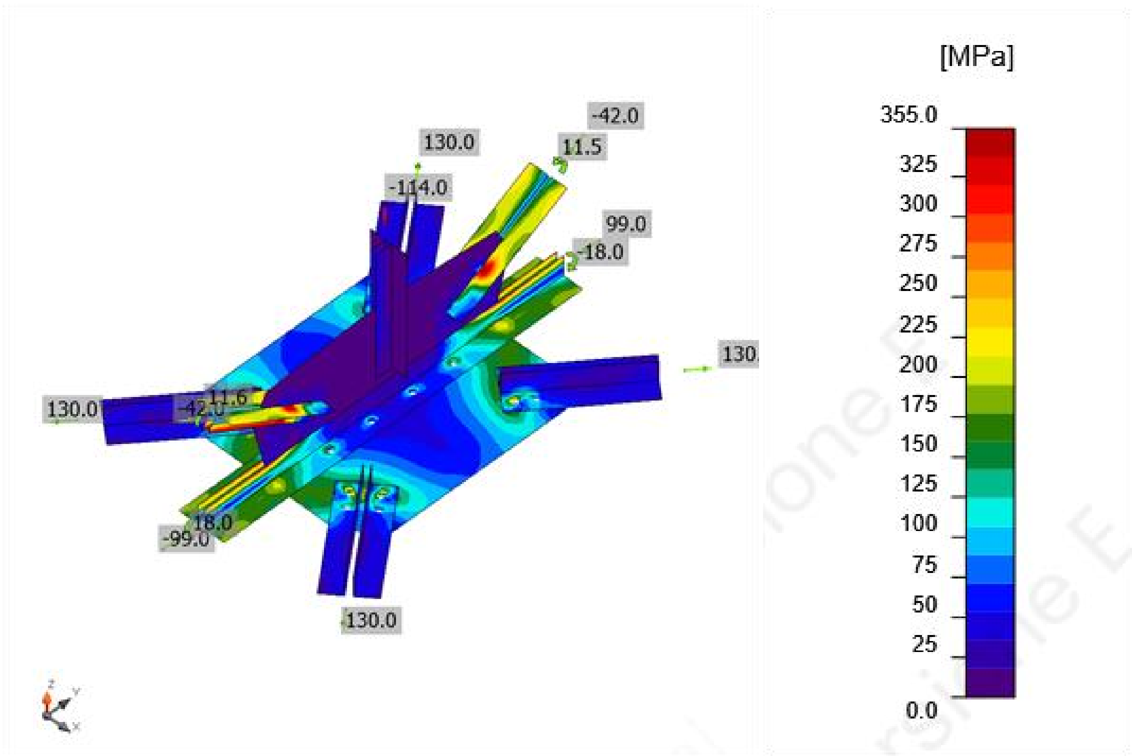

DIAPHRAGM NODE – TYPE B

ST ANALYSIS

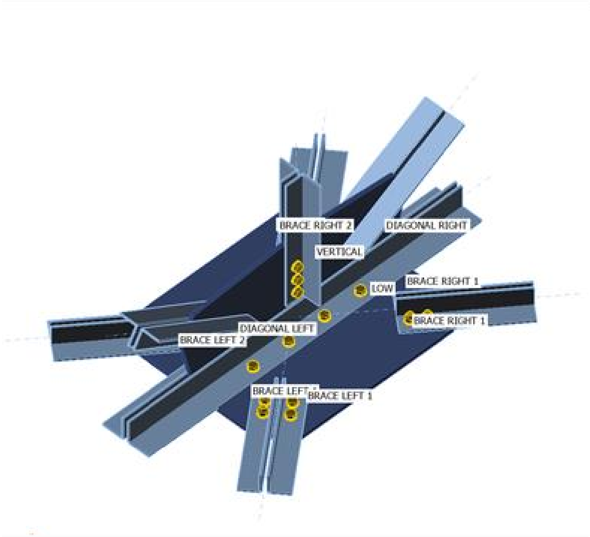

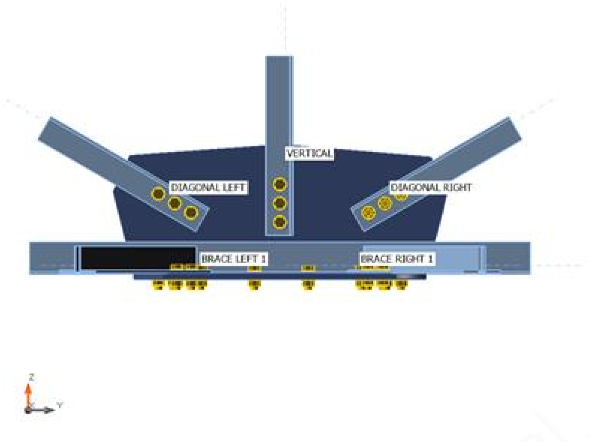

VERIFICATION

Axial stiffnes

N [kN]	**Nj,Rd** [kN]	**dx** [mm]	**St** [MN/m]
-65.0	-715.0	0	286

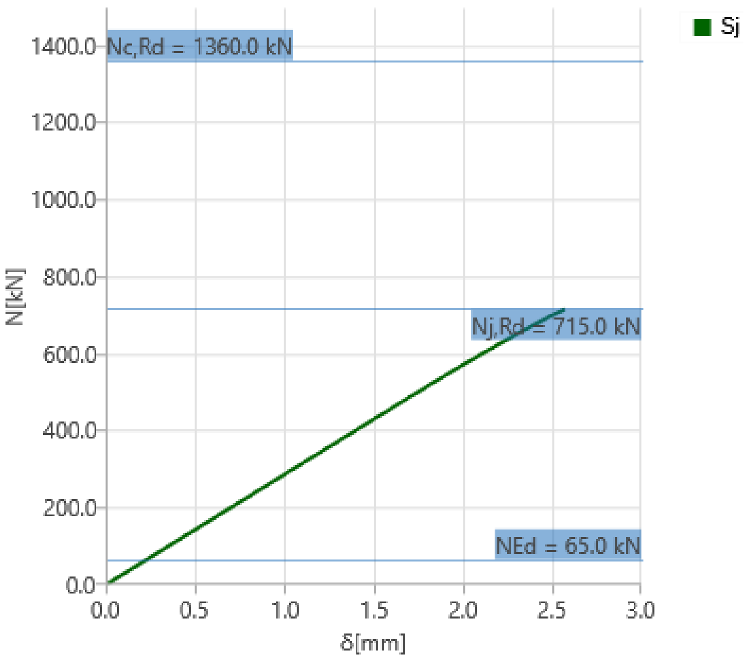

EPS ANALYSIS

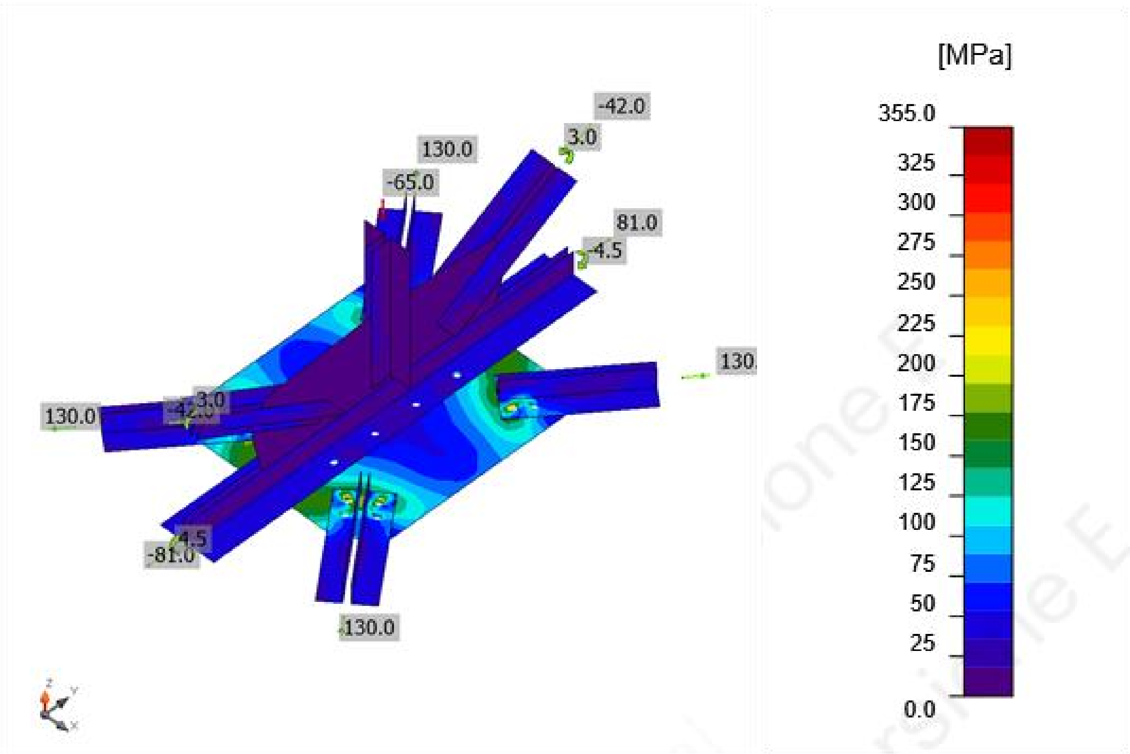

DIAPHRAGM NODE – TYPE ABUTMENT

ST ANALYSIS

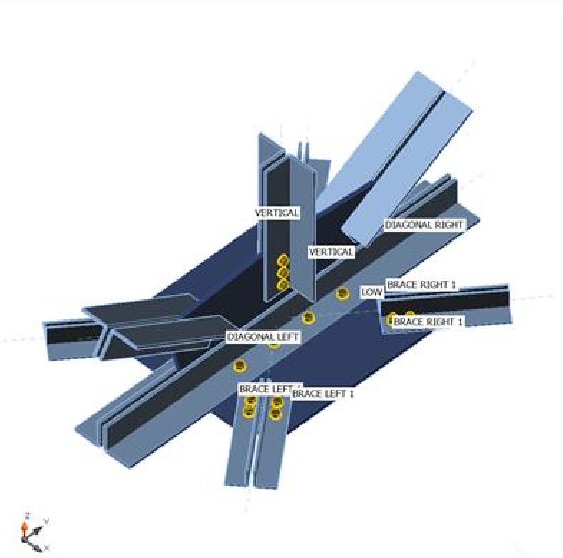

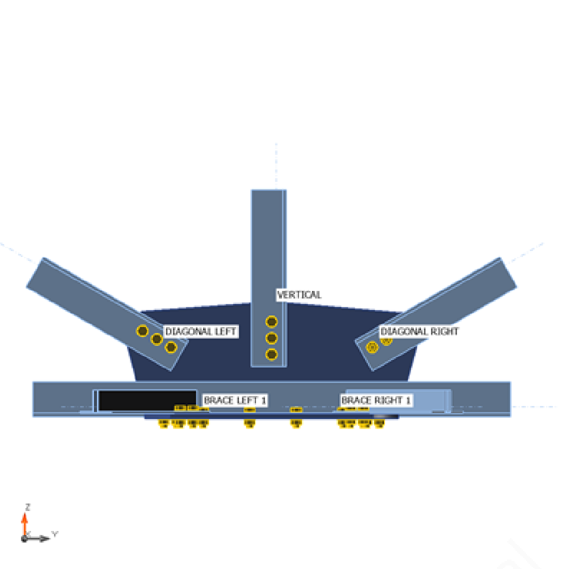

VERIFICATION

Axial stiffnes

N [kN]	**Nj,Rd** [kN]	**dx** [mm]	**St** [MN/m]
-150.0	-1011.3	0	325

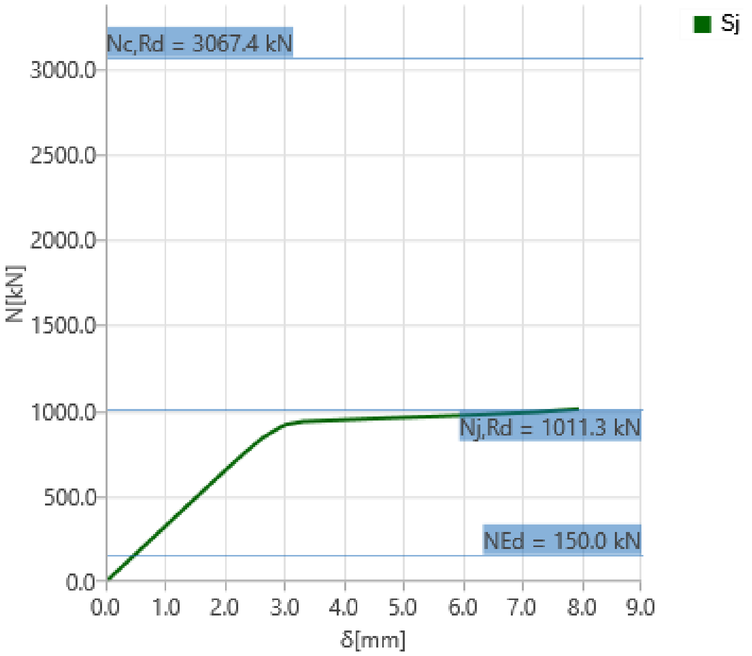

EPS ANALYSIS

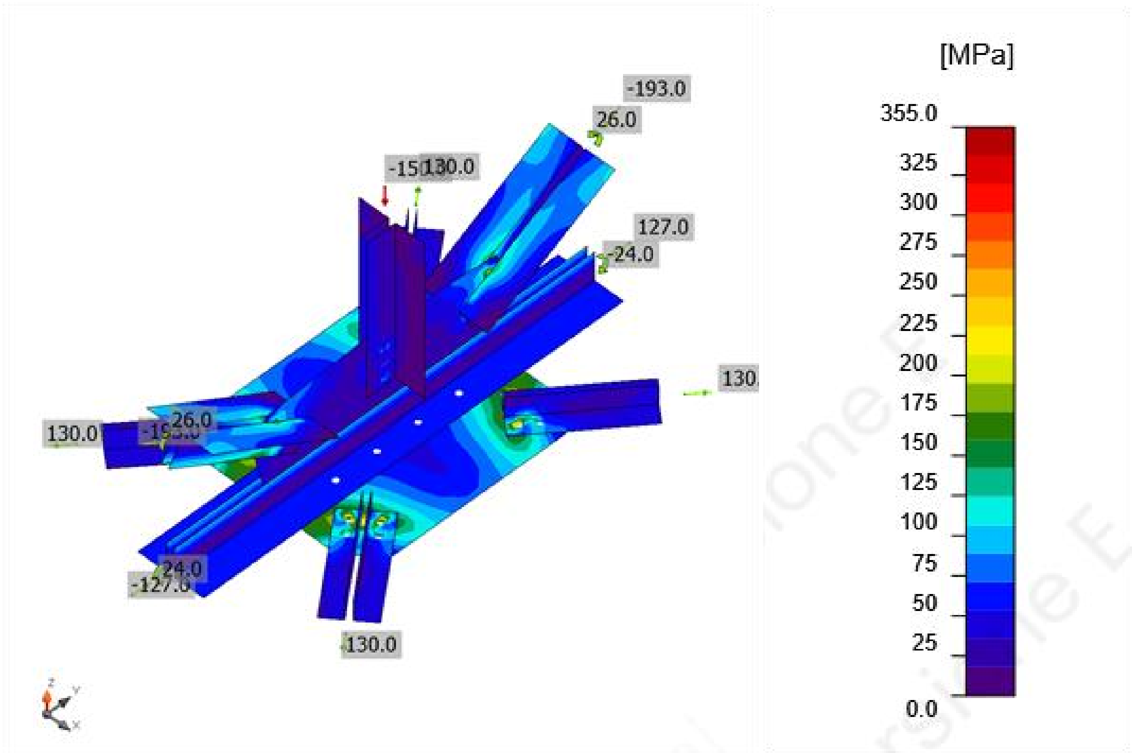

DIAPHRAGM NODE – TYPE PIER

ST ANALYSIS

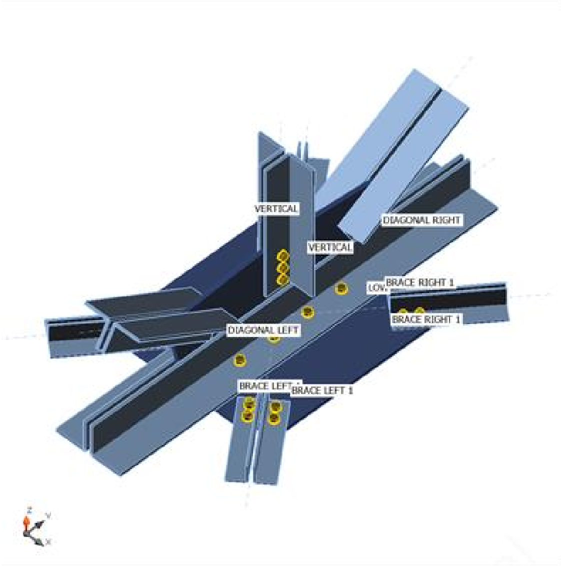

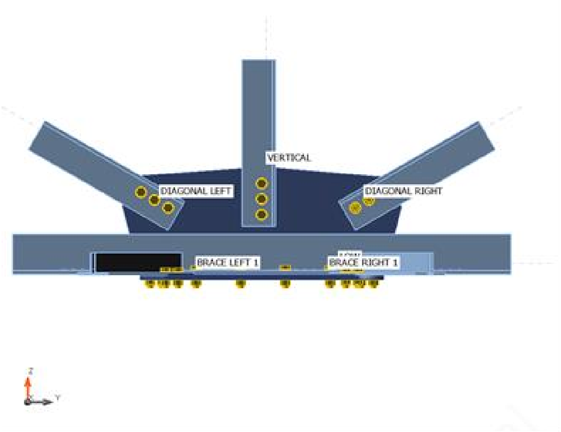

VERIFICATION

Axial stiffnes

N [kN]	**Nj,Rd** [kN]	**dx** [mm]	**St** [MN/m]
-151.0	-1011.0	-1	236

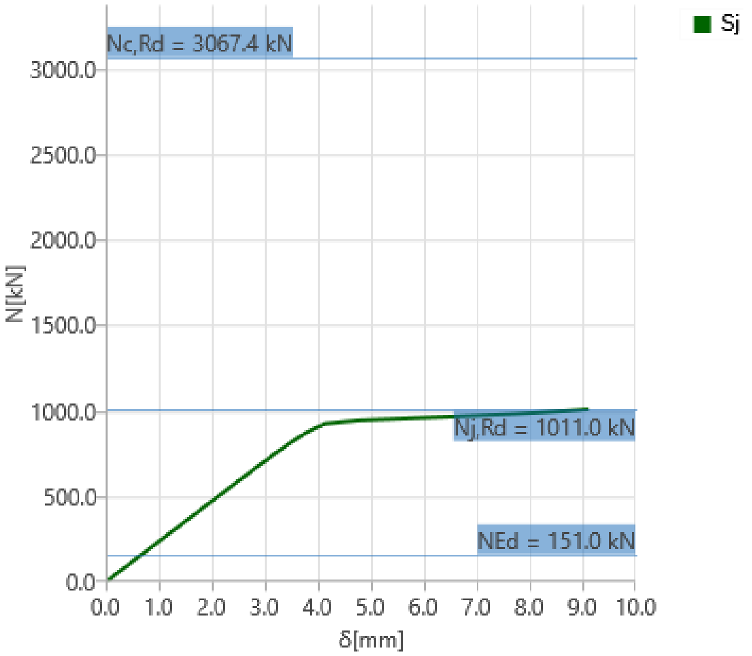

EPS ANALYSIS

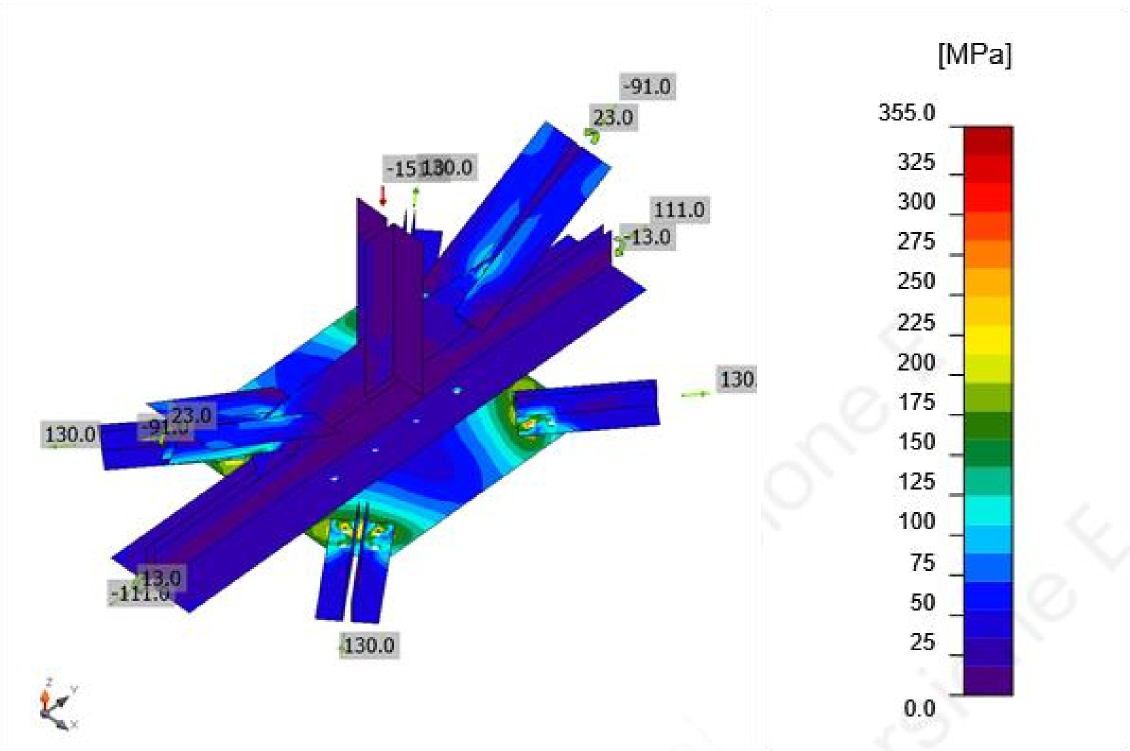

This final table was taken as a reference for the analysis and verification of each profile used for diaphragms and horizontal stiffeners. It was provided by the national association "*Promozione Acciaio*" is the cultural institution that promotes the development of steel constructions and infrastructures in Italy.

PROFILO						
"L" ALI UGUALI						
DIMENSIONI	DIMENSIONI	DIMENSIONI	DIMENSIONI	DIMENSIONI	DIMENSIONI	DIMENSIONI
15x15x3	50x50x3	75x75x6	100x100x16	130x130x8	150x150x12	200x200x18
20x20x3	50x50x4	75x75x7	110x110x6	130x130x9	150x150x13	200x200x19
20x20x4	50x50x5	80x80x6	110x110x7	130x130x10	150x150x14	200x200x20
20x20x5	50x50x6	80x80x7	110x110x8	130x130x11	150x150x15	200x200x21
25x25x3	50x50x7	80x80x8	110x110x9	130x130x12	150x150x16	200x200x22
25x25x4	50x50x8	80x80x10	110x110x10	130x130x13	150x150x17	200x200x23
25x25x5	55x55x4	80x80x12	110x110x11	130x130x14	150x150x18	200x200x24
30x30x3	55x55x5	80x80x13	110x110x12	130x130x15	150x150x19	200x200x25
30x30x4	60x60x4	90x90x6	110x110x13	130x130x16	150x150x20	200x200x26
30x30x5	60x60x5	90x90x7	110x110x14	130x130x17	160x160x14	200x200x28
30x30x6	60x60x6	90x90x8	110x110x15	130x130x18	160x160x15	250x250x18
35x35x3	60x60x7	90x90x9	110x110x16	140x140x8,8	160x160x16	250x250x20
35x35x3.5	60x60x8	90x90x10	120x120x8	140x140x10	160x160x17	250x250x21
35x35x4	60x60x9	90x90x12	120x120x9	140x140x11	180x180x13	250x250x22
35x35x5	60x60x10	100x100x6	120x120x10	140x140x12	180x180x14	250x250x23
35x35x6	65x65x5	100x100x7	120x120x11	140x140x12,5	180x180x15	250x250x24
40x40x3	65x65x6	100x100x8	120x120x12	140x140x13	180x180x16	250x250x25
40x40x4	70x70x5	100x100x9	120x120x13	140x140x14	180x180x17	250x250x26
40x40x5	70x70x6	100x100x10	120x120x14	140x140x15	180x180x18	250x250x27
40x40x6	70x70x7	100x100x11	120x120x15	140x140x16	180x180x19	250x250x28
45x45x3	70x70x9	100x100x12	120x120x16	140x140x17	180x180x20	203x203x19
45x45x4	70x70x8	100x100x13	120x120x17	140x140x18	200x200x15	203x203x22,2
45x45x5	70x70x10	100x100x14	120x120x18	150x150x10	200x200x16	203x203x25,4
45x45x6	75x75x5	100x100x15	130x130x7	150x150x11	200x200x17	203x203x28,6

CHIAVE DI LETTURA					
FACILMENTE REPERIBILE		TEMPI MEDI DI REPERIBILITA		MAGGIORI TEMPI DI REPERIBILITA	